

# Tradespace Model for Planetary Surface Exploration Hopping Vehicles

by  
Phillip M. Cunio

B.S. Aerospace Engineering / B.S. Mechanical Engineering / B.A. German Studies  
University of Florida, 2006

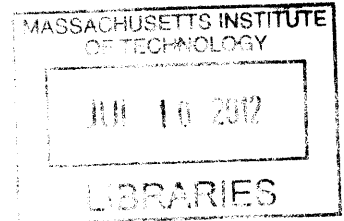
S.M. Aeronautics and Astronautics  
Massachusetts Institute of Technology, 2008

SUBMITTED TO THE DEPARTMENT OF AERONAUTICS AND ASTRONAUTICS  
IN PARTIAL FULFILLMENT OF THE REQUIREMENTS FOR THE DEGREE OF  
DOCTOR OF PHILOSOPHY  
AT THE  
MASSACHUSETTS INSTITUTE OF TECHNOLOGY

JUNE 2012

© 2012 Phillip M. Cunio. All rights reserved.

ARCHIVES



The author hereby grants to MIT permission to reproduce and to distribute publicly paper and electronic copies of this thesis document in whole or in part in any medium now known or hereafter created.

Signature of Author.....  
*Phillip M. Cunio*  
Department of Aeronautics and Astronautics  
May 24th, 2012

Certified by.....  
*Jeffrey A. Hoffman*  
Professor of the Practice of Aeronautics and Astronautics  
Thesis Supervisor

Certified by.....  
*David W. Miller*  
Professor of Aeronautics and Astronautics

Certified by.....  
*Olivier L. de Weck*  
Associate Professor of Aeronautics and Astronautics and Engineering Systems

Certified by.....  
*M. L. Cummings*  
Associate Professor of Aeronautics and Astronautics and Engineering Systems

Certified by.....  
*John Danis*  
Senior Member of the Technical Staff at the Charles Stark Draper Laboratory

Accepted by.....  
*Eytan H. Modiano*  
Chair, Committee on Graduate Students



# **Tradespace Model for Planetary Surface Exploration Hopping Vehicles**

by

Phillip M. Cunio

Submitted to the Department of Aeronautics and Astronautics  
on May 24th, 2012 in Partial Fulfillment of the  
Requirements for the Degree of Doctor of Philosophy  
at the Massachusetts Institute of Technology

## **ABSTRACT**

Robotic planetary surface exploration, which has greatly benefited humankind's scientific knowledge of the solar system, has to date been conducted by sedentary landers or by slow, terrain-limited rovers. However, there are other types of vehicles which can conduct planetary surface exploration. One of these is hopping vehicles, which do not require fluid contact or ground contact in order to move, but instead propulsively balance thrust from their engines against gravity to propel themselves over the surface.

Hopping vehicles are still a nascent technology, however, and no spaceborne hopping vehicles have yet flown. In order to bring hopping vehicles into the decision space for planetary surface exploration missions, in this thesis we provide a framework to understand hopping vehicles' key characteristics and advantages, as well as a tradespace model to size hopping vehicles based on mission characteristics.

The tradespace model takes user-input mission requirements, including target planetary body, scientific payload, and a detailed flight profile, and produces a subsystem-level model of a hopping vehicle which can complete the mission. Information on the operational profile and lifecycle costs of the hopping vehicle is also produced. The tradespace model also permits users to capture results from one model run and compare them to other model runs, or to results produced by other models.

In this thesis, the tradespace model is described, and initial tradespace investigation is performed using the model. Finally, lessons learned are summarized and suggestions are offered for future research. The thesis closes with a summation of the potential offered by hopping vehicles for planetary surface exploration missions in the decades to come.

Thesis Supervisor: Jeffrey A. Hoffman  
Title: Professor of the Practice, Aeronautics and Astronautics

## ACKNOWLEDGEMENTS

Uxor mea, Talitha Cunio, mea familia vera est. For her willingness to follow me so far from home for so long, I am grateful. But for her support, I would expect not to be able to write these words.

I thank all my committee members for their years of advice, encouragement, and moral support. I especially thank Professor Jeff Hoffman for his willingness to back me when I explored things on my own, and when I explored things of a more reasonable nature as well. I thank Professor Missy Cummings for her willingness to gamble and take me in when I was an orphan for the second time. I am glad her lab proved to be so excellent a bridge on which to cast dice. I thank Mr. John Danis for his unflagging support. I thank Professor Dave Miller for his availability and good advice. I thank Professor Olivier de Weck for his support of so much of my work over the years, in so many fields.

I thank other department personnel who have provided me support when I needed it, especially Ms. Kathi Cofield Brazil, Ms. Barbara Lechner, and Ms. Marilyn Good. Kathi gave encouragement when no one else did, and Barbara Lechner provided the last impetus to make things happen when I could not. For providing me exemplary role models, I thank Dr. Erika Wagner and Dr. Alvar Saenz-Otero.

I have also been influenced by other graduate students who preceded me. I thank especially Ryan Boas and Willard Simmons for their positive examples, and think often of others whose examples also shaped much about the way I myself tried to be a good student in later years.

Others who have helped show me the path are Dr. Yves Boussemart, Dr. Luca Bertucelli, and Dr. Jaime Mateus, as well as my officemate, Dr. Ryan Kobrick. Some of the others who have walked it with me, and thereby helped to make the road a little less uncomfortable, are Alex Stimpson, Andrew Clare, Ben Corbin, and Aaron Johnson. I am happy to have been able to name them colleagues.

I have also been able to count myself a member of five different labs while attending MIT, and I therefore should like to express my feelings of regard for the Space Architects, the Man Vehicle Lab, the X-Prize Lab, the Humans and Automation Lab, and the Space Systems Lab. My especial colleagues and collaborators thence over the years have included Alessandro Golkar, Daniel Selva, Matt Smith, and Gwendolyn V. Gettliffe, across several types of projects and student service efforts, and these I thank particularly.

I have, however, been longest a member of the TALARIS project, and I cannot take the time to provide full recognition to all those who participated in it with me, lest I require the use of every blank scrap of writing material housed on campus. I do, however, wish to recognize the many beneficial interactions I have had with Farah Alibay, Ted Steiner, Chris Rossi, Joe Morrow, Eph Lanford, Chris Han, Sarah Nothnagel, Jorge Canizales-Diaz, Todd Sheerin, and Emily Krupczak, and all they have done to advance human knowledge on projects in which I had the honor of also participating. Of my TALARIS colleagues, Bobby Cohanim has also been a steadying influence on many research projects, including my thesis, and a guiding hand on the hardware projects.



My colleague, associate, and best friend Zahra Khan I also thank. Could I but name the celestial object most directly illuminating the period of time in which we began the first of our several dozen collaborations, I would advise her of this; alas, although my ability to recall properly the moment and calculate the zodiac has not diminished since, my facility to distinguish objects of faint color from one another is no more present now than ever, and as such this task would seem insurmountable.

Finally, I should like to recognize my parents and my siblings, of whom I have often thought as I worked.

For three persons who have done parts to bring me to this day, I note an especial gratitude: Marcus Neal Williamson, Sr., his namesake son, and Dr. Mark Sheplak. What feats of cognition I may now be able to perform are rooted in what I observed and was encouraged to attempt when I was younger, and these three have served to provide such encouragement.

I would also like to thank the Science, Mathematics, and Research for Transformation fellowship for funding my degree, and for providing me an opportunity to work in a field I enjoy immediately after graduating.

Last, but undergirding all others, is the Chief Engineer and Architect, access to Whose toybox has ever been among my chief motivations, and Whose continued support of all in my life has been unflagging and central. To that Name I might well dedicate every word I have ever written, as well as those I have not, and I am grateful to find such a source of fascinating things in the world.

# TABLE OF CONTENTS

CHAPTER 1. Introduction .....	13
1.1 Motivation: Hopping Vehicles as an Advancement in Exploration.....	16
1.2 Hopping Vehicles.....	19
1.3 Advantages and Limitations of Hopping Vehicles.....	21
1.3.1 Hopping Vehicle Characteristics .....	21
1.3.2 Hopping Vehicle Advantages .....	26
1.3.3 Hopping Vehicle Limitations .....	30
1.4 Summary .....	32
CHAPTER 2. Background .....	35
2.1 Literature Review .....	35
2.1.1 Hopping Vehicles as a Means of Surface Mobility.....	36
2.1.2 Lunar hopping vehicles .....	36
2.1.3 Mars hopping vehicles .....	39
2.1.4 Other hopping vehicles .....	42
2.1.5 Summary of past theory-centric hopping vehicle designs .....	42
2.1.6 Practical hopping vehicle work .....	44
2.2 Practical hopping vehicles on Earth .....	57
2.3 Summary of past hopping vehicle work.....	58
CHAPTER 3. Hopping Vehicle Model.....	61
3.1 Model Development .....	65
3.1.1 Past Modeling Work .....	65
3.1.2 Notable Hopping Vehicle Models .....	68
3.1.3 Rover Models.....	69
3.1.4 Features of a Hopping Vehicle Model.....	70
3.2 Generating a Hopping Vehicle Model via Formalized Mission Concepts .....	70
3.2.1 Motion and Action Grammars .....	72
3.2.2 Additional Grammar Elements .....	80
3.2.3 Using the Motion Grammar to Describe Hops .....	80
3.2.4 Using an Action Grammar to Describe Additional Behaviors.....	83
3.3 Mission Designers as Users of the Hopping Vehicle Model.....	85
3.3.1 Benefits of a Tradespace Model .....	87
3.3.2 Evaluating a Hopping Vehicle for a Mission.....	88
3.4 Model Details .....	89
3.4.1 Model Overview and Overarching Module .....	90
3.4.2 Payload Module .....	92
3.4.3 Planet Module.....	95
3.4.4 Golombek Model Utilization .....	97
3.4.5 Flight Plan Module .....	101
3.4.6 Operations Plan Module .....	105
3.4.7 Link Budget Module .....	106

3.4.8	Avionics Module.....	108
3.4.9	Propulsion Module.....	110
3.4.10	Physical Configuration Module.....	114
3.4.11	Cost Module Options .....	115
3.4.12	Visualization Module .....	118
3.4.13	Master Parameter Module .....	123
3.4.14	Model Summary.....	125
CHAPTER 4.	Model Validation and User Interface Testing .....	127
4.1	Validation Plan for Model .....	127
4.2	Validation Cases .....	129
4.2.1	Apollo Lunar Module (LM) .....	129
4.2.2	NGL Hopper.....	134
4.2.3	Phoenix .....	136
4.2.4	Viking.....	139
4.3	Cognitive Walkthrough Program and User Interface.....	144
4.3.1	Cognitive Walkthrough Description.....	144
4.3.2	Cognitive Walkthrough Results.....	147
4.3.3	Description of Updated User Interface.....	149
CHAPTER 5.	Initial Tradespace Exploration .....	161
5.1	Model Exercise Plan .....	161
5.1.1	Selection of Tradespace Exploration Missions .....	162
5.1.2	Tradespace Investigation Baseline Hopping Mission .....	162
5.2	Specific Mission Investigation Hops.....	175
5.2.1	Luna Hopping Missions – Shackleton Crater sample return.....	176
5.2.2	Luna Hopping Missions – Mare Tranquilitatis Lava Tube Descent .....	186
5.3	Analysis and Summary of Model Exercise Results .....	221
5.3.1	Tradespace Investigation .....	222
5.3.2	Specific Hopping Mission Investigation .....	224
5.4	Tradespace Investigation Conclusions .....	228
CHAPTER 6.	Conclusions .....	231
6.1	Intellectual Contributions .....	233
6.1.1	Motion and Action Grammar.....	233
6.1.2	Validated Technical Model of Hopping Vehicles .....	234
6.1.3	Early Tradespace Exploration for Hopping Vehicles .....	235
6.1.4	Description of Advantages of Hopping Vehicles.....	236
6.2	Future Work .....	237
6.2.1	Model Improvements .....	237
6.2.2	Tradespace Exploration .....	240
6.2.3	Mission Concept Development.....	240
6.3	Future of Hopping Vehicles .....	241
BIBLIOGRAPHY		243
Appendix A. MATLAB Code .....		259
Appendix B. Excel Databases for Tradespace Model.....		260
B.1.	Planetary Body Database .....	260

B.2. Scientific Instrument Database .....	262
B.3. Engine Database.....	263
Appendix C. User Guide .....	264
C.1. User Inputs .....	264
C.2. Logical Information Flow.....	269
Appendix D. Lower Limit of Gravity for Hopping.....	271
Appendix E. TALARIS History.....	275
E.1 Definition of the TALARIS Project.....	275
E.2 Early Conceptual Designs .....	277
E.2 Initial Prototype Hopper Demonstrator Design .....	278
E.3 Initial Hopper Demonstrator Construction and Testing .....	279
E.4 Hopper Demonstrator Maturation and Flight Testing .....	281
E.5 Further Development and Testing .....	282

# LIST OF FIGURES

Figure 1. OPM diagram of a planetary surface exploration vehicle. .... 22

Figure 2. OPM symbol key. .... 23

Figure 3. OPM models for a hopper (top), rover (middle), and flyer (bottom). .... 23

Figure 4. Motion-related attributes for hopper, rover, and flyer OPM models. .... 25

Figure 5. Guide to fundamental characteristics and key advantages of a hopping vehicle. .... 28

Figure 6. Illustration of hopping mobility used to improve landing accuracy, taken from (7). .... 29

Figure 7. Diagram of concept for hopping vehicle model. .... 62

Figure 8. X, Y, and Z axes for the motion grammar. .... 76

Figure 9. Diagram of model structure, showing software modules in orange, values passed in blue, user inputs in yellow, and master parameters (adjustable by advanced users) in green... 90

Figure 10. Display showing list of available maneuvers. .... 102

Figure 11. Example of a pop-up window showing subsystem mass breakdown. .... 119

Figure 12. Pop-up window showing operational timeline. .... 120

Figure 13. Subsystem mass fractions: model (left columns, blue), Apollo LM (right columns, red).  
..... 133

Figure 14. Subsystem masses: model (left columns, blue), NGL hopper (right columns, red). . 135

Figure 15. Subsystem masses: model (left columns, blue), Mars Phoenix lander (right columns, red). .... 137

Figure 16. Subsystem mass fractions: model (left columns, blue), Mars Phoenix lander (right columns, red). .... 138

Figure 17. Subsystem masses: model (left columns, blue), Viking lander (right columns, red). 142

Figure 18. Subsystem mass fractions: model (left columns, blue), Viking lander (right columns, red). .... 143

Figure 19. Payload selection user entry screen. .... 151

Figure 20. Target planetary body selection user entry screen. .... 152

Figure 21. Flight planning user entry screen. .... 153

Figure 22. Science segment marking user entry screen. .... 154

Figure 23. Example three-dimensional visualization of a hopping flight path. ....	155
Figure 24. Subsystem mass breakdown example. ....	156
Figure 25. Propellant use breakdown example. Maneuver tags are aligned with the solid bar at the top of propellant amount allotted to each maneuver. ....	157
Figure 26. Operations timeline example. ....	158
Figure 27. Textual information output to end screen. ....	159
Figure 28. Total hopping vehicle mass (for a baseline hopping mission) on various planetary bodies. ....	164
Figure 29. Total hopping vehicle mass as a function of horizontal traverse speed on three target planetary bodies. ....	165
Figure 30. Propellant mass fraction for a hopping vehicle on a baseline mission versus target planetary body gravity. ....	166
Figure 31. Subsystem mass breakdown for hopping vehicles on different target planetary bodies. ....	167
Figure 32. Total hopping vehicle mass for different traverse distances and traverse modes. ..	169
Figure 33. Hopping vehicle engine mass for different traverse distances and traverse modes.	171
Figure 34. Propellant mass for various traverse distances and traverse modes. ....	172
Figure 35. Mass breakdown for a series of hopping vehicles with increasingly larger payloads. ....	174
Figure 36. Large-scale view of modeled traverse into a well of eternal night on the floor of Shackleton Crater. ....	181
Figure 37. Operational timeline for a traverse into a well of eternal night on the floor of Shackleton Crater. ....	182
Figure 38. Subsystem mass breakdown for a traverse into a well of eternal night on the floor of Shackleton Crater. ....	183
Figure 39. Mass breakdown comparison for hopping vehicles designed to visit wells of eternal night in Shackleton Crater. ....	184
Figure 40. Traverse path for a descent into a lava tube in Mare Tranquilitatis. ....	189
Figure 41. Subsystem mass breakdown for a descent into a lava tube in Mare Tranquilitatis. ..	190

Figure 42. Operations timeline for a descent into a lava tube in Mare Tranquillitatis. ....	191
Figure 43. Subsystem mass comparison for hopping vehicles designed to explore lava tubes in Mare Tranquillitatis. ....	192
Figure 44. Hopping vehicle traverse path overlaid on a section of Copernicus Crater's floor...	194
Figure 45. Three-dimensional view of hopping vehicle traverse path on a section of Copernicus Crater's floor. ....	195
Figure 46. Operational timeline for a traverse path on a section of Copernicus Crater's floor.	196
Figure 47. Subsystem mass breakdown for a hopping vehicle to traverse a section of Copernicus Crater's floor. ....	197
Figure 48. Propellant use breakdown for a traverse path on a section of Copernicus Crater's floor.....	198
Figure 49. Subsystem mass breakdown for a variant hopping vehicle for exploring Copernicus Crater. ....	199
Figure 50. Subsystem mass breakdown for a hopping vehicle exploring a Martian crater. ....	200
Figure 51. Propellant use breakdown for a hopping vehicle exploring a Martian crater. ....	202
Figure 52. Operational timeline for a stratigraphy survey in Valles Marineris. ....	203
Figure 53. Three-dimensional view of the flight path for a stratigraphy survey in Valles Marineris. ....	204
Figure 54. Subsystem mass breakdown for a hopping vehicle to perform stratigraphy in Valles Marineris. ....	205
Figure 55. Propellant use breakdown for a hopping vehicle performing a stratigraphy survey in Valles Marineris. ....	206
Figure 56. Traverse path for a hopping vehicle retracing MER-A's path. Original image is from (130). ....	208
Figure 57. Operational timeline for a traverse retracing the MER-A mission. ....	209
Figure 58. Three-dimensional view of the flight path for a traverse retracing the MER-A mission. ....	209
Figure 59. Subsystem mass breakdown for a hopping vehicle on a traverse retracing the MER-A mission. ....	211

Figure 60. Propellant use breakdown for a hopping vehicle on a traverse retracing the MER-A mission. ....	212
Figure 61. Three-dimensional view of the flight path for a Titan hopping mission. ....	214
Figure 62. Closeup of three-dimensional view of the flight path for a Titan hopping mission..	214
Figure 63. Operational timeline for a Titan hopping mission. ....	215
Figure 64. Subsystem mass breakdown of a hopping vehicle for a Titan hopping mission. ....	216
Figure 65. Propellant use breakdown for a Titan hopping mission. ....	219
Figure 66. Subsystem mass breakdown for a variant Titan hopping mission. ....	220
Figure 67. Propellant use breakdown for a variant Titan hopping mission. ....	221
Figure 68. Total landed vehicle masses for example missions and flown missions to the same bodies. ....	226
Figure 69. Total costs, in 2011 dollars, for example missions and flown missions to the same bodies. ....	227
Figure 70. Concept for a continuously-editable graphical user interface. ....	239



## **CHAPTER 1. Introduction**

Following in the footsteps of NASA's Project Constellation plans to return to the Moon and send humans to Mars, the flexible path proposed by the Augustine Commission (1) provides a vision for exploring the solar system, and includes provisions for human exploration of the Earth's Moon, Mars, and potentially Near Earth Objects (NEOs). In the meantime, exploration of other planetary bodies by robotic vehicles continues. NASA's Dawn spacecraft is orbiting the asteroid Vesta, the New Horizons spacecraft is approximately halfway to its flyby of Pluto in July 2015, and the Mars Science Lander (MSL) is en route to a landing on Mars in August 2012.

Mars has now been under study by robotic surface exploration vehicles continuously for nearly a decade. The two Mars Exploration Rovers (MERs) and Mars Phoenix have been exploring parts of the surface since 2004, and MSL will likely continue this effort for a long time to come. This sustained exploration campaign has permitted detailed and groundbreaking science to be conducted at different locations on the surface of Mars, and has produced astounding scientific results, including evidence of the presence of water.

The surface exploration of planetary bodies other than Earth has enabled revolutionary advances in our understanding of planetary science. The results produced by human explorers during the Apollo program created a great argument in favor of the high mobility and extremely capable in-situ decision-making abilities of humans (2), but the high cost of the program – about \$115 billion in 2012 dollars (3) - created a counter-argument in favor of robotic exploration.

Improvements in communications technology, avionics, and software have since made teleoperation of robotic vehicles a more viable solution. Using mobile robots with intelligent

human oversight has provided a middle ground between the two limiting cases of inflexible autonomous robots and expensive humans. The MER program embodies the teleoperation approach, and is an excellent example of its merits.

However, in order for robotic planetary surface exploration to continue advancing, the technologies associated with it must advance as well. In particular, technologies associated with improved mobility on the surface of a planetary body are key to further advancement. One such mobility technology, hopping vehicles, will be investigated in detail and modeled in depth in this thesis.

A hopping vehicle is a vehicle which uses its engines to traverse over the surface of a planetary body without the need for ground contact or interaction with a surrounding fluid to provide motive force. A hopping vehicle rests on a planetary surface in between hops, but can traverse from one resting place to the next without regard for the terrain over which it passes. A hopping vehicle can be very similar to a planetary lander, meaning that a lander can be repurposed as a hopping vehicle if it has additional fuel after touchdown, and appropriate guidance, navigation, and control (GNC) capabilities.

Recent developments in technology and the creation of a concept of operations for hopping vehicles, as described in Cohan et al. (4), have shown them to be a viable form of mobility on the surface of a planetary body. However, no vehicles designed as hoppers have yet flown missions in space, or even been constructed to do so, and as such there is limited experience and heritage for hopping vehicles. Thus it is difficult for technical decision-makers to develop

missions incorporating this novel technology. In this thesis, a tradespace model of hopping vehicles, which can provide technical decision makers with additional insight into how hoppers will perform and what other considerations will be when fielding them, will be developed. In this way, a new form of planetary surface mobility will be brought into the mission design space for future planetary surface exploration. Because planetary surface mobility is not meaningful in the context of a gas giant planet, the work done in this thesis is limited to terrestrial planets with a solid surface.

In support of this objective, in this thesis we first define what hopping vehicles are, and describe in the remainder of Chapter 1 their potential advantages and relative position in the array of vehicles which provide surface mobility on planetary bodies. Then a literature survey captures the current state of work on hopping vehicles in Chapter 2. Chapter 3 details a technical model of hopping vehicles down to the subsystem level. Chapter 4 discusses the comparison of model results against historical and planned planetary landers for validation purposes, as well as the development and refinement of the user interface. Chapter 5 describes a series of exercises performed by the model, for the purpose of investigating the tradespace in which hopping vehicles reside and examining some interesting example missions. Additionally, insights gathered into the circumstances under which hopping vehicles are most useful are described. Finally, Chapter 6 summarizes the findings of this thesis, as well as directions for future research.

## **1.1 Motivation: Hopping Vehicles as an Advancement in Exploration**

Uncrewed in-situ exploration of planetary bodies has advanced in a natural progression since its inception, with the Luna 1 mission in January 1959 (5). Prior to this, early historical exploration efforts often consisted of remote observations via the naked eye or telescope. For instance, early astronomers often observed the Earth's Moon, as well as the major inner planets of the solar system. Telescopes enabled further discoveries without approaching the bodies more closely, as when Galileo discovered the four largest moons orbiting Jupiter in 1610.

The advent of space travel in the late 1950s permitted observation from closer to planetary bodies. Initial efforts focused on closer approach with simple instruments, often just cameras. The Soviet Luna program (from 1959 to 1976) and the American Mariner program (from 1962 to 1973) first brought spacecraft to the close vicinity of the Earth's Moon and Venus, and data collected by these vehicles sparked additional interest in exploration.

The first generation of spaceborne exploration vehicles, which included orbiters, flybys, and impactors, progressed to landers, such as the American Surveyor probes (from 1966 to 1968) to the Earth's Moon, and the Soviet Venera probes (from 1961 to 1983) to Venus. The next logical step in exploring a planetary surface after contacting it with a craft would be to contact it in many places by moving over the surface, and the implementation of this phase was first reached in the late 1960s and early 1970s. The American Apollo program was able to utilize humans, together with human-operated vehicles on the later Apollo landings, to provide a degree of flexibility and capability in surface mobility that has not been equaled since. However, during the same time frame, the Soviet Union landed and operated the Lunokhod rovers, which were

teleoperated in real time on the surface of the Earth's Moon without the need for direct human presence (6).

Exploration of planetary surfaces continued, primarily with orbiting observers or landers, in the following decades. Much as the inner planets had been explored via a steady advance of closer contact, culminating in sustained campaigns of exploration, attention turned to the outer planets. The Voyager (in 1977) and late Pioneer probes (from 1958 to 1973) made trips through the outer solar system, making the first flybys of many of the outer planets. As orbiters and some landers (for example, Galileo in 1989 and Cassini-Huygens in 1997) visited the outer gas giant planets and their moons in the 1990s and early 2000s, a number of orbiters were sent to Mars, along with several landers (including the unsuccessful Mars Polar Lander in 1999 and the resurrected Mars Phoenix in 2007). However, the Mars Pathfinder program in 1997 kicked off a new direction, with its roving vehicle that extended the reach of a lander well beyond the narrow circle around the landing site itself. The follow-up Mars Exploration Rovers in 2004 and the Mars Science Laboratory in 2011 capitalized on this success, traveling or planning to travel significant distances on the surface of Mars and extending humanity's knowledge of the surface and its characteristics.

Mobility on the surface of a planetary body is beneficial at a level that a simple lander alone cannot match, but roving mobility has some drawbacks. It is limited by terrain and hindered by low speed. Future evolutions in planetary surface exploration would benefit from transcending these limitations. Just as the ability to move over a planetary surface represented a step change from simply landing on a planetary surface, which was itself a step change from observing the

surface, hopping rapidly and freely over a planetary body's surface will be a step improvement over roving. Hopping vehicles can potentially be used to perform new kinds of tasks in planetary surface exploration, including regional sample collection, science data collection in difficult terrain, and stratigraphy (4), (7).

Hopping vehicles exhibit rapid mobility over long ranges and are free of terrain limitations, and as such are logically a next step in the development of planetary surface exploration. Flying vehicles also exhibit this freedom, but they are limited by the need for an atmosphere to support themselves, and few of the interesting solid planetary bodies in the solar system have atmospheres able to support flight. Flying vehicles may also be limited by terrain needs related to takeoff or landing requirements.

Thus, hopping vehicles represent an excellent option for the next step in the evolution of planetary surface exploration. However, hoppers are as yet a nascent technology. No hopping vehicle has yet flown in space. In order to make hoppers a viable technological option for future planetary exploration missions, it will be necessary for mission designers to understand them, the costs and risks of using them, and the potential advantages of using them. In this thesis, we address these needs by developing a tradespace model of hopping vehicles.

This tradespace model will be able to take a description of a science payload and flight profile on a target planetary body and use initial physics-based models of hopping dynamics and existing engineering models for vehicle and component scaling to produce a description of a hopping vehicle which can perform the desired flight profile with the desired payload. This description

will include details on the total mass, subsystem mass, power levels, and data collection and downlink rates, and will also account for operational aspects of hopping vehicles. This technical information can be used to make changes to the desired payload or flight profile or to evaluate the feasibility of a hopping vehicle for the described mission.

In addition to this tradespace model, we will also contribute in this thesis a motion and action grammar, which is a system to describe flight profile for hopping vehicles and define their motions, as well as perform an initial exploration of the tradespace produced by the model developed in this thesis. This initial tradespace exploration, together with the characteristics and advantages of hopping vehicles listed in Figure 5, can provide guidance to the conditions under which hopping vehicles can best be utilized in planetary surface exploration.

## **1.2 Hopping Vehicles**

Vehicles used to explore planetary bodies can be split into several broad categories, as detailed by Cunio et al. (8). The first distinction that can be made is between spaceborne and surface vehicles. While spaceborne vehicles may include either orbiters or spacecraft which perform flybys, surface vehicles may include sedentary landers or mobile vehicles, such as hopping vehicles or rovers. This thesis is primarily concerned with mobile surface vehicles, as they provide good opportunities for in situ science on broad or varied regions of the planetary surface. Hopping vehicles are a type of mobile surface vehicle.

Mobile surface vehicles may be split into three major subtypes: those that traverse the surface using ground contact, those that traverse using fluid contact, and those that traverse using

propulsive power alone. Ground contact vehicles require a solid surface against which to react. Ground contacting vehicles include walkers, ball-shaped rollers, spring-bouncing vehicles (which could be called 'hoppers,' but are not considered to be hopping vehicles by the definition used in this thesis) and traditional wheeled or tracked rovers. A significant fraction of proposed designs for planetary surface exploration vehicles fall into this class, and all purpose-built surface exploration vehicles to date do as well.

Fluid contact vehicles may react against surrounding fluid via actuators, and may also rely on a surrounding fluid to maintain buoyancy or lift. Vehicles such as a blimp or balloon, a raft or swimmer, and a glider or powered aircraft fall into this category. While a number of proposals for fluid contact planetary surface exploration vehicles exist in the literature, none have yet been fielded on planetary bodies other than Earth.

A vehicle which requires neither ground contact nor fluid contact for propulsion must rely on its own internal propellant, which means that its motion is governed primarily by the law of gravity and its own engine thrust rather than the laws of aerodynamics or hydrodynamics. Like a flying fluid-contact vehicle, this type of vehicle will not always be belly-to-the-ground, meaning that it potentially faces greater risks during operations, but compensates by being able to move without limits imposed by surrounding terrain or atmosphere. A hopping vehicle falls into this class, as it may move about a planetary surface by firing its propulsive hopping engines, and is thus independent of any need for ground contact or fluid contact in order to move. A hopping vehicle does, however, share with a ground contact vehicle (and any fluid-contact vehicle designed not to be in permanent flight) the need to sit at rest on a solid surface in between hops. For most



solid-surfaced planetary bodies in the solar system, this is not a major distinguishing factor, as solid surface is typically present over large portions of or the entire surface of most small rocky bodies. Only Earth is known to possess extensive oceans. This factor would be a consideration in exploring large gas giant planets, but this thesis is only concerned with solid-surfaced planetary bodies.

### **1.3 Advantages and Limitations of Hopping Vehicles**

Understanding the differences between the three major types of mobile planetary surface exploration vehicles is a key step in understanding what the limitations and potential advantages of hopping vehicles are. In this section, we describe these differences and detail how they can produce advantages for hopping vehicles.

#### **1.3.1 Hopping Vehicle Characteristics**

Modeling a moving planetary surface exploration vehicle with the Object-Process Methodology (OPM) will help to clarify the differences. OPM, as described by Dori (9), is a modeling language which abstracts details into either a type of object (tangible thing) or process. This simplification of detail is supplemented by a few key modeling relationships, including decomposition and agency, and is thus able to describe the model desired in the form of a diagram, easily translatable into natural language.

A general model for a moving planetary surface exploration vehicle can be described as a model of a vehicle (object) which performs the processes of moving, collecting data about the planetary body, and sending this data back to Earth. In general, such models should also include the processes of landing and deploying on the planetary body, as shown in Figure 1.

A symbol key describing the icons used in Figure 1's OPM diagram appears in Figure 2.

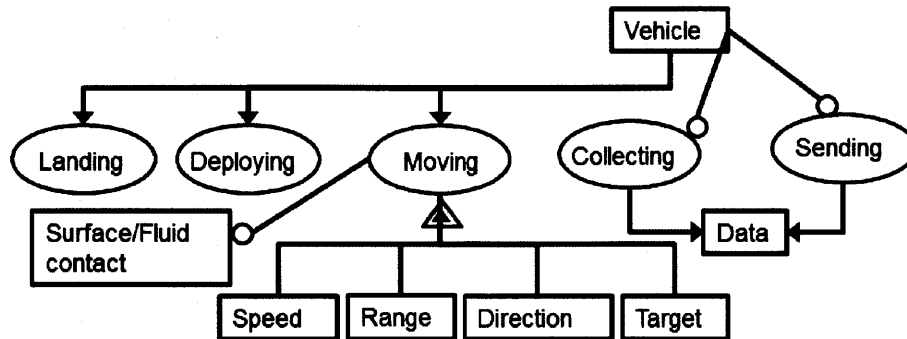


Figure 1. OPM diagram of a planetary surface exploration vehicle.

The nomenclature of OPM indicates that this vehicle is an instrument by which data is collected and sent, and that moving is achieved via the instrument of a contacting ground or fluid. The process of moving has attributes of speed, range, direction, and target. This diagram should not be considered an authoritatively final or exhaustive description of a planetary surface exploration vehicle. Like natural language, OPM can capture the same aspects of meaning in several ways, and can be used to highlight some properties, while suppressing others. For alternative OPM descriptions of a planetary surface exploration vehicle, the reader is encouraged to see Lamamy's doctoral thesis (10).

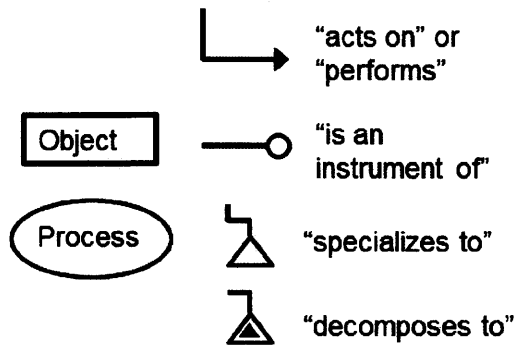


Figure 2. OPM symbol key.

Specializing the OPM description from a general moving vehicle to a hopper, rover, and flyer, specifically (using a hopper, rover, and flyer as exemplifiers of the three major types of moving planetary surface exploration vehicles), we obtain the diagrams in Figure 3.

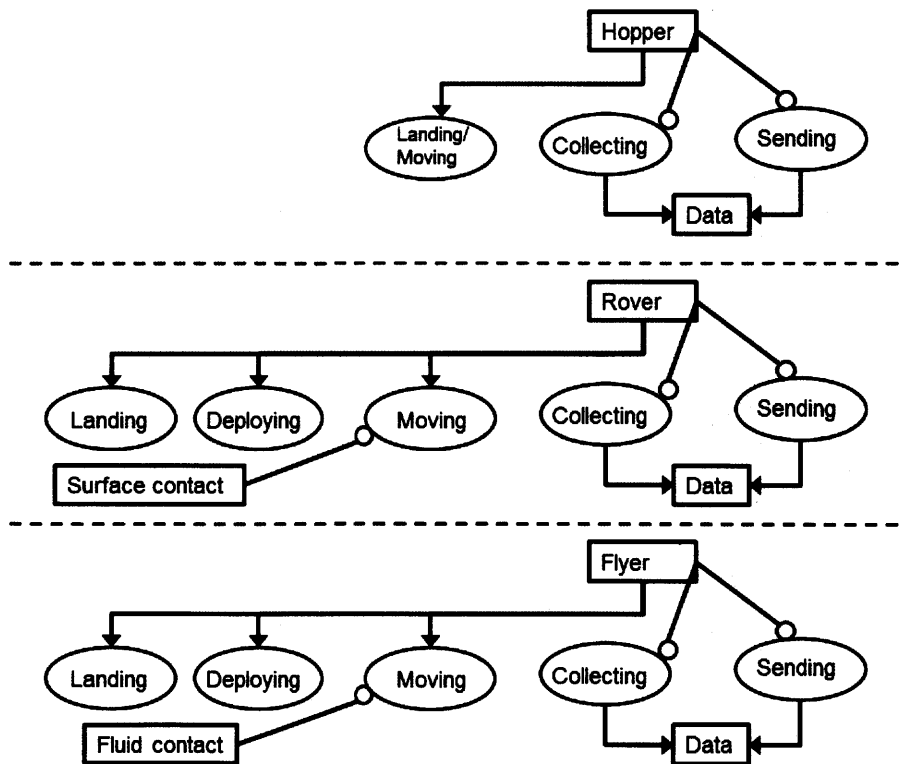


Figure 3. OPM models for a hopper (top), rover (middle), and flyer (bottom).

Figure 3 shows simplified OPM diagrams, focusing on the differences in processes between hoppers, rovers, and flyers. The processes of landing and moving are almost exactly the same in a hopping vehicle, as the process of hopping is typically conducted via propulsive motion, as often terminal descent during landing is also conducted. Additionally, the moving process for hopping vehicles requires no ground or fluid contact during motion, and there is no deployment process, as the vehicle which performs terminal descent can be the very same vehicle which later performs hopping. There is usually a deployment process that must be undertaken to release and activate a ground contact or fluid contact vehicle, as these types of vehicles typically are not able to undergo landing in their mobile configuration, and must be stowed in some way. Notably, however, the processes of collecting and sending science data remain the same for all three types of vehicles.

The next figure (Figure 4) addresses specifically the attributes of the moving process for the three types of vehicles.

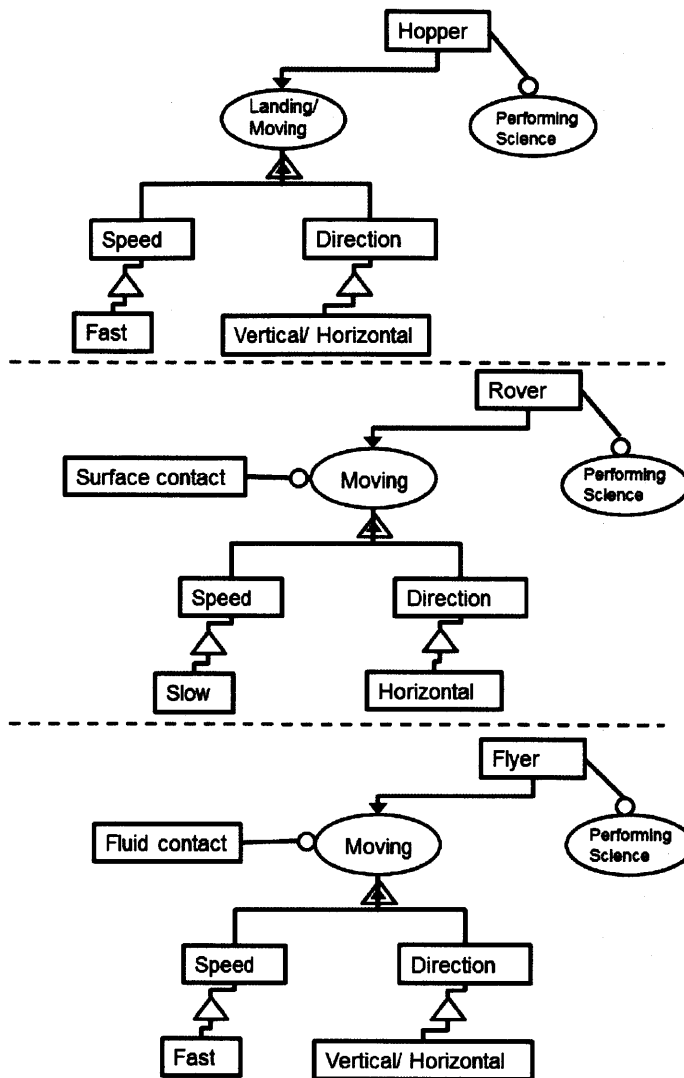


Figure 4. Motion-related attributes for hopper, rover, and flyer OPM models.

Note also that the range and target attributes have been suppressed, as the targeting ability of any of these vehicles is not necessarily a discriminator between it and another type (targeting ability depends on instrumentation, which may be carried by any type of vehicle), and the lifecycle range of one of these vehicles is not clearly a discriminator, either. The MER rovers had a nominally short range, but have so far exceeded it during their lifetimes that their total lifecycle ranges may be comparable to or greater than the lifecycle range of a flyer or hopper, although the

flyer and hopper will be able to traverse this range in a much shorter lifetime. Thus the speed of the moving process remains present as a discriminating attribute. The processes of collecting and sending data, however, have been simplified into a process of performing science, which is similar among all three vehicle types.

Note that flyers and hoppers are fast (top speeds of tens of meters per second), but that rovers are slow (top speeds of centimeters per second). Furthermore, flyers and hoppers may move either vertically or horizontally, while rovers are typically limited to horizontal motion along the planetary surface. Flyers and rovers also require contact with some kind of adjacent medium (ground or fluid) to move, while hopping vehicles do not require it during motion, but only in between hops.

### **1.3.2 Hopping Vehicle Advantages**

This description of the differences among the three major types of moving planetary surface vehicles has led to the identification of several characteristics of hopping vehicles. Although some of these characteristics are not completely unique to hopping vehicles, but are shared with either roving or flying vehicles as well, they still provide insight into what the fundamental advantages of hopping vehicles might be.

The characteristics of a hopping vehicle include the ability to move quickly, the ability to cover long ranges, the ability to move in both horizontal or vertical directions (either separately or simultaneously), and the ability to move without the need for contact with either the ground or with a surrounding fluid. Additional characteristics include the ability to move repeatedly (that is, a hopping vehicle is not a one-shot mover), and an ability to navigate to a precise position, if

supplied with appropriate instruments and guidance capability (see Cohanim's doctoral thesis (11) for more information on hopper navigation and guidance). Finally, the close connection between landing and moving in a hopping vehicle indicates a probable high degree of physical commonality between a landing vehicle and a hopping vehicle.

The fundamental characteristics of a hopping vehicle can be used to create a list of the key advantages of a hopping vehicle. The characteristics combine in ways that flow into advantages, as indicated in Figure 5, below. The figure should be interpreted as an initial assessment of key advantages of hopping vehicles; additional advantages may exist. Furthermore, the advantages listed are not all necessarily unique to hopping vehicles, although some are, and the mix of abilities they represent is unique to hopping vehicles.

The figure should be regarded as an initial guide for thinking about ways to use hopping vehicles.

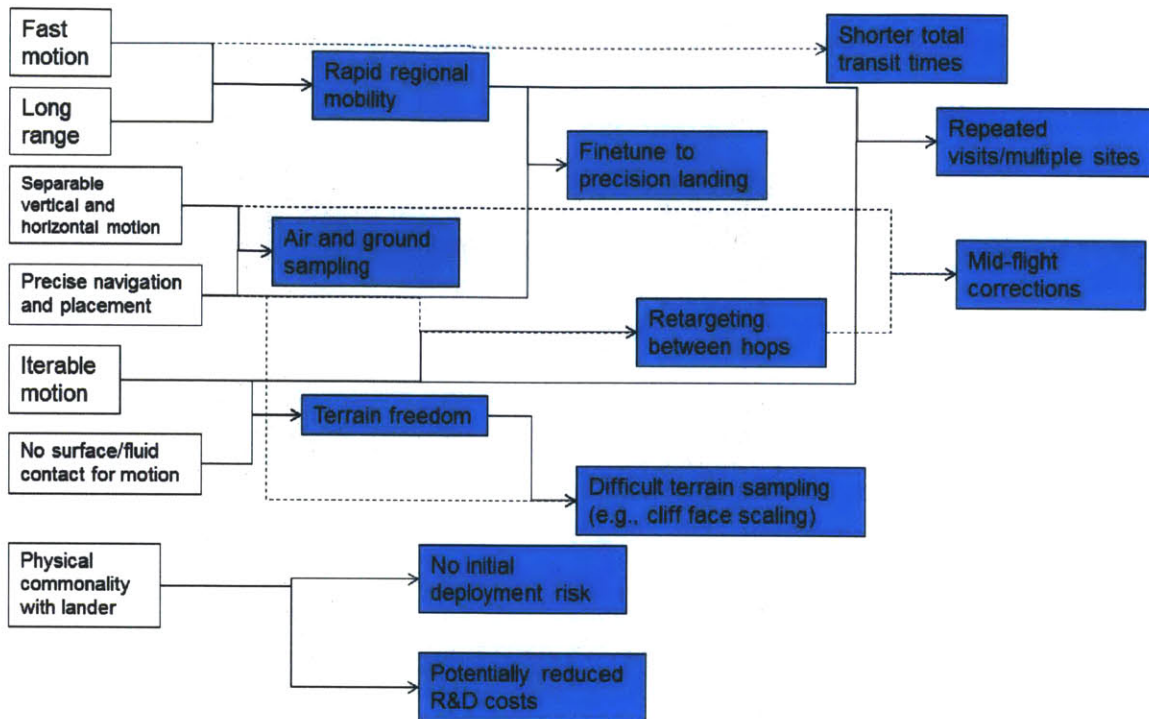


**Figure 5. Guide to fundamental characteristics and key advantages of a hopping vehicle.**

As shown in Figure 5, a hopping vehicle's high speed results in short transit times between points. This is distinguished from a rover's slow transit, but similar to a flyer's speed. Fast motion combined with a long range results in rapid regional mobility, where any spot in a planetary region of several kilometers to tens of kilometers in radius is potentially accessible in a timeframe of seconds to minutes, rather than weeks to years. Rapid regional mobility, combined with a hopping vehicle's ability to perform precise navigational placement, also create an ability to perform precision landing via hopping mobility, wherein a landed hopper traverses to a desired position on a planetary surface via hopping, rather than via landing precisely in the desired spot. This shifts the burden of precision placement away from the initial entry, descent, and landing (EDL) aspect, and can result in essentially a larger initial landing ellipse, with positive effects on the cost and risk tolerance in the EDL guidance, navigation, and control



system. Figure 6 illustrates this concept with the golfing analogy of driving and putting, rather than attempting a hole-in-one with every shot.

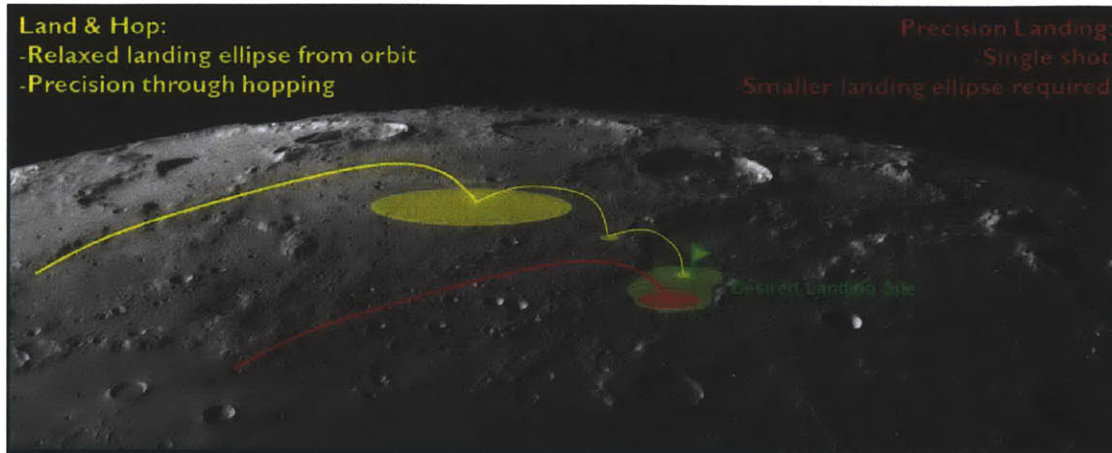


Figure 6. Illustration of hopping mobility used to improve landing accuracy, taken from (7).

The hopping vehicle also possesses an ability to perform sampling of air and ground targets, given that it is free to move vertically as well as horizontally. A hopping vehicle which can perform precise navigation is also capable of performing retargeting and correcting between hops, while resting on a solid surface. This capability, together with the hopping vehicle's ability to move horizontally and vertically independently, results in an ability to perform retargeting during hops, as well.

All of the above advantages are potentially also applicable to flyers, but not always to roving vehicles (precise navigation being a notable exception, as it is available to rovers). Hoppers have some additional advantages, however. A flying vehicle is able to move only when surrounded by fluid, and the actions of taking off and landing are often difficult to perform, due to the need for the flyer to transition from a fluid-supported to ground-supported state. This may result in

flying vehicles which do not touch the ground except immediately after initial deployment. However, a hopping vehicle can easily touch down many times, making it far easier for a hopping vehicle to make more landings, with less risk, than a flying vehicle. This leads to the advantage of repeated visits for hopping vehicles.

A hopping vehicle's comparative independence from a need for ground or fluid contact also affords it terrain freedom. A hopper's ability to hover, as well as to fly up, down, and sideways in careful increments, essentially grants it an ability to move anywhere over any kind of terrain, affording it access to sites that would be nearly impossible for a rover to reach, and difficult for a flyer to reach.

Finally, the commonality between a hopping vehicle and a lander, which is not shared by a flyer or a rover, results in two additional advantages: a lack of initial deployment risk (a hopping vehicle can essentially be a lander with extra fuel), and potentially reduced costs to develop and build a hopping vehicle. A large portion of the costs of any space mission are devoted to designing and testing the vehicles involved; if there are multiple vehicles to develop (such as a lander and a rover), the costs may be greater than if there is just a single vehicle (such as a lander/hopper).

### **1.3.3 Hopping Vehicle Limitations**

Despite these significant advantages, hopping vehicles also have some limitations imposed by their characteristics. For instance, hopping vehicles must rely on their own engines, rather than ground contact or action on a surrounding fluid, to hold them aloft when traversing, and therefore there is a constant propellant requirement for these engines, even when the hopping

vehicle is only hovering in place. This means that hopping vehicles are propellant-limited: their maximum lifetime traverse distance is proportional to the amount of propellant they carry. The only exception would be for a hopping vehicle that is able to refuel periodically or to generate its own fuel from available resources. In contrast, rovers are sufficiently low-powered that they can propel themselves using only solar power, and some flyers that rely on buoyancy effects (such as balloons or floaters) do not require significant amounts of propellant, and can simply drift on fluid currents.

Additionally, hopping vehicles operate under a different risk profile. While they have the advantage of no initial deployment risk, they have the limitation of only performing traverses while relying on their own engines and GNC software to maintain a position aloft over a planetary surface. Failures in propulsion or guidance systems can result in an impact with the surface, which might have severe consequences for the mission. Rovers, which are constantly in contact with the surface while operating, can survive power or processor interruptions without undergoing similar consequences.

Finally, hopping vehicles have an effective minimum efficient hopping distance, imposed by the fact that a hopping vehicle, when landed, is limited to accessing its own footprint and whatever additional area can be reached by extensible mechanisms onboard the hopping vehicle. A hopping vehicle can also take off, traverse, and make a new footprint area accessible to itself, but there is a region, beginning just outside the hopping vehicle's immediate reach, that is nearly as expensive to reach as a more distant region, due to the fact that a hopping vehicle must complete a complete launch and descent cycle to move any distance, and this costs propellant. While a

rover must expend energy approximately linearly according to the range to a target not in immediate reach, a hopping vehicle must expend minimal energy to reach any target within its immediately accessible area, but then must spend a large amount of energy to reach any other target. There is a steep discontinuity in the energy expenditure required to reach a target not immediately accessible. Thus, while a hopping vehicle is a good choice for missions requiring unconventional access (such as cliff faces) or widely-spread sampling, a rover is a more efficient choice for exploring from one rock to the next in a very small area.

Despite these limitations, hopping vehicles still have significant advantages, and these advantages provide additional useful capability for hopping vehicles.

#### **1.4 Summary**

Hopping vehicles, which traverse using pure propulsive power and do not require action against a surface or against a surrounding fluid to move, differ from other planetary surface exploration vehicles (such as rovers or flyers) in that they are free from terrain limitations, can provide rapid regional access, can perform vertical motion as well as horizontal motion, and have physical commonality with landing platforms that may enable reduced research and development costs and reduced initial deployment risk. Although hopping vehicles are also limited by their ability to carry propellant, an increased level of risk during their traverse phases, and an inability to explore rock-to-rock without some minimum expenditure of propellant, they still have the potential to perform useful tasks in planetary surface exploration, such as regional sample collection, difficult terrain access, and vertical stratigraphy.

However, no spaceborne hopping vehicles have yet flown, and hopping technology is still not well understood by decision makers who design planetary surface exploration missions. Past research work on hopping vehicles (described in depth in Chapter 2) does not include any high-granularity models of hopping vehicles, and typically the simpler models that are used are not rooted in an analysis of all the key characteristics and potential advantages of hopping vehicles. These older models also are not able to consider operational aspects of a hopping mission (such as mission timelines), and many models have not been validated against physical hardware.

In order to bring hopping vehicles into the decision space for planetary surface exploration mission designers, in this thesis we develop a tradespace model for hopping vehicles, which will be able to take a description of a science payload and flight profile on a target planetary body and generate a technical description of a hopping vehicle which can perform the desired mission. The information in the description, which will include subsystem-level details of the hopping vehicle and second-by-second mission timelines, can be used to evaluate the feasibility of a hopping vehicle for the described mission.

The hopping vehicle model we develop in this thesis provides for easy comparison of hopping vehicle designs, by creating a tradespace of hopping vehicle designs. Users of the model can review information about individual hopping vehicle designs, or can review information about multiple hopping vehicle designs at once, in order to make comparisons more easily.

Furthermore, the tradespace model is validated against three spaceborne planetary landers (which are similar to hopping vehicles), and one mature design for a soon-to-be-built planetary hopping vehicle.

The tradespace model will be supported by a description of characteristics and advantages of hopping vehicles. Additionally, the results of initial tradespace exploration performed using the model, will be provided. This information together will serve to illustrate how hopping vehicles can best be used to explore the surfaces of terrestrial planetary bodies.

## **CHAPTER 2. Background**

This chapter describes some of the background for the thesis research effort, including past work on developing hopping vehicles from both theoretical and practical standpoints.

### **2.1 Literature Review**

This thesis builds on past designs and past missions for hopping vehicles to develop a concept of what hopping vehicles can do, and also examines past models of hopping vehicles. The development of hopping as a viable surface mobility concept is traced from the Apollo era to the present. Existing hopping vehicle models are also evaluated and compared to the model developed in this thesis.

Hopping research in the past has focused either on theoretical designs and the theoretical uses of hopping vehicles, or on practical designs and modeling and the practical use of hopping vehicles. The theoretical design of hopping vehicles focuses on what missions hopping vehicles may undertake, and is generally centered on one of two planets: the Moon or Mars. Streams of research stretch from the Apollo program era to the early 21st century. Practical research focuses more on how hopping vehicles should undertake these missions, or on the hopper vehicle. Streams of practical research tend to be more recent, beginning around the time of the renewal of interest in space exploration kicked off in the mid-2000s by the Constellation program and the Google Lunar X-Prize (12).

### **2.1.1 Hopping Vehicles as a Means of Surface Mobility**

The paradigm of exploring a remote planetary body via surface mobility dates to the Apollo era. The first pre-planned physical motion on the surface of a planetary body was carried out by the astronauts themselves as they walked about on the surface. However, the precursor mission Surveyor VI first moved in an untargeted way in a short hop of a few meters, by reigniting its engine after landing (13).

The exploration of a planetary body followed a progression in the late 1950s and early 1960s from flybys to hard landings (impacts on the surface at high speed) to soft landings (touchdowns on the surface at low speed). Once soft landings on a planetary surface had been attained, exploring the planetary body via surface mobility was the next logical step. Just as the progression from flyby to soft landing shows a series of steadily closer encounters with a planetary surface, so it should be expected that the advance of technology in mobility over a planetary surface will show a steady progression of close encounters with more and more regions spread over a wider fraction of a planetary body's surface.

### **2.1.2 Lunar hopping vehicles**

The Apollo astronauts were the first means of surface mobility, but it was quickly realized that astronauts could do more if they had some form of mechanically-assisted mobility, and several concepts were developed during the Apollo program. The concept of a vehicle which would hop in some fashion over the surface of a planetary body originated in the Apollo program, although the proposed hopping vehicles were replaced on actual flight missions by the more conventional



lunar rover. These proposed hopping vehicles were legged hoppers, using pistons instead of propellant (14), (15), (16), (17).

A manned hopping vehicle was later proposed as a possible means of improving astronaut mobility on the surface of the Earth's Moon, as part of the later work on Project Apollo. The standing platform design proposed by Sandford (18) and detailed by Carey and Stricklin (19) was intended as a means to increase astronaut mobility on the lunar surface. Although the inherent mobility afforded by a hopping platform was a driver for the design effort, the specific characteristics and advantages of a hopping vehicle were not described, and the project was never flown.

Although these projects never achieved flight status, and the legged hopper was a variation of a walking vehicle more than a true propulsive hopping vehicle, other projects in later years built upon the concept of a hopping vehicle used to explore planetary surfaces.

Lunar mission discussions involving hopping vehicles include Mankins, Vallerani, and Della Torre (20), which discusses from a high-level view the importance of various system-level properties for robotic missions on the Moon, Mars, and other bodies in the solar system. It describes briefly the importance of some system-level properties, such as commonality and reconfigurability for a space exploration system, and then lays out some examples of lunar exploration mission architectures. In the process, the high importance of advanced surface mobility is emphasized. Long-range point-to-point access and access over extreme terrain are both indicated to be key features of a successful lunar robotic exploration strategy, and hoppers

are specifically mentioned as a feasible architecture option, although analysis of the effects of hoppers on a mission architecture is not presented, and no hopper model is shown either.

Uwe (21) considers large ballistically-propelled hopping vehicles (87 metric tons at takeoff) as part of a lunar transit system encompassing large portions of the lunar surface. The hopping vehicles deliver up to 30 tonnes of cargo using liquid oxygen and liquid hydrogen (LOX/LH<sub>2</sub>) propellants (generated not specifically in-situ but by large-scale production facilities at the lunar poles), and are found to be useful in situations where transport demand in a large network around the Moon is somewhat limited, as they provide in these circumstances a more favorable ratio of mass moved per cost than other options (including electric rovers, a maglev rail system, and mass drivers).

Donahue and Fowler performed a study (22) in the context of the early-1990s First Lunar Outpost (FLO) initiative (23). It analyzes, as part of the overall study, a second-site capability for a lunar lander over a distance of a few thousand kilometers. While the analysis is not extensive, it does distinguish initially between ballistic (or two-burn) hops and hover hops (continuous burn). The two-burn transfer is described as more efficient, especially at distances over about 300 km. (Further analysis and comparison of ballistic and hover hops appears in Section 3.2 of this thesis.) The analysis notes that landers will have advanced GNC capabilities, probably suitable for hopping, already installed, and will only need mature propulsion systems (with additional fuel and restartable engines) to conduct hops, and further proposes that crew rescue or rover recovery might make good justifications for developing second-site hopping capability.

Vallerani et al. (24) also describes a hopping vehicle in the context of a larger lunar transportation architecture. In this paper, a 2000-kg dry hopping vehicle delivers 200 kg of payload via ballistic hops. The initial design is expanded to a “cluster” design, in which a set of hopping vehicles are connected side-to-side fly the hops. The main “central carrier” is envisioned as a main base, rover hangar, science platform, or fuel repository/generation plant. Sidestacks, other hopping vehicles which are connected to the side of the main vehicle, can be boosters to enable the stack to land, and can separate and perform autonomous hopping missions or deliver samples and crew back to lunar orbit. This approach permits a degree of commonality in the design process as well. The authors also distinguish between “reaction mobility,” which is generated by ballistic expulsion of propellant, and “surface mobility,” which is generated by intermittent or continuous ground contact. Several different monotype and hybrid mobility architectures are compared, and the authors conclude by recommending what is essentially a hybrid hopper/rover with wheels or treads for maximum mobility on the Moon.

### **2.1.3 Mars hopping vehicles**

The concept of hopping vehicles on Mars often appears either in comparison to or as part of a portfolio of other exploration vehicles, such as flyers or rovers, and using in-situ resource utilization (ISRU) techniques to fuel themselves.

Hoffman, Niehoff, and Stancati (25) compare a theoretical ballistic hopper and a theoretical Mars airplane using  $\text{CH}_4/\text{CO}_2$  and  $\text{CO}/\text{O}_2$  ISPP (In-Situ Propellant Production) schemes. In the end, it is discovered that  $\text{CH}_4/\text{O}_2$  is a preferred propellant option, that hoppers which carry their

own ISPP suites are preferred to those which must hop back to a dedicated refueling station, and that the maximum total range of a Mars hopper is about 1030 km (using ISRU technology of the day). This range is only accomplished using two hops and ballute/parachute for braking on descent. This performance is limited in part by the fact that the delta-V needed to travel 1500 km is greater than that needed to achieve orbit, and this 1500-km distance still represents less than 7.5% of Mars' circumference. A fixed-wing Mars ISPP airplane was found to be able to achieve 6650 km of range (although the authors note that it does not carry its own ISPP gear, and must return to base for refueling). Although detailed consideration was not given to the mechanics of flight in the Martian atmosphere or the relative dangers of repeatedly landing a ballistic hopper or aerodynamic flyer, and no analyses on these topics were shown, the flyer was a preferred option in this early study.

Following this, Sercel, Blandino, and Wood (26) propose a somewhat more detailed concept for an ISPP-enabled hopper on Mars. This hopper masses 2225 kg dry, and uses O<sub>2</sub>/CO fuel (with refueling between hops) to cover ranges of up to 1000 km in 15-minute suborbital hops. It is noted that these hops could also be a starting point for a sample return launch, and that reliability and terrain roughness (upon landing) may be issues for future concern. A similar study of an ISPP-enabled hopper was done by Zubrin (27), which describes the use of diborane with ISPP-derived CO<sub>2</sub> to fuel Mars hoppers. The hopping vehicle design is comparatively simple, with a nominal hop distance of 500 km.

Zubrin (28) also takes a much broader look at mobility and ISRU, and discusses the potential for various ISRU techniques used in combination with exploration vehicles on Mars. The paper

distinguishes between three types of vehicles: surface vehicles, which use “wheels, treads, half-tracks, or even motorized legs,” ballistic vehicles “employing rocket propulsion,” and atmospheric vehicles, which include balloons and jet- or rocket-propelled aircraft. It also notes that long ranges (on the order of hundreds or thousands of kilometers) can theoretically be attained by flying vehicles, and recommends  $\text{CH}_4/\text{O}_2$  propellants for ground vehicles or raw  $\text{CO}_2$  (heated by nuclear energy) for flying vehicles. There is, however, no discussion of cost, as the paper is meant to encourage the use of ISRU and provide an initial survey of its potential utility.

Landis, Linne, and Taylor (29) describe the use of cryogenic propellants, namely  $\text{O}_2$  and  $\text{CO}$ , derived from the Martian atmosphere for use in a ballistic hopper to explore the Martian surface. One of the primary drivers for the use of a hopper is its ability to sidestep the terrain-based limitations of surface rovers. The hopper is proposed to separate from a lander after touchdown, and then to hop autonomously for hundreds of meters at a time, using this ability to serve as a science and technology demonstrator on the surface of Mars. Although the authors recognized the high mobility advantages a hopping vehicle has, they did not consider its ability to mitigate deployment risk by essentially being the same vehicle as the lander. This paper was revised and expanded to create (30), which also describes some potential science payload objectives for such a hopper: aerial photographs, meteorological and atmospheric data, and geological measurements at sites that would be isolated from rovers by rugged terrain.

Shafirovich, Salomon, and Gokalp (31) analyze and compare the range performance of hoppers using either in-situ-derived  $\text{CO}_2/\text{Mg}$  or Earth-transported nitrogen tetroxide/monomethyl hydrazine (NTO/MMH) propellants. Designing a hopper using a simple model for power

systems, ISRU systems, and propulsion systems, they determine that a CO<sub>2</sub>/Mg hopper can provide better range performance (longer hops and more of them) than a hopper using more conventional rocket fuels. The total range covered is estimated as 10-15 km over 180 sols for a 200-kg hopper, using a series of 10-15 hops. Although this is not explicitly compared to rovers, this analysis does help to clarify the advantageousness of an ISRU-utilizing hopper design.

#### **2.1.4 Other hopping vehicles**

Powell, Maise, and Paniagua (32) describe using a hopper with a nuclear thermal rocket engine to visit the inner moons of Jupiter, Pluto and Charon, or Mars. The hopper, with a dry mass of 1080 kg, would access multiple sites on these planets (and potentially even deploy a subsurface autonomous probe on Europa), collect samples with a science payload, and then return to Earth. An extension of the hopper's main engine to use hydrogen or carbon dioxide, extracted from water ice or planetary atmospheres, as an in-situ-derived propellant is also proposed. Although this hopper is unique in the use of a nuclear propulsion system (and therefore incorporates an advanced propulsion technology into hopping vehicle technology), the concept is developed to a level more akin to the other theory-centric designs than to a working design. However, it also expresses the aspirations to high-performance exploration ability that is also characteristic of hopping vehicle designs.

#### **2.1.5 Summary of past theory-centric hopping vehicle designs**

The theoretical work on hopping vehicles started with designs for legged hoppers, which were displaced by the Apollo Lunar Rover. Although there was no immediate follow-up, the concept was picked up in later decades by Martinez-Cantin (33) and Montminy, Dupuis, and Champiaud

(34), which focused on using hopping legged vehicles on the Moon or on a Near Earth Object (NEO).

Theoretical work done on lunar hoppers brought to light some potential advantages of hopping vehicles over other forms of transportation, or as part of a transportation network, as in (21), (31) or (24). Work done on Mars hoppers developed the unique abilities of hopping vehicles, including their ability to use ISRU (28), (35), and their ability to access otherwise unreachable parts of the surface (30).

There was a growing awareness of the fact that hopping vehicles should be separated from other surface exploration vehicles, and a slowly increasing development of the details of hopping vehicles' unique abilities.

However, there are also a few key weaknesses in these studies. Most work focused on the use of hopping vehicles for fairly specific missions (28), (35), (22), rather than looking at a wide range of things hopping vehicles could do. Most works also focused on one key advantage of hopping vehicles (the ability of hopping vehicles to move great distances in short periods of time), and did not investigate the other capabilities conferred on hopping vehicles by their means of propulsion, nor examine how these capabilities could be utilized in new ways. Furthermore, past theoretical hopper designs were paper designs only, and had not been validated, nor did they have realistic modeling of subsystems. There has been to date no published concerted campaign of in-lab development hand-in-hand with mission design and theoretical investigation of the capabilities of hopping vehicles for planetary surface exploration. Although NASA's lunar

landing research vehicle (36), developed in the context of Project Apollo, was a sustained and focused effort of Earth-gravity testing and mission design, capped off with extremely successful flight validation, the purpose of the vehicle developed was simply to land on and return from the Moon, not to hop around the surface and explore it at length.

#### **2.1.6 Practical hopping vehicle work**

The creation of Project Constellation in 2004 (37) and its proposed return to the Moon rejuvenated interest in planetary surface exploration in a number of areas, hopping vehicles among them. Although Project Constellation has now been canceled, new work on hopping vehicles has begun, including on a manned hopper for transportation of humans around the surface of the Moon (38), the development of a hopper/lander bus testbed at NASA Ames and Marshall, and the creation of a student testbed hopper at the University of Southern California (39). The Space Systems Lab at MIT has also been a source of additional, and ongoing, work on hopping vehicles, done in the context of the Google Lunar X-Prize contest (40), (41), (42).

These hopping vehicles are often seen as the next phase of advancement in planetary surface mobility, and are intended to be utilized as single vehicles carrying scientific instruments around a planetary body. They thus represent an addition to the current paradigm of landers/rovers as a means of exploring a planetary surface, while still operating within the same context. These hopping vehicles have also often been the subject of attention at a more detailed level, including careful analysis of subsystem hardware, modeling, and other practical issues affecting flight. With few exceptions, practical hopping vehicle research has also been done in the context of existing hardware, usually a flight prototype.



### **2.1.6.1 LEAPFROG**

The LEAPFROG (Lunar Entry and Approach Platform for Research on Ground) hopper, built and operated at the University of Southern California (39) was designed as a low-cost proof-of-concept demonstrator, and used commercial off-the-shelf (COTS) components to keep costs manageable. The vehicle flies using a single JetCat P-200 engine, with 12 nitrogen-fueled thrusters providing attitude control. Integration was performed at USC by students, and total flight time was expected to be approximately 180 seconds. As of 2010, the vehicle had undergone component tests and hot-fire strapdown tests. Since then, further published progress updates have not been made available, although conversations between the author of this thesis and students involved in the LEAPFROG project (43) indicate that, after one brief test flight, the vehicle underwent a damaging crash, and has not flown again since.

Barnhart, Sullivan, and Will (44) provide additional insight into the driving forces behind the LEAPFROG demonstrator. In addition to broader goals of providing hands-on experience for engineering students, the project seeks to be used as a risk-reduction tool for lunar flight technologies and techniques. The vehicle was conceived with the purpose of flying “Apollo-like landing approaches,” through which various (never specified in detail, but said to include lunar-qualified flight sensors) technologies and techniques could be tested. A second emphasis in the LEAPFROG project was an iterative design-test-repeat cycle, conducted by students and modeled after industry and government aerospace projects. This cycle was expected to manifest itself in a multi-generational fashion, with successive iterations of the LEAPFROG hopper

becoming more capable as the vehicle gradually began to incorporate space-qualified hardware and to use hot-fire bipropellants instead of air-breathing engines for main propulsion.

Although LEAPFROG was conceived with the intention of buying down risk, both technologically and programmatically (by exposing students to the inherent risks of flight testing early in their careers), there was no formal description of risks, uncertainties, or a defined path ahead. The underlying design philosophy of LEAPFROG is obtaining hands-on experience for students, rather than a defined test objective.

The LEAPFROG hopper resulted in the development of flight hardware and flight design documents, including at least first-order system models, but details were not published. The project personnel paid close attention to hopper design and subsystems, but did not consider the broader issue of what a hopper's unique advantages are and how best to use them in various mission contexts.

#### **2.1.6.2 Project Alshain**

Another example of current research is found in work by Space Systems Lab at the University of Maryland (38), (45). This work focuses on the design of a single-person lunar hopper, which uses short-range ballistic propulsive maneuvers, as a means of extending astronaut mobility on the lunar surface. Although this project was a theoretical hopper design, with no hardware component, the attention paid to subsystems in (38) and the acknowledgment of the detailed ways this hopper might be used in (45) make this paper a bridge between theory-centric and

practical hopping vehicle research. However, there is still not a lot of acknowledgment of the advantages of hopping vehicles beyond their ability to traverse long distances rapidly.

#### **2.1.6.3 NASA Marshall/Ames Hopper and Project M/Morpheus Testbed**

There has also been a stream of practical hopping vehicle development within NASA, with a working prototype being built at NASA Ames, and a copy and successor vehicle being built and operated at Marshall. This stream focuses on uncrewed exploration, and the vehicle is intended to be used as a hardware and software testbed. However, although the potential utility of this vehicle in hopping applications has been noted, it is primarily a lander testbed. Therefore, less study was made of the ways the development of this vehicle could be guided by the unique capabilities of hopping vehicles, and most work focused on simply building and testing the hardware.

The Morpheus lander testbed (formerly called Project M) is another such vehicle being developed by NASA (46). Morpheus is another example of a testbed vehicle with the ability to be used to improve hopping software and propulsion technology, but which is primarily focused on use as a lander testbed.

#### **2.1.6.4 Masten/Armadillo**

A second practical hopper research stream includes the two separate vehicles being developed by Masten Space Systems and Armadillo Aerospace. These vehicles have actually flown hop-like profiles on Earth, even though they were originally developed to demonstrate lander technology as part of the Northrop-Grumman Lunar Lander Challenge. There has only been limited

publication of details on these landers by Frampton et al. (47) and Collins et al. (48), and what has been published mostly focuses on GNC, engines, or flow dynamics. This stream of research is intended to produce advancements in subsystems (such as GNC or engines), rather than to promote a whole new type of mobility.

#### **2.1.6.5 TALARIS and related work**

A significant and ongoing stream of practical research on hopping vehicles can be found in work ongoing at MIT's Space Systems Lab and the Charles Stark Draper Laboratory as part of the Terrestrial Artificial Lunar And Reduced gravity Simulator (TALARIS) project. In addition to a growing body of research on guidance, navigation, and control (GNC) for hopping vehicles, work has been ongoing on the development and flight of a hopping vehicle testbed (40), (41), (42), and on possible theoretical applications of hopping technology (4), (8).

The design, development, and operation of a hardware testbed is described in detail. Cunio et al. from 2009 (40) describes the initial development of the vehicle, including the genesis of the concept of dual propulsion systems for hopping. The first propulsion system serves to offset the weight of the vehicle to provide an environment dynamically similar to the one that would be encountered on the Moon or Mars, or another planetary body. The second propulsion system operates within this emulated environment, and is specifically built to mimic the impulsive operation of rocketry. The prototype testbed conducts flight tests, as detailed by Cunio et al. from 2010 (41) in a student-heavy and densely populated urban setting. This necessarily led to restrictions on feasible propellants, leading to the use of compressed nitrogen thrusters. However, the use of a weight-offsetting propulsion system and safe propellants permitted the

completion of a full design, build, and test cycle, culminating in flight tests. This in turn permitted the maturation of vehicle design, operations concepts, and flight software, which led to further development efforts on more advanced vehicles in more realistic test environments (49). Additional information on the hardware testbed and its history can be found in Appendix E of this thesis.

In the meantime, the inherent advantages of hopping vehicles and the possible applications of these are described in another substream of research. Cohanim et al. (4) first describes some of the advantages of hopping vehicles, and associates them with a specific hopper mission concept. However, Cunio and Cohanim (50) and Lanford (51) expand these concepts.

Michel's thesis (52) examines hopping vehicle performance in the hover-hop (fixed-attitude/fixed-altitude) mode. Setting a background for hopping mobility by briefly examining the history of landings on other planetary bodies and the history of using rovers for surface mobility on other planetary bodies, Michel recognizes that rovers are limited to accessing small areas of a planetary surface (as, necessarily, are landers), and are also usually limited to smooth terrain. Michel recognizes a broad range of potential means of surface mobility, and generates a highly subjective weighting in each of ten subcategories of versatility for each. Propulsive hopping vehicles (requiring no ground or fluid contact to move) are found to be the highest-ranked option, and landers are found to be the second-highest-ranked option.

The remainder of the thesis focuses on the trade between hoppers and landers, specifically between exploring large areas of the surface of a planetary body using a single hopping vehicle

and using a fleet of landers. Options for hopping vehicles, including dropped payloads, staging, and ISRU, are also presented. The option for ISRU is explored by listing a few potential ISRU options from the technical literature. Finally, the hover-hop method is selected over the ballistic hop method for operational reasons (including better views of the surface during traverse and the ability to make course corrections in flight) and for technical reasons (lower required engine thrust). The hover-hop, also known as the fixed-altitude, fixed-attitude (or FA-FA) hop, involves a hopping vehicle traversing in a quasi-steady state while holding itself in a constant attitude relative to the surface. A ballistic hop, which follows a ballistic arc, involves burning propellant to rapidly achieve a high velocity at a steep angle and then shutting down engines for the majority of the trajectory.

Given these constraints, hopper mass is estimated on a subsystem basis, using a model originally developed by Howard et al. (53). Subsystems modeled include structure, propulsion, power, and payload. Other systems are not modeled. Using a seven-phase model of the hover-hop maneuver (ascent, horizontal boost, boost with hover, gliding hover, horizontal deceleration, de-boost, and descent), a hopper mission is modeled. Input parameters include local gravity, engine  $I_{sp}$ , number of hops performed and distance traveled during each hop (all hops performed on a given mission must traverse the same distance in Michel's model), hover height, fixed payload mass, and dropped payload mass. Optimization of the system mass is incorporated locally to deliver a minimum value for the mass of engines, tanks, and propellant. Numerical optimization is used, but not full numerical simulation of the hop. This optimization extends to the engine firing parameters during each hopping flight.

From a number of runs with the optimization tool, closed-form analytical relationships were estimated for various parameters. The closed-form estimate is given, and enables estimation of minimized hopper mass if given values for number of hops, distance of hops, and fixed and dropped payload masses. Finally, a view of a 3-dimensional plot showing the trade between equal hopper and lander equivalent masses is shown.

Simplifications in Michel's work include a lack of attention paid to surface characteristics and atmospheric effects, as well as a lack of detail in subsystems. Additionally, the model is only concerned with lunar missions, and furthermore uses a set of constraints and automatic optimization to deliver a single answer. This, however, greatly reduces its ability to examine several options for missions and to address hopping missions with flexibility and granularity in modeling. Additionally, no attention is paid to costs, and only some attention (the seven-phase model of a hop) is shown to operational issues.

Middleton's thesis (54) focuses on examining the performance of hoppers via modeling and simulation. Middleton develops his own tool, but is focused as much on the need to predict how well prototype performance on Earth will match vehicle performance in space as on anything else. He examines two fundamentally distinct types of hops: ballistic and hovering hops. His model of a hopping vehicle focuses on the propulsion system, including parameters such as wet mass and engine specific impulse, and makes the assumptions that the vehicle has perfect and instantaneous navigation, control, and actuation. The model focuses heavily on the upper end of performance; e.g., it outputs the best possible results based on given inputs. The primary

mechanics of the simulation center on vehicle performance and dynamics, and are not broken down by subsystem.

While hops are broken down into phases appropriate for ballistic or hover hops, idealizations are made in calculating them. However, hops are simulated on a step-by-step basis.

With this basic simulation of a hopping vehicle, Middleton addresses issues of optimal choices for launch angle, initial thrust-to-weight ratio and engine burn time. The new model provides information useful for minimizing fuel use (in terms of delta-V) or traverse time. Middleton concludes that a ballistic hop is theoretically more fuel-efficient than a hover hop, but notes that neither of the hop maneuvers is modeled as granularly as they would be executed, and that other factors, such as the ability of GNC to perform precision maneuvers and the need for payloads to undergo a vibration-free coast period, play a key part in tradeoffs. However, the ease of testing in the lab conferred by the hover hop maneuver means it is preferred for the TALARIS hopping vehicle.

The remainder of Middleton's thesis includes a more detailed simulation of the TALARIS hopping vehicle, focusing on flight performance and engine characteristics (and adding drag characteristics). The simulation is run for a 30-meter traversing hop on the Earth, at a height of a few meters. The primary concern is whether the TALARIS hopper prototype vehicle will be able to perform the hop, given the amount of fuel it carries as designed. Additional information on the total traverse time, total fuel burned, and other factors as a function of initial burn time is



considered. The baseline distance planned to be traversed was scaled down based on preliminary results from Middleton's work.

Notably, the effects of drag from the atmosphere on Earth are also analyzed. Drag is shown to have a positive effect on fuel consumption under certain conditions (it replaces fuel that would otherwise be needed to decelerate the vehicle), although the effects are also small enough as to be essentially negligible under expected flight conditions.

An additional modeling and simulation effort was conducted to understand the degree to which the TALARIS hopper and the lunar vehicle that the team one day expects to fly are similar. This simulation model includes more detailed modeling of the guidance system and control system, and is intended in part to make it possible to isolate the effects of the Earth environment on the hopper. For this reason, the model is heavily modularized. Noise is also programmed into the model, in the form of uncertainty in the actuators. Monte Carlo runs with this model revealed that the disturbances as modeled are not typically large enough to cause major issues for Earth testing or lunar flight. For the Monte Carlo simulation, over 1000 runs showed a 98% success rate, where success was defined as having enough fuel to complete a planned hop without large trajectory deviations in spite of disturbances.

The conclusion Middleton makes is that the TALARIS prototype can emulate a lunar hop very well. Barring a very high standard deviation in electric ducted fan (EDF) force uncertainty (on the same order as the force they generate nominally), the vehicle should perform well enough to complete a hop in the lab. Unfortunately, later experience with EDFs indicates that the smallest

amount of EDF noise can cause hop failure; this dynamic was not detected by Middleton because it only occurs in reality or in 6-DOF simulations.

Middleton also focuses on vehicle flight performance on the Earth's Moon. Middleton's modeling did not extend to the subsystem level, and did not consider costs. Although some attention was paid to both uncertainty and operational issues, neither was fully addressed. The most significant limitation, however, was this thesis' limitation to the TALARIS vehicle and its immediate planned successor, the not-yet-built NGL lander. This caused the thesis to focus on questions of optimization and similarity of results, rather than of tradespace exploration and feasibility of results or existence of alternate options.

Lanford's thesis (55) centers on the use of hopping vehicles for planetary exploration, and provides a number of example missions, as well as analysis of the policy context for the use of hopping vehicles as part of a national program of space exploration. Lanford uses a technical model of hopping vehicles adapted from work done by Michel (52) and Yue et al. (53), with some updates. While Lanford thus incorporates the current available state-of-the-art in hopping models into his work, he does not have available fully-detailed models of all hopper subsystems, and his operational hopping models are not completely detailed. Lanford develops more granular models of hopping vehicle mission profiles by combining the results of Middleton's and Michel's models (see especially p. 115 of Lanford), but this is accomplished by moving inputs and outputs from one model to the other by hand – there is not an integrated modeling tool to mix ballistic and hover hopping modes of traverse.

Lanford also looks at the inherent advantages afforded by hopping mobility. In addition to the advantages of rapid regional mobility, terrain freedom, and precision landing, with shifted operational risk profiles and potential cost reduction via commonality with landers, taken from (8), Lanford adds the advantages of generally precise navigation and traverse, the ability to make direction changes in mid-maneuver (if performing a hover hop), or between maneuvers, the ability to deliver low-altitude ground coverage, the ability to deliver temporary presence in a harsh environment and then escape, and the ability to make repeated samples of the atmosphere and ground. Lanford notes, as have others, the disadvantages that hopping vehicles are as-yet unproven by space flight, may have a higher development cost than a pure lander, are fuel-limited, and accrue higher amounts of risk by undertaking hopping maneuvers. Lanford then adds the disadvantages that a hopper has limited mission duration, and may also disturb its landing site upon touchdown or launch. Lanford also notes how some factors that are a combination of the target's characteristics and mission characteristics may arise, including the potential for environmental hazards or corrosion, access to Earth for communication, and access to the Sun for solar power.

After adding a policy implications discussion, which touches on the ways in which hopping vehicles may use their inherent flexibility to further a program of space exploration, including by serving as robotic precursors or human assistants, and touching on how new mobility may enable new uses of remote presence (a theme explored in detail in (50)), Lanford also examines the list of planetary bodies that can be targeted by hopping vehicles. Lanford adds to the traditional bodies of Luna and Mars the larger asteroids, Galilean moons of Jupiter, the Saturnean moons, and even suggests some trans-Neptunian bodies. Lanford's thesis concludes with a series of

exemplar missions to Luna, Mars, and Saturn's moon Titan. Lanford examines and sizes hopping vehicles for the distribution of science network nodes, a multiple-sample return in the South Pole Aitken (SPA) basin region, an excursion into or near the permanently-shadowed regions of Shackleton Crater, and dropping into lunar surface features that appear to be deep pits or open caverns, as well as for a trip down into and up out of the Valles Marineris, into similar pits or open caverns on Mars near Mons Arsia, and even a potential human or heavy-cargo hop to the Isidis Planitia region, as well as an initial exploration of lakeshore regions near the Kraken Mare on Titan.

All of these hopping missions showcase interesting examples of missions for which hopping vehicles are uniquely suited. The cavern trips show how terrain freedom can be exploited, and the ILN distribution utilizes the range of hopping vehicles to best advantage. The combination of speed and range that hopping vehicles provide, plus their precision ability, enables the missions to Kraken Mare and the SPA basin. The Valles Marineris hop shows how rapid long-range mobility and terrain freedom can be combined, and the quick hop into and out of Shackleton Crater combines terrain freedom and rapid mobility.

However, Lanford's thesis still relies on hopping vehicle models which are not very detailed. Some hopper subsystems are modeled incompletely (or not at all), and hopping maneuvers are limited to two types, without a high degree of granularity for either type of maneuver. This high degree of granularity is important, however, as acknowledged by Middleton (54). Furthermore, Lanford includes no integrated model, and does not incorporate assessments of design/build costs, operational costs, or technology risk into his models. A more-detailed model, including

more dynamics (and especially feedback between the first levels of design of each subsystem) would be a logical follow-up to Lanford's work.

## **2.2 Practical hopping vehicles on Earth**

One area of hopping vehicle development that has seen much less progress than might be expected is Earth-based hopping vehicles. Despite the wide variety of transportation that already exists on Earth, vehicles which hop using only their own propulsive power are not common. Ground transportation such as automobiles and rail relies on surface contact, and aircraft and oceangoing vessels rely on fluid action. The reason for this is that Earth is a comparatively high-gravity world (in fact, it has the highest gravity of all the terrestrial planetary bodies in our solar system), and that it has a comparatively dense atmosphere (see Appendix B for more data on gravity and atmospheric density for other terrestrial planetary bodies). As such, vehicles which rely on fluid contact (flyers) are capable of performing at a level of mass efficiency which far exceeds that of hopping vehicles on Earth. A flying vehicle on Earth is capable of a much longer duration of sustained flight than a comparably-sized hopping vehicle, a fact which is clearly illustrated by the heavy dominance of rotor-driven and gas turbine-driven technology over rocket-driven technology in the field of personal flight systems, as described by White and Lewis (56). Helicopters thus are far more cost-effective in an environment where the gravity and atmospheric density are as high as on Earth.

However, this is not the case on all other terrestrial planetary bodies, and in fact many have very low or negligible atmospheric density, meaning that flying vehicles are not at all effective there. While helicopters may thus be more effective than hopping vehicles in many low-altitude

applications, they are heavily dependent on atmospheric density, and as such some Earth applications, such as rescue and rapid response in high altitude mountain regions, may still be feasible subjects for hopping missions. Additionally, a helicopter is not structurally or functionally similar to any sort of vehicle that can make a planetary entry and landing, so exploration of any distant planetary surface via a helicopter would still require the deployment of the helicopter, with all the attendant initial operational risk and programmatic need to develop multiple vehicles that this entails, but which are not associated with the use of a hopping vehicle.

### **2.3 Summary of past hopping vehicle work**

In summary, early interest in hopping vehicles included a vision of hopping vehicles as mechanical-legged range enhancing tools for crews on the Moon. This vision was never fully realized, and although mechanical-legged hoppers were proposed for other missions, these other missions were scientific in nature, and tended also to display reliance on advancements in robotic technology, such as miniaturization, materials advances, and systems and controls technology developments. Other hopping vehicle designs were often envisioned as part of a broader technology demonstration or scientific research plan, such as when hoppers were seen as key components of a lunar transportation network or as ISRU demonstrators and mobility enablers for Mars exploration. Interestingly, the concept of a tripartite description of unmanned mobility on planetary bodies, with mobility styles roughly separated into rovers, hoppers, and flyers, was developed fairly early, although it is seen most clearly in Zubrin's work (28).

The stream of hopping vehicle research that proposed interesting and unique missions for hopping vehicles also resulted in early assessments of the advantages and characteristics of

hopping vehicles, which were slowly added to as research continued and stretched beyond the Moon to Mars and even other planetary bodies in the solar system.

Another area of research on hopping vehicles sought to develop them as physical hardware, usually for the purpose of technology development, rather than for their unique advantages and potential to bring about a new era in planetary surface exploration. This research often focused on specific subsystems (such as GNC or propulsion) or a high-level design of the entire hopping vehicle system, and very often was backed by the presence of a physical testbed or prototype.

Past work in the TALARIS project, especially by Lanford (55), sought to unite these two streams by developing a concept of the types of missions hoppers might undertake, and by using models of hopping vehicles to understand the sizing of the hoppers which would undertake these missions. Lanford built on models by Middleton (54), which was based in part on early work done with prototype hardware, and by Yue et al. (53) and Michel (52), which was built on an early understanding of hopper subsystems and of hopper missions.

However, some gaps still remain. Models of hopping vehicles are still in an early stage of development; they are not sufficiently granular nor exhaustive in terms of the operations they permit, they rely on models of subsystems which are not modeled in detail and which have usually only first-order coupling (if any) between all subsystem models. Previous models do not incorporate the dimensions of lifecycle cost, including development, build, and operations costs, nor of technological risk. Furthermore, there is as yet no integrated model that incorporates all the pieces of modeling capability previously developed. For example, although the ballistic-arc

hop and the hover-hop trajectories have both been described as feasible and useful for a hopping vehicle, they must be modeled with separate tools and the results combined by hand.

Therefore, there is a need to develop an integrated model of hopping vehicles, which should incorporate several key features, including: an ability to model subsystems and subsystem interactions, as well as operations, with a high level of granularity; a record of validation against examples of actual spaceborne vehicles; lifecycle cost estimates, including operational costs; a grounding in an understanding of the key abilities of hopping vehicles to perform uniquely in planetary surface exploration missions; and the ability to investigate more than just a single point design for a hopping vehicle or hopping mission.

The tradespace model presented in Chapter 3 of this thesis possess all these features, and as such is a viable means of bringing hopping vehicles into the decision space for future planetary surface exploration.



### **CHAPTER 3. Hopping Vehicle Model**

In this thesis, we combine an understanding of the capabilities of hopping vehicles (4), (8) with practical systems engineering knowledge as well as physics-based models to produce a physically grounded and operationally realistic tradespace model for hopping vehicles as a means of planetary surface exploration. This model will be able to analyze formally described hopping mission concepts and generate detailed information about the physical design of the hopping vehicle which will be able to perform the mission. The model will be validated via subsystem-level mass comparison to planetary landers and proposed hopping vehicle designs, and will be used to make initial assessments of the tradespace of hopping vehicle missions, in order to identify some ways in which hopping vehicles can contribute to planetary surface exploration.

In this chapter, background work on hopping vehicles from Chapter 2 of this thesis will be used to develop an overarching model for the tradespace in which hopping vehicles exist. This tradespace can be used to support analysis of mission concepts for hopping vehicles by providing a framework to formalize hopping vehicle mission concepts, and then mapping the formalized concepts onto a design space for hopping vehicles. This hopping vehicle design space will include physical characteristics of the hopping vehicles, such that users of the model will be able to assess the mass, cost, and other characteristics, including some technology choices, of a hopping vehicle that can be built to fly the formalized mission.

The model will serve to map function to form, in that a prescribed list of hopping vehicle motions (such as vertical ascent, then hovering traverse) can be used to generate a hopping

vehicle design (such as an 80-kg hopping vehicle carrying 10 kg of propellant). These hopping vehicle designs can also be mapped to cost estimates and can have their operational profiles mapped onto a timeline. This will result in the availability of key information to users of the model, such as total cost to build such a hopping vehicle, relative mass of each subsystem on the hopping vehicle, and approximate level of operational intensity at mission control over the lifetime of the mission.

This concept appears in Figure 7 below.

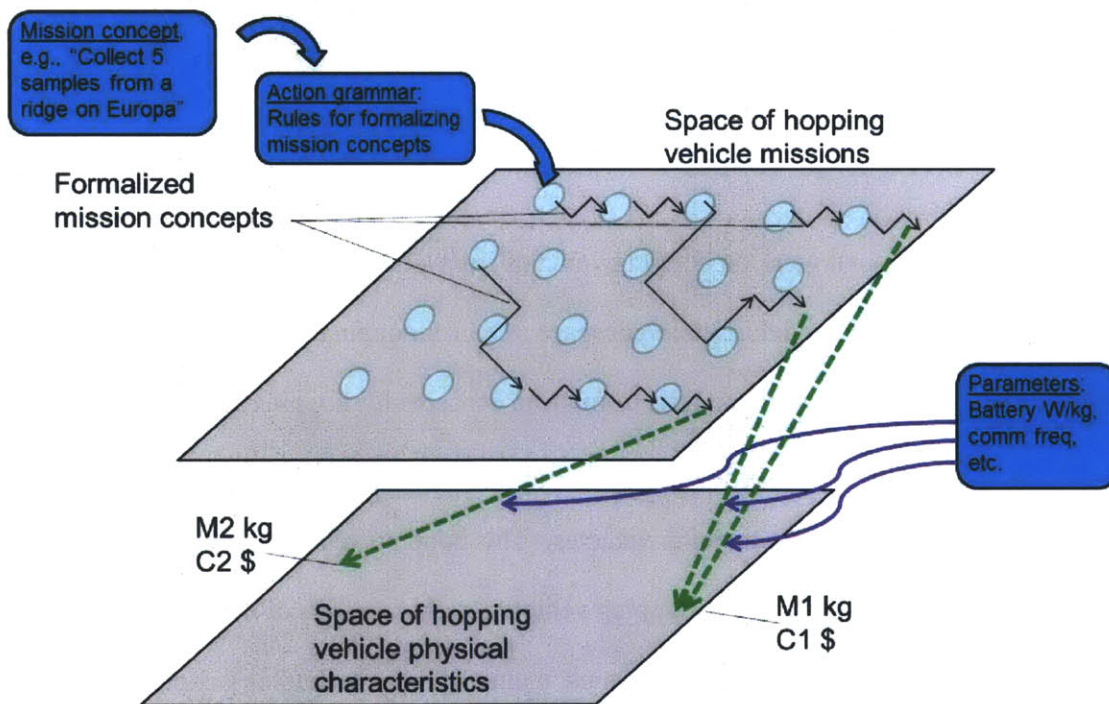


Figure 7. Diagram of concept for hopping vehicle model.

Figure 7 shows how the space of hopping vehicle missions (which is shown subdivided into elementary actions a hopping vehicle might perform, as indicated by the dotted regions in the

plane) can have traces of actions made through it. Each trace connects a series of elementary actions to describe a complete hopping vehicle mission. A series of such elementary actions, connected by a trace, defines a mission. This mission is formalized from a mission concept (a mission concept is a simple, short description of a desired science activity or series of science activities) via an action grammar, which contains rules and a vocabulary for describing mission concepts in the action space. Each hopping vehicle mission can then be mapped onto a physical description of the hopping vehicle which will be able to perform it, including such details as the relative mass of subsystems. This mapping is aided by a catalogue of physical parameters, including performance characteristics of key subsystem components, as well as some choices for subsystems from small sets of possible technology options. The parameter catalogue can be updated by advanced users of the model.

The tradespace model developed in this thesis creates an early-phase picture of what the final hopping vehicle will be. It should be noted that various sets of hopping actions may result in similar physical characteristics, as the mapping is not necessarily one-to-one from function to form. Some differing mission concepts may result in similar mass and cost estimates for their hopping vehicles. However, the early-phase picture, especially with aspects of cost, operations, and subsystem details included, can be very valuable to designers of planetary surface exploration missions.

The designer of a planetary surface exploration mission will have some set of objectives in mind, and will be interested in performing these objectives within appropriate cost, risk, and schedule limitations. This thesis will be primarily concerned with exploration by means of vehicles that

are semiautonomous, with high-level operational decisions made by humans in teleoperational oversight. Objectives for these missions will typically be scientific in nature, and there will be some set of scientific instruments which can help to achieve these objectives. Mission designers will be interested in moving these scientific instruments around the surface of a planetary body and operating them in order to achieve their objectives (moving and operating scientific instruments may occur sequentially or simultaneously, depending on mission needs). However, there are multiple ways to move scientific instruments around a planetary body, each with different cost, risk, and schedule implications.

The model created in this thesis provides a way for planetary surface exploration mission designers to obtain additional insight into the performance, cost, risk, and schedule characteristics of a planetary surface exploration mission conducted by hopping vehicles. The desired performance can be mapped into the functional space of hopping vehicle actions, and the model's mapping of this onto physical form aspects of a hopping vehicle provides information on the costs of the mission. The technology choices included in the model will cast light onto the risk aspects, and the operational descriptions provided will clarify aspects of the schedule of the project. Programmatic schedule can also be estimated based on the total cost, and some aspects of the development program, such as the relative design work needed for each subsystem, can also be determined from the granularity provided by the physical form description.

The model provides a insight into a hopping vehicle design that would be able to perform a specific mission. This insight, provided at a relatively early phase in the design lifecycle, can be

used to make a decision as to whether to proceed with detailed design and construction of the hopping vehicle. The model's outputs on cost and risk could be compared to available resources and risk tolerance, which could lead to a go/no-go decision on proceeding with a hopping vehicle design. Additionally, the model's outputs could be compared to those of a different model, such as a model of a lander vehicle or a rover vehicle (like the one created by Lamamy (57), (10)), so that mission designers could make a choice between a hopping vehicle and a different kind of planetary surface exploration vehicle.

### **3.1 Model Development**

This section describes the design of a hopping vehicle model. The hopping vehicle model consists of a series of MATLAB code modules, fed by Excel databases. Code for the model is shown in Appendix A, and the Excel databases are shown in Appendix B. The model runs from the MATLAB command line, and generates textual and visual output on the screen, as well as an archive of information about inputs, outputs, and parameters that is stored in a new Excel file. This chapter describes past modeling work and each module of the model developed in this thesis.

#### **3.1.1 Past Modeling Work**

Many of the papers discussed in Chapter 2 include some effort to model a hopping vehicle. Table 1 contains a list of various hopping vehicle models developed in the literature.

The columns contain information about the models. Note that the columns range from left to right roughly along a spectrum of theoretical underpinnings to empirical validation. For

instance, the leftmost column indicates whether a model has been created in the context of a well-developed understanding of the range of unique abilities displayed by a hopping vehicle, and the next column to the right indicates whether the model was created to describe a mission enabled by hopping or which is in some way tied to hopping vehicles. Both of these are theoretical underpinnings for the concept of utilizing hopping vehicles.

The presence of some sort of performance model is indicated in the third column. Typically, even a simple hopping vehicle model includes an equation to model the hopping vehicle's use of propellant on a hop. This is generally used to estimate the amount of propellant a hopping vehicle will need to perform its mission. This may be (and often is) as simple as a calculation of the fuel required to propel a vehicle in a ballistic arc over a certain distance. A performance model allows the calculation of some value for some cost, say distance covered for total vehicle mass. The next column indicates whether the vehicle is described in some detail at the subsystem level – a model facet which enables more careful analysis of the likely cost of developing and building the vehicle, and which could potentially provide insight into the relative complexity or cost of the vehicle's subsystems. These models may vary in detail, with some models incorporating detail on only a few subsystems, while others exhaustively describe all subsystems. Typically, hopping vehicle subsystems are sized either using a parametric estimate from the amount of propellant needed for the full mission, or based on some of the mission parameters (e.g., payload mass), or based on a standard subsystem model.

The last two columns describe matching between the hopping vehicle model and the actual hopping mission. A realistic operations model makes some attempt to account for the step-by-

step operation of a hopping vehicle, instead of simply calculating performance and mass characteristics and ignoring all subtleties. Finally, the last column indicates whether there has been any effort to match output from the model to actual vehicles in the real world. This is often a difficult step, as no spaceborne hopping vehicles exist yet, although validation can be made against prototype vehicles in the lab or against similar spaceborne vehicles.

**Table 1. Comparison of previous hopping vehicle models.**

<b>Model</b>	<b>Considers hopper unique abilities?</b>	<b>Involves hopper mission concept?</b>	<b>Performance model?</b>	<b>Detailed subsystem model?</b>	<b>Realistic operations model?</b>	<b>Validated sections of model?</b>
Sercel, Blandino, Wood 1987 (26)			X	X		
Donahue, Fowler 1993 (22)		X	X	X		
Zubrin 1992 (28), Hoffman 1982 (25)		X	X			
Hendry 2007 (39)			X	X		
Landis 2000 (29), Beal 2009 (38)		X	X	X		
Vallerani 2006 (24)			X	X		
Shafirovich 2006 (31), Powell 2006 (32)		X	X	X		
Masten, Armadillo				X		X
Yue 2010 (53)/ Michel 2010 (52)		X	X	X		
Middleton 2010 (54)		X	X		X	X
Lanford 2011 (55)	X	X	X	X		
Cunio 2012	X	X	X	X	X	X

As can be seen Table 1, there is currently no model for hopping vehicles that extends from theoretical underpinnings such as unique abilities and mission capabilities of hopping vehicles all the way to practical aspects, such as realistic consideration of operations and validation of the model. While some previous modeling work, especially Yue et al. (53), Michel (52), and

Middleton (54), can be used as a building block, it is necessary to build an entire model from the ground up, using physical principles and empirical engineering relationships where possible.

### **3.1.2 Notable Hopping Vehicle Models**

Prior work done in the context of the Google Lunar X-Prize at MIT and at the Charles Stark Draper Laboratory has focused on the modeling of hopper dynamics, and on the modeling of hopper subsystems. For instance, a simulation of hopper dynamics was developed by Middleton (54), and an assessment of the capabilities of hoppers, built on a detailed subsystem sizing model, was also developed by Yue et al. (53). These works advocate the use of the hover-hop trajectory, rather than the ballistic-arc trajectory, for practical reasons, and develop models of vehicle capability based on an analysis of this trajectory. These works provide a starting point for modeling the behavior of hopping vehicles in an operationally realistic fashion.

#### **3.1.2.1 Middleton's TALARIS Model**

Middleton (54) models a hopper with explicit attention paid to the hopper's ability to remain stable in flight. He focuses on the trajectory the vehicle will fly, and is able to make some comparison between his model's results and the TALARIS prototype vehicle as a means of validating his model.

#### **3.1.2.2 Michel et al. Hopper Model**

Yue et al. (53), with Michel (52), and followed by Lanford (55) model hoppers using several standardized assumptions to model their hopping vehicle missions, and a standard model of subsystems, taken from (58) to describe their hopping vehicles. Although this is an improvement



from the simpler mathematical models used in prior work, their model still does not permit a high degree of flexibility in hopping vehicle operations, and was not used to address hopping vehicles' unique abilities, until picked up and used by Lanford (55). Additionally, it is not validated by comparison to existing vehicles.

### **3.1.3 Rover Models**

Exploration of planetary surfaces via mobility has been the subject of research since humans first walked and drove around the Moon, and since then, most mobility on the surface of planetary bodies has been studied in the context of roving vehicles. The history of planetary surface exploration via roving extends from Apollo (59) and Lunokhod (60) to the present-day Mars rovers, including Pathfinder (61), the very long-lived MER rovers (62), and MSL rover (63) scheduled to land on Mars in August 2012.

Due to the success of mobility via roving over the surface of Mars, attention was paid to modeling roving vehicles at early design stages. To this end, Lamamy (10) developed a model for roving vehicles, which takes mission parameters entered by the user and generates a detailed model of the roving vehicle which can carry out this mission. Lamamy is able to validate his work via comparison to actual roving vehicles, and draws repeatedly on an extensive base of knowledge at NASA's Jet Propulsion Laboratory to create his model.

This thesis seeks to create a similar result for hopping vehicles.

### **3.1.4 Features of a Hopping Vehicle Model**

Past models of hopping vehicles have typically been focused on a single mission or single hopping vehicle design, and did not often compare multiple hopping vehicle designs, although sometimes hopping vehicle designs were contrasted to roving or flying vehicle designs. Previous hopping vehicle models have typically not been complex, and have included primarily a few simple interrelationships between vehicle subsystems. Hopping vehicle models have typically not made many detailed assessments of cost, especially development cost, have never included a realistic model of operations or of operations costs, and have given limited consideration to how the unique advantages of hoppers may enable entire new missions.

This work seeks to fill these gaps, by providing an initial look at the types of missions hopping vehicles can do, both on the Earth's Moon and on other bodies in the Solar System, how their capabilities are uniquely enabled by their properties, and how operationally-realistic factors affect these capabilities. This work aims to expand the conception of hopping vehicles beyond point designs for specific missions and create a means of evaluating hopping vehicle performance for many different missions in many different places around the Solar System. This work is also undergirded by validation against actual flight vehicles. The combination of theoretical work and hardware-based validation seeks to provide a realistic tradespace to investigate the performance of hopping vehicles.

## **3.2 Generating a Hopping Vehicle Model via Formalized Mission Concepts**

The size and physical characteristics of a hopping vehicle are heavily driven by mission-related design choices. A mission consists essentially of moving certain scientific instruments around the surface of a planetary body, and a hopping vehicle tends to grow rapidly and exponentially in

mass as the distance to be moved increases. Therefore, the selection of the maneuvers to be made, the selection of the scientific instrument payload, and the selection of the planetary body on which the instruments are to be moved all drive the rest of the hopping vehicle design characteristics.

The process of using a hopping vehicle tradespace model requires formalization of a mission concept so the mission concept can be analyzed. A mission concept is driven by needs, such as the need of a scientist to know more about the dynamics of formation of other planetary bodies, or about whether life or organic compounds are present on other planetary bodies. The mission concept is a short statement of a desired series of activities to fulfill the need. An example would be the need to know whether carbon compounds are present 6 inches below the surface of the Valles Marineris region on Mars. This need results in a plan to use a spectrometer on samples drilled from the top and bottom of the canyon. This concept is sufficiently developed to be formalized into a hopping vehicle mission.

All formalized mission concepts are applicable to hopping vehicles – in this thesis, we focus on providing mission designers with insight into the design requirements for a hopping vehicle, and not on generating a detailed comparison of hoppers, rovers, and flyers, as rover modeling tools already exist and planetary flyer technology is even more nascent than hopping technology.

The formalization of a mission concept includes formal detailing of the instruments to be used, providing a reference name, parameters for the volume, mass, heat rejection, power requirements, and costing data, including costing parameters and relative level of maturity.

The formalization of a mission concept also includes detailing of the surface characteristics of the planetary region to be studied. This includes selecting the planetary body by name from a database, or entering a new planetary body or region in terms of atmospheric density, gravitational level, and local and regional surface roughness.

Finally, the formalization of a mission concept also includes formal detailing of the flight profile itself. This is especially important, as the detailing of the mission concept involves careful analysis of the hopping maneuvers to be performed. These maneuvers directly drive propellant costs and directly affect engine sizing, therefore strongly affecting all other physical aspects of the vehicle. To analyze these maneuvers carefully a motion grammar must be developed. The formalized hopper mission concept can then be evaluated or compared to other mission concepts in detail.

### **3.2.1 Motion and Action Grammars**

Much as the grammar of a language describes the ways in which the words that make up the vocabulary of the language can be assembled into meaningful sentences, a maneuvering grammar describes the ways in which the various maneuvers that a hopping vehicle can perform can be assembled into hops. Just as a language can create a nearly infinite number of sentences, so can a hopping vehicle with six degrees of freedom perform a nearly infinite number of hops, where a hop is any series of maneuvers that begins with a takeoff and ends with a touchdown. To be able to describe the hops that the vehicle should perform, it is necessary to formalize a series of rules describing the ways in which hopping vehicles may string together individual maneuvers to perform a hop. Furthermore, it is necessary to understand what individual

maneuvers can be performed. In a language, these rules for combination and lists of the elements that could be combined constitute a grammar and a vocabulary; here we stretch the term 'grammar' slightly to include both; as such, a motion grammar for hopping vehicles will describe the elementary maneuvers such a vehicle can make, and the rules governing how they may be ordered with respect to one another.

The concept of a motion grammar is similar to the shape grammar concept, originally advanced by Stiny and Gips (64), which provides an example of pattern generation using a system specific to the type of pattern being generated.

The elementary maneuvers in a maneuvering grammar for hopping vehicles are based on an assessment of all the possible modes of movement for a vehicle with six degrees of freedom. Assuming that there are six degrees of freedom for a hopping vehicle, and assuming that each of these six degrees of freedom can be either in motion or not in motion at any time, there are  $2^6 = 64$  total possible modes of motion. However, not all of these are feasible modes of motion for a hopping vehicle, and some are essentially repeats of another mode of motion, so it is necessary to elucidate the elementary maneuvers and eliminate impractical or unnecessary maneuvers. The end result is a list of the fundamental motions a hopping vehicle can realistically perform.

Accordingly, as a formal motion grammar may include motion in any of the three translation axes (X, Y, and Z) or any of the three rotation axes ( $\theta$ ,  $\psi$ , and  $\phi$ , about the X, Y, and Z axes). The directionality of the motion is not considered to be a distinguishing feature in most cases – a motion consisting of a translation or rotation in a positive sense is considered the same as a

translation or rotation in a negative sense. This is because motion in the positive or negative sense is energetically equivalent, and the model does not need to distinguish the direction of motion. The one exception is motion in the vertical ( $X$ ) axis. Motion in the negative  $X$  direction can be construed either as simple descent (which may pass below the nominal ground level if the descent is down into a terrain feature) or as a descent to the ground and a touchdown. This difference is handled practically in the model by setting a flag to mark all touchdowns.

Furthermore, intentionality must be present for a given mode to be present. Minor disturbances are ignored in naming modes. For instance, a translation with minor disturbances in the rotational axes does not count as two or more mixed motion modes, but as a translational mode. The modes are meant to be idealized elementary motions for a hopping vehicle. Assembling these elementary maneuvers into a sequence according to the grammar will result in a fully described hop, from takeoff from the surface of the planetary body to touchdown on the surface after completing the hop.

### **3.2.1.1 Vocabulary for a Motion Grammar**

Initially, there are 64 possible modes of motion. Table 2, below, illustrates these.

**Table 2. Full list of motion modes for a hopping vehicle, used to develop a motion grammar.**

Number	X	Y	Z	$\theta$	$\phi$	$\psi$	Range motion	Tip motion
1	-	-	-	-	-	-	Steady hover	
2	-	-	-	-	-	X	Steady hover	Yaw
3	-	-	-	-	X	-	Steady hover	Pitch
4	-	-	-	-	X	X	Steady hover	Pitch-yaw
5	-	-	-	X	-	-	Steady hover	Roll
6	-	-	-	X	-	X	Steady hover	Roll-yaw
7	-	-	-	X	X	-	Steady hover	Roll-pitch
8	-	-	-	X	X	X	Steady hover	Full wobble
9	-	-	X	-	-	-	Downrange slide	
10	-	-	X	-	-	X	Downrange slide	Yaw
11	-	-	X	-	X	-	Downrange slide	Pitch
12	-	-	X	-	X	X	Downrange slide	Pitch-yaw
13	-	-	X	X	-	-	Downrange slide	Roll
14	-	-	X	X	-	X	Downrange slide	Roll-yaw
15	-	-	X	X	X	-	Downrange slide	Roll-pitch
16	-	-	X	X	X	X	Downrange slide	Full wobble
17	-	X	-	-	-	-	Crossrange slide	
18	-	X	-	-	-	X	Crossrange slide	Yaw
19	-	X	-	-	X	-	Crossrange slide	Pitch
20	-	X	-	-	X	X	Crossrange slide	Pitch-yaw
21	-	X	-	X	-	-	Crossrange slide	Roll
22	-	X	-	X	-	X	Crossrange slide	Roll-yaw
23	-	X	-	X	X	-	Crossrange slide	Roll-pitch
24	-	X	-	X	X	X	Crossrange slide	Full wobble
25	-	X	X	-	-	-	Angle slide	
26	-	X	X	-	-	X	Angle slide	Yaw
27	-	X	X	-	X	-	Angle slide	Pitch
28	-	X	X	-	X	X	Angle slide	Pitch-yaw
29	-	X	X	X	-	-	Angle slide	Roll
30	-	X	X	X	-	X	Angle slide	Roll-yaw
31	-	X	X	X	X	-	Angle slide	Roll-pitch
32	-	X	X	X	X	X	Angle slide	Full wobble
33	X	-	-	-	-	-	Ascent/descent	
34	X	-	-	-	-	X	Ascent/descent	Yaw
35	X	-	-	-	X	-	Ascent/descent	Pitch
36	X	-	-	-	X	X	Ascent/descent	Pitch-yaw
37	X	-	-	X	-	-	Ascent/descent	Roll
38	X	-	-	X	-	X	Ascent/descent	Roll-yaw
39	X	-	-	X	X	-	Ascent/descent	Roll-pitch
40	X	-	-	X	X	X	Ascent/descent	Full wobble
41	X	-	X	-	-	-	Ascent/descent downrange	
42	X	-	X	-	-	X	Ascent/descent downrange	Yaw
43	X	-	X	-	X	-	Ascent/descent downrange	Pitch
44	X	-	X	-	X	X	Ascent/descent downrange	Pitch-yaw
45	X	-	X	X	-	-	Ascent/descent downrange	Roll
46	X	-	X	X	-	X	Ascent/descent downrange	Roll-yaw
47	X	-	X	X	X	-	Ascent/descent downrange	Roll-pitch
48	X	-	X	X	X	X	Ascent/descent downrange	Full wobble
49	X	X	-	-	-	-	Ascent/descent crossrange	
50	X	X	-	-	-	X	Ascent/descent crossrange	Yaw
51	X	X	-	-	X	-	Ascent/descent crossrange	Pitch
52	X	X	-	-	X	X	Ascent/descent crossrange	Pitch-yaw
53	X	X	-	X	-	-	Ascent/descent crossrange	Roll
54	X	X	-	X	-	X	Ascent/descent crossrange	Roll-yaw
55	X	X	-	X	X	-	Ascent/descent crossrange	Roll-pitch
56	X	X	-	X	X	X	Ascent/descent crossrange	Full wobble
57	X	X	X	-	-	-	Ascent/descent angle range	
58	X	X	X	-	-	X	Ascent/descent angle range	Yaw
59	X	X	X	-	X	-	Ascent/descent angle range	Pitch
60	X	X	X	-	X	X	Ascent/descent angle range	Pitch-yaw
61	X	X	X	X	-	-	Ascent/descent angle range	Roll
62	X	X	X	X	-	X	Ascent/descent angle range	Roll-yaw
63	X	X	X	X	X	-	Ascent/descent angle range	Roll-pitch
64	X	X	X	X	X	X	Ascent/descent angle range	Full wobble

Note that, if the rotational motions are defined as roll, pitch, and yaw, and the translational motions are defined as steady hover (no motion), slides (translational horizontal motion) downrange or crossrange, and ascents/descents, groupings in the maneuvering grammar become apparent. Various combinations of hovering, translations horizontally, ascents or descents, and rolling, pitching, or yawing motions make up the entirety of the elementary maneuvers in the motion grammar.

For the purposes of this work, the X axis direction is defined as being in the vertical (antiparallel to the gravity vector) direction, the Z axis points along the direction of travel, and the Y axis forms the right-handed triplet. These axes are shown in Figure 8. The hopping vehicle shown has a quadruple-engine architecture, which is the default engine architecture in the technical model developed in this thesis.

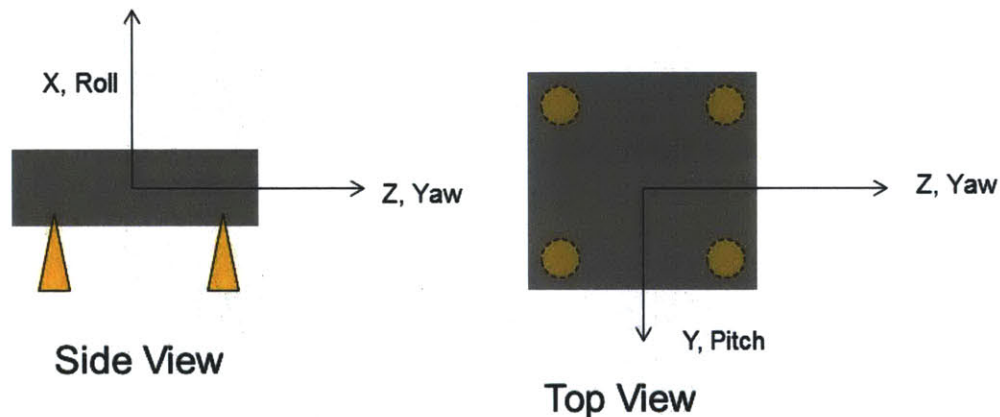


Figure 8. X, Y, and Z axes for the motion grammar.

Reducing the number of feasible motion modes can be done by eliminating any mode where rotational movements are performed in three axes simultaneously – these are very complex



maneuvers, and not likely to be utilized in the real world. After this cut, 56 elementary maneuvers remain. A second cut can be made by analogizing between maneuvers that include a roll-yaw component and maneuvers that include a roll-pitch component. Any particular orientation of the hopping vehicle in three-dimensional space can be attained by a combination of rolling and pitching or by a combination of rolling and yawing, provided there are no restrictions on the order in which the rolling, pitching, and yawing are done. Therefore, roll/pitch combinations are similar to roll/yaw combinations, and all roll/pitch combinations can be cut, leaving 48 elementary maneuvers.

Yet a third cut can be made by looking closely at downrange and crossrange motion. It is reasonable to assume that a hopping vehicle will only move in straight lines, and therefore any horizontal motion can be composed of segments of downrange and crossrange motion.

However, a hopping vehicle will not perform zig-zags as it moves; it will simply fly in a straight line at an appropriate angle in the crossrange-downrange plane (here, the Y-Z plane). Since the coordinate system for hopping maneuvers is not fixed to any geological feature of a planetary surface, it is simpler to model any horizontal motion as being in a straight line along an arbitrary axis of motion, with changes in direction being applied by rolling the vehicle about the X axis to point in a new direction, which will also roll the motion axis (as it is vehicle-fixed). A simple radial description of horizontal motion is used here, where a certain distance is covered at a given angle. Given this radial distance convention, we can further simplify discussion to the concept of alongrange motion, which incorporates horizontal motion in a straight line. Any motion which can be described as a combination of downrange and crossrange motion in

surface-fixed axes can be described as a combination of alongrange motion and rolling motion in the hopping motion grammar. The elimination of explicit crossrange and downrange components in favor of alongrange motion leaves 24 elementary maneuvers. While this set of 24 is a reduced list of possible elementary maneuvers, some of the maneuvers remain very complex, and are not feasible here.

Of these 24 remaining elementary motions, some are still more realistically feasible than others. Examining the remaining modes, it can be seen that some, such as roll-yaw combinations during steady hover, ascent, or forward motion, would result in complex dipping motions simultaneous with attempts to maintain or increase altitude or move forward. Similarly, a pitch-yaw combination during steady hover is essentially an attempt to perform a very complex spiraling scanning maneuver, and is unlikely to be feasible. These cuts leave 18 elementary maneuvers.

Additional maneuvers which are very complex are those which specify either rolling, pitching, or yawing while performing forward motion during an alongrange slide, or pitching or yawing during an ascent or descent. After these cuts, 13 elementary maneuvers remain.

A final cut can be made by looking at maneuvers which incorporate any element of pitching and yawing in combination with each other. After this, 11 elementary maneuvers remain, as shown in Table 3. Maneuver numbers are arbitrary, and assigned to afford later convenient reference.

**Table 3. List of eleven feasible elementary motions for a hopping vehicle.**

<b>Num.</b>	<b>X</b>	<b>Y</b>	<b>Z</b>	<b><math>\theta</math></b>	<b><math>\phi</math></b>	<b><math>\psi</math></b>	<b>Mode name</b>
1	-	-	-	-	-	-	Steady hover
2	-	-	-	-	-	X	Steady hover with crossrange scan
3	-	-	-	-	X	-	Steady hover with downrange scan
4	-	-	-	X	-	-	Steady hover with horizon scan
5	-	-	X	-	-	-	Alongrange slide
6	X	-	-	-	-	-	Ascent/descent
7	X	-	-	X	-	-	Ascent/descent with spiral scan
8	X	-	X	-	-	-	Ballistic launch and glide
9	X	-	X	-	-	X	Ballistic launch and glide with sidescan
10	X	-	X	-	X	-	Ballistic launch and glide with trackscan
11	X	-	X	X	-	-	Ballistic launch and glide with horizon scan

Note that maneuvers 8-11 are described as ‘ballistic.’ These maneuvers are associated with the ballistic hop mode, where the hopping vehicle moves in a ballistic arc over a long distance instead of in short and relatively straight segments. These maneuvers include simultaneous translation in the X (vertical) and Z (alongrange) axes, which represents the motion of the vehicle following a large impulse delivered quickly in the direction of motion. Therefore, maneuvers 8-11 include at least some periods of coasting, when the hopping vehicle travels without its main propulsion system operating. All the other maneuvers are constant-burn, meaning that small impulses are continually applied. Although a ballistic hop is a more traditional hopping maneuver, and may be advantageous in that it offers a relatively disturbance-free coasting phase, the alongrange slide (also called a hover hop of a fixed-altitude, fixed-attitude traverse) offers closer views of the nearby terrain, plus the ability to stop and move in a different direction at any moment.

### **3.2.2 Additional Grammar Elements**

The motion grammar now includes a list of the elementary maneuvers making up the vocabulary for a hopping vehicle, which can be connected to form a description of a hop. A few basic rules provide guidance in organizing the elementary maneuvers into coherent hops.

First, every hop must begin and end with a vertical ascent or descent maneuver. This represents a sheer vertical takeoff and a sheer vertical touchdown, which bookend any other maneuvers carried out during the hop. Secondly, any touchdown must be immediately preceded by a landing cycle, which is an alongrange maneuver (number 5) which seeks out a safe landing footprint. The length of the landing cycle is driven by the Golombek model (65), (66) of the planetary body's surface roughness. Thirdly, any ballistic maneuver (numbers 8-11) must be preceded and postceded by an instance of an alongrange tilt (number 3), as this represents the alignment change between the default steady hover mode and the tilted ballistic travel mode. Fourth, every elementary maneuver is self-contained: it includes allowances for starting and stopping the described motion, as well as executing it. Finally, the steady hover mode is assumed as the default mode. Transitioning from any one elementary maneuver to another always involves passing through the steady hover mode, even if only instantaneously. If a mission designer wishes, he or she may explicitly place extended-length steady hover maneuvers in between all other maneuvers; otherwise they are not directly accounted for in the maneuver list which describes a hop.

### **3.2.3 Using the Motion Grammar to Describe Hops**

Using the 'vocabulary' of the elementary maneuvers and the 'grammar' of the rules, it is possible to describe a hop as one would describe a grammatical sentence, composed of smaller elements

(words or elementary maneuvers). Once a hop is described, it can be strung together with other hops to describe a campaign of hopping that constitutes a complete mission. An entire program of scientific exploration on another planetary surface can be described in detail using the motion grammar developed in this thesis.

Once the maneuver list has been developed through the motion grammar, and the payload and planetary body have been specified, the mission concept is considered formalized. An example of a formalized mission concept is moving a mass spectrometer from the landing point through a hovering traverse across 500 meters of flat terrain, over a 4-meter crater rim, and hovering slowly 7 meters down the crater rim's inner face before touching down on the crater floor, and then performing in-situ science while landed.

To create this description, a mission designer can select elementary maneuvers from the list of eleven possible elementary maneuvers, within the relatively light restrictions applied by the grammar rules. When connected completely from takeoff to touchdown, this list of maneuvers describes a hop. Several hops in series describe a mission. Because the motion of the hopping vehicle is such an important driver of its abilities and of its design, this list of maneuvers for one or more complete hops (which we can refer to as a flight profile) is a major user input and starting point for sizing the hopping vehicle.

However, once the flight profile is created, the flight profile needs to be translated into fuel used or delta-V required. To do this, some parameterization of each maneuver in the flight profile is required, as seen in Table 4.

Num.	X	Y	Z	$\theta$	$\phi$	$\psi$	Mode name	Sizing parameter	Governing parameter
1	-	-	-	-	-	-	Steady hover	Time	-
2	-	-	-	-	-	X	Steady hover with crossrange scan	Degrees	Deg/sec
3	-	-	-	X	-	-	Steady hover with downrange scan	Degrees	Deg/sec
4	-	-	X	-	-	-	Steady hover with horizon scan	Degrees	Deg/sec
5	-	X	-	-	-	-	Alongrange slide	Distance	Max V
6	X	-	-	-	-	-	Ascent/descent	Distance	Max V
7	X	-	X	-	-	-	Ascent/descent with spiral scan	Distance/Degrees	Max V, deg/sec
8	X	-	X	-	-	-	Ballistic launch and glide	Distance	-
9	X	-	X	-	X	-	Ballistic launch and glide with sidescan	Distance/Degrees	Max V, deg/sec
10	X	-	X	-	X	-	Ballistic launch and glide with trackscan	Distance/Degrees	Max V, deg/sec
11	X	-	X	X	-	-	Ballistic launch and glide with horizon scan	Distance/Degrees	Max V, deg/sec

Table 4. List of eleven elementary maneuvers and associated parameters.

Additionally, a simple convention for describing mission flight profiles will be used. This convention uses maneuver tag numbers, followed by parameter values in parentheses, to indicate individual maneuvers in a mission. If the maneuver is to be marked as a science segment, it will be bolded. If additional information is required to be input by the user, such as the direction of a traverse or a binary flag for a touchdown maneuver, it will be included in the parentheses. For example, the maneuver sequence 6(25) – 5(500@90) – 6(-25/1) – **13(300)** – 14(900) compactly describes a full mission. The first and third terms describe an ascent to 25 m and a descent and touchdown from 25 m, respectively. The second term describes a 500-m hovering traverse (or alongrange slide), in an angular direction of 90 degrees by the compass. The fourth term describes a science segment lasting five minutes, while the fifth and last describes a communications segment lasting fifteen minutes. This convention will be applied in this thesis whenever a mission profile is described numerically.

### **3.2.4 Using an Action Grammar to Describe Additional Behaviors**

Much as the motion grammar describes how the hopping vehicle moves, an action grammar is a means for systematically describing how a hopping vehicle behaves overall. Accordingly, an action grammar is a superset of the motion grammar, and includes possible actions a hopping vehicle can undertake that involve no motion, as well as any rules for the order in which it must undertake them.

The action grammar used in this thesis will include an action vocabulary of six elementary types of actions, including moving, collecting data, transmitting data to Earth, performing internal housekeeping and maintenance, recharging, and sleeping.

The elementary action category of moving includes a large number of lower-level motions, which are all contained in the motion grammar detailed in the previous section of this thesis. The other action categories represent other key actions carried out during a planetary surface exploration mission. For instance, the main value delivery function of such a mission is the collection of data, and transmitting that data to Earth is a key supporting function. In addition to these three categories of actions, other supporting functions include maintaining the exploration vehicle's capacity to continue to move, collect data, and transmit it to Earth. These functions are split here into the three categories of housekeeping, recharging, and sleeping. These three categories of action are distinguished by the differences in data generation and power use that they require.

The housekeeping function refers to any action wherein internal computational actions may be taken. This function includes a power requirement for passive power to the instruments, plus

base power to the main avionics. It also includes some small amount of data generated for later analysis by the mission control staff, which is uplinked during the next communications segment. Because the amount of housekeeping data is typically not significant compared to the data generated during a science mission segment, that amount of data is simply piggybacked onto the science segment's communications backlog.

The recharging function refers to housekeeping or similar functions which are carried out without generating any data that must be uplinked to the mission control station later in the mission. Thus, this action category includes passive power to the scientific instrument payload as well as avionics base power, but no data generation. Finally, the sleep function is intended to cover last-ditch situations or very low-power situations, where everything but base power to the avionics is shut down.

Any situation where the vehicle is moving is described by the motion grammar, and any motion segment can be a science segment as well, when the payload is operating. Payload operations can also occur when the vehicle is resting on the surface of the planetary body (not moving). However, the other action categories can only occur when the vehicle is not moving. The action grammar is intended to provide an exhaustive description of possible actions for periods when the vehicle is sitting. Accordingly, they must describe situations when the payload is not being used actively (and thus is drawing no more than passive power), and when a communications segment is not occurring. Any communications segment must occur while the vehicle is sitting on the surface and not using its science payload.



Thus, if the vehicle is moving, its actions can be described using the motion grammar. If it is running instruments, it is either sitting or moving, but can do nothing else. If it is communicating, it cannot be moving or running its payload. When it is sitting (i.e., not moving), not running its payload, and not communicating, the other three action categories can be used to describe what it is doing. Table 5 clarifies where the various descriptions apply.

<u>Providing instruments with passive power?</u>	<u>Generating data to transmit later?</u>		
		<u>Yes</u>	<u>No</u>
	<u>Yes</u>	<i>Housekeeping</i>	<i>Recharging</i>
	<u>No</u>	<i>Not applicable</i>	<i>Sleep</i>

Table 5. Applicability conditions for non-moving action grammar modes.

Note that only one possible action category is not used, as it is not sensible to generate data during a period when even the instruments are not being provided with passive power. The generation of housekeeping data implies that power is available to provide passive power to the scientific instrument payload.

### 3.3 Mission Designers as Users of the Hopping Vehicle Model

The goal of this thesis is to create a model that will bring hopping vehicle technology into the space of possible options for exploration missions on the surfaces of planetary bodies in our solar system.

To create such a model, it is necessary to understand the needs of the intended users. The intended users are people who make or support the making of high-level decisions about unmanned missions to explore the surfaces of other planetary bodies in our solar system. These

users would most likely be program managers, chief mission engineers, or their support staffs. Such users would be interested in understanding the programmatic costs and risks of fielding a hopping vehicle to perform a mission, and in being able to evaluate how changes in the mission might affect these costs and risks. Since many key decisions about such missions are made early in the design lifecycle, the tradespace model developed in this thesis will be applicable to these early design stages. The tradespace model will generate results that will be useful during Phase A or pre-Phase A work to define a mission, and will help missions designers decide whether to proceed with a hopping vehicle design to the next phase.

A mission is defined here as a concept involving the movement and use of a scientific instrument or set of scientific instruments around the surface of a planetary body. A planetary body is a planet, asteroid, Near-Earth Object (NEO), comet, or moon in the solar system. Although gas giant planets fall within this definition, for the purposes of this thesis, planetary bodies will consist of those bodies which have solid surfaces and upon which a physical landing can occur.

Therefore, a good example of an early-phase mission concept would be “perform spectrometry on soil samples from the rims and floors of craters on Mars.” A mission which requires a scientific instrument to be moved around a planetary body is amenable to hopping. It may also be amenable to the deployment of a fleet of landers, rovers, or some other form of surface motion, but in this thesis we focus on the details of performing the mission via hopping technology. This early-phase mission concept can be rephrased as a need of the mission designers. The mission designers need to take a given action with given items, and the action needs to have certain attributes (e.g., its exact location). The mission designers are willing to

trade resources and take risks to meet this need, and are interested in exploring some alternative means of meeting their needs as well.

### **3.3.1 Benefits of a Tradespace Model**

In order to assess a hopping vehicle for a mission, mission designers should also be able to evaluate the effects of small changes in the design parameters. Typically science requirements (the decisions made about what measurements to capture, and where and when to capture them) drive the development of high-level mission technical requirements. For the purposes of this thesis, the science requirements are encapsulated in the mission concept, and the selection of some high-level technical requirements is carried out by formalizing the mission concept. For instance, the flight profile describes high-level mission requirements.

However, once the requirements have been defined (in this case, via the formalization of the mission concept), mission designers may wish to make tradeoff analyses, for which they will wish to understand the effects of changes in the mission target planetary body, payload, or flight profile on the resulting technical characteristics of the hopping vehicle which can perform the mission.

Tradeoff analyses are critical in space systems engineering work, and often focus on the effects of a change that would be beneficial to one subsystem as applied to all other subsystems, and the mission as a whole. Tradeoffs may include the sizing of various subsystems or the selection of technologies for subsystems, and mission designers will seek to optimize the benefits of the mission within available technical, financial, and programmatic resources (67). For this purpose,

it is beneficial to have a tradespace model, which can produce individual point designs, but which also can support analysis of multiple designs or comparison of designs with different characteristics.

### **3.3.2 Evaluating a Hopping Vehicle for a Mission**

In order to assess how a mission might be addressed with a hopping vehicle, mission designers need to know what resources must be spent on the hopping vehicle, and also desire to know the sensitivities of the resource levels to small changes in the mission. Mission designers also are often interested in the risks inherent in committing their resources, and in the trades between cost, performance, schedule, and these risks.

Accordingly, a mission designer needs a way to evaluate a mission. We here assume perfect performance – that is, we assume that a mission as specified by a mission designer will be carried out as specified, and that no significant component or system failures will occur. Mission designers must also evaluate cost, schedule, and risk. The costs in which a mission designer is interested include development cost, build cost, and operations cost. For the purposes of this thesis, schedule will be addressed by the cost dedicated to development and build (with the rationale that money for a development project can be spent on a few people for a long period, or many people for a short period), and also addressed in later life cycle stages via detailing the operational lifecycle of a hopping mission.

Risks will be assessed via Technology Readiness Levels, or TRLs. Because most technologies that might be used on a hopping vehicle are technologies relatively common on other space

exploration vehicles, such as power systems, communications systems, and thermal control systems, they are likely to be of a relatively high TRL. Payload technologies may be at TRL 6 or 7, but this is fairly common for a payload, as it is not common for a payload instrument to be flown multiple times. Typically it is replaced by the next generation of advanced technology. However, the engine used on a hopping vehicle may or may not be at a high TRL, and thus the TRL of the hopping vehicle's engine serves as a proxy for risk in the development process.

In addition to generating means of addressing development cost, build cost, operations cost, and risk assessments for the entire system, the model developed in this thesis will also prepare a breakdown of the subsystems on the hopping vehicle, enabling further insight into the development process for mission designers.

The means of specifying a mission's performance, the details of estimating costs and risks, and other descriptions of the model's internal machinery are described in Section 3.4.

### **3.4 Model Details**

The hopping vehicle model is composed of a linked series of MATLAB scripts. One overarching script manages the entire process, calling other submodules, initializing variables, and writing stored search history to an external Excel file. There are thirteen submodules, which will be described in detail in the following sections. Altogether, these submodules and the overarching module work to generate a technical model of a hopping vehicle, including cost and operational concerns.

### 3.4.1 Model Overview and Overarching Module

The hopping vehicle model relies on a series of modules, linked together in MATLAB, to design and size a hopping vehicle. These modules are linked together by one overarching module, which calls the other modules at appropriate points and tracks major variables in the program. A view of the structure imposed on the overall model is seen in Figure 9.

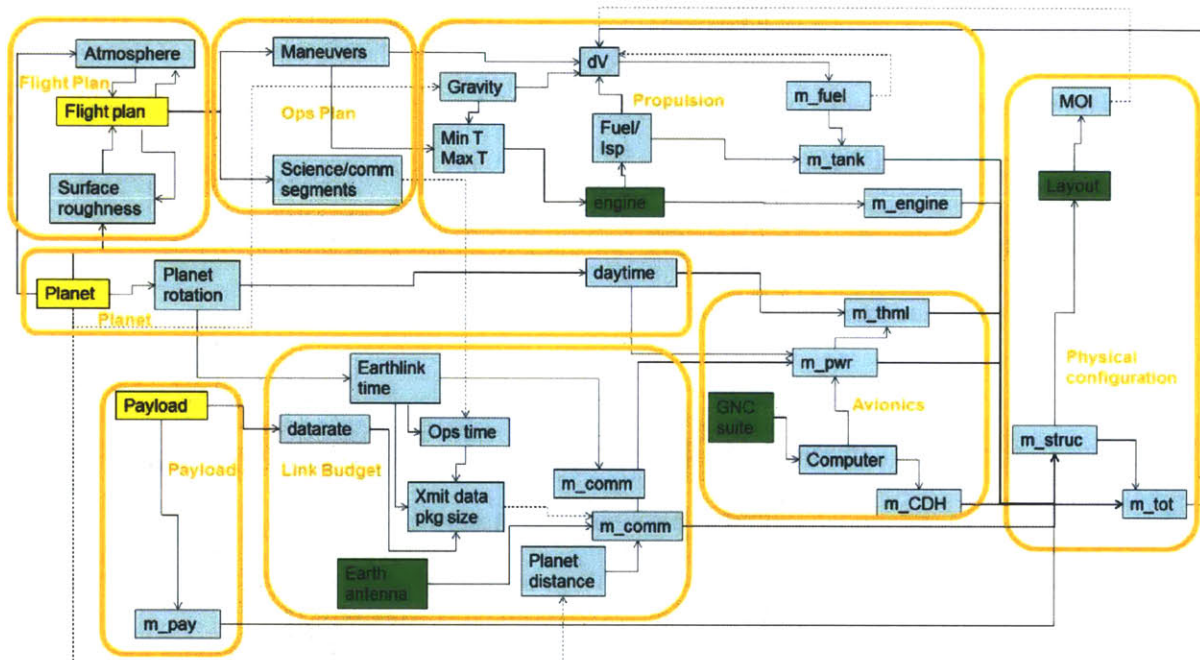


Figure 9. Diagram of model structure, showing software modules in orange, values passed in blue, user inputs in yellow, and master parameters (adjustable by advanced users) in green.

In Figure 9, blue boxes represent information values created and passed in the model. Yellow boxes represent user-input values, and green boxes represent parameters or automatically selected values. The values in green boxes can also be changed by advanced users of the model. Separate modules of code are highlighted and named in orange. Modules related to cost

estimates, master parameters, visualization, and the overarching code are eliminated for clarity. Thus, Figure 9 shows the mass-based hopping vehicle sizing routine in some detail.

The model is differentiated into three major segments. The first segment includes the Planetary Body and Payload modules, as well as the Flight Plan and Operations Plan modules. This segment collects and collates user input, which in turn represents a formalized version of a hopping vehicle mission concept.

The second segment analyzes the user input to create a subsystem-level model of a hopping vehicle. It includes the Link Budget, Avionics, Propulsion, and Physical Configuration modules. Additionally, it includes a loop structure to size the hopping vehicle's propulsion system. This loop structure is governed by the Overarching module, and iterates between the Propulsion and Physical Configuration modules. The Propulsion module first estimates a propellant amount and a tank size based on an initial mass estimate, and then feeds the information to the Physical Configuration module, which collates all mass information and creates a new mass estimate, based on this information and the output of the Avionics and Link Budget modules. This new mass estimate is then fed back to the Propulsion module, which repeats the iteration based on the revised mass estimate. This process continues until the revised mass estimate and the old mass estimate converge within a certain tolerance. This tolerance is set from the master parameter list, and can be adjusted by an advanced user.

Once this convergent mass estimate is reached, the results are wrapped in a margin factor. Both the margin factor and the iteration tolerance can be adjusted by an advanced user. Finally, the

third segment of the model is activated. This segment includes the Cost and Visualization modules, as well as the later sections of the Overarching module. This segment is used to generate outputs for the user.

### **3.4.2 Payload Module**

The Payload module allows the user to select science instruments to be used as the hopping vehicle's payload. The module draws from a database of science instruments, into which seven existing science instruments have been entered. The database is in Excel, and the user is able to enter a new science instrument into the database easily.

The original database is designed to accept new additions easily because new scientific instruments are constantly being created, and typical motivation for exploring a new planetary surface includes a need to study it using new scientific tools. Ideally, a user would simply enter a few key parameters related to a scientific package available for use in hopping missions; however, building the model with only this mode of input would require that all users be familiar with scientific instruments, and would thus render the model more difficult for some users.

Accordingly, a series of seven scientific instruments, used for a small range of purposes, was assembled and preloaded into the database. While the database is intended to permit users to load in their own instruments, the preloaded instruments permit rapid selection of a roughly analogous or interesting science package.



The seven preloaded instruments include the Alpha Particle X-Ray Spectrometer (APXS), the ChemCam, a drilling/coring device based on the Rock Abrasion Tool (RAT), a panoramic camera, a precision camera, a simple magnetometer, and a Sample Analysis Bay, which is a combination of several chemical sensors into a large package, and which is intended to provide detailed information from in-situ analyses of soil, rock, or gas.

All the seven preloaded instruments were based on data available for existing scientific instruments. Data was collected on the mass, volume, active power requirement, and passive power requirement (if any) for the instruments, using several sources describing the instruments. Instrument data collection rates were also captured or inferred from information on instrument capabilities, and where possible, an approximate amount of analysis time necessary for a given amount of instrument data was collected, or estimated based on turnaround times and approximate complexity of the data and probable number of analysts needed. Development and build costs were also collected, or estimated from information available regarding the size of the contracts for instrument construction. For scientific instruments added by the user to the database it is assumed that this information will be available or can be estimated.

The APXS was based on a similar tool aboard the Mars Science Laboratory (MSL) (68), (69). Cost information is estimated from (70).

The ChemCam, a combination of a precision camera and a ranged spectrometer (71), (72) , is used to select samples for further analysis, and is currently flying on MSL. Its cost was estimated based on the costs estimated for other spectrometers and cameras.

The driller/corer tool was based on the MER's Rock Abrasion Tool (RAT) (73). Cost was estimated from (74) and a few assumptions about the prominence of NASA contracts in the firm's quoted annual revenue. The cost was split 95%-5% between development and building.

The panoramic camera instrument was based on the mast camera instrument on MSL, and its precursor on the MER missions (75), (76), (77). Cost information was taken from (78) and (79).

The precision camera was based on the Mars Hand Lens Imager onboard MSL (80), (81), (82).

The magnetometer was given simple assumed characteristics, as a magnetometer is in general a straightforward instrument and simple to develop.

The complex Sample Analysis Bay was based on similar scientific sample analysis suites carried on Viking (83) and MSL (84), (85).

The Payload module displays a list of available instrument names to the user via the command-line interface. The user selects one or more instruments to form the payload and indicates when selection is complete. After checking for and eliminating input errors, the program summarizes the mass, volume, power, data rates, and other information for the entire payload. For the remainder of the model, the entire payload will be considered to act as a single unit, as this allows for conservative estimates of the payload requirements and simultaneously simplifies the user interface somewhat, in that the user need not specify a detailed operating profile for each separate instrument (this is a reasonable simplification, as often instruments will act in concert).

### **3.4.3 Planet Module**

The planet selection module permits the user to select a planetary body on which to operate. The module generates a list of planetary bodies in the solar system which could be feasible targets for hopping missions. The user can then select a planetary body, which sets the planetary body characteristics for the rest of the modules. The characteristics set are the planetary body's gravity, atmospheric density, length of diurnal cycle, minimum and maximum surface temperatures, and average orbital distance from the Sun. An additional parameter set is the typical Golombek parameter for the planetary body's surface, which is the typical percentage of the planet's surface covered by rocks. This parameter is used in calculations related to the landing cycle, and is described in detail in Section 3.4.4.

The planetary bodies included in the feasible list are those which might be targets for hopping missions. They include the rocky inner planets, certain moons of the outer planets (and Earth's moon, Luna), as well as the larger minor planets. The list is intended to cover a range of targets, and is not necessarily meant to be exhaustive. None of the bodies on the list are small enough that they would be targets more for rendezvous and docking-type operations than landing-type operations, as is the case with Phobos and Deimos, the two moons of Mars.

The entire list appears in Table 6. Notable bodies on it are Luna and Mars, which are the two best-explored planetary bodies (and still a source of significant interest for scientific, mining, and potentially colonization purposes) and are likely to be among the first targets considered for any hopping vehicle mission. Other notable bodies include Titan and Europa, moons of the gas giant

planets which may contain volatiles in significant amounts, as well as several of the larger minor planets, including Ceres in the inner solar system and Pluto, Eris, and Makemake in the outer system. The larger asteroids round off the list, although they are much smaller than most of the other bodies on it.

Further expansion of the list is possible, given the advances in understanding of the solar system which have occurred in the last decade alone. However, the list currently includes a range of bodies from throughout the solar system, and as such is a reasonable starting point for investigating hopping vehicle missions.

**Table 6. Potential planetary body targets for hopping.**

<b>Number</b>	<b>Name</b>	<b>Type</b>
1	Earth	Planet
2	Venus	Planet
3	Mars	Planet
4	Ganymede	Moon - Jupiter 3
5	Titan	Moon - Saturn 6
6	Mercury	Planet
7	Callisto	Moon - Jupiter 4
8	Io	Moon - Jupiter 1
9	Luna	Moon - Terra 1
10	Europa	Moon - Jupiter 2
11	Triton	Moon - Neptune 1
12	Eris	Dwarf planet
13	Pluto	Dwarf planet
14	Titania	Moon - Uranus 3
15	Rhea	Moon - Saturn 5
16	Oberon	Moon - Uranus 4
17	Iapetus	Moon - Saturn 8
18	Makemake	Dwarf planet
19	Charon	Moon - Pluto 1
20	Umbriel	Moon - Uranus 2
21	Ariel	Moon - Uranus 1
22	Ceres	Dwarf planet

#### **3.4.4 Golombek Model Utilization**

The current standard for surface roughness in a local area of a planetary body is a model originally proposed by Golombek and Rapp (86). This model describes the distribution of rocks of a certain diameter or larger, and can relate rock height to rock diameter as well. The model, which is a power law with fit parameters derived from analysis of data from the Viking landing sites on Mars and from some Earth analogue sites, is also indicated by Golombek and Rapp to be logically consistent with the current understanding of fracture mechanics and fragmentation mechanisms for rocks. The model is driven by these derived fit parameters and an estimate of the total area covered by rocks in the local region. The fact that the fit parameters have been

fine-tuned based on data from multiple planetary bodies indicates that the model can be generalized to other planetary bodies as well – the surface roughness indicated on any planetary body will be a function of the total rock coverage at that location on the planetary body. The total rock coverage parameter varies from location to location on a given planetary body, with Mars having a modal coverage of 6%, with minima near 1% and maxima near 40% (for small regions) or even 100% (for the inner rims of craters) (86).

Golombek et al.'s follow-up paper (87) supports this original analysis of ground coverage by noting that rock height is typically half of the rock diameter. Because the hazard of relevance for a lander or hopping vehicle is the height of a rock, as landing with one footpad on a high rock may result in tipping or falling during touchdown, this relationship allows an assessment of what portion of total ground area is unsafe for touchdown. If a certain rock height is known to be too high for a safe landing, the Golombek model can predict what percentage of the total ground area will be covered by rocks of that height or larger, if given as an initial parameter the total fraction of ground covered by rocks. Because the power-law model is not an exact match for reality, at the lower diameter end of the scale, the data tend toward saturation, with the fractional coverage rising. At larger diameters, the data drop off, with the Golombek model overpredicting the prevalence of rocks above about 0.8 m in diameter. Thus the Golombek model is conservative for larger diameter rocks.

However, total ground coverage by rocks is a parameter that varies from one planetary body to the next, and often from one region of a planetary body to another as well. For the purposes of this model, a small distribution of total rock coverage fractions was estimated. Three relative

levels of coverage (low density, medium, and high density) were chosen, based on information from (65) which indicates that 5% rock coverage is a good model for low density coverage, while 12% is a good model for medium coverage and 30% is a good model for high-density coverage. These three densities map approximately onto high-coverage craters, less dense crater fields, and background areas; however, for purposes of this model, it will be assumed that one density captures the character of the entire planetary body's surface. While this is not completely realistic, it is reasonable, in that some planetary bodies, like Earth and Mars, have global weather and geologic activities which may be expected to break down rocks, while airless and remote bodies like the moons of Uranus or Saturn can probably be expected to display very rough features over most of their surfaces. Furthermore, while any given patch of ground has one applicable coverage fraction, a hopping vehicle will very likely see several types of ground during its mission or even during one hop, and as such an average coverage fraction is a more meaningful assessment of the coverage at a hopping vehicle's probable landing site. While more detailed mission design would require specific rock coverage estimates for the sites being considered, the model developed in this thesis is for initial design work, and as such it is reasonable to use an average coverage fraction.

Translating fractional surface coverage by rocks into effects on hopping vehicles is accomplished by translating the coverage into an additional flight distance for a hopping vehicle. Since coverage is stochastic, clear areas (areas free of hazardous rocks) will be scattered throughout the terrain in between the rocks. The distance between any randomly-selected spot on the surface and the nearest clear area large enough for a hopping vehicle to touch down is a probabilistic function of the rock coverage.

This probabilistic rock coverage problem was already addressed by Bernard and Golombek (66), which provides a method to calculate the number of hazardous rocks and guidance for calculating the risk of mission failure given this information and knowledge of the size of the lander. It is also possible to calculate the risk of landing on a hazardous rock of a given size if hazard avoidance capability exists. From this information, a model for hopping vehicle landing cycles was developed, which relies on a conservative model of a hopping vehicle's size and clearance requirements (the model assumes a hopping vehicle with a footprint 2.5 m on a side, and 0.25 m clearance vertically). This model generates the probability of mission failure (due to landing on a rock too large for the hopping vehicle to handle), given that the hopping vehicle can traverse a short distance laterally and thus cover more ground. As the hopping vehicle covers more ground, it passes over multiple landing sites, as the surface is modeled as a series of footprint-sized landing sites tiling the surface. Given that Golombek and Bernard's (66) assumption that rock distributions are independent remains true, the probability of landing on a hazardous rock drops as the hopping vehicle encounters multiple landing sites, due to the increase in the probability of finding at least one site with no hazardous rocks.

The landing mode of a hopping vehicle is assumed to consist of a vertical descent to near the surface of the planetary body, followed by a short lateral traverse just above the surface until a suitable landing footprint is located. Mathematically, this is modeled as a descent vertically down to the surface, plus a lateral traverse at reduced speed. Raising the lateral distance traversed during the landing cycle then drops the chances of landing on a hazardous rock; it is assumed that traversing a distance such that the probability of failure is less than 1% is sufficient



to guarantee a safe landing. As such, the model takes the relative total ground coverage by rocks as an input and can be used to find a necessary traverse distance to have a 99% chance of a safe touchdown during the landing cycle. For the conservative hopping vehicle model used here, the landing cycle traverse distance extends from 39.5 m (for a heavily-covered 40% rock region) to 0.75 m (for a very lightly covered 5% rock region). These traverse distances, and the delta-V costs they incur, are added into the delta-V costs already incurred by the flight profile mapped out by the user.

Because we have very limited knowledge of the terrain of many small planetary bodies in the solar system, it is assumed that this lateral landing traverse must always be undertaken during every hopping vehicle landing. Fine-tuning of the traverse distance for different planetary bodies is accomplished by making an analogy between known rock coverage levels on the two planetary bodies with explored surface areas (Luna and Mars) and unexplored bodies. This allows the general Golombek surface roughness model to have some specific applicability to a target planetary body, simply by inputting the average rock coverage for the target planetary body into the model.

### **3.4.5 Flight Plan Module**

After the user has selected a science payload and a target planetary body, he or she will input the list of maneuvers and operations that the hopping vehicle should perform. This is the final step in formalizing a mission concept into an analytical description of a hopping vehicle mission, and relies on user understanding of the action grammar described earlier in this chapter, as well as some user knowledge of the mission concept.

The Flight Plan module displays a short list of the available maneuvers in the mission grammar, as seen in Figure 10.

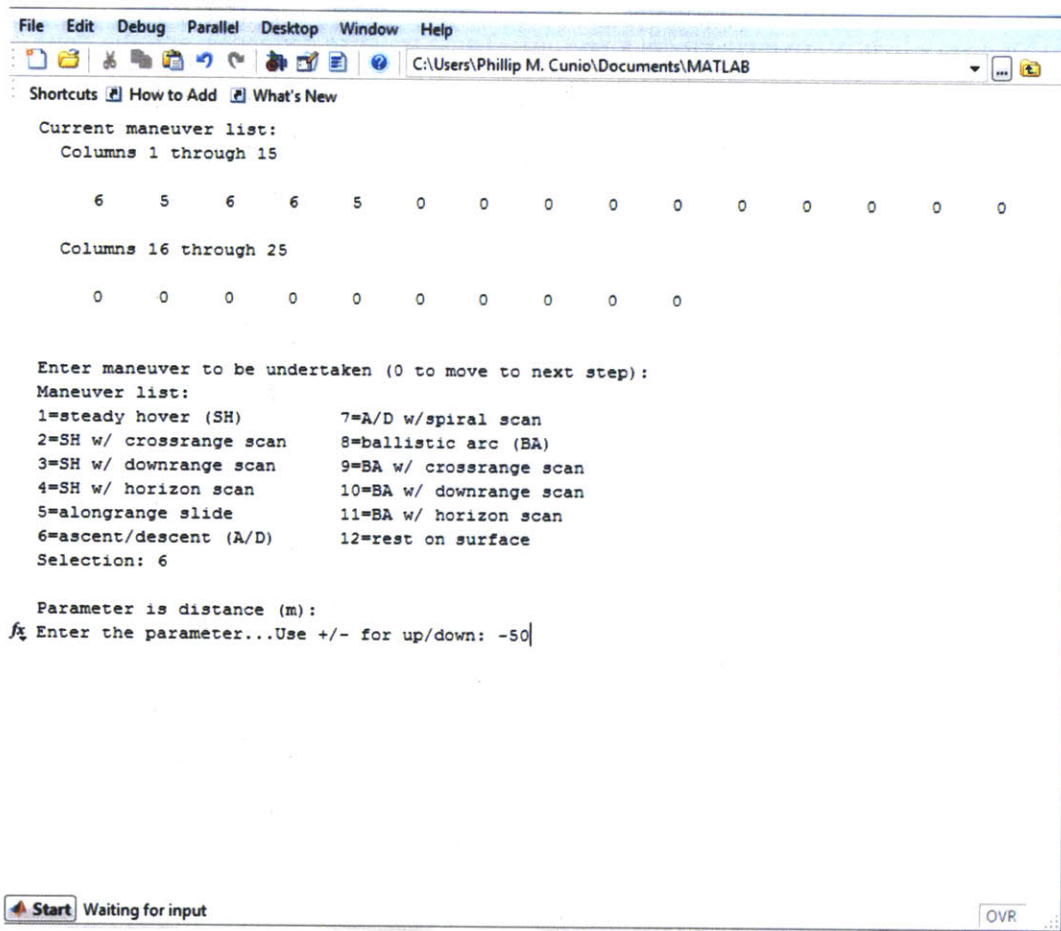


Figure 10. Display showing list of available maneuvers.

The model lists the 12 maneuvers in the motion grammar, and asks the user to select one by number. Once the user has selected a maneuver, the program displays a line listing the parameters used to size the maneuvers. The parameter used depends on the maneuver selected. For instance, maneuvers without lateral translation or rotation rely on a time parameter

(examples are resting on the surface or hovering steadily). Maneuvers with lateral translation are sized by distance covered (vertical translation is also sized this way), and maneuvers with rotation are sized by the angle through which the vehicle rotates.

For each maneuver on the list, a delta-V cost, scaled according to the sizing parameter, is calculated. For instance, a steady hover must counteract the planetary body's gravity, and so a delta-V cost equal to the planetary body's gravitational acceleration is assessed for every second of hover time. For translational and rotational motions, assumptions about reasonable speeds and accelerations are used to size delta-V costs.

Finally, delta-V costs for the entirety of the mission are added together, resulting in a total delta-V used. This is later used in an overall sizing routine for the hopping vehicle.

Maneuvers on the list are described in detail in Sections 3.2.1 to 3.2.4. However, available maneuvers consist of eleven motions (including ascent/descent, horizontal translation, various rotary scanning motions, and parabolic ballistic arcs), plus a twelfth maneuver, resting on the surface. Resting on the surface implies that the vehicle is not moving and engines are not running, but there are several actions which can be undertaken when the engines are not running. These actions include collecting science data (via operating the science payload), transmitting science data back to Earth via the communications subsystem, performing internal housekeeping, allowing the batteries to recharge, or entering a power-conserving sleep mode. These actions have different consequences, chiefly on the power demands. Science data collection requires sufficient power to operate the payload (which depends on the active power demands of the

payload); transmitting data back to Earth requires running the communications equipment (which depends on the time allotted to the communications period, and the distance to Earth – these are detailed further in Section 3.4.7); internal housekeeping permits the science payload to be reduced to passive power levels, but creates a small amount of housekeeping data which will be transmitted back to Earth at the next communications opportunity; and sleep mode powers down the science payload and turns off everything but the base power required to keep the vehicle alive.

The Flight Plan module also runs a Golombek routine on the accumulated maneuvers, wherein every touchdown maneuver incurs an additional delta-V cost proportional to the surface roughness of the planetary body. This accounts for the need a hopping vehicle has to traverse laterally a short distance to find a safe landing spot (it is assumed that onboard GNC sensors and software are capable of locating and selecting such a spot).

Additionally, the Flight Plan module accounts for atmospheric drag. It locates maneuvers which include a lateral traverse in the hover-hop mode (those tagged 5) or those which include a ballistic lateral traverse (those tagged 8, 9, 10, or 11), and calculates the additional delta-V that would be lost in performing such a traverse, then adds makeup delta-V to the maneuver. The delta-V lost is calculated by assuming a conservative size for the hopping vehicle, then calculating the drag force and estimating the impulse lost to it. Drag force is a direct function of atmospheric density, which can be calculated from knowledge of the atmospheric pressure on the surface of the planetary body, coupled with a small assumption about the average size of the molecules that make up the atmosphere (a molecular weight of 10 g/mol is assumed, as this

presupposes some mix of oxygen, nitrogen, and carbon in monoatomic form with a smaller amount of more complex molecules, such as carbon dioxide, methane, or diatomic gases). The consequence of this assumption is that drag force, and delta-V lost to drag, drops to negligible levels as the atmospheric pressure on planetary bodies becomes effectively zero.

The Flight Plan module assumes hopping vehicle operation begins with the hopping vehicle sitting on the surface of the target planetary body, and thus does not account directly for landing operations. This helps to maintain a tradespace model that is agnostic to the landing method (which may vary widely from one mission to another), and that is easy to use to evaluate a hopping mission on its own merits. The model produces the characteristics of the hopping vehicle that will begin the mission from rest on the planetary surface, and mission designers can account for the landing and other mission phases as appropriate using the information supplied about the hopping vehicle itself.

#### **3.4.6 Operations Plan Module**

Additional formalization of the mission concept is created by the user through interaction with the Operations Plan module, which tags each maneuver created during the Flight Plan module with additional important information. Each maneuver is tagged with flags indicating whether the mission segment is a science segment and whether it is a communications segment.

The Operations Plan module also produces four logs of actions taken. A power log tracks the power level required at each mission segment (some differentiation is generated by the fact that flight maneuvers require powering the GNC package, while surface actions do not), while a data

log tracks the amount of data accumulated onboard the hopping vehicle. A similar log, the analysis log, tracks the amount of analysis work required that has accumulated (this is driven by the amount of data accumulated). The communications log tracks mission segments when communications links occur, and resets the data and analysis logs to zero, as a communications interval represents a downloading of all information onboard the hopping vehicle to a ground station.

The information developed in the Operations Plan module permits detailed analysis of the power levels required for a hopping mission, as well as of the major operational actions (flight, science, and communications). The module also generates a timeline, which plots each mission segment along a time axis, and permits overlaying of key information on that timeline by mission segment. Since each mission segment is not necessarily of the same length as other segments, this permits a moment-by-moment view of the mission as planned, permitting additional insight into the operational aspects of the mission.

#### **3.4.7 Link Budget Module**

The Link Budget module is the first of a series of hopping vehicle modules that work together to size the hopping vehicle bus. These modules, the Link Budget, Avionics, Propulsion, and Physical Configuration modules, generate a size for the hopping vehicle's dry bus mass, based on the power and communications requirements implied by the choice of science payload, operational profile, and target planetary body.

The Link Budget module begins this process by tracking mission segments when communications are occurring, and looking up the necessary link rate, which is calculated based on the data backlog accumulated at the beginning of the communications mission segment and the time the communications segment lasts. Thus every communications segment is assumed to exhaust the data backlog accumulated up to that point.

A link budget is then calculated, based on models from (58) and (88). Key parameters for the link budget, including the transmitting antenna efficiency and size, are set as master parameters for the model, and given sensible default values which can be changed by advanced users. The maximum transmission data rate is calculated from inputs given by the user in previous steps. The choice of receiving antenna at Earth can be set to the 34-m dishes used by NASA's Deep Space Network, the 70-m dishes used by the Deep Space Network (this is the default setting), or a user-defined other dish. This allows for some range in the operational aspects, as the choice of which receiving network to use can be a major programmatic decision.

Link margin is also set according to a master parameter with a reasonable default value, as is the transmitting frequency, and losses are calculated. From the link budget equation, required transmitting power can be calculated. This transmitting power is then added into the power log, and a mass for the chosen antenna size is also estimated. Thus, communications requirements are translated into mass and power requirements onboard the hopping vehicle.

### 3.4.8 Avionics Module

The Avionics module sizes most of the remaining electronics onboard the hopping vehicle. A commonly used processor module, the RAD750 board, is selected as the primary command and data handling (CDH) component, and is given an overhead wrap factor to account for additional hardware and redundancies, including a backup processor module. A wiring factor is also added to account for wiring, and a base power level is created. This power level represents the minimum required for the hopping vehicle to function, and power in sleep mode will not drop below this level.

Additionally, a guidance, navigation, and control (GNC) package is added, with its own mass and base power requirements. The GNC package is assumed to be active only during flight segments, and is assumed to focus on the hardware sensors. Any GNC software running on the CDH system is not accounted for specifically, as it is assumed to execute automatically under appropriate limitations, and is further assumed to fit under the power requirement of the CDH subsystem. Standby power for the GNC package and for any mission executive software necessary to activate it is assumed to fit under the base power level for the processor.

The mass and power for the GNC system are set by master parameters for the model, which default to values based on the sensors and architecture used on the TALARIS hopping vehicle prototype, which assumes that this architecture is viable for spaceborne hopping vehicles. The default mass and default power for the GNC package are based on the use of an IMU and multiple laser rangefinders, as used on the TALARIS prototype hopping vehicle (42).



The power system is sized by developing a detailed power log, which is based on base power, communications power, science payload power, and GNC power (for flight segments).

Maximum power requirements are determined from this power log. Then power system architecture is selected based on the distance from the planetary body to the Sun. If the distance is less than 5 AU, a solar-array-and-battery architecture is selected; otherwise an RTG-based architecture is selected. In both cases, after determining the power subsystem architecture type, a characteristic parameter of power density for each architecture type is used to size the power subsystem. For solar array and battery architectures, allowances are made for the end-of-life degradation solar arrays usually experience, and then the solar arrays are sized as well.

The thermal subsystem is also sized, by performing a thermal analysis. For this, the maximum and minimum temperatures on the planetary body are used. This assumption provides maximum generality for analyzing thermal conditions on the target planetary body, but as a consequence cannot account for seasonal or regional temperature variations in depth. For this thermal analysis, radiative heat transfer from the Sun and from the planetary body are considered, as is convective heat transfer from the atmosphere of the planetary body. Conduction, which would normally be expected to occur through the footpads, is ignored, as heavy insulation can be used on footpads. Furthermore, on a planetary body with very thin or no atmosphere, radiation will dominate, and a thick atmosphere will cause convection to dominate over conduction.

Convection is scaled by the planetary body's atmospheric density, so a thin atmosphere will produce very negligible convection, as would be expected. Radiative heat transfer from the Sun is a function of the solar irradiance at the planetary body's distance from the Sun. The baseline

solar irradiance is scaled down by the appropriate distance, and this power is assumed to be absorbed with a given absorption coefficient, which is set based on the master parameter list, and is thus defaulted to a reasonable value, with the ability to be updated by advanced users.

Radiative heat transfer away from the vehicle to space and between the vehicle and the planetary body is set based on the temperature of the planetary body and the vehicle, with the temperature of space set to 3 Kelvin. Absorptivity and emissivity parameters are again set in the master parameter list.

After running a complete thermal balance, the vehicle will be found to need either heaters, radiators, or both, depending on where the vehicle's temperature falls relative to the range of temperatures exhibited on the planetary body. Radiator mass and volume are selected appropriately, as are heater mass. Heater mass is based on a radioactive spaceflight heater developed by the Department of Energy (89).

### **3.4.9 Propulsion Module**

The Propulsion module also relies on a database generated from an Excel file, as do the Planet and Payload modules. This database contains information on characteristics of a small number of rocket engines, selected as exemplars. The engines are sized from relatively small (a hundred newtons of thrust) to large (tens of thousands of newtons of thrust or more), and are all throttleable.

The database, which is detailed further in Section 3.4.9.1 and shown in Appendix B, includes the DM-LAE, Bell 8414, R-40A (the Shuttle's RCS engine), MR-80B, LMDE, TR202, and RL-10B engines. The maximum thrust, fuel/oxidizer type and specific impulse, engine mass, and maximum throttle ratio are included in the database, as well as an estimate for the Technology Readiness Level of the engine.

The Propulsion module sorts the engines by maximum thrust level and by throttling ratio, where throttling ratio is the percentage of maximum thrust by which engine output is reduced when running at minimum thrust (that is,  $R = (T_{max} - T_{min})/T_{max}$ , such that a larger throttling ratio is better). The required maximum thrust and throttling ratio are determined based on the maneuver list input into the Flight Plan module and the sizing routine that the model runs. The smaller engines are not physically throttled, but are pulsed. For the purposes of this thesis, pulsing is treated as effectively able to deliver throttling ratios of 0.20.

After sorting the engines, the Propulsion module determines which engine can deliver the required maximum thrust, and which can be throttled down far enough to deliver the required minimum thrust, where minimum thrust is defined by the highest thrust that will still produce a thrust-to-weight ratio of less than unity in a fuel-emptied hopping vehicle.

Following this, the lowest-mass feasible engine is selected, and model parameters related to the engine's propellant specific impulse are set. Additionally, a propellant tank mass is calculated, based on the amount of fuel required for the maneuver set.

This module works with a baseline engine architecture of four engines, throttled appropriately, as is used on the TALARIS hopping vehicle prototype (41). Additional leverage in the model is provided to the user in the form of the ability to force the model to select a given engine, which allows for the user to mandate the use of a particular technology. The user can even enter the parameters of a specific engine technology into the Excel database and then force selection of that engine.

After setting engine parameters based on the selected engine, the module also sizes the propellant tank. The propellant tank is sized by calculating the mass of propellant required, and then estimating the mass of the fuel tank based on the mass of the fuel. A propellant margin is first added, and then the tank mass is set to 15% (a conservative estimate, according to (58)) of the propellant mass.

#### **3.4.9.1 Engines in the database**

The engines used to populate the engine database are meant to represent a cross-section of available engine technology. Among these engines are both historical examples, such as the engines used by the Surveyor probes (90), and engines currently in development, such as the advanced RL-10 designs (91). A range of maximum thrust and maximum throttle ratio is used; engines range from small and not deeply throttled (the DM-LAE (58)) to very large and with very deep throttling (the TR-202 (92)).

The seven engines selected to form a representative sample are seen in Table 7. The engines were sorted into categories of maximum thrust and maximum throttle ratio, arranged in

approximately ascending order in the table. Note that, due to the default architecture of four engines per hopping vehicle, each engine only needs to produce a quarter of the maximum required thrust by itself.

Where an engine typically used a non-storable propellant, an estimate for the specific impulse of a storable fuel was substituted into Table 7. This affected the TR202 and the CECE/RL-10B engines, with the specific impulse for a different, storable fuel being substituted for the actual fuel; for example, methane is substituted for liquid hydrogen, with a corresponding decrease in specific impulse.

**Table 7. Engine selection table.**

<b>F<sub>eng</sub> = T<sub>max</sub>/4</b>	<b>R = (T<sub>max</sub>-T<sub>min</sub>)/T<sub>max</sub></b>	<b>Engine Name</b>	<b>Propellant Type</b>	<b>Engine Isp [s]</b>	<b>Engine Mass [kg]</b>	<b>References</b>	<b>TRL (est.)</b>
0-500 N	20	DM-LAE	N <sub>2</sub> O <sub>4</sub> /N <sub>4</sub> H <sub>4</sub>	315	4.54	(58)	8
0-500 N	90	Bell 8414	N <sub>2</sub> O <sub>4</sub> /N <sub>4</sub> H <sub>4</sub> -UDMH	254	3.86	(93)	6
500 – 5000 N	20	R-40A/ Shuttle RCS	N <sub>2</sub> O <sub>4</sub> /MMH	281	10.25	(94), (95), (58)	9
500 – 5000 N	90	MR-80B	Hydrazine	204	7.68	(96)	7
5000- 50,000 N	75	LMDE	N <sub>2</sub> O <sub>4</sub> /N <sub>4</sub> H <sub>4</sub> -UDMH	300	224.1	(97)	9
5000- 50,000 N	90	TR202	LOX/LH <sub>2</sub> -> LOX/CH <sub>4</sub>	309 (est.)	127.3	(92)	4
250,000 N	90	CECE/ RL-10B modification	LOX/LH <sub>2</sub> -> LOX/CH <sub>4</sub>	275 (est.)	301.8	(91), (98), (99)	5

Finally, Technology Readiness Levels (TRLs, (100)) were estimated for each of the engines in the database. Because the LMDE has flown successfully on the Apollo LM many times, it was rated at TRL 9. The R-40A/Shuttle RCS engine was also rated 9, for similar reasons. The DM-LAE was also assessed as very mature, and has flown in space, and so was rated at TRL 8.

Because the MR-80B only flew once, it is rated at TRL 7. Other engines with less development history, such as the Bell 8414, CECE/RL-10B, and TR202, were rated at TRL 4, 5, or 6, based on whether the latest available published paper describing them indicated breadboard, component, or system-level functionality having been demonstrated.

#### **3.4.10 Physical Configuration Module**

The Physical Configuration module is used to size the structural mass of the vehicle. It takes in the masses of all the other subsystems, and aggregates them into a bus mass. The bus mass is based on the assumption that a hopping vehicle will have a fairly straightforward subsystems design, and that the major subsystems (power, payload, avionics and GNC, and thermal) can be aggregated physically into a simple body, much like is done for planetary landers like Viking and Phoenix, or like the Mars rovers, which use a body structure to contain and support internal electronics and power systems, with actuation systems and science manipulators placed external to the main body.

The Physical Configuration module aggregates the power, thermal, CDH, communications, payload, and tank masses into a bus mass. Structure mass is then assumed to be a fraction of this total dry bus mass. The vehicle total mass is then calculated by adding the dry bus mass, the engine mass (for four engines), the structure mass, and the propellant mass. This represents the total mass landed on the surface of the planetary body.

The Physical Configuration module does not actually manage configuration or physical layout of components, but it includes hooks for additional functionality that can be added to the module, including calculations related to the volume of the bus and its various component subsystems, as well as the moment of inertia of the whole hopping vehicle. This functionality may be activated in a later version of the model.

The Physical Configuration module runs in a sizing loop with the Propulsion module to set the final vehicle size.

#### **3.4.11 Cost Module Options**

The cost of a hopping vehicle development and operations effort is assessed in the Cost module. The Cost module first sets an inflation factor (which can be set from the master parameter list), which updates 2010 dollar amounts to a future dollar amount. The Cost module is baselined in 2010 dollars, so all results are internally generated in 2010 dollar amounts.

The Cost module produces cost estimates for development, building, and operations costs for the hopping vehicle it considers. Five separate models are available for development and building cost estimation, and the model permits advanced users to select which one to use. All of the cost models are mass-based cost estimating relationships, as this is the most appropriate type of cost model to apply at an early design stage.

#### **3.4.11.1 Draper/MIT CE&R Cost Model**

The default cost model is the Concept Estimation and Refinement (CE&R) set of cost models, developed in 2005 by Draper Laboratory and MIT (101). The CE&R models were developed for use in the Constellation program, and were intended to be applicable to the development of advanced vehicles, without precedent or precursor. This model is thus not as useful for cost estimation of a single satellite in a series, but is appropriate for any project where there is little or no heritage. Thus, any exploration vehicle intended to visit a planetary body which has never been visited before, or any novel exploration vehicle, would be a good fit for modeling with this cost model. A planetary surface exploration hopping vehicle is a good fit here.

The CE&R model is also able to generate some granularity. Using it, separate development and build costs for the hopping vehicle's propulsion, communications, payload, and bus can be generated. The CE&R model includes explicit ability to account for these costs for propulsion systems, in the form of a cost estimation routine for Mars ascent propulsion. This cost estimation routine is applied to the mass of the engines and tank of the hopping vehicle. The communications system is analogized to the surface communications model used in the CE&R suite, and the remainder of the bus is accounted for via the CE&R suite's surface rover modeling relationship. This is reasonable, as the bus of a hopping vehicle is similar in many ways to the bus of a roving vehicle, although the engines and tankage are not. Payload costs come from the Payload module, where they are directly entered into the database by the user, or selected from the pre-existing database entries.

The CE&R modeling relationships include separate development and build costing relationships, making it easy to break these numbers out for the user of the hopping vehicle model.



#### **3.4.11.2 Small Spacecraft Cost Model**

Additional available cost estimating relationships include the aggregated SSCM (Small Spacecraft Cost Model), with parameters taken from (102). This relationship relies on the dry bus mass of the vehicle, so the bus is here revised to include the engines and tankage, as well as the communications system. This model generates a TFU (Theoretical First Unit) cost, which includes development and building of one unit. This cost is broken out into development and build costs artificially by means of a build cost fraction, which is set in the master parameter list. The building cost fraction sets a fraction of the TFU cost as being required for building, rather than development.

The SSCM 8.0, which is a complex function of the communications requirements, power requirements, and propulsion system mass, is also available. It similarly generates a TFU cost, which is artificially broken into development and build costs.

#### **3.4.11.3 Unmanned Spacecraft Cost Model**

The Unmanned Spacecraft Cost Model (USCM), which also relies on dry bus mass and creates a TFU cost, is available as another alternative, taken from (102).

#### **3.4.11.4 Spacecraft Vehicle Level Cost Model**

The final available cost estimating relationship is the Spacecraft Vehicle Level Cost Model (SVLCM), available online (103). It also relies on a dry bus mass estimate, and generates a TFU cost.

#### **3.4.11.5 Operations Costs**

Operations costs are calculated in only one way, unlike development and build costs. They are rooted in three cost sources: personnel, facilities, and communications time. Personnel costs are calculated by assessing the length of the mission timeline, as defined by the model user, and calculating the number of active work days required. The number of team members (which is set in the master parameter list) is then multiplied by this number of workdays and an average cost per person for a worker.

A wrapper on the number of personnel is used to set facility costs. The final cost element, the cost of communications, is set based on the communications system specified by the user. If the user selects either the 70-m or 34-m Deep Space Network antenna as a ground link, the appropriate cost for the amount of communications time specified is generated, according to the official aperture fee formula (104). If the user has selected a user-defined communications antenna, an appropriate cost, scaled from the DSN values, is used.

These three sources of operations costs (personnel, facilities, and communications time), which are based on the operations plan specified by the model user, are then summed to arrive at a total operations cost for the hopping vehicle.

#### **3.4.12 Visualization Module**

Visualization of results is created in the Visualization code module. The Visualization module generates and collates key information about the hopping vehicle design, and then displays it on

screen for the user. Some information is displayed as text in the command window, and some is displayed in pop-up windows. Additional descriptions of the user interface can be found in Chapter 4 of this thesis.

Key information displayed in the command window includes the maximum link data rate required, the type of power system onboard the hopping vehicle, and total development, build, and operational costs.

Additional key information is displayed in pop-up windows. The first pop-up window displays a subsystem mass breakdown of the hopping vehicle. Figure 11 shows this window.

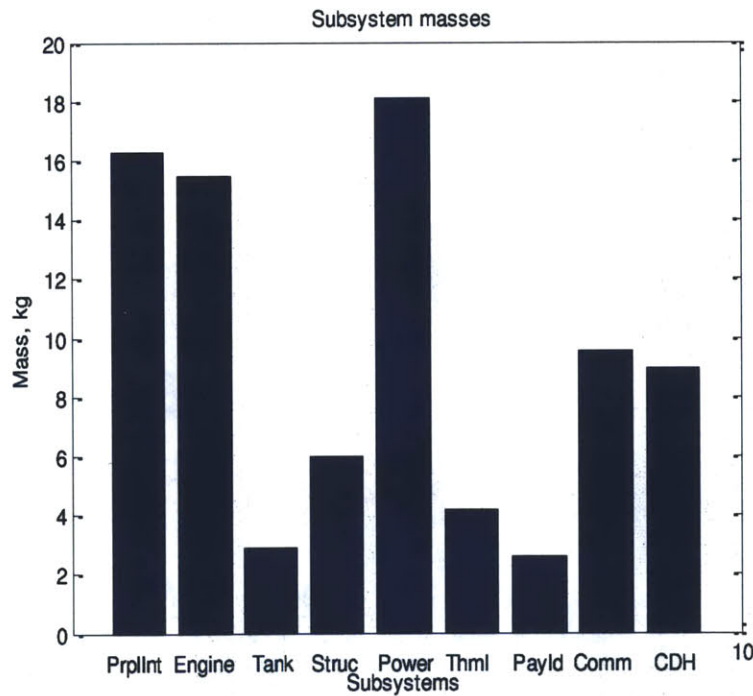


**Figure 11. Example of a pop-up window showing subsystem mass breakdown.**

Each subsystem is listed with its calculated mass. This window allows the user to see the relative mass of each subsystem with respect to the others. This information can then be used in making further design decisions, including possibly whether to attempt to reduce the mass of some subsystems or to estimate the amount of budget and design personnel that should be allotted to each subsystem for further studies.

The second pop-up information window lays out a timeline for the hopping vehicle's operations. The timeline is created by assessing the actions specified for each mission segment in the Flight Plan and Operations Plan modules. Every mission segment is described as Flight, Datalink, or Science. Flight segments occur when the vehicle is in motion, executing any of the 12 maneuvers on the maneuver list, save for maneuver 12 (sitting still on the surface). Science segments occur when the science payload is being operated. Figure 12 shows an example, with each segment also labeled for clarity.

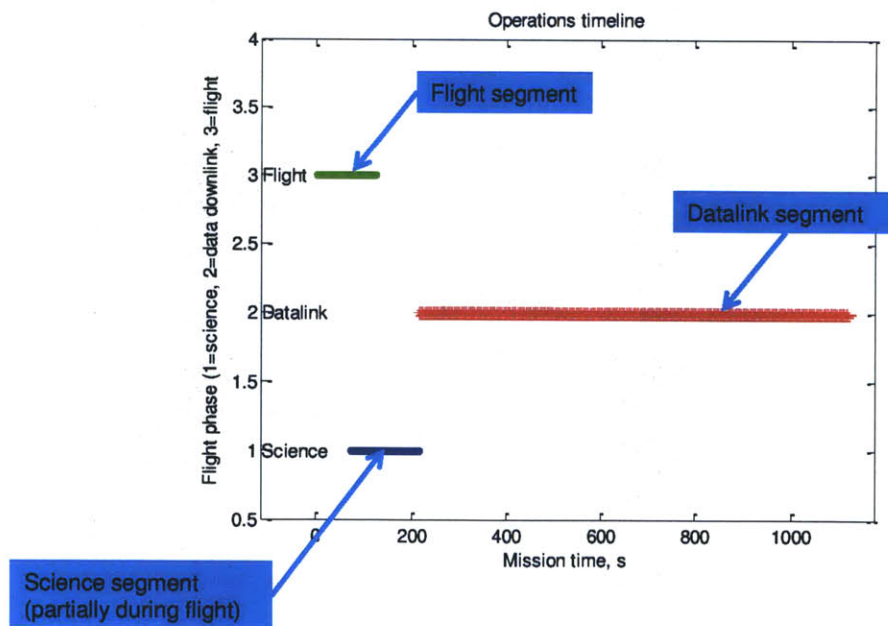


Figure 12. Pop-up window showing operational timeline.

The three types of mission segments, Flight, Science, and Datalink, are plotted on the time axis. The time axis is generated by calculating the length of each mission segment and summing them together. Then each mission segment is plotted on the time axis for the duration of the segment. The plot shows each type of segment being either active or inactive, such that the hopping vehicle is doing one of these actions or is not. Datalink segments must be Datalink segments alone, but Flight segments can also be Science segments (as seen in the figure above). Science segments may occur in conjunction with a Flight segment or alone. In the plot, the segment labels are displayed at different line height for visual clarity, although there is no other distinction between the segment types implied by the line. The lines are labeled to show which mission segment they represent.

Table 8 details the specific actions the user can assign the vehicle, and how they are labeled in the operations timeline pop-up window. Note that Recharge and Sleep modes do not appear in the operations timeline, as the operations timeline is intended to provide the user additional information about the operations aspects of the vehicle related to Earth-based support requirements. That is, there will presumably exist some requirements for support, oversight, or analysis during (or possibly before or after) these mission segments, and these support requirements will translate to certain numbers of people required, or certain aspects of support being available, differently at different mission segments. For instance, a Flight segment will probably require some attention, but not the same sort of attention that a Datalink segment, which will downlink information relevant to mission science goals, will require. The operations

timeline allows the user to assess how these different levels of support will exist over the duration of the mission.

**Table 8. Action grammar mapping to mission segment type.**

<b>Maneuver/Action number</b>	<b>Description</b>	<b>Mission segment type</b>
1-11	Motion grammar maneuver	Flight
12	Rest on surface	N/A
13	Operate payload	Science
14	Transmit data	Datalink
15	Housekeeping	Datalink
16	Recharge	N/A
17	Sleep	N/A

Finally, the Visualization module also supports later post-hoc analysis of missions, as well as conversion and storage of missions modeled, via the collection of all user-input information, as well as a slate of key output values, and gathering them into a single-line matrix. This single-line matrix is a mission entry, and this is stored as a MATLAB variable. If the user creates multiple hopping vehicle missions, multiple mission entries are also created and stored in MATLAB.

Following the final mission that the user wishes to model, the mission entries are all written to an Excel file, one mission entry per column. This feature allows the user to conduct additional analyses and comparisons of multiple missions, as well as to store information about the search history of the user. With this storage ability, users can vary a single parameter through several modeling iterations of one mission, and then use Excel tools to assess the effects of that parameter upon any other mission output. They can also stop work, save their search history, and then return where they left off some time later.

### **3.4.13 Master Parameter Module**

Although the model currently requires user input only for the selection of payload, target planetary body, and flight maneuvers and other operational actions, the hopping vehicle design it generates is a function of more than just these user choices.

In addition to the user choices, a series of parameters that affect the design is also captured in the model. These parameters can be changed by advanced users of the model (even during model runtime), but are set to reasonable defaults for most purposes. In this way, a novice or casual user can still use the model to investigate characteristics of hopping vehicles for given missions, but an advanced user can redesign a hopping vehicle with an improved thermal system or some other feature.

There are 42 parameters in the list, which is created in the Master Parameter module. These parameters are described in Table 9. The parameters are distributed throughout the remaining code modules, according to the details of the requirements for a hopping vehicle design process.

Table 9. List of master parameters and default values.

<u>Tag #</u>	<u>Parameter</u>	<u>Default Value</u>	<u>Module</u>	<u>Tag #</u>	<u>Parameter</u>	<u>Default Value</u>	<u>Module</u>
1	dV for starting/stopping rotation of hopper	$\pi/15$ m/s	Flight Plan	22	Power system efficiency in eclipse	0.60	Avionics
2	dV for starting/stopping lateral/vertical motion of hopper	15 m/s	Flight Plan	23	Power system efficiency in sunlight	0.80	Avionics
3	Speed at which final landing traverse occurs	2 m/s	Flight Plan	24	End of life degradation fraction	0.85	Avionics
4	Mass of hopper used for drag calculations	250 kg	Flight Plan	25	Energy density of batteries	45 W-hr/kg	Avionics
5	Drag coefficient	1.5	Flight Plan	26	Battery depth of discharge	0.50	Avionics
6	Drag area	2.25 m <sup>2</sup>	Flight Plan	27	Force engine selection?	Binary 0/1	Propulsion
7	dV for starting/stopping ballistic flight	40 m/s	Flight Plan	28	Number of vertical engines on hopping vehicle	4	Propulsion
8	Margin factor for uplink rate	1.10	Link Budget	29	Design margin fraction	1.3	Overarching
9	Uplink frequency	8.45 billion Hz	Link Budget	30	Inflation factor from 2010 dollars	1.0375	Cost
10	Transmitting antenna diameter	0.5 m	Link Budget	31	Selection of cost model	Ordinal numeral 1-5	Cost
11	Transmitting antenna efficiency	0.55	Link Budget	32	Initial hopping vehicle mass estimate	250 kg	Overarching
12	Link margin	2 dB	Link Budget	33	Mass difference limit in iterator	10 kg	Overarching
13	Transmitting antenna thickness	0.05 m	Link Budget	34	Fraction of TFU cost used as build cost	0.10	Cost
14	Transmitting antenna density	750 kg/m <sup>3</sup>	Link Budget	35	Enable runtime updates to master parameters?	Binary 0/1	Overarching



<u>Tag #</u>	<u>Parameter</u>	<u>Default Value</u>	<u>Module</u>	<u>Tag #</u>	<u>Parameter</u>	<u>Default Value</u>	<u>Module</u>
15	Receiving antenna selection	Ordinal numeral 1-3	Link Budget	36	Persons on mission control team	10 people	Cost
16	Hopping vehicle temperature	300 K	Avionics	37	Facility cost wrapper	\$5000/person	Cost
17	Radiator emissivity in IR	0.9	Avionics	38	Solar array efficiency	0.15	Avionics
18	Absorptivity	0.4	Avionics	39	Power required to run GNC hardware	15 W	Avionics
19	Radiator temperature	335 K	Avionics	40	Mass of GNC hardware	4 kg	Avionics
20	Radiator thickness	0.005 m	Avionics	41	Housekeeping data generated per segment	3 kb	Operations Plan
21	Radiator density	2700 kg/m <sup>3</sup>	Avionics	42	Use advanced entry mode?	Binary 0/1	Overarch

Use of these master parameters enables more control over the design of a hopping vehicle for advanced users.

### 3.4.14 Model Summary

All of the modules described in this chapter are integral components of the tradespace model for hopping vehicles that we develop in this thesis. The tradespace model is able to take mission inputs, including a specified payload, a target planetary body, and a planned flight profile, and use these to produce a hopping vehicle design. The tradespace model includes subsystem-level models and interactions between these subsystem models, and as such is able to produce a subsystem-level mass breakdown for the hopping vehicle design.

The hopping vehicle design also includes information on the technology readiness level for the hopping vehicle's engine, as well as operational information, including a timeline of mission activities, as well as a catalogue of data captured by the scientific payload, stored onboard the hopping vehicle, and downlinked to Earth. All of this information is potentially useful to mission designers for evaluating a hopping vehicle for a mission. The subsystem-level mass breakdown provides significant insight into the hopping vehicle design, in that it can be used to calculate the initial and final total mass of the hopping vehicle (the propellant required is included in the mass breakdown), and can be used to infer the relative design effort required for each subsystem (smaller subsystems typically require less design attention than larger subsystems).

The subsystem-level mass breakdown is also useful for model validation purposes. Because it provides a granular look at the inner workings of a hopping vehicle, it can be used to compare, on a subsystem-to-subsystem basis as well as on an overall level, a hopping vehicle design produced by the tradespace model and an actual physical spaceborne vehicle. Although no spaceborne hopping vehicles have yet flown, spaceborne landers (which are similar to hopping vehicles) have flown, and these can be used, together with mature spaceborne hopping vehicle designs, for validation of the tradespace model developed in this thesis. Chapter 4 describes the validation process in detail.

## **CHAPTER 4. Model Validation and User Interface Testing**

After developing a model to show the design tradespace for a hopping vehicle, it will be necessary to demonstrate that confidence in the model's results is merited. However, the model cannot be validated against an actual spaceflight hopping vehicle, as such a vehicle does not currently exist.

Validating the model once it has been constructed will be done primarily via "equivalent-hop" comparison to vehicles that have been constructed. Because no spaceflight hopping vehicles have been built, most of the vehicles used will be planetary landers, which have characteristics similar to hopping vehicles. The exception is the Next Giant Leap (NGL) Google Lunar X-Prize team's hopping vehicle, which has been designed in some detail, but which has not been built. While other hopping vehicles are in early stages of design, most of the information related to their physical and operational characteristics is proprietary, and thus unavailable.

### **4.1 Validation Plan for Model**

The validation process will be conducted by using the model to create a hopping mission similar to the actual landing vehicle's mission (or, in the case of the NGL hopper, the actual hopping mission). The hopping vehicle model will generate a hopping vehicle design down to a subsystem-level mass breakdown. This generated mass breakdown will then be compared to the known subsystem mass breakdown of the actual landing (or hopping) vehicle.

The total mass of the generated hopping vehicle design can be compared to the total mass of the landing (or hopping) vehicle, and the subsystem mass breakdowns can be compared for relative

size of the subsystems as well. If these match well across a range of comparisons between generated hopping vehicle designs and actual landing (or hopping) vehicles, then the model can be considered validated. This validation method is similar to one seen in McCloskey's thesis on rover mobility models (105), where validation for the rover modeling framework occurs for subsystems (the mass of subsystems is seen to be within 14% of actual JPL rover subsystems, cf. Lamamy (10)), and for the whole mission (compared to MER).

The landing vehicles used as a validation basis for the model's output will be vehicles that have landed on Luna or Mars. Full comparison, of all subsystems against all hopping vehicle designed subsystems, will be carried out against the Apollo Lunar Excursion Module (LM) and the NGL hopper, both of which landed on Luna, and against Phoenix and Viking, which landed on Mars. Because the model is intended to apply to spaceborne hopping vehicles, validation will focus on comparison against actual spaceborne vehicles. Validation against the TALARIS prototype hopping vehicle is not feasible, as the prototype is intended to operate in a laboratory environment. Thus, although the prototype was used to develop hopping software, its subsystems were built to emulate the lunar environment and operate in it, rather than to operate in a real space environment. Accordingly, rad-hard equipment and vacuum-ready materials were not used; additionally, the electric ducted fan system used to offset Earth's gravity and create a lunar dynamic environment by offsetting 5/6 of the prototype's weight is a large parasitic mass and requires a very large dedicated power system. Although this subsystem is essential for operation of the prototype, it has no analogous counterpart on any spaceborne hopping vehicle. Therefore, validation of the model's spaceborne output against a laboratory-based real prototype would not be viable.

## 4.2 Validation Cases

### 4.2.1 Apollo Lunar Module (LM)

For comparison to the Apollo LM, the hopping vehicle model was given a set of inputs intended to correspond to the actual LM landing. Accordingly, the planetary body was set to Luna. The maneuver list could not be set to a mission that would correspond exactly to the maneuvers performed by the LM as it landed, but key parameters of the LM's flight profile were adapted. For instance, the average time from Powered Descent Initiation (PDI) to engine shutdown for a landing on Luna was 739 seconds (106). Apollo 15 required almost exactly this amount of time to land, so it is selected as an exemplar of the Apollo LM. Because the action taken by the lander during this time was very similar to simple hovering (it burned its engine all the way down to the touchdown point), the maneuver list assembled for the model focused on a hovering maneuver. The maneuver consisted of a long hover, bracketed by a low launch and descent, followed by a brief science and communications period on the surface. If the maneuvers are listed in sequence, with maneuver tag numbers appearing first, followed by the parameter in parentheses, and with science segments bolded (flight segments are marked by maneuvers 1-11, and maneuver 14 marks a communications segment), then the maneuver sequence is: 6(25) – 1(739) – 6(-25) – **13(10)** – 14(30). Science is performed in the second-to-last segment, and communication occurs during the last phase. The very short times for the science and communications segments are due to the fact that the LM actually did not perform much surface science itself, and communications were handled in flight rather than in bulk batches after touchdown. However, the structure of the action grammar for hopping vehicles requires that

these actions be included after a hopping touchdown, so they must be modeled here. As modeled, they are relatively inconsequential.

Additionally, the payload is simplified somewhat. For the LM, the payload is humans, and the vehicle is actually two vehicles together, the ascent and descent stages. For the purposes of validation, the entire upper stage of the LM is set to payload. Because the LM thus effectively gains a very large payload mass fraction (this is realistic, as any human mission has a large overhead in crew systems, which can effectively be considered payload), the payload for the model's hopping vehicle must also be upgraded in some way. This was done by selecting one item from the payload science instrument database, and artificially inflating its mass until the mass fraction roughly matched the mass fraction for the LM. The Sample Analysis Bay was thus bumped up to a mass of 300 kg (from 15 kg), resulting in a more realistic mass fraction for the payload.

The end result of this validation attempt was a look at a hopping vehicle which delivered a massive payload back to the lunar surface after a long period (about twelve and a half minutes) of hovering at a low altitude. This is approximately analogous to the actual flight profile of the Apollo LM.

Because the Apollo LM was much larger than any robotic hopping vehicle could expect to be, the validation analysis is conducted on the basis of subsystem mass fractions.

Additionally, the model output a development cost of 1018 \$M, and a build cost of 62 \$M, in 2011 dollars. The hopping vehicle was designed to mass 1482.3 kg. For the sake of comparison, the Apollo LM massed 16434 kg, and the “payload” (ascent stage) was 4971 kg (107). Thus there is still roughly a factor of 10 in terms of mass difference between the very large hopping vehicle designed here, and the Apollo LM. This is still not unreasonable, as the LM carried humans, while the hopping vehicle would not.

Information on the mass distribution of most Apollo subsystems, including GNC, radar (rendezvous and landing), descent engine and propellant, ascent engine and propellant, RCS, electrical power system (EPS), ECLSS (both ascent and descent), onboard explosives, and instruments, was taken from the NASA Lunar Handbook Systems Manual (108); all precise values are taken from Apollo 15.

Additional information about subsystems was collected from various sources. Information about the shape, composition, size, and pressure of the fuel tanks was used to calculate a mass estimate for the propellant tanks of the Apollo LM (107). With the exception of this propellant tank subsystem and the communications subsystem, actual mass estimates were available for many of the Apollo LM’s subsystems, although they had to be organized into the scheme used for the hopping vehicle model.

The vehicle’s structure mass was not given explicitly, but (109) indicates that it was about 1/15 of the fully-loaded vehicle mass, which permitted an estimate. Included in this was the landing gear estimate, taken from (110). Thermal insulation on the landing gear was also given as 14%

of the landing gear weight, permitting estimate of the total thermal system insulation mass as 14% of the total structural mass, or 0.933% of total mass (110).

Additionally, an estimate for the wiring on the LM, about 200 kg, was provided in (111). This was scaled between the ascent and descent stages proportionally to their mass, and added to the GNC, radar, and instruments to estimate CDH/avionics mass. The explosives were grouped in with the structure mass, and the RCS system was grouped as a whole in with the engines. Ascent engines were included in the payload mass, as was ascent propellant, given that this stage is delivered unused to the lunar surface.

All this information together permits accounting for all but about 1% of the LM's mass. It is assumed that this remaining mass fraction includes the communications subsystem. It is not possible to assess the subsystems at a deeper level of detail with currently available information, so some assumptions have necessarily gone into this assessment.

The resulting subsystem mass breakdown from the hopping vehicle is compared to the subsystem mass breakdown of the Apollo LM in Figure 13. The plot shows subsystem masses as a fraction of total vehicle mass (the entire hopping vehicle or the descent and ascent stages of the LM), with each class of subsystem given its own block. In each block, the mass fraction for the model-designed hopping vehicle appears in blue on the left side of the block, and the Apollo LM's mass fraction for the same subsystem appears in red on the right side of the block.



Note that, while subsystem masses and mass fractions could be assessed for every subsystem in the Apollo LM except the communications subsystem (sufficient information on the mass of components of the communications subsystem could not be located), the communications subsystem mass fraction must be less than 0.0133, given the distribution of the other mass in the Apollo LM against its total mass.

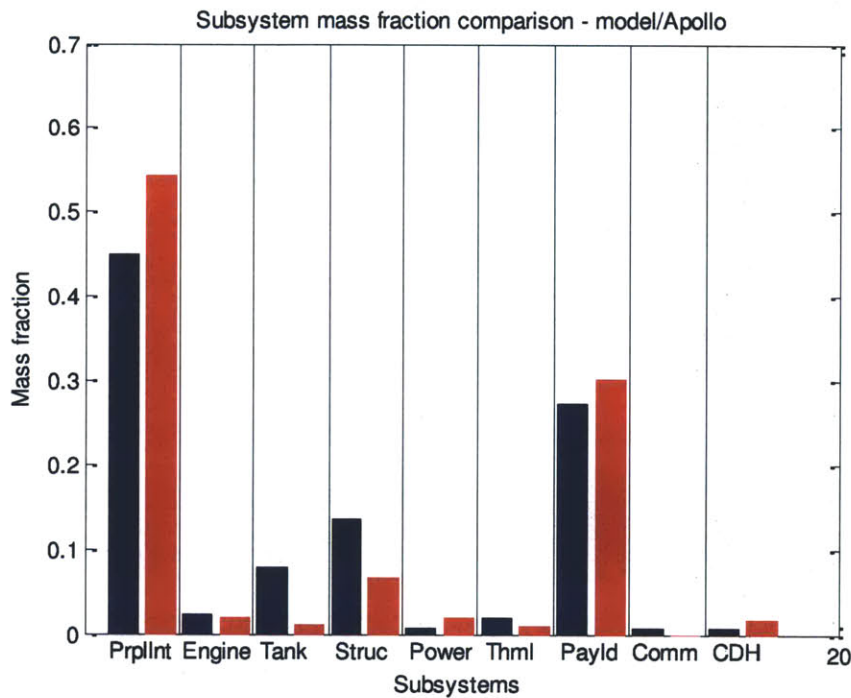


Figure 13. Subsystem mass fractions: model (left columns, blue), Apollo LM (right columns, red).

Note the generally good correspondence between the subsystem mass fractions of the model-designed landing vehicle and the Apollo LM. In a vehicle heavily dominated by its payload and propellant masses, the hopping vehicle model shows reasonable sizing for the CDH and other avionics, communications, thermal control, and power subsystems. The engine is also reasonably well accounted for in the plot. The major differences appear in the tank and structure

subsystems. While the correspondence in these subsystems is not exact, it is close enough that some confidence can be placed in the model results.

For instance, the structural mass fraction for the model-designed hopping vehicle is in the neighborhood of 15%, while the LM has a structural mass fraction of about 8%. This is in part because the model-designed hopping vehicle has conservative assumptions for its structural mass, while the LM was specifically designed to be extremely light-weight. As indicated in (112), this structure mass fraction is in the super-efficient regime, while the model-designed hopping vehicle has a more typical structural mass fraction.

These results indicate good comparability at the subsystem level when the hopping vehicles are scaled up to the level of the LM.

#### **4.2.2 NGL Hopper**

The NGL hopping vehicle is in an early design stage (layouts and breakdowns exist, but full, finalized drawings and operational prototypes do not yet exist). Acquisition of a mass breakdown estimate, taken from somewhere in the design cycle between Preliminary Design Review (PDR) and Critical Design Review (CDR), permitted calculation of subsystem mass fractions for the NGL hopping vehicle (113).

The NGL hopper is 131.4 kg total. Its mission profile involves a 500-m hop on the Earth's moon, carrying a camera. Accordingly, Luna was again selected as the target body, with a payload consisting only of a camera (the precise camera from the scientific instruments

database). However, the NGL hopper also performs some of its own terminal landing delta-V with the same hardware that later performs the 500-m hop. Thus, a significant fraction of the mass of the NGL vehicle is terminal descent propellant. Therefore, the mission profile had an extended hovering section included, to account for the fuel burned during the terminal descent. The extension of the hovering time was estimated from the delta-V requirement for the landing phase, scaled by the ratio of the NGL hopper's engine specific impulse to the designed vehicle's engine specific impulse (a more realistic value). The final mission profile is given as 6(25) – 1(373) – 5(500@90) – 1(10) – 6(-25/1) – 13(60) – 14(900). Note that the hopping vehicle runs its payload (the camera) both during and after flight, and that the communications segment at the end of the mission is rather lengthy, as there is much data to be downlinked.

The subsystem mass breakdown appears in Figure 14.

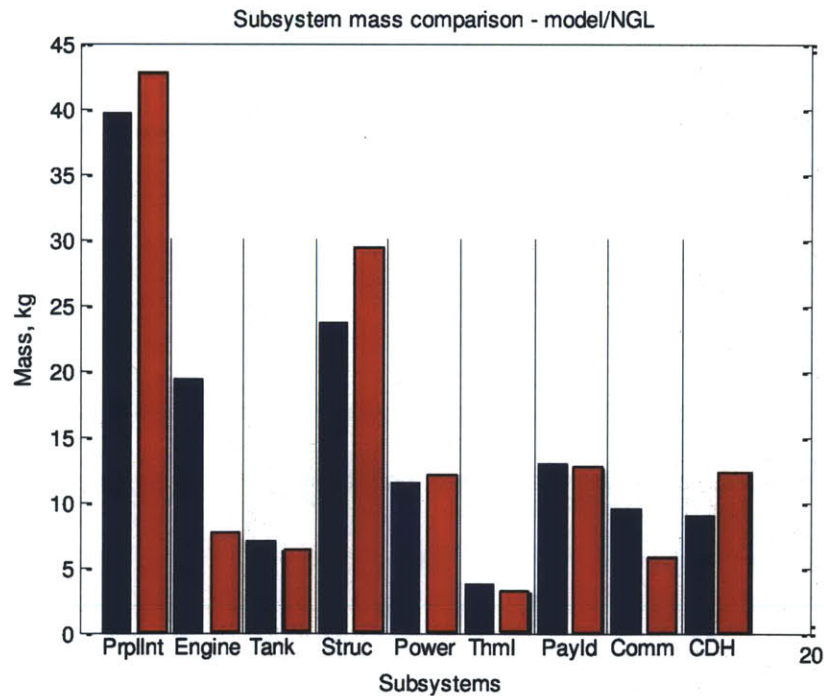


Figure 14. Subsystem masses: model (left columns, blue), NGL hopper (right columns, red).

The total mass of the model-designed hopping vehicle is 136.7 kg, which is very close to the NGL design's 131.4 kg estimate. All subsystems match closely or nearly closely, with the exception of the engine. This is in part because the NGL hopper can use a custom-built engine, while the model-designed hopping vehicle is set to use one of a small set of off-the-shelf engines. The engine selected by the model for the hopping vehicle was the Bell 8414, which is the smallest engine with high throttling, and it is therefore the closest engine on the list to the performance characteristics of the engine that the NGL hopper will use.

One other changed attribute is reflected in Figure 14: the thermal subsystem received an upgrade when it became clear that the model was generating a very large set of thermal radiators. The parameter governing radiator surface temperature was bumped up to 375 K from 335 K, indicating high-temperature radiating capability must be required or at least considered for this mission. This is partly due to the model's thermal analysis, which must size systems to handle extreme low and extreme high temperatures – it might also be possible to land a hopping vehicle such that it did not encounter high temperatures during its operational period.

### **4.2.3 Phoenix**

The Mars Phoenix lander underwent a landing procedure similar to those of Apollo and the NGL hopper. The mission profile was set to a short launch, followed by an extended hover and a landing. After touchdown, science and communications take place.

The final mission profile is 6(25) – 1(40) – 6(-25/1) – **13(900)** – 14(900). The hover time was set based on actual mission times during the Phoenix mission, as described in (114).

Additionally, the payload was updated again to match the actual payload, with the Sample Analysis Module standing in for the payload. This payload was set to 45 kg and 250 W, to match Phoenix. The results appear in Figure 15, which shows a subsystem mass breakdown.

Information on the subsystem masses for Phoenix was primarily gleaned from (115), although many of the numbers were confirmed from other sources, including confirmation of payload mass (approximately) from (84), confirmation of peak power levels from (116), and a description of the EDL flight profile from (114). Multiple sources also listed the Phoenix lander as massing 350 kg (117), (118), although (115) described a total mass of 381 kg.

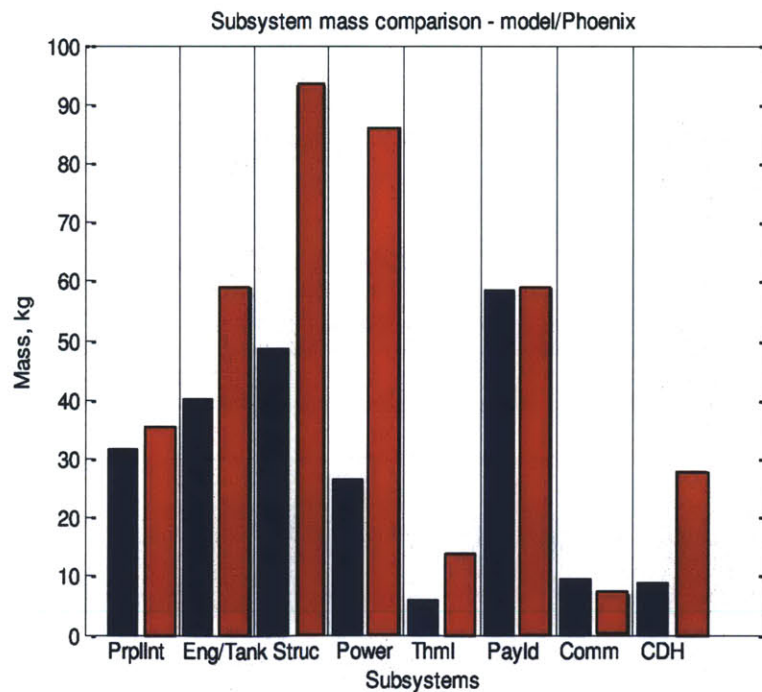
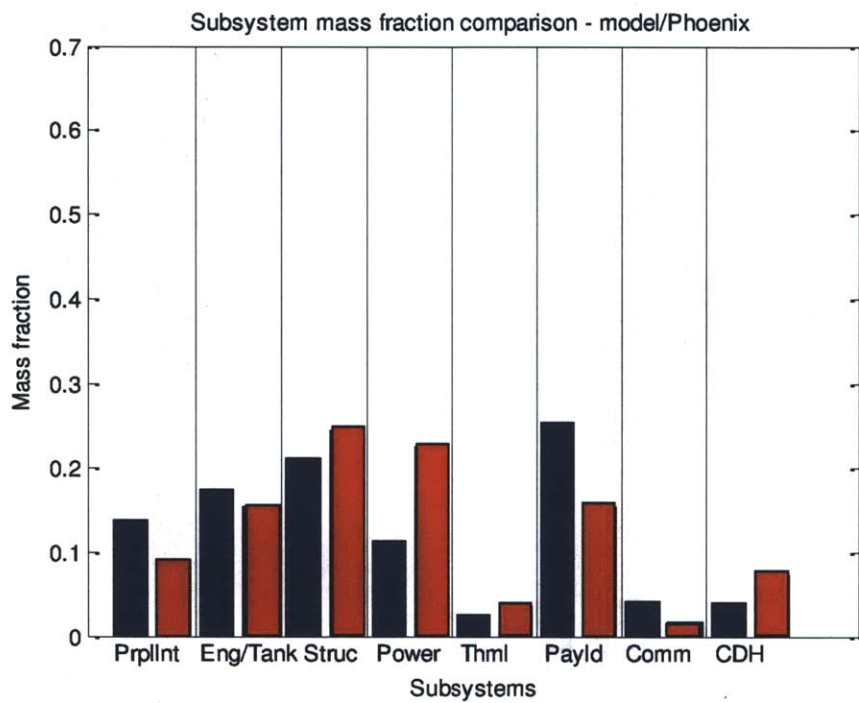


Figure 15. Subsystem masses: model (left columns, blue), Mars Phoenix lander (right columns, red).

The model-designed hopping vehicle has a total mass of 229.96 kg, as opposed to Phoenix’s actual 350 kg. The biggest differences are in the structure and power subsystems. Structure is different because the total estimate for the hopping vehicle is low – the structural mass fractions are very close, as seen in Figure 16. This indicates that the difference in power system mass is primarily responsible for the difference in structural mass.



**Figure 16. Subsystem mass fractions: model (left columns, blue), Mars Phoenix lander (right columns, red).**

However, the power system differential requires some additional consideration. As noted in (116), the electrical power system on Phoenix underwent a “real workout” during the EDL phase, due to the need to drive multiple pyrotechnics at once, and the need to fire cold pyrotechnics (which nearly doubles the current required to ignite them). This phase included

expected peak currents of up to 50 amps (a factor of ten over the typical load). This delivery of high current loads had to be undertaken during a phase which prevented the use of solar arrays, and was immediately followed by a Martian night, throughout which solar arrays would remain ineffective. Accordingly, the EDL and first night on the surface demanded both a high level of performance and a sustained performance from the battery system, which is the best explanation for the increased mass required of the power system. No such intensive battery discharging sequence is modeled for the hopping vehicle, which explains the disparity in this subsystem.

As an additional element of validation, the National Space Science Data Center entry for Phoenix (119) lists a total cost for the Phoenix program as \$417 million. The model-designed hopping vehicle, despite generating a total vehicle mass of somewhat less than the actual Phoenix lander, generated cost estimates of \$421 million to develop the hopping vehicle, and \$35 million to build. Together, these costs are \$456 million in 2011 dollars, which is equivalent to \$420.33 million in 2007 dollars (120). Thus, the CE&R cost model (101), used as the default cost estimator in the hopping vehicle model, and which generates a cost estimate based on mass, but includes some subsystems-level granularity, has closely reproduced a cost estimate for a validation mission in equivalent dollars, even though the mass estimate was slightly different.

#### **4.2.4 Viking**

A final validation run was made against the Viking landers. Detailed mass breakdown data on the Viking landers was not available either from the open literature or from contact with mission designers (a difficult process anyway, as the missions were launched nearly forty years prior to



this writing), but available technical data permitted estimation of the mass of many of the component subsystems on the Viking landers.

The Viking flight profile was set in a similar fashion as the Apollo and Phoenix profiles. The actual Viking lander performed a powered descent after using aerodynamic deceleration and a parachute. The document reporting on the Viking landers' performance (121) describes the terminal descent as occurring from a height of roughly 1460 m, with a starting velocity of 53.3 m/s. Assuming that the lander decelerated to an eventual speed of roughly 0 m/s, and estimating an average descent speed of one-quarter of the maximum speed, the total hovering time was set to 110 seconds. Thus the final flight profile was 6(25) – 1(110) – 6(-25/1) – 13(900) – 14(900). A low-fidelity simulation of the descent from that altitude, which postulated equal drops in speed during equal distance increments until a speed of roughly 2.5 m/s was reached, after which the lander proceeded smoothly to the surface before flaring to a stop right before touchdown, estimated a total flight time of 113 seconds.

The Viking-equivalent payload in the model was also set such that it would amount to 91 kg and would draw roughly 50 W at maximum demand. Technical information on power, structure, propulsion, and payload subsystems was available from NSSDC (122). Structural mass was estimated from a description of the size of Viking's main structural members and their composition. Tank and thermal masses were estimated from guidelines in SMAD (58). No reliable information was available for CDH/Avionics or communications. Landing gear mass was estimated based on the same mass fractions that occurred in Apollo.



Some additional masses had to be estimated and then subtracted out of the total given Viking lander mass of 576 kg. This included the masses of the bioshield assembly, the aeroshell and base cover, the parachute, and the parachute mortar. The parachute mass was known, and the parachute mortar mass was estimated by scaling from Phoenix. The parachute system on Phoenix was a scaled version of the Viking parachute system (123), and the diameters of both mortar systems are known (124). The Viking mortar mass was then assumed to be equal to the Phoenix mortar mass, scaled by the mortar diameters.

Using the geometry and composition of the aeroshell, base cover, and bioshield, density and volume were estimated, which provided mass estimates. The mass of the non-lander items (base cover, bioshield, aeroshell, parachute, and mortar) was subtracted from the total mass of the lander at entry. The remaining subsystem components, estimated or given, accounted for 91.5% of the remaining system mass. Although the provenance of this subsystem mass breakdown is less rigorous than the other three vehicles used for validation, the additional datapoint may still provide useful insight.

In fact, the initial estimate from the model resulted in a power system mass that was extremely different from the Viking lander's actual power system mass. Further inspection indicated that the Viking landers used nuclear thermoelectric power, rather than solar arrays and batteries. When this became clear, the hopping vehicle model was changed to force the power system to scale with the parameter for RTG power sources, rather than for solar array/battery power sources. With this update, the hopping vehicle generated a result very similar to the actual Viking lander, as seen in Figure 17.

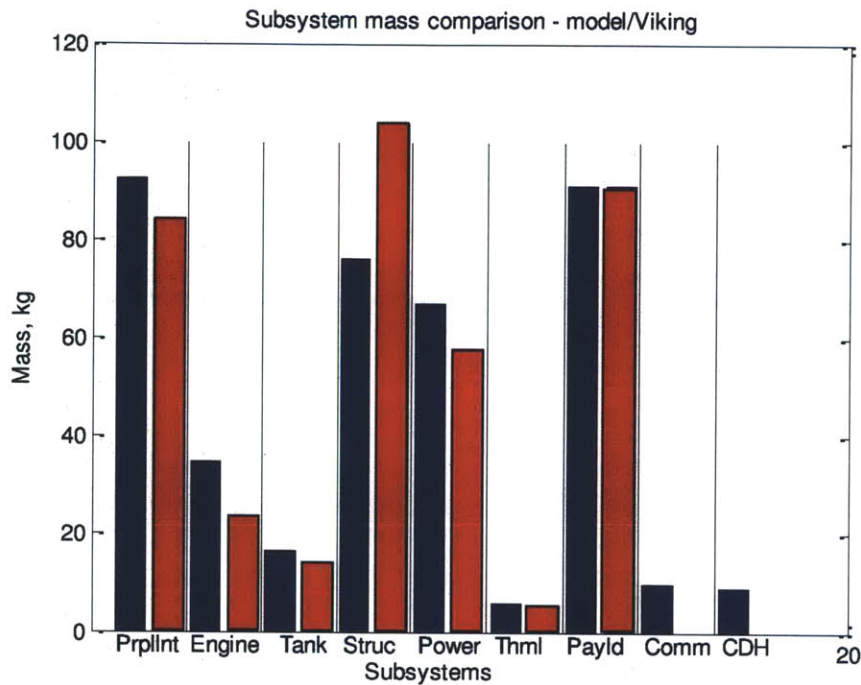


Figure 17. Subsystem masses: model (left columns, blue), Viking lander (right columns, red).

There is no comparison basis for the communications and CDH/avionics subsystems, but most of the other subsystems match well, including the propellant, thermal, and tank subsystems. There is again some offset in the engine masses, but it is not extensive. The power system masses are very similar, indicating that the hopping vehicle model can roughly accurately reproduce an RTG-based power system at a scale that matches actual flown vehicles, as far as can be ascertained.

Some difference is visible in the structure subsystem, but this difference fades somewhat when it is considered in light of mass fractions, as in Figure 18. Additionally, the model results in a mass estimate of 401.7 kg for the hopping vehicle, while the Viking lander was approximately

413 kg after the EDL accoutrements were removed. Additionally, the engine selected by the model, the MR-80B, is the engine descended from the actual Viking engine (125).

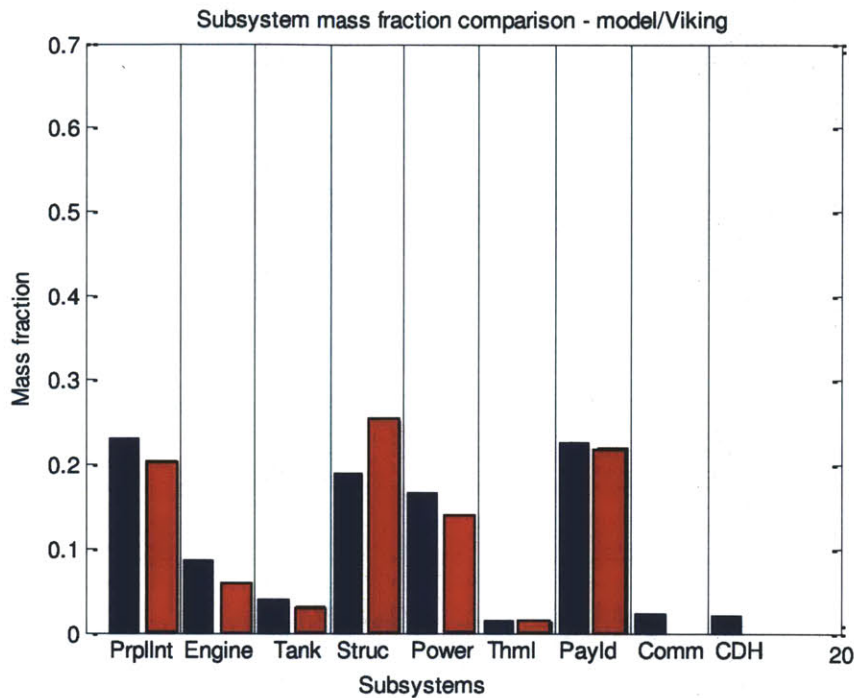


Figure 18. Subsystem mass fractions: model (left columns, blue), Viking lander (right columns, red).

To provide some insight into the overall effectiveness of the model, it is possible to examine each of the subsystems modeled for each of the four validation cases and to compare each to its hardware analogue (when data is available). Comparing each subsystem mass fraction from the validation cases to its hardware analogue (e.g., comparing the model's output for a Viking-like mission's structure subsystem to the actual Viking structure subsystem), the largest error in any predicted subsystem mass fraction is 10.8 percentage points. Therefore, any single modeled subsystem mass fraction does not mismatch the actual hardware subsystem mass fraction by more than 11% of the total vehicle mass. Furthermore, the average difference in subsystem mass

fractions between the model output and hardware subsystems is 0.042, which provides evidence that overall the correspondence between the model's output and what data is available is good, and the model can be considered validated.

### **4.3 Cognitive Walkthrough Program and User Interface**

In addition to validating the engineering side of the hopping vehicle model, attention was paid to the user interface side of the model. The existing user interface was constructed to provide basic functionality of the model, rather than an optimized user experience, and as such an item of remaining future work would be the further development of the user interface.

A program of cognitive walkthroughs was created and executed in order to verify that the user interface as designed can perform acceptably. This section briefly describes the cognitive walkthrough program and some of the feedback generated from the walkthrough campaign, as well as the user interface in its current state. A user guide to the tradespace model's software appears in Appendix C.

#### **4.3.1 Cognitive Walkthrough Description**

A cognitive walkthrough is an exercise commonly used in the field of human factors, as a method for usability inspection. A cognitive walkthrough, wherein a user interface is tested by means of the guided completion of tasks by a test user, allows the system to be evaluated from the user's perspective. A cognitive walkthrough typically involves a series of tasks for a test user to complete, after the test user has received initial training on the use of the interface. A

guide, who is often an expert on or developer of the interface, will usually be present to interact with the test user during the cognitive walkthrough process (126).

The cognitive walkthrough is often used as a tool for early assessment of a user interface. It is not typically a part of formal, experimentally-rigorous evaluations or comparisons of user interfaces. It generally produces both a set of observations about how the user interface enables or hinders the test user in performing the assigned tasks, and a set of reactions or recommendations from the test user. Either or both of these products may then be used to improve or change the user interface.

The cognitive walkthrough process was applied to the hopping vehicle model in a straightforward way. Seven test users were given a simple demographic survey, then shown a sequence of training slides on the model. While the test users reviewed the training material, the model's creator was present to supplement training verbally. The test users were then shown a demonstration of the use of the model, either via a screen-capture video or via an in-person demonstration of the model by the model's creator. After reading a description of the tasks, the test users were then given a printed copy of the tasks and given control of the hopping vehicle model. At all points of the cognitive walkthrough, test users were permitted to ask questions, and periodic dialogue was initiated to elicit feedback from and provide interim guidance to the test users.

The three tasks given to test users were taken from the set of basic tasks that a novice user of the hopping vehicle might wish to accomplish. The first task was for the test user to formalize a

mission concept and enter it into the model. To perform this task, the test user would read a text description of a mission concept, written by the model creator. The text description described goal actions from a scientific point of view, and provided some detail on parameters (example: “Take a sample from a spot 75 m laterally and 15 m down from the starting position”), but left the exact implementation of the concept to the test users. The mission concept described was the collection of a sample on Mars from a crater floor, and the return of that sample to a site nearby, where an ascent vehicle could transfer the sample and return it to Earth.

The second task required the test users to pick out specific details of the resulting hopping vehicle design and report them. This task primarily investigated the ability of the test users to locate information in the model interface.

The third task required test users to compare model outputs. The test users received a detailed description of a hopping vehicle mission, including specifications for payload and maneuver sequence. The test users were asked to enter this mission into the model and then compare the resulting outputs to the hopping vehicle they themselves had designed in the first task they completed (formalizing a mission concept from a text description). Then test users were given a set of information about a rover which could perform the same sample collection mission and asked to compare the hopping vehicles to the rover as well. Rover information was generated from a rover modeling tool developed by Lamamy (57), (10).

Finally, users were asked to select a preferred vehicle (their own hopping vehicle, the pre-designed hopping vehicle, or the rover) to perform the mission, and were asked to register the level of confidence they had in their results.

The three tasks given to test users correspond to initial formulation and investigation of hopping vehicle mission concepts, assessment of details of a hopping vehicle mission concept, and comparison of either two hopping vehicle missions or one hopping vehicle mission and one mission by another type of vehicle. All of these tasks correspond closely to actions that might be undertaken by mission designers interested in a hopping vehicle mission.

#### 4.3.2 Cognitive Walkthrough Results

The cognitive walkthrough was undertaken by seven people, six of whom were graduate students and one of whom was a practicing engineer. The cognitive walkthrough test users included three females and four males. Five test users were between the ages of 18 and 25, one was between the ages of 26 and 35, and one was between the ages of 45 and 55.

Results from the cognitive walkthrough program are shown in Table 10.

Table 10. Summary of cognitive walkthrough results.

User	Gender	Occupation	Time to complete first model run [min]	Error in reading results?	Error in entering information?	Choice of vehicle	Confidence in choice
1	F	Student	11	N	Y	Own hopper	4.5
2	F	Student	6	N	Y	Own hopper	--
3	M	Student	11	N	Y	Own hopper	3.5
4	M	Student	11	N	Y	Own hopper	4.5
5	F	Student	17	N	N	Prescribed hopper	4
6	M	Engineer	9	N	Y	--	--
7	M	Student	8	N	N	Own hopper	5

Table 10 indicates the gender and occupation of each user, as well as the time the user required to complete his or her first model run – that is, to go from a written mission concept statement to a mass estimate from the tradespace model. The average time required to use the model for the first time is 10.4 minutes. Table 10 also indicates whether test users made any errors in reading information from the model interface after completing their first model run (their second task), and whether test users made any errors in entering information into the model during either their first or third task. Finally, the test users' choices of preferred vehicle and their confidence in this choice are shown.

Notably, five of the seven test users made at least one entry error, but most were able to notice and recover from the error. One user even restarted the entire entry process to recover from an error. However, no errors were made in locating and assessing information presented by the model's user interface, and thus all users showed an ability to evaluate hopping vehicle designs easily. The errors that users made could easily be corrected, either in the model or by simply abandoning one model run and starting another (which takes only minutes at worst, and seconds at best).

The confidence shown by test users in their choice of preferred vehicles (the third task) tended to be high, with an average value of 4.3 out of 5, although two test users did not express a confidence level. Every user but one selected a preferred vehicle (his or her own design for a hopping vehicle, a prescribed design for a hopping vehicle, or a rover), and of those who selected, all chose a hopping vehicle, with all but one choosing the design of his or her own hopping vehicle. Some users explicitly indicated a preference for a hopping vehicle due to its



ability to deliver increased performance (moving larger payloads to more places, more quickly), despite the rover design presented being lighter in mass than the hopping vehicles.

While this may be a bias effect induced by the fact that users had to invest significant thought into designing their own hopping vehicles, there is also indication that users are able to understand and evaluate hopping vehicles based on concrete technical aspects, including mass, mission time, and payload, as well as based on less-tangible aspects, like risk and terrain freedom.

The cognitive walkthroughs conducted have indicated that the tradespace model is initially comprehensible to a user with some basic technical background, and that the information it presents to users is able to be assimilated and used to make further decisions regarding hopping vehicle missions. Although this does not represent a full-scale user interface evaluation, it shows the initial usability of the interface and points the way to future improvements, which are discussed in more detail in Chapter 6.

### **4.3.3 Description of Updated User Interface**

The updated user interface includes four user entry screens, via which the user enters information about the hopping vehicle's payload, target planetary body, and flight profile. The user interface produces one screen during the flight profile creation, a three-dimensional visualization of the hopping vehicle's path which is actively updated while the user enters information. It also produces four additional visualization screens after completing a model run. One of these is a simple text listing of key design parameters, while the other three are pop-up plots. The pop-up

plots display the subsystem mass breakdown, operational profile, and propellant use breakdown for the hopping vehicle designed.

#### **4.3.3.1 User Entry Screens**

The four user entry screens are used to enter important modeling information. The first screen, shown in Figure 19, provides a list of available scientific instruments (pulled from the Excel database) and allows the user to add them one at a time to the vehicle's payload. The second screen, in Figure 20, performs a similar series of actions for the target planetary body. The user can select and confirm a planetary body from a list, and then enter it and move on to the rest of the model.

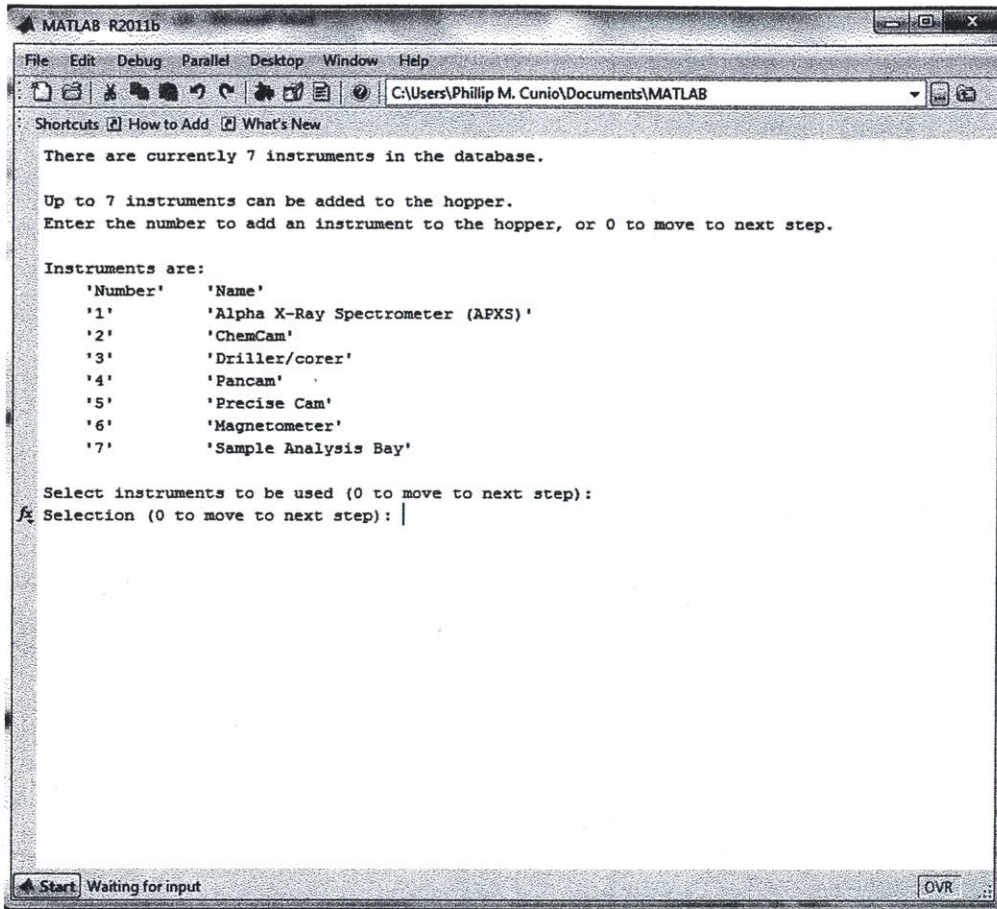


Figure 19. Payload selection user entry screen.

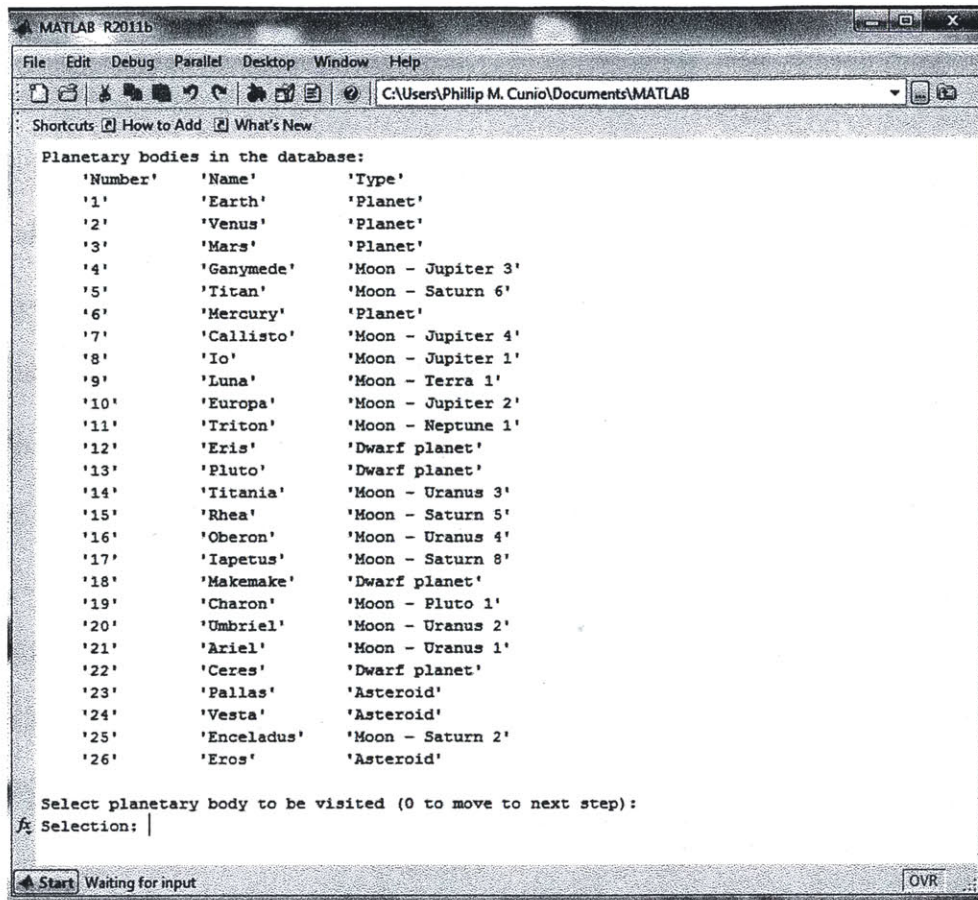


Figure 20. Target planetary body selection user entry screen.

The third and fourth user entry screens are used to input information about the flight profile and other actions taken by the hopping vehicle. The third screen, seen in Figure 21, shows a list of possible maneuvers (taken from the motion grammar) and permits the user to select a sequence of them, one at a time. The screen guides the user by listing previous maneuvers at the top, and prompting for sizing parameters and other ancillary information for each maneuver as it is entered. The fourth screen, seen in Figure 22, steps back through each maneuver and prompts the user to flag it as being a science segment or not. Science segments can occur during flight or during resting on the surface. If a surface resting segment is marked as not being a science

segment, the user interface prompts for the segment to be marked as either communications, sleeping, housekeeping, or recharging.

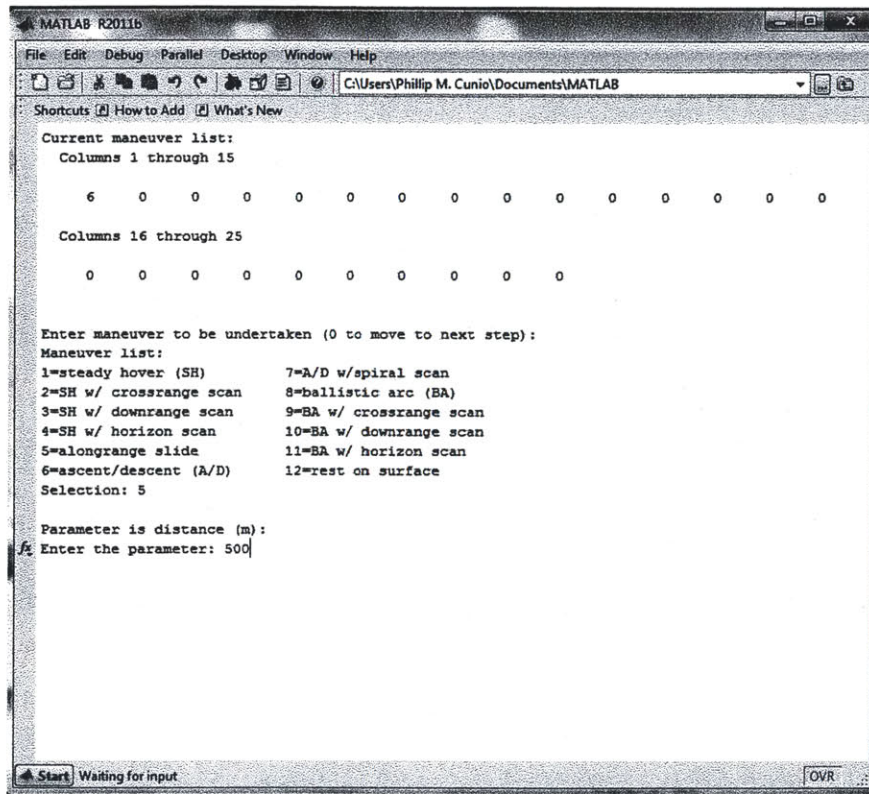


Figure 21. Flight planning user entry screen.



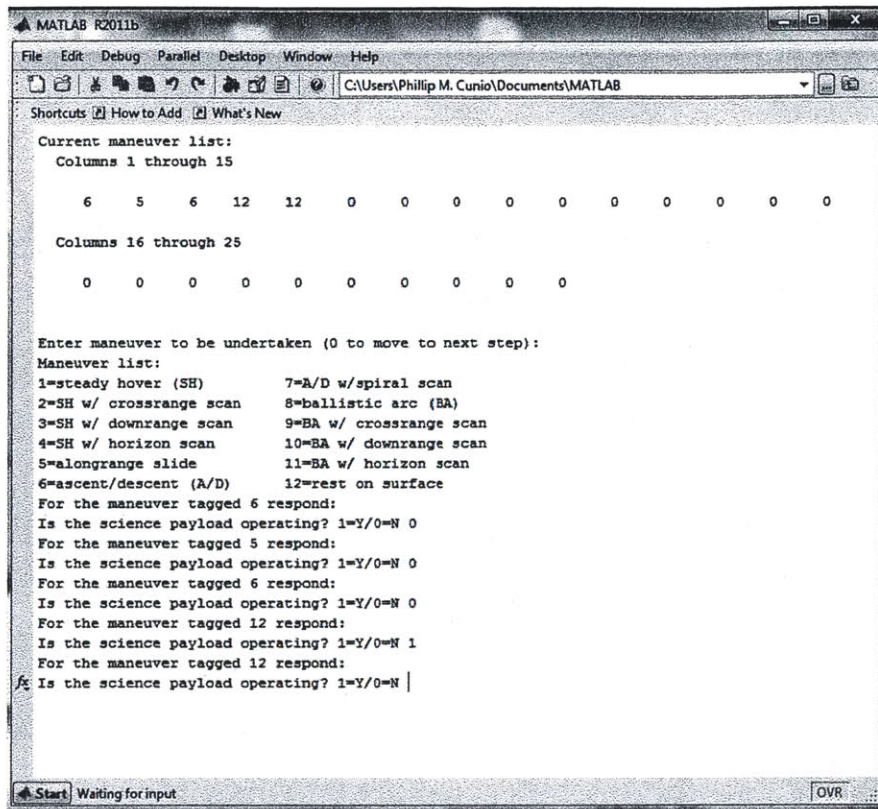
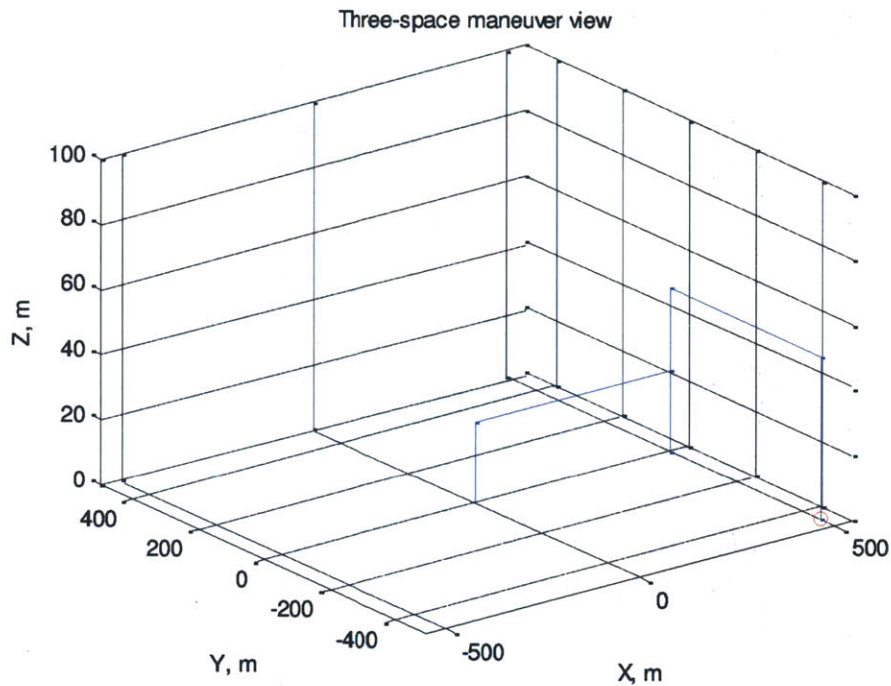


Figure 22. Science segment marking user entry screen.

#### 4.3.3.2 Actively Updated Screens

In addition to the user entry screen seen in Figure 21, the user interface also produces an actively updated three-dimensional plot of the flight path as the user enters the flight profile. An example of this is seen in Figure 23. Note that the path generates blue lines to plot the course of the hopping vehicle. A red circle marks the vehicle's current location, as flight paths often recross themselves, and it would be easy for a user to become confused. The visualization appears with only a wireframe background for simplicity (which actively scales the axes as the path length grows), but future iterations could be updated to include available imagery of the surface of the target planetary body as such imagery becomes available.



**Figure 23. Example three-dimensional visualization of a hopping flight path.**

#### **4.3.3.3 End Visualization Screens**

The user interface also produces four end visualization screens to describe the model's results. The first, seen in Figure 24, is a subsystem-level mass breakdown of the designed hopping vehicle, which permits the user to evaluate and compare subsystems. The second figure, seen in Figure 25, is a propellant use breakdown, which marks the total propellant mass into fractions for each maneuver performed. The third, seen in Figure 26, is a timeline showing operational activities, namely whether science, flight, and communications segments are occurring at any time during the prescribed mission. Note that science and flight segments may occur separately or simultaneously, but communications segments must occur in isolation.

The final end screen is a simple text display of useful information about the design, as seen in Figure 27.

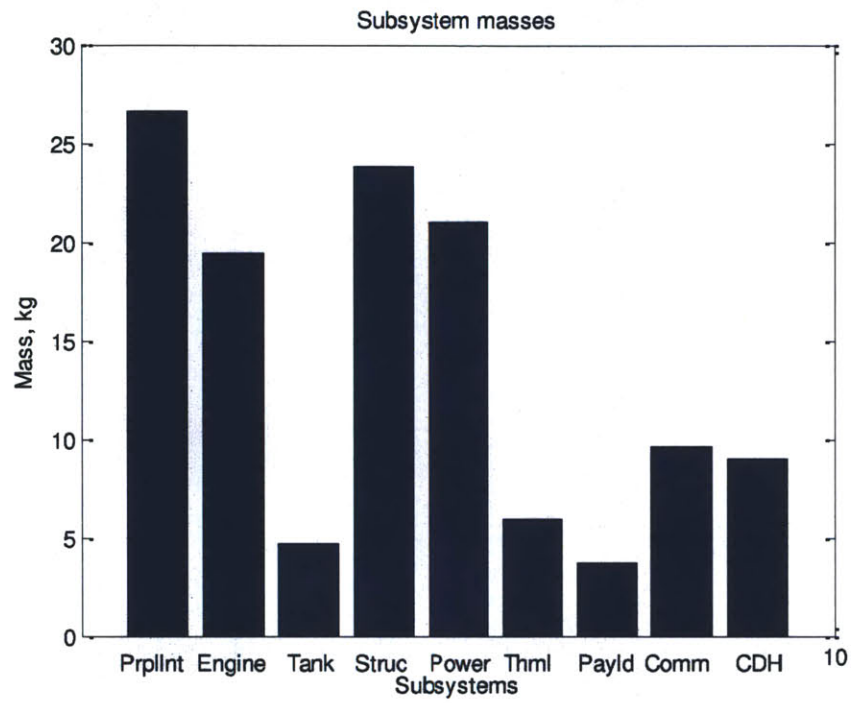
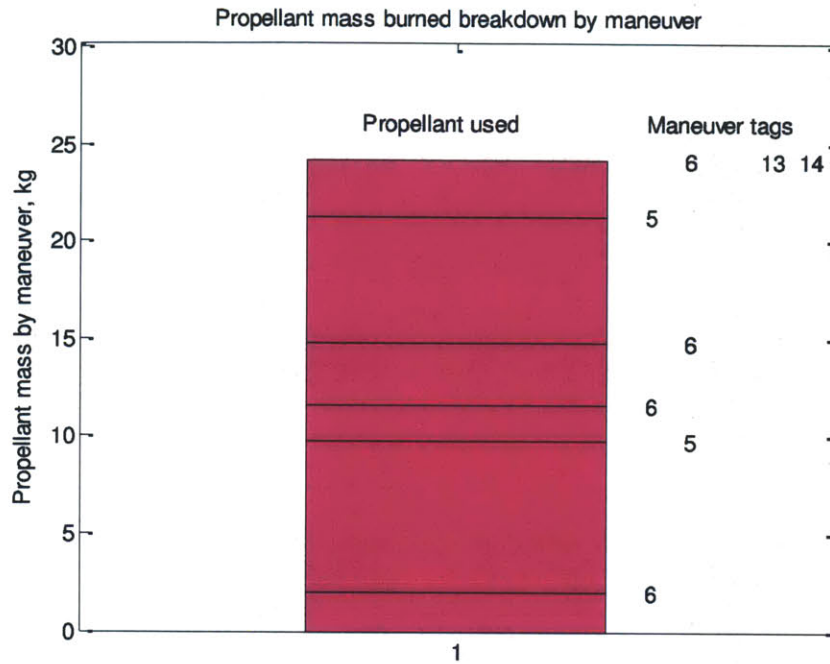


Figure 24. Subsystem mass breakdown example.





**Figure 25. Propellant use breakdown example. Maneuver tags are aligned with the solid bar at the top of propellant amount allotted to each maneuver.**

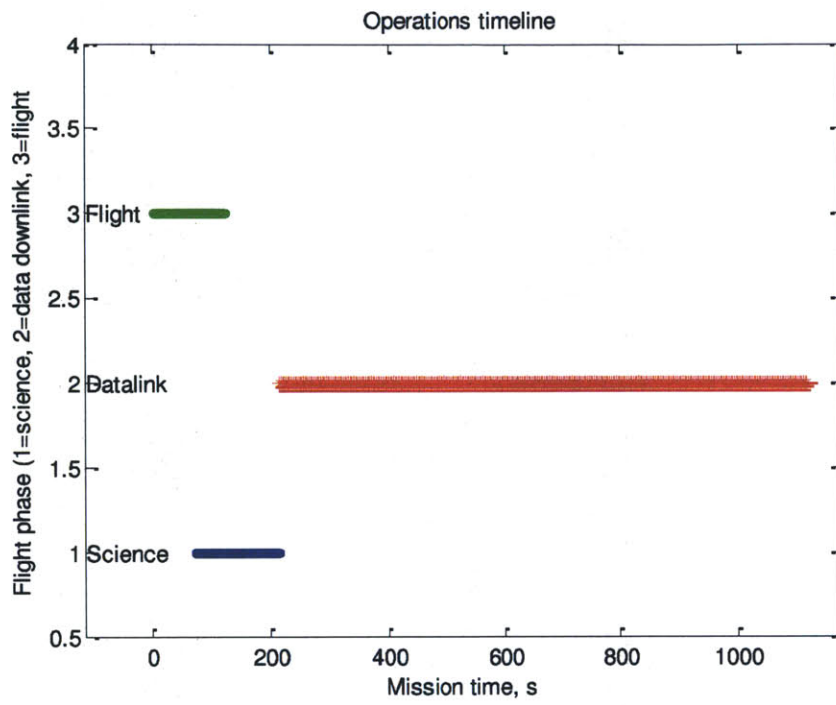
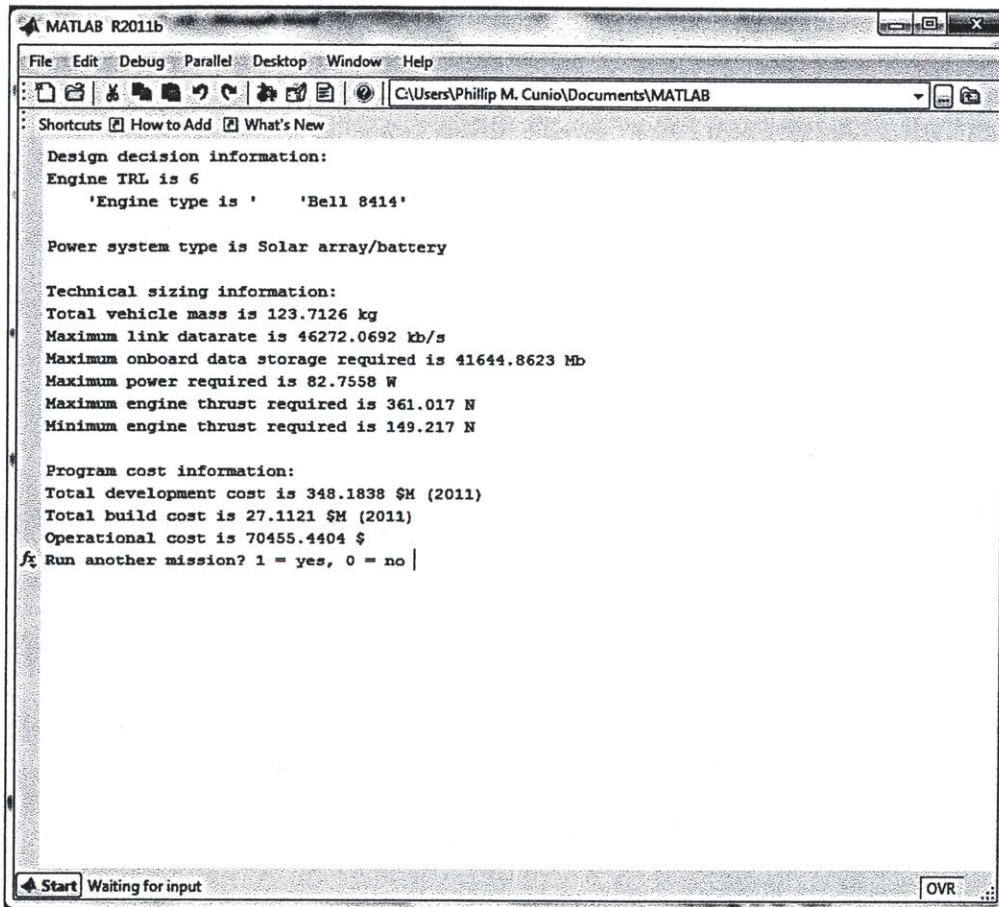


Figure 26. Operations timeline example.



```
MATLAB R2011b
File Edit Debug Parallel Desktop Window Help
C:\Users\Phillip M. Cunio\Documents\MATLAB
Shortcuts How to Add What's New
Design decision information:
Engine TRL is 6
'Engine type is ' 'Bell 8414'
Power system type is Solar array/battery
Technical sizing information:
Total vehicle mass is 123.7126 kg
Maximum link data rate is 46272.0692 kb/s
Maximum onboard data storage required is 41644.8623 Mb
Maximum power required is 82.7558 W
Maximum engine thrust required is 361.017 N
Minimum engine thrust required is 149.217 N
Program cost information:
Total development cost is 348.1838 $M (2011)
Total build cost is 27.1121 $M (2011)
Operational cost is 70455.4404 $
fx Run another mission? 1 = yes, 0 = no |
Start Waiting for input OVR
```

Figure 27. Textual information output to end screen.

Examples of some of these results, taken from tradespace investigation model runs, will appear in Chapter 5 of this thesis.



## **CHAPTER 5. Initial Tradespace Exploration**

In Chapters 1 and 2 of this thesis, the need for a tradespace model of hopping vehicles was motivated, and hopping vehicles were described in terms of their advantages and potential uses.

In Chapter 3, the details of a tradespace model were given. In this chapter, the output of the model on several example runs will be described.

### **5.1 Model Exercise Plan**

Exercise of the hopping vehicle model will be conducted in two broad fields: tradespace investigation and specific mission investigation. Tradespace investigation will involve running series of hopping missions in the model such that changes occur along a single axis, and thus the broad curves of behavior that the model shows can be plotted. These broad curves will in turn provide insight into the ways in which hopping vehicles can be most useful for exploring other planetary surfaces. Axes investigated will include the planetary body axis, such that different choices of target planetary body are examined; the traverse axis, which stipulates different types and distances of traverse over a planetary surface; and the payload size axis, which examines the effects of larger payloads.

Specific mission investigations will focus on the modeling of specific mission concepts that have been previously elucidated as of interest for hopping vehicles, or that may be compared to other missions in revealing ways. These exercise runs will also provide insight into the ways in which hopping vehicles can be most useful, but will investigate specific points in the tradespace, rather than broad curves.

### **5.1.1 Selection of Tradespace Exploration Missions**

This section details why specific missions were selected for tradespace investigation or specific mission investigation, and describes the entries made. Comparison to similar missions modeled using the hopping vehicle model developed in this thesis are then made.

### **5.1.2 Tradespace Investigation Baseline Hopping Mission**

For tradespace investigation purposes, it was necessary to construct a baseline hop, a simple set of maneuvers which might be of interest on any planetary body. The baseline hop chosen for this is the GLXP-derived hop, consisting of a 25-m ascent, followed by a 500-m hovering traverse and then a 25-m descent. Science and communications mission segments follow this. This baseline hop is conducted on every planetary body in the catalogue, followed by more detailed investigation of the effects of variations in payload mass, maneuver sequence, and various master parameters on the results.

Initial investigation of this hopping mission sequence showed some interesting results. For instance, the planet Venus, despite its solid surface and notionally attractive gravity, is not amenable to hopping missions. The planet's surface is sufficiently hot that a thermal system sized to deal with it according to the constraints of the model developed in this thesis is unrealistically large. Furthermore, the planet's atmosphere is extremely dense, resulting in high drag whenever a flight maneuver is attempted. Taken together, these aspects render Venus untenable as a target for hopping vehicles. The history of Venusian exploration, with few successes among many attempts (and even those successes short-lived on the surface), bears out this conclusion.

Other planetary bodies are similarly difficult to approach as hopping mission targets. The moon Io and the planet Mercury have similarly extreme temperatures, resulting in similarly outsized requirements for thermal systems. Because the thermal systems required on these planetary bodies are so large, there is carryover of excess mass into the structural subsystem, and consequently into the propulsion requirements, resulting in rather large hopping vehicles.

Additionally, the moon Titan has similarly stringent thermal constraints, but these stem from the cold temperatures experienced on the surface of Titan. Although the moon at its coldest is not colder than many relatively airless planetary bodies, the thick atmosphere serves to wick heat away from the hopping vehicle, especially if the vehicle is moving steadily through the atmosphere. Furthermore, the vehicle is always hotter than Titan, as the maximum temperature is also low, so it must always be heated or else losing heat. To maintain a constant steady-state temperature, a large mass of thermoelectric heaters is required.

Finally, the Earth is somewhat anomalous as a hopping mission target. The Earth, in addition to having the highest gravity of any planetary body on the list of potential target bodies, also has a comparatively dense atmosphere, increasing drag effects, and displays a range of temperatures such that a hopping vehicle might need both heating and cooling components in its thermal system.

Leaving aside the four special cases of Io, Mercury, Titan, and Earth, the results for total hopping vehicle mass seen in Figure 28 are obtained.

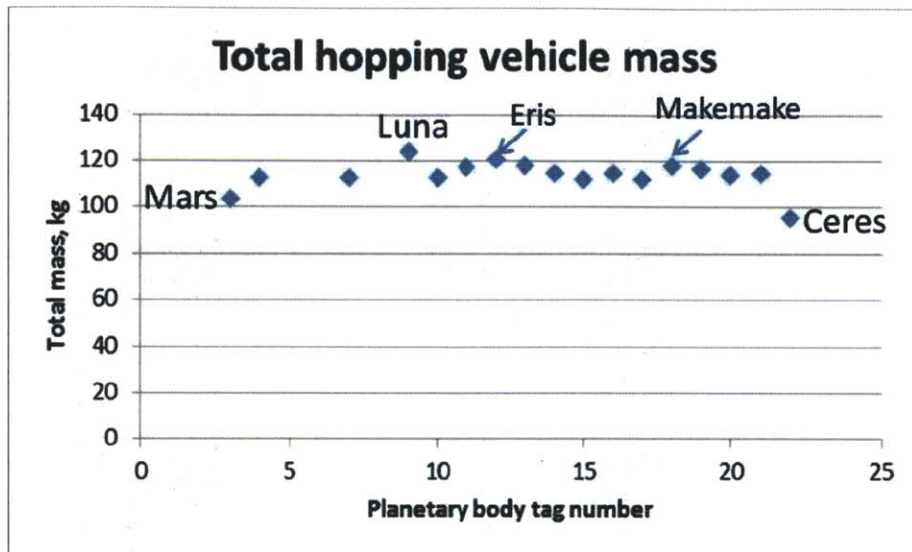


Figure 28. Total hopping vehicle mass (for a baseline hopping mission) on various planetary bodies.

Figure 28 shows the calculated total hopping vehicle mass for each planetary body (excluding Venus, Io, Mercury, Titan, and Earth), listed by their number in the catalogue of potential hopping mission targets. The planetary bodies in the catalogue (listed in full in Table 6) are arranged loosely by descending gravity, but certain bodies are picked out. Luna is the planetary body closest to Earth, but also has a difficult thermal environment which requires both heating and cooling. Accordingly, the thermal system for a Luna hopping vehicle is larger than the average thermal system for a hopping vehicle at one of the other target planetary bodies. This is not quite offset by the low power level required for communications from Luna to Earth (given their relative proximity).

Two other bodies with large (in comparison) masses for hopping vehicles are those most distant from the Sun and from the Earth: Eris and Makemake, the outer dwarf planets beyond Pluto.



Their relative increase in total mass is a consequence primarily of their need for additional power to transmit data back to Earth. At the furthest right of the plot, the minor planet Ceres has the advantages of very low gravity and relatively close proximity to Earth, leading to a lessened need for a high-power communications system. The low temperature of Ceres also ensures that heaters are needed, but cooling subsystems are not.

Interestingly, except for the impossible case of Venus and the four special cases of Io, Mercury, Titan, and Earth, the total masses of the hopping vehicles fall within or near a band from 100 kg to 120 kg.

Looking at traverse speed for fixed-altitude, fixed-attitude hops (or hover hops) on the special-case planetary bodies of Earth and Titan yields additional insight. The standard hopping mission was performed on Earth and Titan (the two dense-atmosphere planetary bodies that are otherwise feasible for hopping missions), and on Mars for comparison. Figure 29 shows the total hopping vehicle mass as a function of horizontal traverse speed for the three planetary bodies.

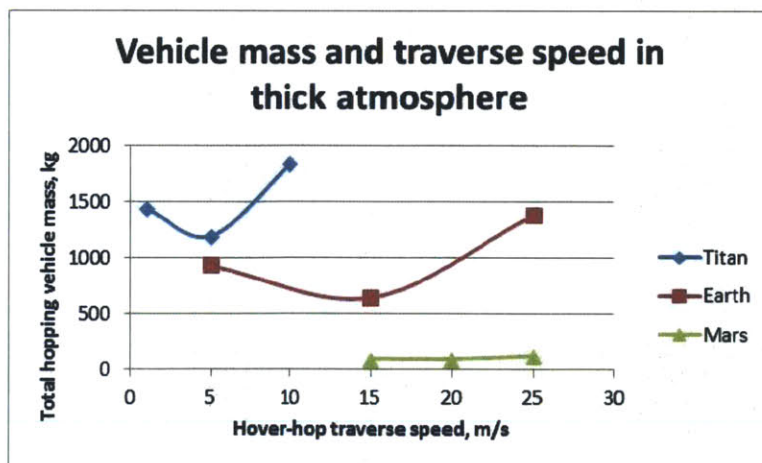


Figure 29. Total hopping vehicle mass as a function of horizontal traverse speed on three target planetary bodies.

The existence of a convex curve is clear for Earth and Titan. The curve is also present for Mars, but is less apparent, with a minimum at a traverse speed near 20 m/s. This implies that optimum traverse speed is a function of atmospheric density. This may be true; however, total hopping vehicle mass is a function of gravity as well as atmospheric density, so the true optimum traverse speed varies on several axes. However, the presence of a minimum in Figure 29 suggests that the optimum speed exists.

Some indication of the effect of planetary body gravity on the total mass of a hopping vehicle is given by Figure 30, which shows the effect of propellant mass fraction (the fraction of total vehicle mass given over to propellant) versus gravity.

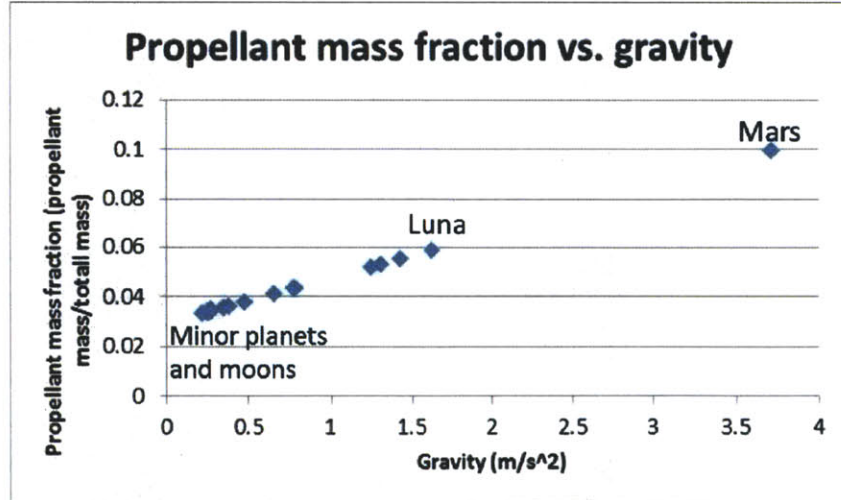


Figure 30. Propellant mass fraction for a hopping vehicle on a baseline mission versus target planetary body gravity.

As would be expected, there is an approximately first-order correlation between propellant mass fraction and the planetary body's gravity. Some bodies, including Mars and Luna (the two bodies with highest gravity) are indicated on the plot, as is a cluster of minor planets and moons with similar gravity levels.

Additional insight can be obtained by looking at the full mass breakdown for each planetary body. This appears in Figure 31.

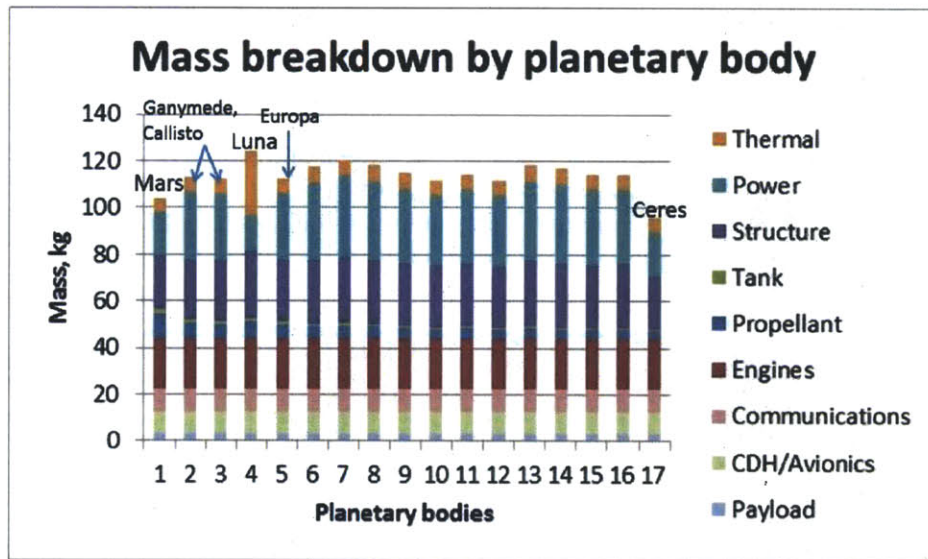


Figure 31. Subsystem mass breakdown for hopping vehicles on different target planetary bodies.

Note that, as previously seen, all planetary bodies indicate hopping vehicles which fall within a band from roughly 100 kg to 120 kg. Mars and Ceres are slightly lower, while Luna is slightly higher, within this band. Note also that certain subsystem masses, such as CDH/Avionics, payload, and communications, are constant among all planetary bodies. This is because the same payload is specified for each mission, and a similar CDH/avionics subsystem reflects the fact

that hopping vehicles need not perform exceptionally different computations from one mission to the next. The communications subsystem mass is constant because a standard set of communications equipment is assumed to be part of a basic hopping vehicle bus, and because variations in the link budget are handled via increasing the transmission power. The similarity of the basic mission profile, even across a reasonable range of gravities, permits the use of the same engines on every mission as well.

Differences between planetary bodies do not appear until the propellant is examined. Propellant varies from one planet to the next as a roughly first-order function of gravity, as seen in Figure 30. This in turn feeds a difference in the mass of the structure subsystem, although the structure subsystem is also influenced by the mass of the power subsystem, which in turn is related to communications requirements. The thermal subsystem is primarily driven by temperature ranges on the planetary body, and the thermal system also feeds into the mass of the structure subsystem. There are additional feedbacks between the structure and the propellant mass, which are also captured in the model.

With this basic assessment of the hopping vehicle tradespace completed, attention can be paid to the effects of varying other inputs. For instance, a traverse across a long distance can be made either via the alongrange slide or a ballistic arc. These two different travel methods correspond to what is known as a fixed-altitude, fixed-attitude (or FA-FA) hop, also called a hover-hop, and to a ballistic arc. Conventional wisdom holds that a ballistic arc is a more energetically efficient means of performing a traverse, but this is not always accurate. Operational considerations, such as the fact that a vehicle cannot likely perform a ballistic kick from a position resting on the

surface of a planetary body, and as such must launch and hover up to a starting altitude before beginning ballistic flight, affect the traverse. Such a process must generally be repeated in reverse after finishing a ballistic traverse. As first noted by Middleton (54), this operational overhead chips away at the efficiency gained in a ballistic traverse. This type of consideration is captured by the hopping vehicle model developed in this thesis in the form of action grammar rules, which describe the proper method by which a ballistic maneuver can be modeled.

In an effort to assess how ballistic and hover-hop traverses are distinguished in the model developed for this thesis, simple hops with increasing traverse distance were modeled. The simple hops took place on Mars, which was selected as a baseline planetary body. The results are in Figure 32.

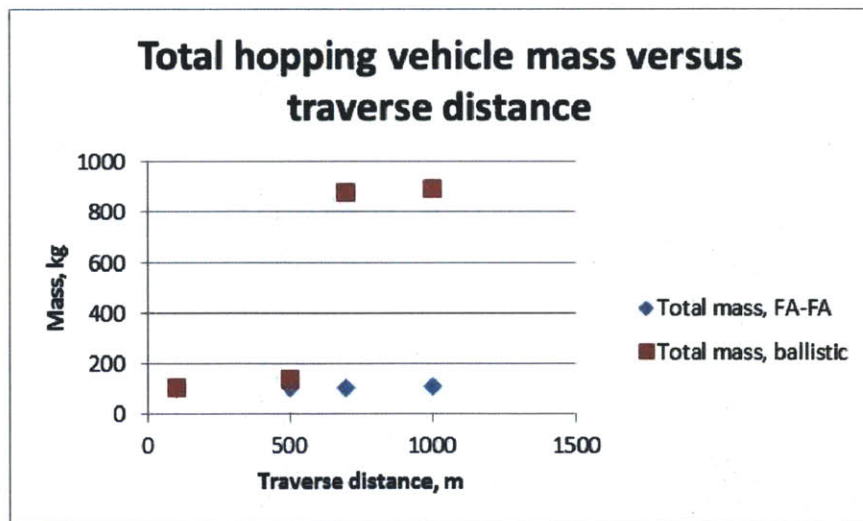


Figure 32. Total hopping vehicle mass for different traverse distances and traverse modes.

Figure 32 indicates that there is only a minor increase in total hopping vehicle mass as traverse distance increases for hover-hops, attributable to the increase in propellant required to keep the



hopping vehicle aloft as it traverses the additional distance. However, there is a much larger increase in total mass for the ballistic arc traverse method with increasing traverse distance.

The reason for this is visible in Figure 33. As traverse distance increases, so does the delta-V that must be delivered by the engines to move the vehicle that distance. A longer traverse distance equates to a higher required delta-V at the start of the ballistic arc maneuver, which in turn equates to a higher required thrust, assuming that the delta-V must all be delivered in a given short period of time.

As the required thrust increases, so typically does the engine mass. However, another aspect of the situation is that an engine with higher maximum thrust, if given an otherwise similar flight profile and an otherwise similar hopping vehicle bus and payload mass, must be capable of throttling down further from its max thrust in order to permit landing after the ballistic arc has been completed. In short, the difference between the maximum and minimum thrust levels required during the mission increases, which means that the throttling ratio must increase as well. Stricter engine requirements often lead to the selection of larger engines, which in turn adds a cascade of mass to the design of the hopping vehicle. Therefore, traversing a longer distance in a ballistic arc maneuver tends to increase required engine mass. This effect is seen in Figure 33.

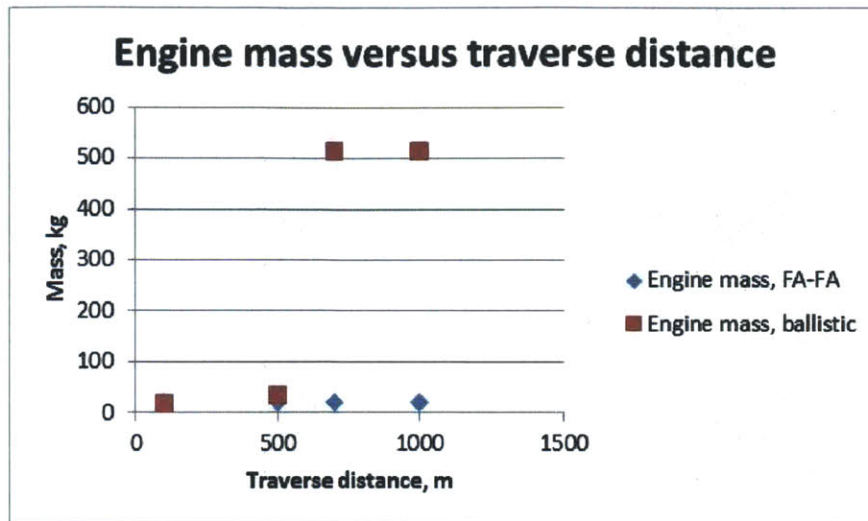


Figure 33. Hopping vehicle engine mass for different traverse distances and traverse modes.

The engine mass for the hover-hop traverse remains constant, as the same engine has a much wider range of viability for this type of maneuver. However, as traverse distance increases for the ballistic arc, engine sizes goes up. The step up to a larger engine between the 100-m ballistic arc traverse and the 500-m ballistic arc traverse is apparent; a larger step from that to the 700-m ballistic traverse is caused by the need to step to the next size engine in the engine database. Because the engine database is not exhaustively filled with every existing deep-throttleable engine, the jump from the engine at the 500-m ballistic traverse to the engine at the 700-m traverse is significant. There are no engines sized between the smaller one that permits a 500-m traverse and the larger one that permits a 700-m traverse. This is a limitation of the model, but the ability of the model to accept and analyze additional engines, which is based on the ability of the user to enter information about a new engine into the Excel engine database, is a way around this limitation. Either the user can look up and enter an engine with intermediate parameters between those of the 500-m traverse engine and the 700-m traverse engine, or the user can specify a custom engine design and force its selection to see how it would affect the results.

The engine architecture also plays a role here, in that the four-engine architecture of a hopping vehicle used in the tradespace model means that a jump to the next largest engine size has a multiplied impact. Other engine architectures, which are not yet supported by the tradespace model but which may be supported by future versions, could change the height of the step impact of an engine size change.

Although it cannot be claimed that the dynamics of stepping up to the next engine size are completely captured here, because the model developed in this thesis does not claim to have an exhaustive list of available deep-throttling engines and because it is still possible to build or purchase custom engines which meet parameters in between what appears in the database, the general shape of the dynamic has been captured. Traversing farther via ballistic arc may result in a need to use an engine so much larger that it offsets the advantages of using a ballistic arc trajectory in the first place. This may even have additional cascade effects, as seen in Figure 34.

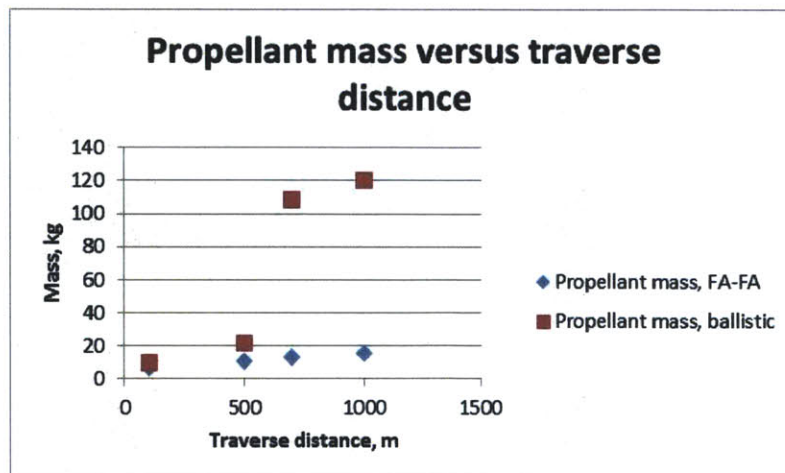


Figure 34. Propellant mass for various traverse distances and traverse modes.



Figure 34 shows the propellant mass increasing for a hover-hop traverse, and similarly increasing with large discontinuities for a ballistic traverse. The propellant mass for the ballistic traverse includes both additional propellant for the additional distance traveled, but superimposed on this increase in propellant mass are the step changes in propellant that come from the need to add heavier engines, with their attendant structure as well. This leads to the ramped-stairstep effect seen in propellant mass for ballistic arc traverses.

In the end, while it cannot rigorously be concluded that a hover-hop traverse trumps a ballistic arc over any given distance, the effect identified here is counter to the conventional wisdom. Therefore, careful analysis should be applied to a traverse in a given situation to determine whether a hover-hop or a ballistic arc is preferred. The model developed in this thesis is one way of performing such analysis.

Another type of useful study is an investigation of the effects of increasing payload mass on a baseline hopping mission. To conduct this investigation, the baseline hop was varied by taking one payload element (the Sample Analysis Bay) and adding instances of it to the baseline payload (which did not include this payload). First one instance was added, then two, then one more at a time until five instances were onboard the hopping vehicle. This resulted in a steadily-increasing payload mass. The mass breakdowns as a function of the number of Sample Analysis Bays aboard appears in Figure 35.

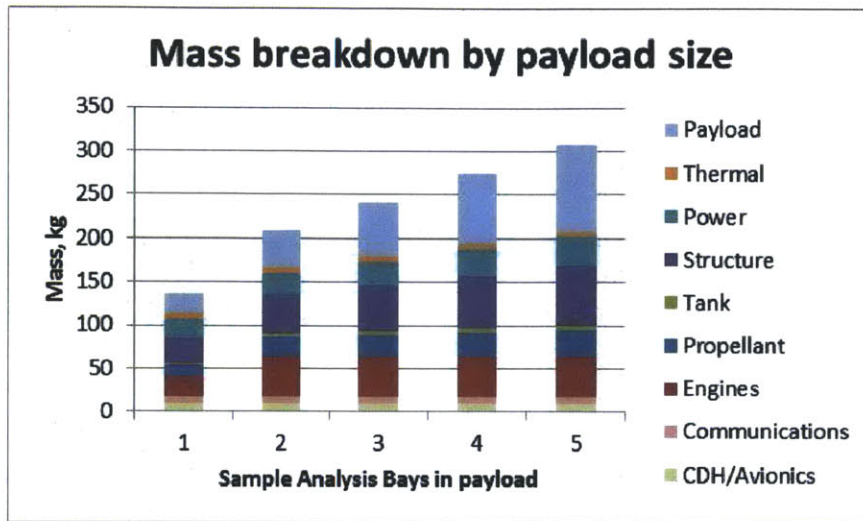


Figure 35. Mass breakdown for a series of hopping vehicles with increasingly larger payloads.

Note that, as payload mass increases linearly, there is also a linear increase in the total mass, with the exception of the jump from one to two Sample Analysis Bays in the payload. This is due to an increase in engine mass, driven by a change to the next size engine, that occurs between one and two Sample Analysis Bays aboard. If the payload mass were to be increased further, then eventually another step change in engine mass would occur, with a correspondingly large jump in total mass, even though the overall trend of punctuated linear rise in total mass would persist.

The baseline GLXP hop, conducted on every planetary body, provides a starting point for analyses of the effects of other user inputs on hopping vehicles designed by the model. The model includes two additional axes that are easily controllable by a user: the payload contents, and the maneuver sequence. Some investigation of the effects of variation in the maneuver type and payload mass was conducted, and the resulting curves through the hopping vehicle tradespace were analyzed.

However, this does not constitute a full and rigorous exploration of the tradespace that can be explored by the hopping vehicle model. Such detailed and formal investigation of the tradespace, using techniques developed explicitly for the purpose, is left to future work. The goal of tradespace investigation for this thesis is simply to arrive at an early picture of the main trends in the tradespace. Because hopping vehicles are still a nascent technology, little knowledge of design tradespaces relating to them exists. The initial tradespace investigation conducted in this thesis seeks to develop some knowledge, but not to exhaust it.

## **5.2 Specific Mission Investigation Hops**

In addition to general tradespace exploration, a few specific hopping missions are modeled. Some of these specific missions are drawn from prior suggestions in the literature; others are developed to take advantage of the unique abilities of hopping vehicles or to provide a point of comparison between hopping vehicles and rovers.

Missions undertaken on Luna include a sample return mission at Shackleton Crater, a sample return mission in the Copernicus crater region, and a descent into a lava tube in the Mare Tranquillitatis. On Mars, a mission to investigate the stratigraphy of the Valles Marineris and a separate mission to repeat a portion of the MER-A rover's traverse of the Columbia Hills are modeled. Additionally, a mission to hop around the shore of Kraken Mare on Titan is modeled.

Hopping vehicle design results presented for each of the example missions are found to be feasible for the selected missions. A feasible hopping vehicle design, while not precisely defined, can be understood to mean that the hopping vehicle design produced is both relatively

balanced (meaning that the design's mass distribution is not dominated completely by one subsystem without reason, and that the distribution of mass among subsystem is reasonable) and that the overall hopping vehicle mass is not too large to consider flying it. There is some element of judgment in this assessment, but it would be safe to assume that a feasible hopping vehicle must be no larger than the largest vehicle previously landed on another planetary body. To date, this is the Apollo LM, with a total wet mass of about 16,400 kg, of which about 7000 kg was landed on the lunar surface. Accordingly, a feasible upper mass limit for a hopping vehicle is in the middle thousands of kilograms upon the start of its mission.

Of the example missions presented in this section, all except the Titan mission and its lighter variant are less than 600 kg. As this is approximately the mass of the Viking lander (122), it is reasonable to consider a hopping vehicle design of this size or smaller feasible. The Titan mission and its variant, presented in Section 5.2.2.4, are in the range of 2000-3000 kg, and thus are less massive than the Apollo LM. Although this mission is thus near the outer edge of feasibility, it is still smaller than the largest vehicle ever landed on another planetary body.

### **5.2.1 Luna Hopping Missions – Shackleton Crater sample return**

In his master's thesis, Lanford (55) describes the relationship between hopping mobility and national policy and exploration objectives. As part of his thesis, he describes in detail missions on three planetary bodies which might be specifically enabled by hopping vehicles. Lanford's work was completed with knowledge of the advantages of hopping vehicles, as detailed in Chapter 1, and is aimed at "portraying hoppers in the most general conditions where they could operate, and showcasing both the capabilities and versatility of the hopper concept."

Some of the missions Lanford proposes are appropriate for re-examination in the context of the hopping vehicle model developed in this thesis. The first of these is a mission at the Shackleton Crater region on Luna, intended to gather samples from a shadowed area of Luna's surface.

Lanford specifies a hop into a permanently shadowed region of the lunar surface, near the rim of Shackleton Crater. Shackleton Crater is unique in that its region provides proximity to both peaks of near-eternal light, where the high latitude and elevation result in mountaintops where the sun almost never sets, and permanently-shadowed regions down in the crater, where sunlight has not fallen directly for billions of years. The well-irradiated regions are attractive locations for a permanent human-crewed outpost, and the nearby wells of eternal night may have been collection points for frozen volatiles, and are suspected to harbor frozen water.

Accordingly, sending a vehicle into the regions of shadow to collect a sample and return it to the regions of light for analysis is an intriguing prospect. Lanford formalizes his mission as carrying 55 kg of payload from a spot 4 km vertically up and 5 km away laterally to a target site at a well of eternal night and back to the crater rim.

The hopper Lanford proposes for this mission has a total mass of 126 kg, of which 25.3 kg is a propellant with a specific impulse of 300 seconds. The mass breakdown of this hopping vehicle is seen in Table 29 in Lanford (55).

With the more-detailed hopping vehicle model developed in this thesis, it is possible to model subsystems in much more detail than was afforded by the model available to Lanford, and to describe missions in more depth as well. Initial mission designs quickly showed that a traverse of 5 km laterally and 4 km vertically was not feasible. Hopping vehicles designed to follow this flight path showed diverging mass estimates in the model – meaning that the iterating mass estimates for the subsystems and the propellant mass would not converge on a viable solution. This is caused mathematically by the fact that more propellant requires a bigger tank and often larger engines, which in turn require more structure, which altogether require the addition of yet more propellant to perform a given traverse. This facet of hopping vehicle sizing dynamics corresponds to realistic issues encountered in the design of aerospace vehicles, and is more accurately captured by the subsystem granularity and interactions present in the model developed in this thesis than in the model available to Lanford.

Essentially, there is an upper limit to the feasible size of hopping vehicles that can be accurately represented in the model developed in this thesis. This is in part due to the divergence in total vehicle mass described above, but also partly caused by the fact that larger engines which work on vehicles carrying extensive amounts of fuel must also be throttled very low when these engines have burned off most of that fuel. The necessary performance specifications often exceed those for which the engines are rated. Forcing an engine choice can alleviate this problem and permit convergence of the sizing algorithm, but can also result in lessened realism in the model results.

A traverse of this length on Luna diverges. However, a traverse of slightly smaller scope could potentially deliver similar mission performance, without requiring the hopping vehicle to traverse the full distance Lanford specifies. Since the exact locations of the wells of eternal night are not perfectly known now, it is possible that some may exist closer to the crater rim, and not so deeply down from the crater rim peaks. Furthermore, if a human-crewed base is located near the crater rim, humans may be able to traverse some distance down and into the crater before deploying a hopping vehicle. In this scenario, a hopping vehicle might need to traverse a much smaller distance to access a well of eternal night.

Accordingly, the flight profile selected for this mission included a lateral traverse of 1500 m, with a total vertical change of 1000 m between starting/ending elevation and sample target elevation. A hopping vehicle deployed by a crew could quickly make a trip to a distant well of eternal night, recover a sample or just take science data, and then hop back to a location near the humans. This would enable human presence somewhere inside the crater, but also extend the total reach of humans or their technology to the deepest recesses of the lunar south polar region.

In order to model this mission, some master parameters were updated. The minimum temperature on the surface of Luna was updated to 30 K, to reflect possible conditions inside the wells of eternal night, and the thermal system on the hopping vehicle was correspondingly upgraded to reflect increased range of thermal conditions it will encounter. Radiator temperature for thermal control was upgraded from 335 K to 375 K, reflecting a need to develop an enhanced thermal system for the periods of time when the hopping vehicle is resting on the sunlit surface of Luna, before and after it descends into the well of eternal night. This upgrade has been found

to be desirable in any hopping vehicle sent to Luna. Furthermore, the default vehicle temperature was changed to 280 K, reflecting the need to create and deploy cold-tolerant mechanisms and electronics onboard a hopping vehicle which will descend into Shackleton Crater. Finally, given the large vertical distance which is traversed twice in this flight profile, the vertical speed of the hopping vehicle was changed from the default value of 3 m/s to a higher 15 m/s. Because there is effectively no atmosphere on Luna, there will be no additional drag losses from this change.

The model developed in this thesis sizes a thermal system based on an assumption of steady-state. The steady-state assumption is not completely applicable to a situation where a hopping vehicle does not stay for more than a few hundred seconds in a well of eternal night. However, the assumptions made by the thermal model used in this thesis are biased toward the production of a conservative mass estimate for the thermal subsystem. A full and detailed thermal analysis would be required to find a more accurate estimate for the mass of the thermal subsystem, and the result produced by the model developed in this thesis is intended to provide an initial starting point for such a full thermal analysis.

The flight profile selected includes a series of maneuvers intended to get the hopping vehicle from a station further up the crater slope to a lower point and then back. The profile is described by 6(10) – 5(1500@180) – 6(-950/0) – 4(360) – 6(-50/1) – **13(300)** – 6(1000) – 5(1500@0) – 6(-10/1) – 14(300). The plotted profile appears in Figure 36.



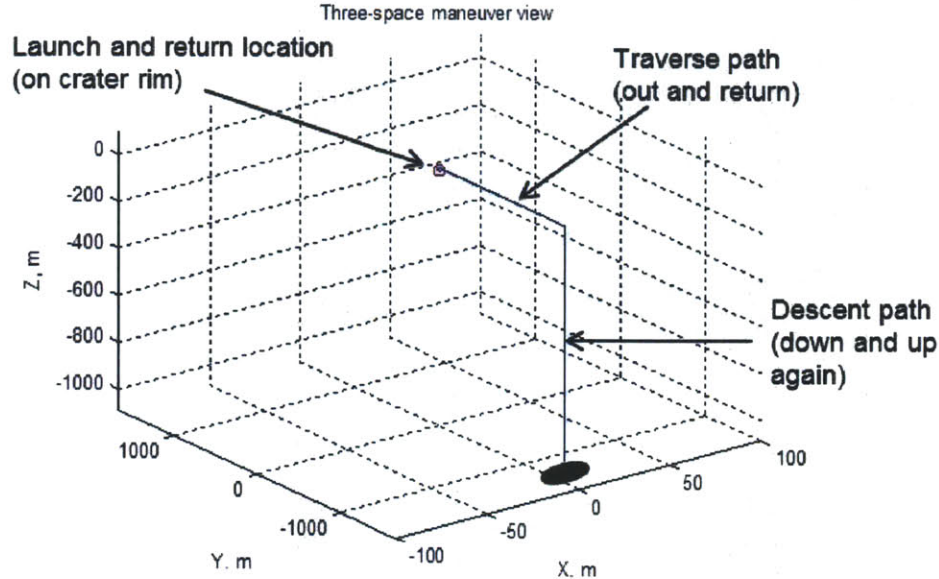


**Figure 36. Large-scale view of modeled traverse into a well of eternal night on the floor of Shackleton Crater.**

The profile this formalizes includes a short launch to clear terrain, then a traverse into the crater, followed by a descent to near the crater floor, a full-circle scanning maneuver to locate possible samples, and a final descent to the surface. After a very quick sample recovery procedure, the hopping vehicle relaunches to traverse height and returns to its launch position. There it touches down and radiates a radio signal for a short time, until located by mission control on Earth or recovered by EVA astronauts on Luna. For this mission, and for all the example missions following it in this chapter, the appropriate lengths of time periods for science and communications segments were estimated. Although the time of a communications segment can be set by the user, it is up to the user to ascertain that the hopping vehicle will maintain a line of sight to Earth during the entire communications segment. For the purposes of this thesis, it will be assumed that a line of sight is maintained during each communications segment shown.

The operational profile of this mission appears in Figure 37.

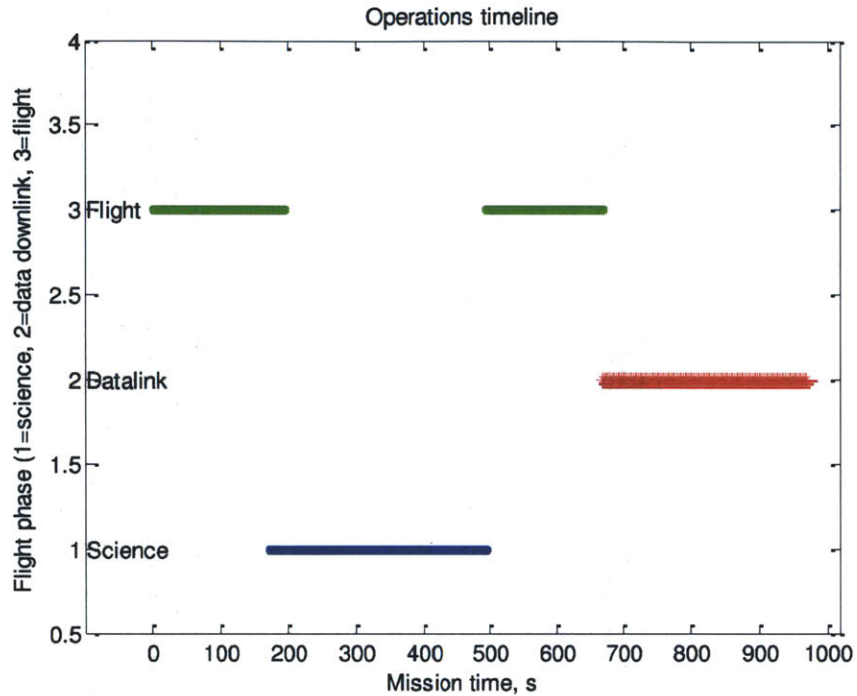


**Figure 37. Operational timeline for a traverse into a well of eternal night on the floor of Shackleton Crater.**

Note the comparatively high ratio of the total flight time to the total operational time. This is an effect of the large distances that must be traversed, including the vertical portion of the traverse. Comparatively short communication and science time segments are included, but this is done partially in consideration for the likelihood that the hopping vehicle should only spend a short period of time in a well of eternal night.

The mass breakdown for the hopping vehicle design generated appears in Figure 38.

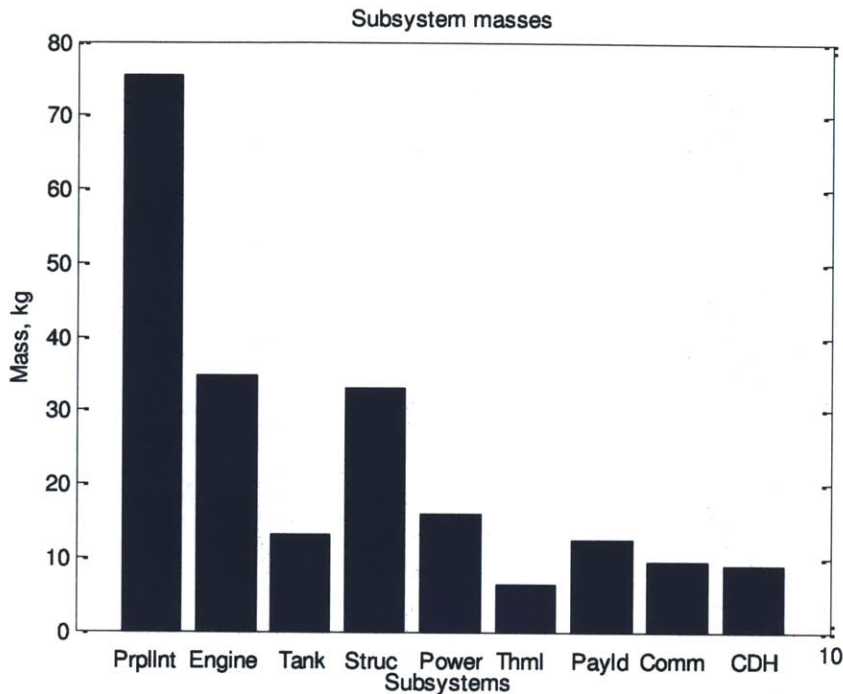


**Figure 38. Subsystem mass breakdown for a traverse into a well of eternal night on the floor of Shackleton Crater.**

Notably, the propellant is the major mass component. The entire hopping vehicle masses about 210 kg. The upgraded thermal system is the cause of a comparatively reduced mass required for the thermal subsystem; however, this comes at the cost of the need to develop and build the upgraded thermal system, which is not explicitly captured by the model, but must be noted by the user.

This mission also was not able to select an engine and converge without assistance. The model had to have an engine forced, and as such, additional development may be required for a new or upgraded engine for this hopping vehicle.

These insights stem from the basic fact that this is a very ambitious and long traverse for a hopping vehicle. However, the model indicates that it is within the realm of potential feasibility, and therefore is a candidate for detailed design and further investigation. A brief summary of the hopping vehicle’s technical characteristics appears in Table 11.

**Table 11. Technical characteristics of a hopping vehicle for a descent into a well of eternal night on Luna.**

<u>Design decisions</u>		<u>Technical sizing</u>		<u>Cost information</u>	
<b>Engine</b>	MR-80B (TRL 7)	<b>Total mass</b>	210.2 kg	<b>Dev cost</b>	468 \$M
<b>Power type</b>	Solar array/battery	<b>Max data rate</b>	312700 kb/s	<b>Build cost</b>	29.3 \$M
		<b>Max onboard data storage</b>	93810 Mb	<b>Ops cost</b>	70.5 \$K
		<b>Max power</b>	65 W		
		<b>Max thrust</b>	508 N		

Figure 39 shows a comparison between the hopping vehicle designed here and the vehicle designed by Lanford, on a subsystem basis.

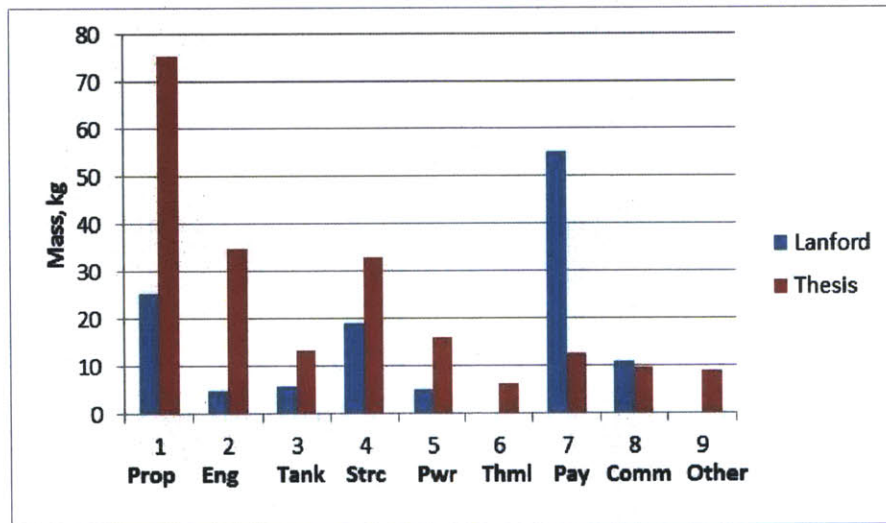


**Figure 39. Mass breakdown comparison for hopping vehicles designed to visit wells of eternal night in Shackleton Crater.**

Note that the major differences in Propellant, Engine, and Structure are a consequence of the increased need for propellant and its cascading effects. Additionally, somewhat larger engines are required, and furthermore, four engines are required by the baseline architecture of the model developed in this thesis, while Lanford's model assumes only a single engine.

The payload difference is caused by the fact that Lanford selected a large payload to account for margin, while the model used in this thesis only drew from the catalogue of available scientific instruments. Only a few instruments would be required to land, retrieve a sample, and then return with it.

As will be seen in comparison to missions modeled on those taken from Lanford's thesis, hopping vehicle designs generated by the model developed in this thesis typically are more massive than those developed by Lanford. This is due in significant degree to the underlying hop model used by Lanford, which was originally developed by Michel (52). This source model has key limitations, and uses only simple parametric models to estimate masses for tanks, engines, and vehicle structure. While the parametric relationships are somewhat useful, the engine parametric model is derived from Michel's assumption of a single-engine vehicle, and relies on data taken from a relationship between engine thrust and engine mass empirically derived from a dataset including mainly engines used on launch boosters. Thus, the parametric relationship does not capture the type of deep-throttling engines that would likely be used in a hopping vehicle. Furthermore, CDH/avionics, thermal systems, and GNC are not modeled explicitly in the Michel model, and are instead wrapped into payload. Finally, the Michel model also has simplifying assumptions of 300 seconds for the specific impulse of every fuel/engine

combination, and a single simplification of the hopping maneuver process. The Middleton model (54), with which Lanford supplements his analyses, also makes no modeling at the subsystem and subsystem-interaction levels. The overall effect is that the Michel-Lanford model has less granularity, and therefore does not capture many of the realistic effects that invariably add to initial mass estimates.

### **5.2.2 Luna Hopping Missions – Mare Tranquilitatis Lava Tube Descent**

Another mission investigated by Lanford is hopping down into recessed geological features of the lunar surface, including some like the Mare Tranquilitatis lava tubes. These tubes, visible in lunar photographs, are recessed pits in the surface of Luna that may have been caused by lava flowing out of tubes before hardening. The exact nature of their interior features is unknown, but may provide a window into the composition of Luna's upper crust if it can be investigated at close range.

Lanford proposes a traverse from a kilometer away to the edge of a Mare Tranquilitatis pit, followed by a descent into and return from the pit, which is estimated to require the ability to traverse 200 m horizontally and 120 m vertically. The total hopper payload estimated is 63 kg, with the overall hopper being described by a total mass of 104 kg, including 3.9 kg of propellant, 1.6 kg of propellant tank, 3.9 kg of engine, 5 kg of power systems, 11 kg of communications systems, and 15.6 kg of structures.

For this thesis, the hop into and out of the lava tube will be modeled. The thermal system is assumed to have undergone an upgrade, such that the radiators radiate thermal energy at 375 K,

rather than the standard specified 335 K. However, the vehicle is not assumed to have a requirement to be cold-tolerant, as in the Shackleton Crater mission. Given the possible difficulty of navigating out of a lava tube after touching down on the floor of the tube, it was assumed that navigational upgrades would be required. Accordingly, the mass of the GNC system was bumped from 4 kg to 6 kg, and the power was bumped from 15 W to 25 W. These upgrades capture the need to pay additional attention to hardware requirements for a mission like this, although they may reflect either improved capability or increased redundancy. Any additional complexity required in the development of navigational software is not captured.

Operationally, the mission was modeled in more granular detail than Lanford's model permits. A simple payload, consisting of a panoramic binocular camera instrument, was selected. The flight profile, described as 6(10) – 5(1000@180) – 6(-10/1) – **13(900)** – 14(1800) – 16(1800) – 6(5) – 5(200@90) – 1(10) – **7(-125/1)** – **13(900)** – 6(110) – 4(180) – 6(15) – 5(200@270) – 6(-5/1) – 14(7200), allows entry into the lava tube from a location emplaced on or near the tube's outer edge on Luna's surface, after the kilometer traverse to approach the tube, plus a brief information-gathering stop on the edge of the tube. Following this is a transmission period to send data back to Earth, and then a waiting period during which mission control can make a decision to enter the tube or abort, and communicate it to the hopping vehicle. The hopping vehicle then traverses horizontally to the center of the lava tube's edge at a low height of 5 m above the lunar surface, hovers for ten seconds to ensure navigational stability and to locate a safe landing site, and then descends down to the floor of the tube and touches down. The hopping vehicle then takes pictures of the interior of the lava tube for 15 minutes, after which it ascends to near the top of the lava tube, taking a 180-degree rotational scan before it reaches the

top of the tube to perform a navigational fix and ensure it is still able to exit the tube without impacting an obstacle on the way. The hopping vehicle then traverses back over to the edge of the tube's entrance and touches down, after which it transmits its collected imagery back to mission control on Earth.

Although this hopping vehicle mission concept works in isolation, it also shows potential as a human-machine collaborative exploration effort. Instead of having a hopping vehicle emplaced near a lunar lava tube by a landing vehicle, the hopping vehicle could be placed there by a crew of EVA humans, potentially as they make an exploration traverse over the Mare Tranquilitatis. The humans could collect imagery and information around the rim of the lava tube, emplace or offload the hopping vehicle, and then proceed on their traverse while the hopping vehicle powers up, descends into the lava tube, returns, and then downlinks its collected data to Earth. The humans could then conceivably even retrieve the hopping vehicle on a return traverse for later use.

The three-dimensional view of the hopping traverse appears in Figure 40.



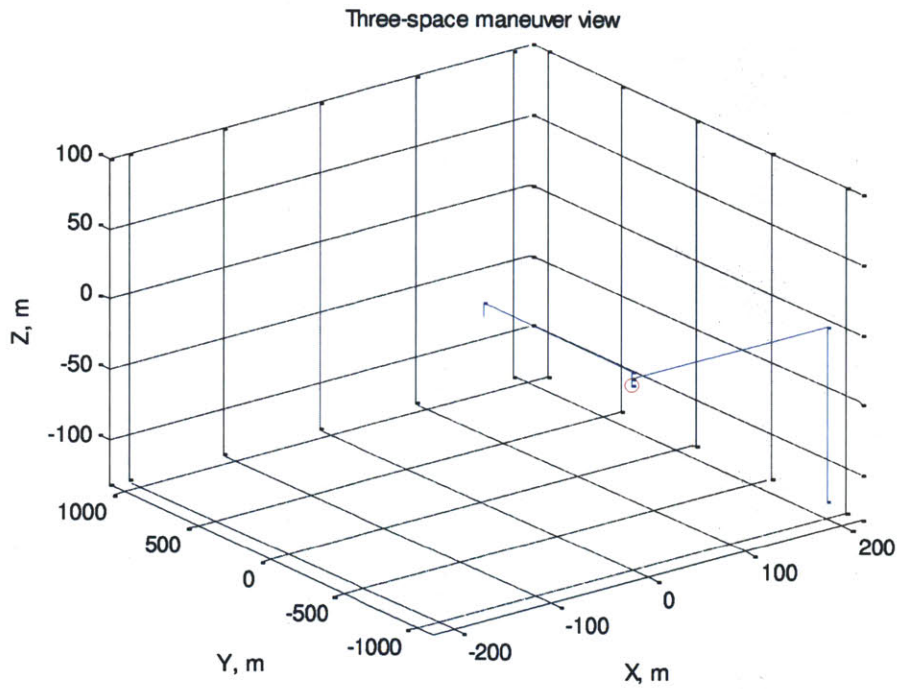


**Figure 40. Traverse path for a descent into a lava tube in Mare Tranquilitatis.**

Additionally, Figure 41 shows the mass breakdown of the hopping vehicle sized to perform this mission.

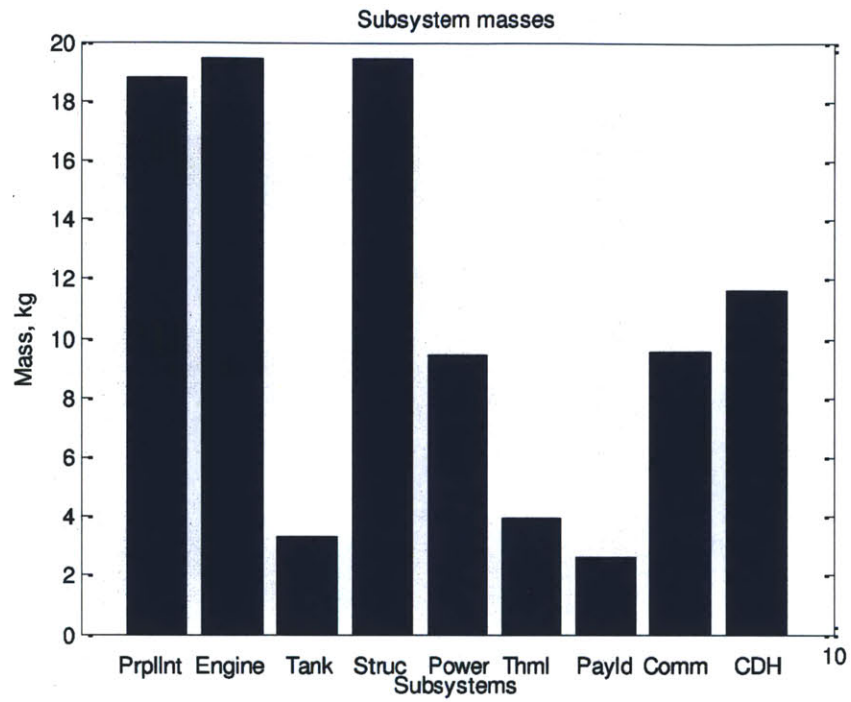


**Figure 41. Subsystem mass breakdown for a descent into a lava tube in Mare Tranquilitatis.**

The mission does not require a very large propulsion fraction as designed, and accordingly seems feasible.

The operations timeline for the mission as designed appears in Figure 42.

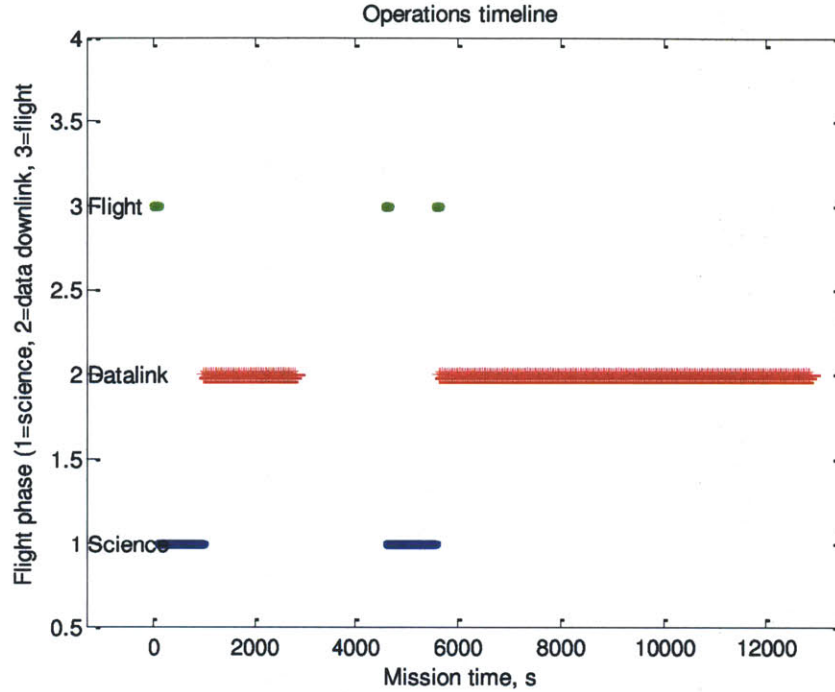


**Figure 42. Operations timeline for a descent into a lava tube in Mare Tranquillitatis.**

Note that the hopping vehicle takes two separate intervals to communicate with the ground and downlink data. Also note that the relative ratio of hopping time to total mission time is very small, as a consequence of the fact that the hopping vehicle moves very rapidly, even over relatively long distances.

A comparison on a subsystem mass basis between Lanford's designed hopper and the hopping vehicle appears in Figure 43. Note again that Lanford's model does not capture all the subsystem interactions of the model used in this thesis, although the two vehicles are overall similar in size.

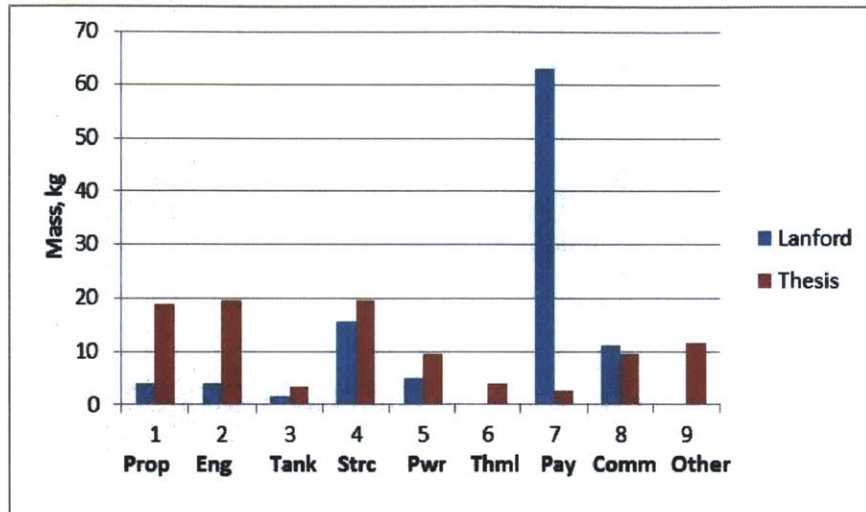


Figure 43. Subsystem mass comparison for hopping vehicles designed to explore lava tubes in Mare Tranquilitatis.

Table 12 summarizes the design of a hopping vehicle for exploring lava tubes in the Mare Tranquilitatis region of Luna.

Table 12. Technical characteristics of a hopping vehicle for exploring lava tubes on Luna.

<u>Design decisions</u>		<u>Technical sizing</u>		<u>Cost information</u>	
<b>Engine</b>	Bell 8414 (TRL 6)	<b>Total mass</b>	98.2 kg	<b>Dev cost</b>	305 \$M
<b>Power type</b>	Solar array/battery	<b>Max data rate</b>	147,456 kb/s	<b>Build cost</b>	23.0 \$M
		<b>Max onboard data storage</b>	278,004 Mb	<b>Ops cost</b>	79.4 \$K
		<b>Max power</b>	48.8 W		
		<b>Max thrust</b>	243.4 N		

### 5.2.2.1 Luna Hopping Vehicle Missions – Copernicus Crater

Copernicus Crater is a large geological feature on Luna that has played a significant role in assigning relative geological age to features of Luna’s surface (127). Further exploration of the features in and around Copernicus Crater would contribute greatly to the development of knowledge about Luna’s history (and, in turn, Earth’s history).

Copernicus Crater is very large, and includes a number of smaller features in and around its own selenography. Key science objectives for exploring Copernicus Crater include the exploration of features which provide insight into the stratigraphy in the region and the collection of samples from multiple locations around the crater floor. These science objectives might feasibly be accomplished by a vehicle which lands on the inner floor of the crater, as had been planned for one of the later canceled Apollo missions (127).

A hopping mission could therefore consist of an exploration of several features of the floor of the crater. Figure 44, taken from (128), shows a series of interesting selenological features closely grouped on the floor of Copernicus Crater. A traverse, as laid out by the heavy yellow lines in the figure, could visit two intermediately-sized hills, a rille, and a partially-filled crater while traveling only a few kilometers total. The vertical traverse heights are estimated.

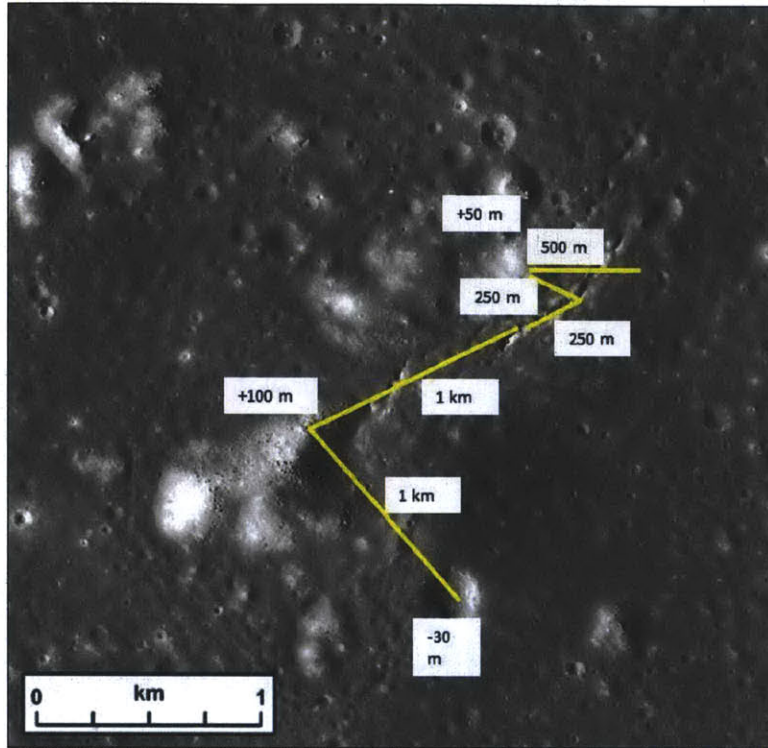
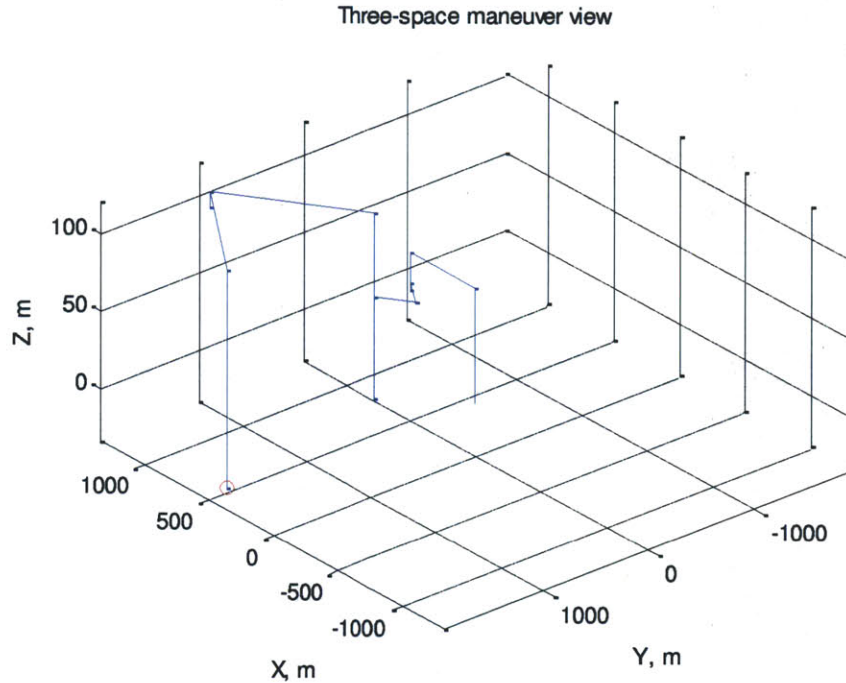


Figure 44. Hopping vehicle traverse path overlaid on a section of Copernicus Crater's floor.

As plotted in the hopping vehicle model, this mission is as appears in Figure 45.



**Figure 45. Three-dimensional view of hopping vehicle traverse path on a section of Copernicus Crater's floor.**

A mission profile of 6(75) – 5(500@90) – 6(-25/1) – **13(1200)** – 14(3600) – 6(5) – 5(250@315) – **5(250@45)** – 6(-65/1) – **13(1200)** – 14(3600) – 6(120) – 5(1000@45) – 6(-10/1) – **13(1200)** – 14(3600) – 6(10) – 5(1000@315) – 6(-140/1) – **13(1200)** – 14(3600) is proposed for this mission. Note that there are four separate science periods, all twenty minutes each and followed immediately by a communications segment. These science periods reflect visits to the first hill, the rille, the second hill, and the filled crater. In order to perform the science, a payload including a driller/corer tool to collect samples, a panoramic camera to capture imagery, a spectrometer (the APXS), and a magnetometer are included in the hopping vehicle's payload.

The operational timeline, seen in Figure 46, shows the operational tempo, including the science and communications segments.



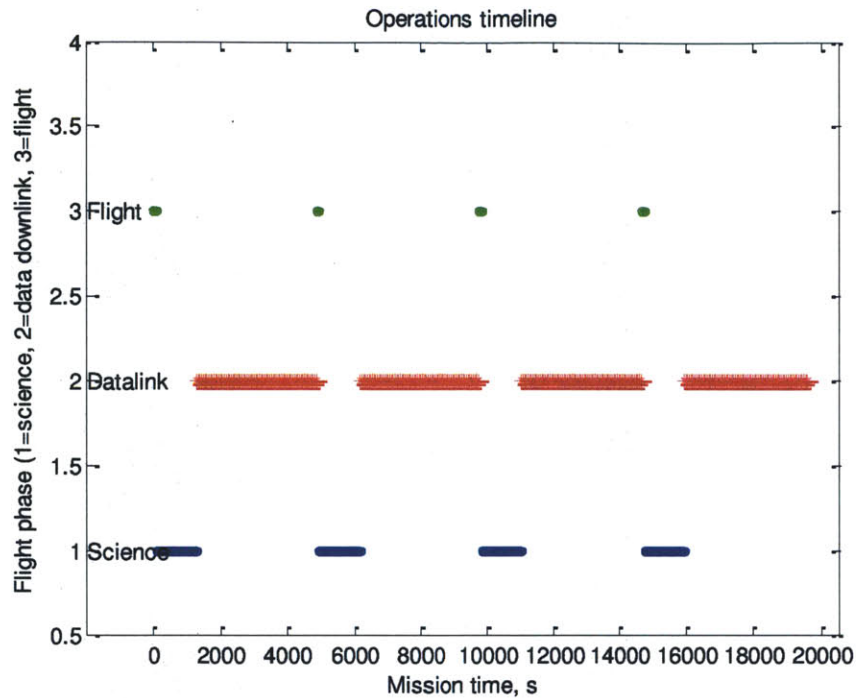


Figure 46. Operational timeline for a traverse path on a section of Copernicus Crater’s floor.

Notably, even with several fairly lengthy science segments and communications segments occurring during the mission, the entire profile can be completed in less than a quarter of a day. Even greatly increasing the length of the science and communications segments would not alter the fact that a hopping vehicle can complete the physical motions required to traverse the distances required for a mission like this on the order of tens or hundreds of seconds, where a roving vehicle might require tens or hundreds of hours.

The resulting hopping vehicle (which also includes the same upgraded thermal system, with a radiator temperature of 375 K, that is also onboard the other lunar hopping vehicles), has a total mass of 127.4 kg. Table 13 summarizes this hopping vehicle design.



**Table 13. Technical characteristics of a hopping vehicle for traversing a section of Copernicus Crater's floor.**

<b>Design decisions</b>		<b>Technical sizing</b>		<b>Cost information</b>	
<b>Engine</b>	Bell 8414 (TRL 6)	<b>Total mass</b>	127.4 kg	<b>Dev cost</b>	370.6 \$M
<b>Power type</b>	Solar array/battery	<b>Max datarate</b>	99,921 kb/s	<b>Build cost</b>	25.7 \$M
		<b>Max onboard data storage</b>	359,716 Mb	<b>Ops cost</b>	83.8 \$K
		<b>Max power</b>	52.8 W		
		<b>Max thrust</b>	303 N		

The mass breakdown for this hopping vehicle is seen in Figure 47.

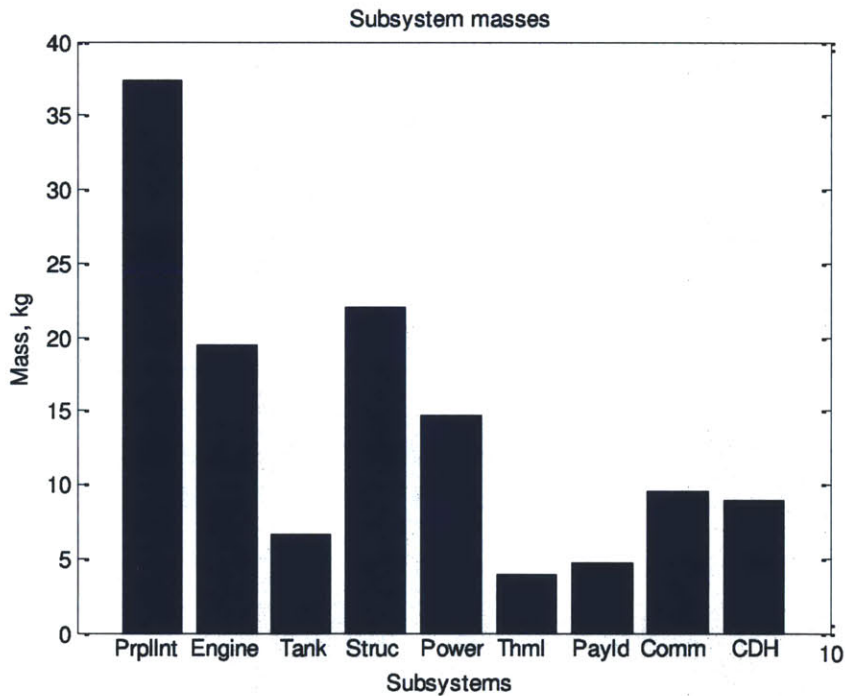


**Figure 47. Subsystem mass breakdown for a hopping vehicle to traverse a section of Copernicus Crater's floor.**

Note that, with the lengthy maneuvers included in this mission, the hopping vehicle's mass fraction of propellant approaches 0.25.

The distribution of propellant mass expended, broken down by maneuver, is seen in Figure 48.

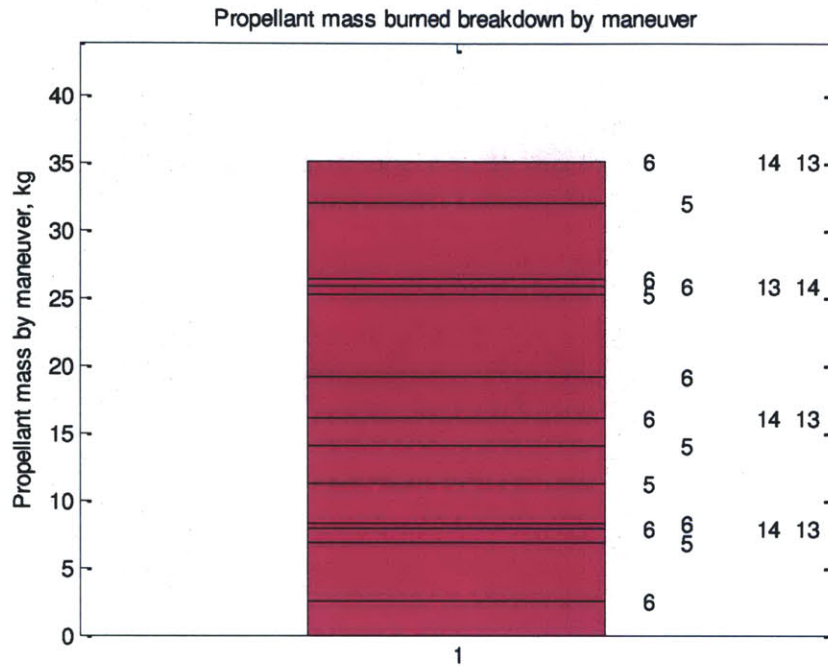


Figure 48. Propellant use breakdown for a traverse path on a section of Copernicus Crater's floor.

Note that three major traverses (the first traverse, and the two long 1-km traverses) require the largest portions of propellant by mass.

For additional insight, it is possible to investigate two variations on the basic Copernicus Crater mission. The first variation is the same as the original mission, except with the thermal system returned to its normal capability (and the master parameter of radiator temperature set back to 335 K from 375 K).

The characteristics of this mission appear in Table 14, and the subsystem mass breakdown is seen in Figure 49.

**Table 14. Technical characteristics of a variant hopping vehicle for exploring Copernicus Crater.**

<b>Design decisions</b>		<b>Technical sizing</b>		<b>Cost information</b>	
<b>Engine</b>	MR-80B (TRL 7)	<b>Total mass</b>	233.3 kg	<b>Dev cost</b>	502.1 \$M
<b>Power type</b>	Solar array/battery	<b>Max datarate</b>	99,921 kb/s	<b>Build cost</b>	34.6 \$M
		<b>Max onboard data storage</b>	359,716 Mb	<b>Ops cost</b>	83.8 \$K
		<b>Max power</b>	52.8 W		
		<b>Max thrust</b>	552 N		

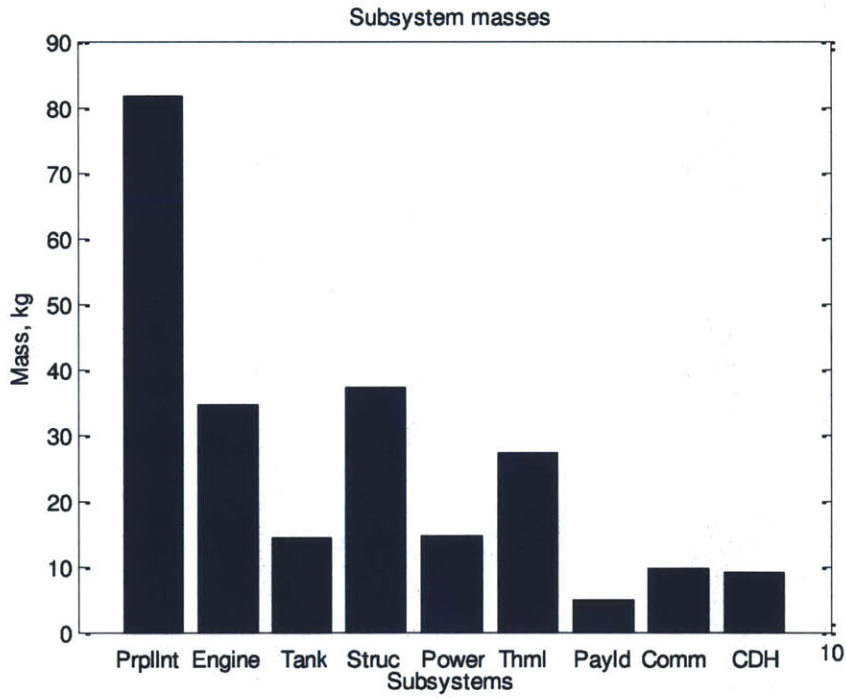


**Figure 49. Subsystem mass breakdown for a variant hopping vehicle for exploring Copernicus Crater.**

Note that the effect of the larger thermal system is to cause a jump in engine size, structure mass, and correspondingly propellant and tank mass. However, the overall design is still a feasible hopping vehicle.

A second variation on the basic Copernicus Crater mission is a version of the same mission on Mars. A Mars Copernicus mission would include the exact same payload and flight profile, but would take place on Mars, and would thus highlight the differing effects of the different targeted planetary body. The upgraded thermal system would remain in place.

The mass breakdown generated for this variation appears in Figure 50, followed by Table 15 containing the technical details.

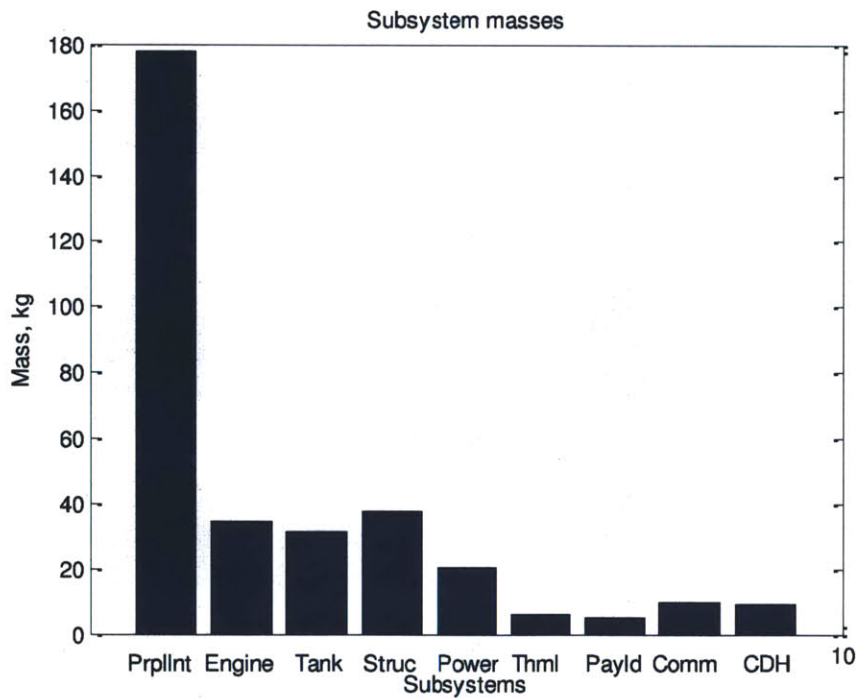


Figure 50. Subsystem mass breakdown for a hopping vehicle exploring a Martian crater.

**Table 15. Technical characteristics of a hopping vehicle for a hopping vehicle exploring a Martian crater.**

<b>Design decisions</b>		<b>Technical sizing</b>		<b>Cost information</b>	
<b>Engine</b>	MR-80B (TRL 7)	<b>Total mass</b>	330.7 kg	<b>Dev cost</b>	590.4 \$M
<b>Power type</b>	Solar array/battery	<b>Max data rate</b>	99,921 kb/s	<b>Build cost</b>	31.9 \$M
		<b>Max onboard data storage</b>	359,716 Mb	<b>Ops cost</b>	83.8 \$K
		<b>Max power</b>	84.0 W		
		<b>Max thrust</b>	869 N		

Notably, while a small increase is seen in engine size (driven in part by the expanded range of thrust requirements), a larger increase in total propellant mass is seen. This is again driven partly by the increased gravity on Mars, and partly by the cascading effects of carrying additional mass in terms of engines, tank, and supporting structure.

A breakdown of fuel consumption by mass, as seen in Figure 51, shows similar shape to the breakdown on Luna. Three traverses consume the largest chunks of fuel (and more absolute mass of fuel on a higher-gravity planetary body).



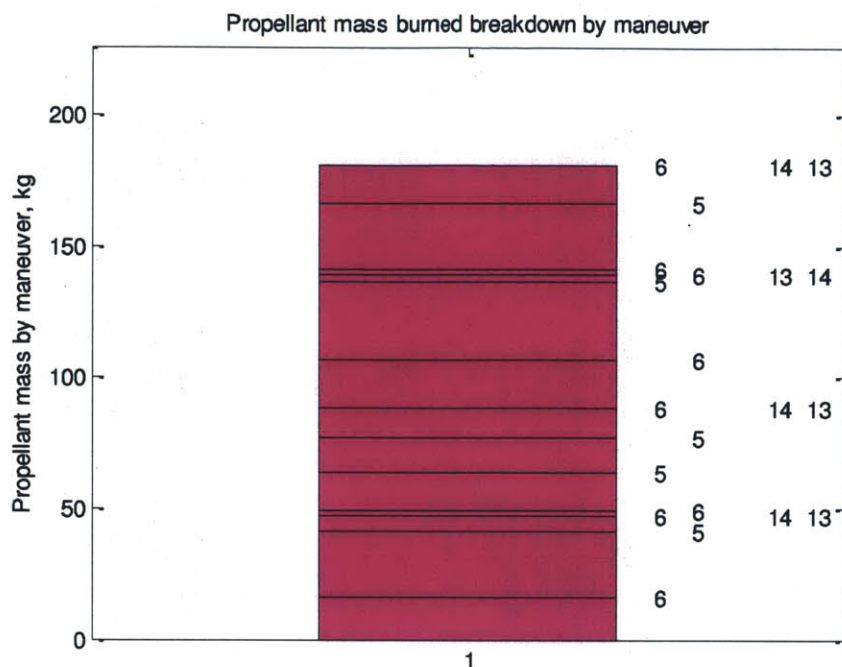


Figure 51. Propellant use breakdown for a hopping vehicle exploring a Martian crater.

### 5.2.2.2 Mars Hopping Missions – Valles Marineris Stratigraphy

Another mission of potentially great interest to a hopping vehicle mission designer is a stratigraphic survey carried out inside the Valles Marineris terrain feature on Mars. Valles Marineris is a massive canyon that runs a long distance over the surface of Mars, and close survey of the walls of the canyon may provide insight not only into the geological history of Mars but also into the substrate composition below the topsoil.

Using a model with all master parameters set to nominal values, a payload of two cameras (one for a panoramic overview, and one paired with a ranged spectrometer for detailed evaluation of chemical makeup) and a magnetometer was selected. This payload should permit analysis of several facets of the stratigraphy as the hopping vehicle passes over the canyon face.

Because the canyon is extremely large, there is an incredibly wide variety of depths and face terrain from which to select as a target. For the purposes of this mission, a location approximately 1 km deep, with faces that slope at an average of 45 degrees, will be used.

The mission will include a stairstepping traverse down the sloping canyon face, followed by a 1-km traverse along the canyon floor to trace the horizontal evolution of the stratigraphy. The corresponding flight profile is 6(5) – 5(100@180) – 6(-100/0) – 5(200@180) – 6(-200/0) – 5(200@180) – 6(-200/0) – 5(200@180) – 6(-200/0) – 5(200@180) – 6(-200/0) – 5(100@180) – 6(-100/0) – 1(10) – 5(1000@90) – 6(-10/1) – 14(7200). The operations timeline for this profile appears in Figure 52.

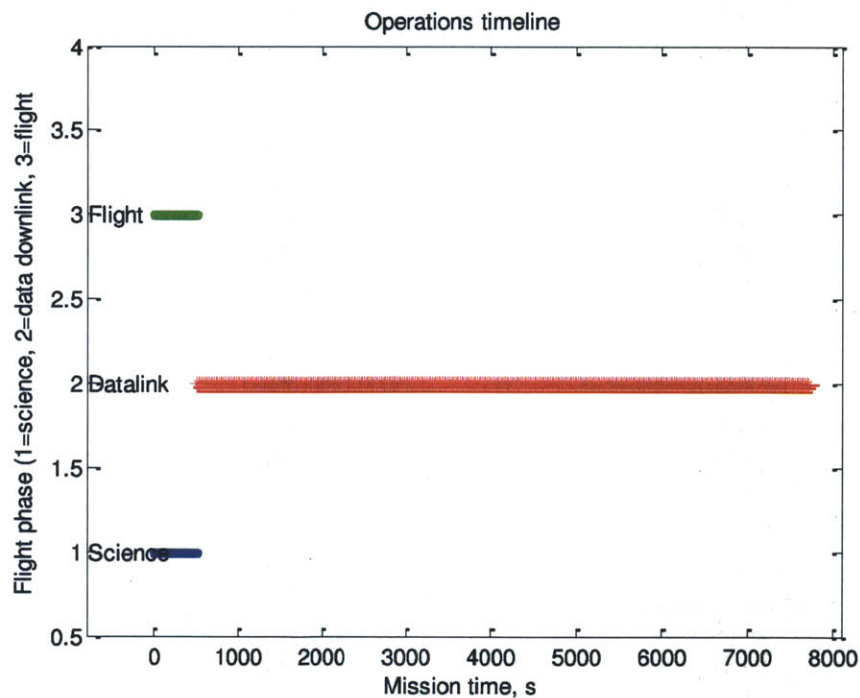


Figure 52. Operational timeline for a stratigraphy survey in Valles Marineris.

Note that science activities occur essentially throughout the entire flying traverse, creating a constant stream of data. Note also that the flight is rather lengthy, as the hopping vehicle must traverse more slowly vertically down than it does horizontally (to maximize exposure to the canyon face). A vertical traverse speed of 3 m/s is used here.

A visualization of the traverse in three-dimensional space appears in Figure 53.

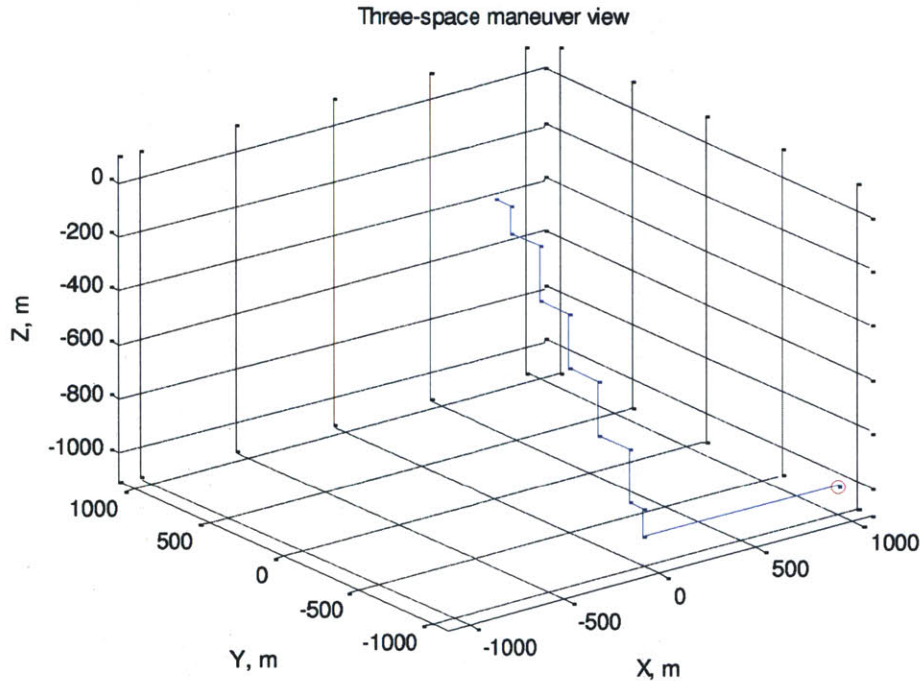


Figure 53. Three-dimensional view of the flight path for a stratigraphy survey in Valles Marineris.

The resulting design characteristics appear in Table 16.



**Table 16. Technical characteristics of a hopping vehicle for performing stratigraphy in Valles Marineris.**

<b>Design decisions</b>		<b>Technical sizing</b>		<b>Cost information</b>	
<b>Engine</b>	MR-80B (TRL 7)	<b>Total mass</b>	598.8 kg	<b>Dev cost</b>	752.5 \$M
<b>Power type</b>	Solar array/battery	<b>Max data rate</b>	20,423 kb/s	<b>Build cost</b>	34.8 \$M
		<b>Max onboard data storage</b>	147,047 Mb	<b>Ops cost</b>	74.9 \$K
		<b>Max power</b>	75.7 W		
		<b>Max thrust</b>	1576 N		

Following this is the subsystem mass breakdown, in Figure 54.

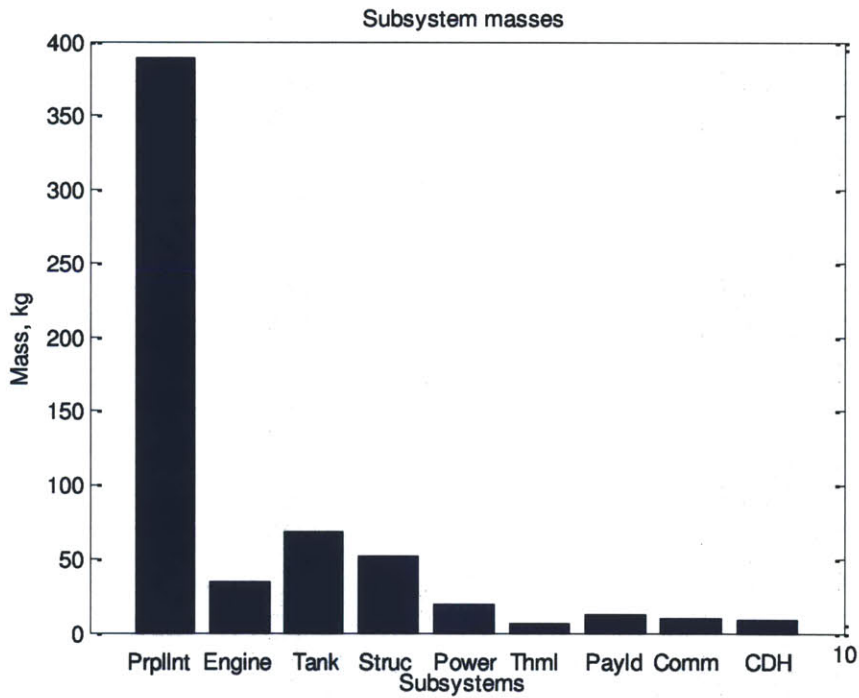


**Figure 54. Subsystem mass breakdown for a hopping vehicle to perform stratigraphy in Valles Marineris.**

Note that the comparatively high gravity of Mars and the long, slow vertical traverses have resulted in the need to carry a large amount of propellant.

The amount of propellant burned per maneuver is seen in Figure 55. Note that, although the horizontal traverse along the canyon floor requires a significant amount of propellant itself, the larger and earlier phases of the stairstepping phase require yet more propellant, as they naturally are carrying around a large mass of propellant to be used later in the mission.

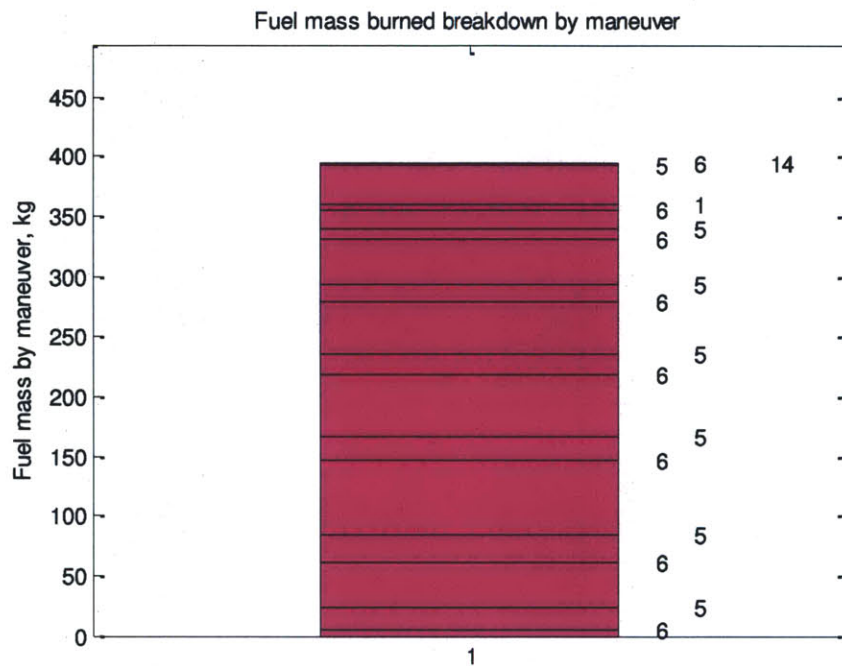


Figure 55. Propellant use breakdown for a hopping vehicle performing a stratigraphy survey in Valles Marineris.

### 5.2.2.3 Mars Hopping Mission – MER-A Retracing

An interesting point of comparison between hopping vehicles and other planetary surface exploration vehicles could be created by repeating a significant portion of a rover traverse with a hopping vehicle.

A portion of the traverse made by the MER-A rover, named *Spirit*, was therefore duplicated in the hopping vehicle model. The traverse portion selected was that from Sol 1 to Sol 502, during which time the MER-A vehicle traveled from a location nearby Bonneville Crater to the crater, and then from there to the low peaks of the Columbia Hills, passing the smaller Missoula and Lahontan craters on the way. The rover then climbed gradually to the peaks of the Columbia Hills, at around 50 m elevation.

Although the rover made periodic stops to perform science activities on the way to the Columbia Hills, the hopping vehicle cannot do the same. The hopping vehicle can, however, visit each of the most interesting sites along the traverse route.

Based on the information at (129), the MER-A rover typically took a few days to make science observations, and drove anywhere from about ten to about one hundred meters in a day when heading toward a distant goal. To match this traverse with a hopping vehicle, an overall view of the MER-A rover's path was obtained and tracks were laid on it to assess the distances between the largest and most interesting targets visible on the map. Figure 56 shows the route, with the rover's path traced in light yellow and the hopping vehicle's path in heavy yellow.

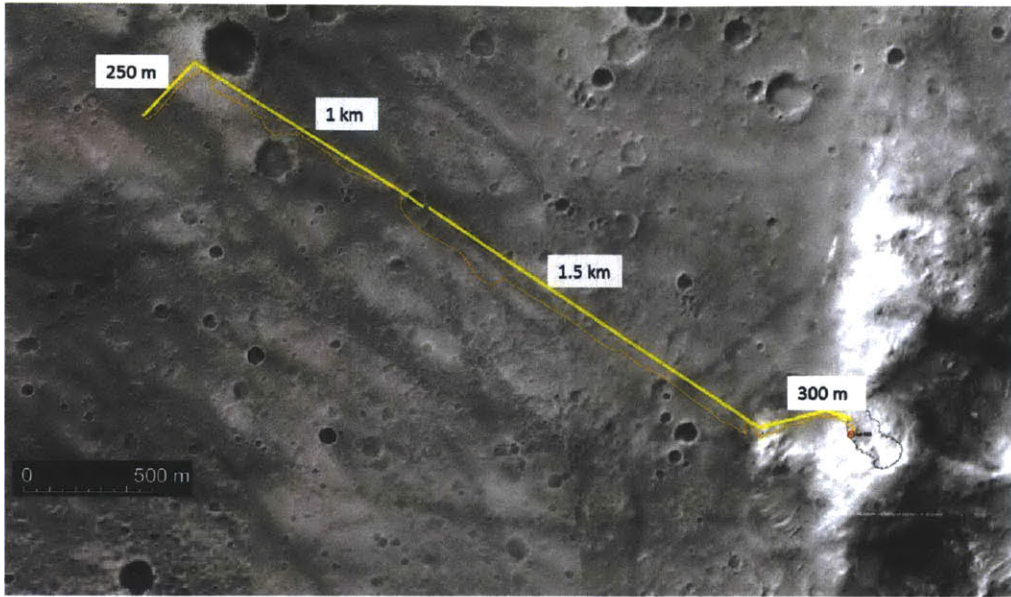


Figure 56. Traverse path for a hopping vehicle retracing MER-A's path. Original image is from (130).

The hopping vehicle's path consists of four major legs: the first is a traverse from the starting point to Bonneville Crater, followed by a traverse to Lahontan Crater (bypassing Missoula Crater along the way). Following this, a long traverse leg leads to the base of the Columbia Hills, and then a 300-m lateral traverse combined with 50 m of vertical rise leads to the peaks of the Columbia Hills.

This traverse path, including stair-stepping up to the top of the Columbia Hills before touchdown, is described by 6(10) – 5(250@45) – 6(-10/1) – **13(7200)** – 6(10) – **5(1000@135)** – 6(-10/1) – **13(7200)** – 6(10) – 5(1500@135) – 6(-10/1) – **13(7200)** – 6(10) – 5(100@90) – 6(15) – 5(100@90) – 6(15) – 5(100@135) – 6(15) – 1(10) – 6(-10/1) – **13(7200)** – 14(28800). This describes a mission with four touchdown science segments, and one flyby science segment (for the trip by Missoula Crater). The mission terminates with an eight-hour data downlink segment.

The resulting mission profile appears in Figure 57. Below that, in Figure 58, appears the three-dimensional view of the mission.

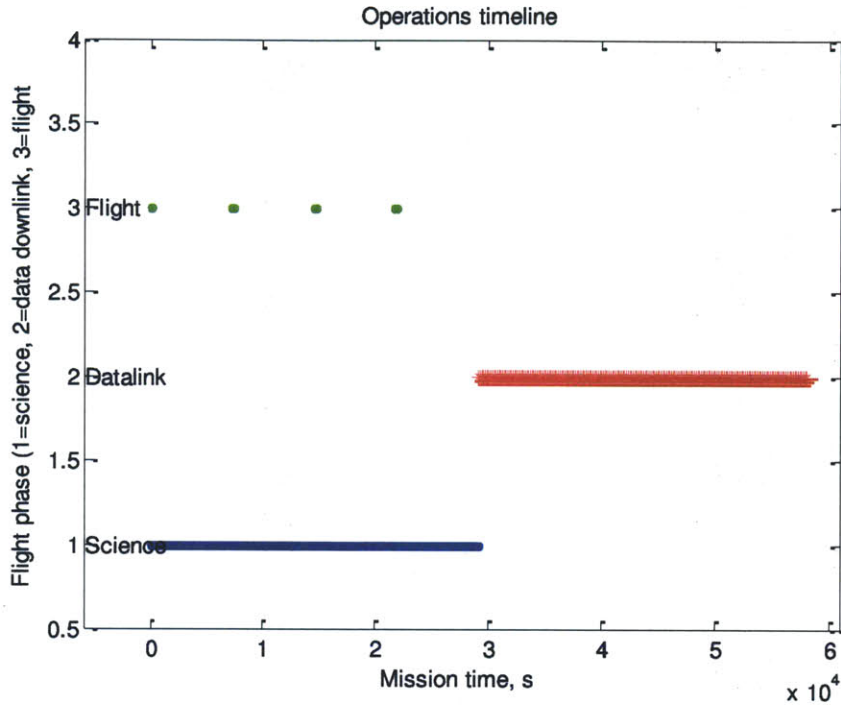


Figure 57. Operational timeline for a traverse retracing the MER-A mission.

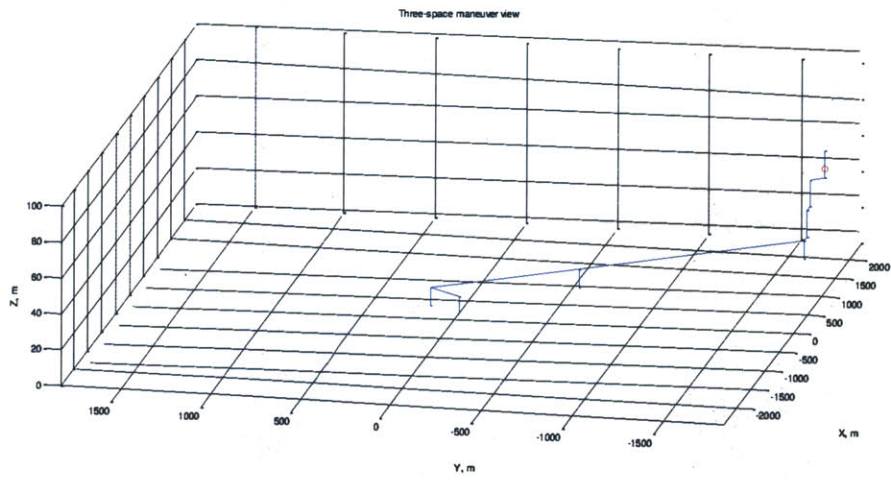
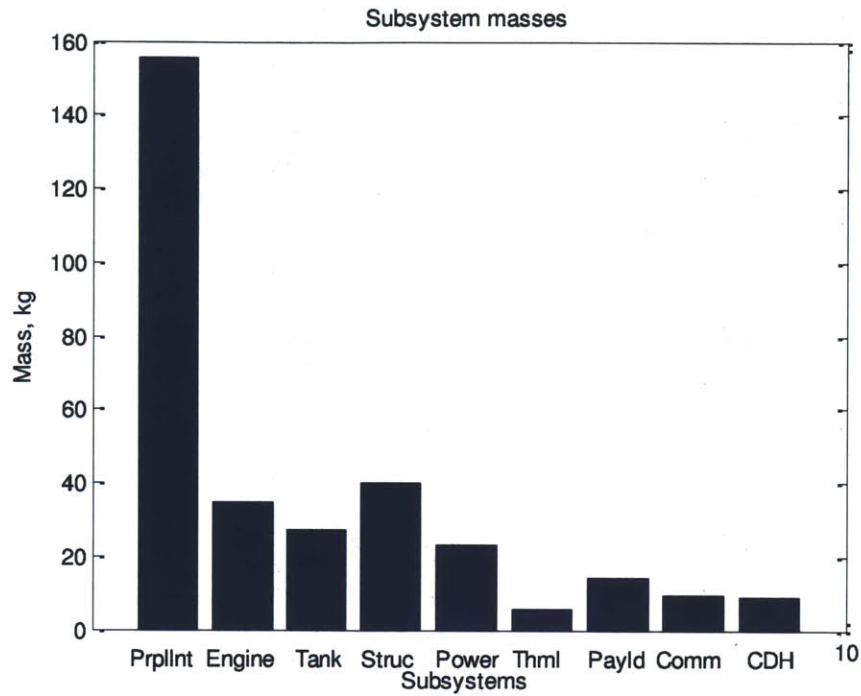


Figure 58. Three-dimensional view of the flight path for a traverse retracing the MER-A mission.

Note the lengthy duration of the science activity period versus the communications period – as designed, this hopping vehicle delivers 8 hours of scientific information during an 8-hour communications period, and requires less than a full day’s time to do so, as the mission segments during which the hopping vehicle is moving are very short compared to the total mission duration. Admittedly, this timeline relies on the assumption that only two hours are needed to perform basic science at any touchdown site; while the model explicitly sizes the power system to be able to perform scientific activities this way, it is less clear what the detailed physical limitations of performing science from a landed hopping vehicle might be. Therefore this mission profile is suggested as a baseline, with the acknowledgment that future investigation into or practice of hopping vehicle operations might cause the parameters used in this baseline to be revised.

The onboard payload of MER-A consists of two cameras, three spectrometers, one rock abrasion tool, and an array of magnets (131). A corresponding hopping vehicle payload, drawn from the available scientific instrument catalogue, would include two cameras (one panoramic, one for close-up imagery), two spectrometers (one single, one paired with a camera), and a magnetometer, as well as a sample collection tool. This payload comes very close to matching the payload aboard the MER-A rover.

The resulting subsystem mass breakdown appears in Figure 59.



**Figure 59. Subsystem mass breakdown for a hopping vehicle on a traverse retracing the MER-A mission.**

Once again, propellant mass constitutes a major proportion of the total vehicle mass. Figure 60 shows a breakdown of the propellant mass by maneuver.



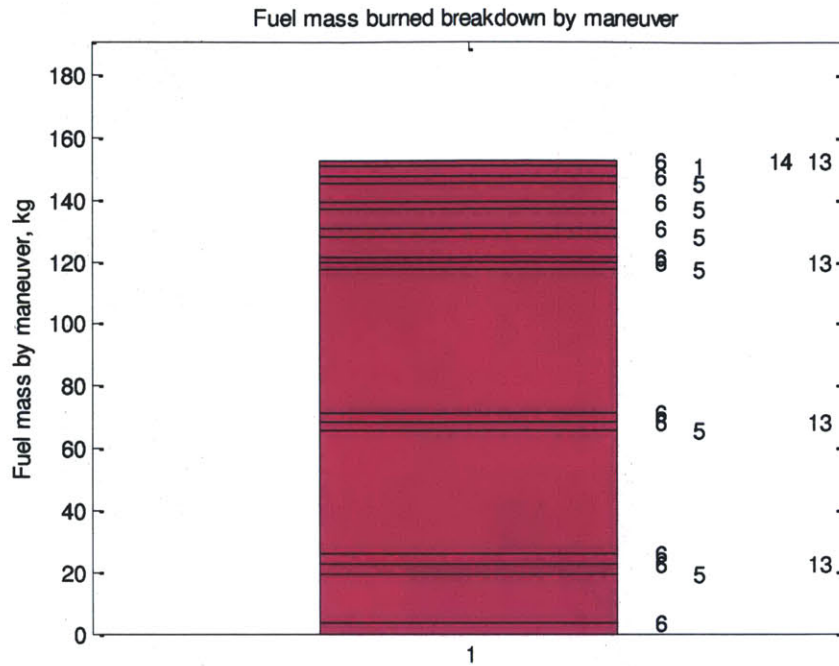


Figure 60. Propellant use breakdown for a hopping vehicle on a traverse retracing the MER-A mission.

As could be expected, the two long traverses (one 1000 m, one 1500 m) take a large amount of the propellant; although the aggregate of the sequence of climbs and traverses which constitutes the stairstep up the Columbia Hills takes nearly as much propellant overall.

The distinguishing characteristics of this mission appear in Table 17.

Table 17. Technical characteristics of a hopping vehicle for retracing the MER-A mission.

Design decisions		Technical sizing		Cost information	
Engine	MR-80B (TRL 7)	Total mass	319.4 kg	Dev cost	593.4 \$M
Power type	Solar array/battery	Max datarate	296,717 kb/s	Build cost	33.6 \$M
		Max onboard data storage	8,545,456 Mb	Ops cost	113.3 \$K
		Max power	93.2 W		
		Max thrust	875 N		



#### 5.2.2.4 Titan Hopping Mission

Another potentially interesting mission proposed by Lanford is a mission to Titan, Saturn's largest moon. Titan has been shown to have lakes of volatiles on its surface, including a methane sea named Kraken Mare. A visit to explore the shores of Kraken Mare, including potentially visiting some of the offshore islands, would be a great scientific endeavor and a huge boost to our knowledge of Titan's surface conditions.

Lanford indicates that the investigation of the atmosphere via several high-altitude sounding hops would also be of great scientific interest. Accordingly, a hopping mission was designed on Titan with a flight profile of 6(25) – 5(200@180) – 6(-25/1) – **13(900)** – 6(25) – 5(200@90) – 6(-25/1) – **13(900)** – 6(25) – 5(200@0) – 6(-25/1) – **13(900)** – 14(1800) – **6(1000)** – 6(-1000/1) – 14(28800).

An overview of the flight profile appears in Figure 61, followed by a closeup of the low-level (not atmosphere sounding) portion of the profile, in Figure 62.

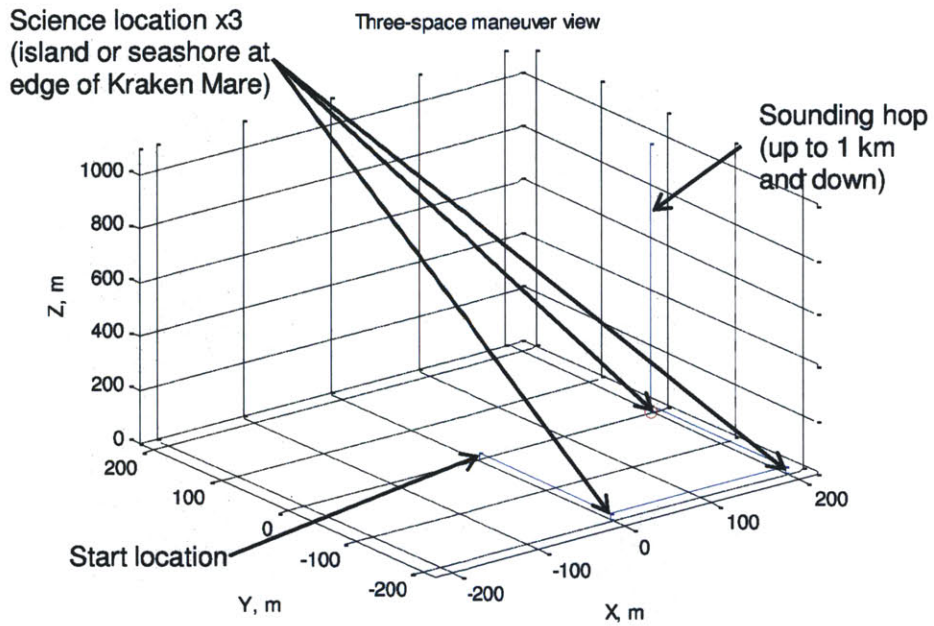


Figure 61. Three-dimensional view of the flight path for a Titan hopping mission.

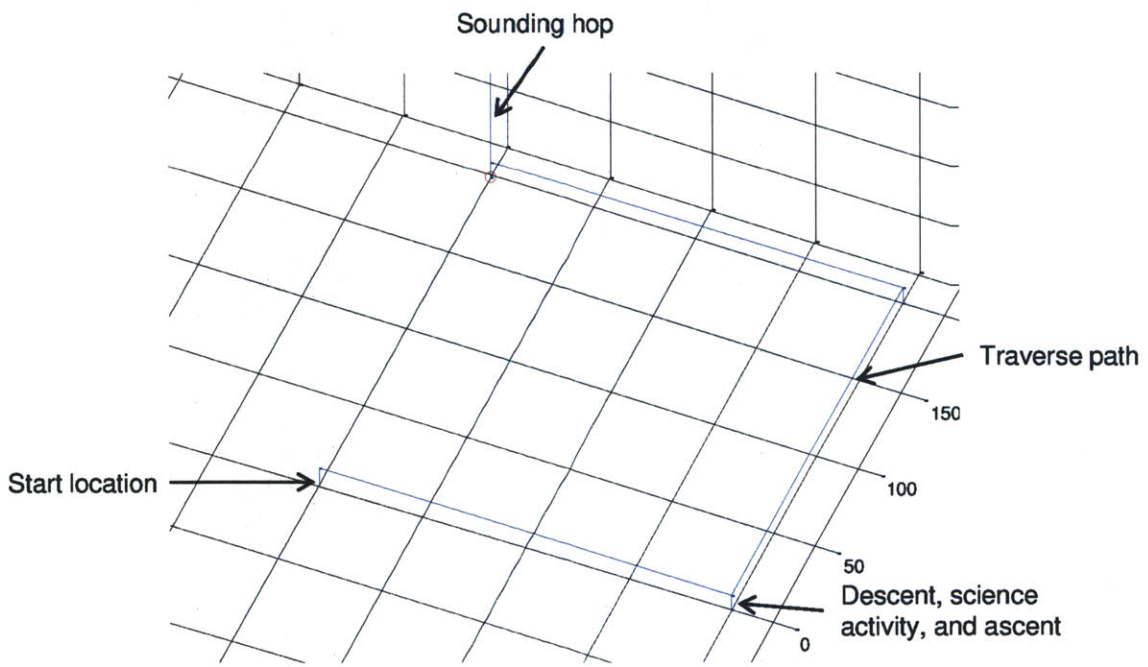


Figure 62. Closeup of three-dimensional view of the flight path for a Titan hopping mission.

Note that the mission as designed permits a hopping vehicle to visit three spots on or near the shore of Kraken Mare before performing a sounding hop.

A plot of the operational timeline appears in Figure 63. The sample collection times are kept necessarily short, as the conditions on the surface of Titan are known to be difficult, and even with a capable thermal system, it is not guaranteed that a hopping vehicle could survive an extended period on the surface. This may factor in favor of a hopping vehicle, as its high traverse speed would permit it to perform a number of exploration activities before it encountered malfunctions due to thermal stresses.

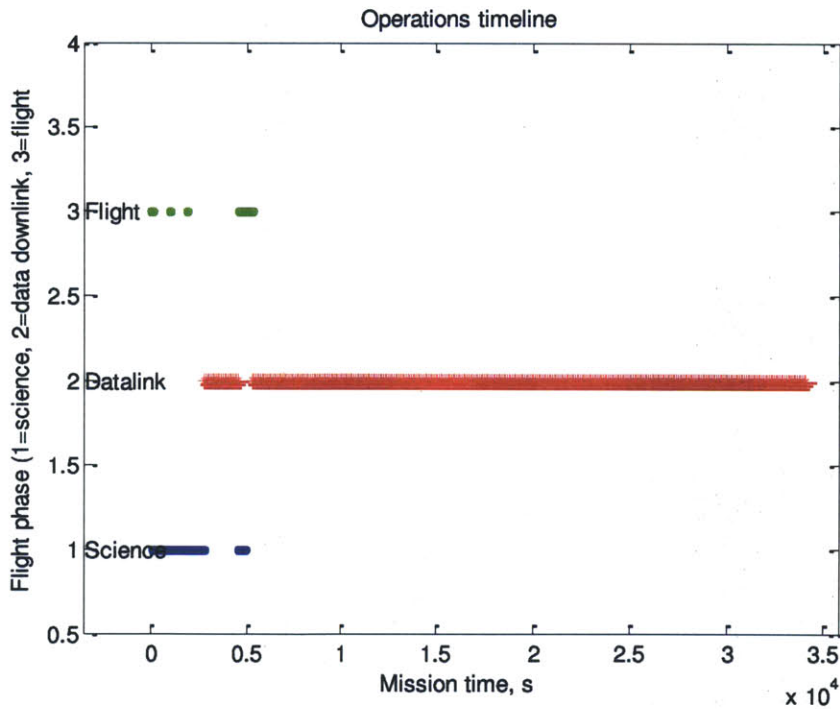


Figure 63. Operational timeline for a Titan hopping mission.

The payload selected for this mission included a spectrometer, drilling/coring sample collection device, a panoramic camera, and a Sample Analysis Bay to perform in-situ analysis. A summary of the technical characteristics of this hopping vehicle appears in Table 18.

**Table 18. Technical characteristics of a hopping vehicle for a Titan hopping mission.**

<b>Design decisions</b>		<b>Technical sizing</b>		<b>Cost information</b>	
<b>Engine</b>	TR-202 (TRL 4)	<b>Total mass</b>	3123.2 kg	<b>Dev cost</b>	1,834.6 \$M
<b>Power type</b>	Nuclear/RTG	<b>Max datarate</b>	442,373 kb/s	<b>Build cost</b>	163.7 \$M
		<b>Max onboard data storage</b>	796,271 Mb	<b>Ops cost</b>	108.2 \$K
		<b>Max power</b>	106.5 W		
		<b>Max thrust</b>	16,716 N		

The mass breakdown appears in Figure 64.

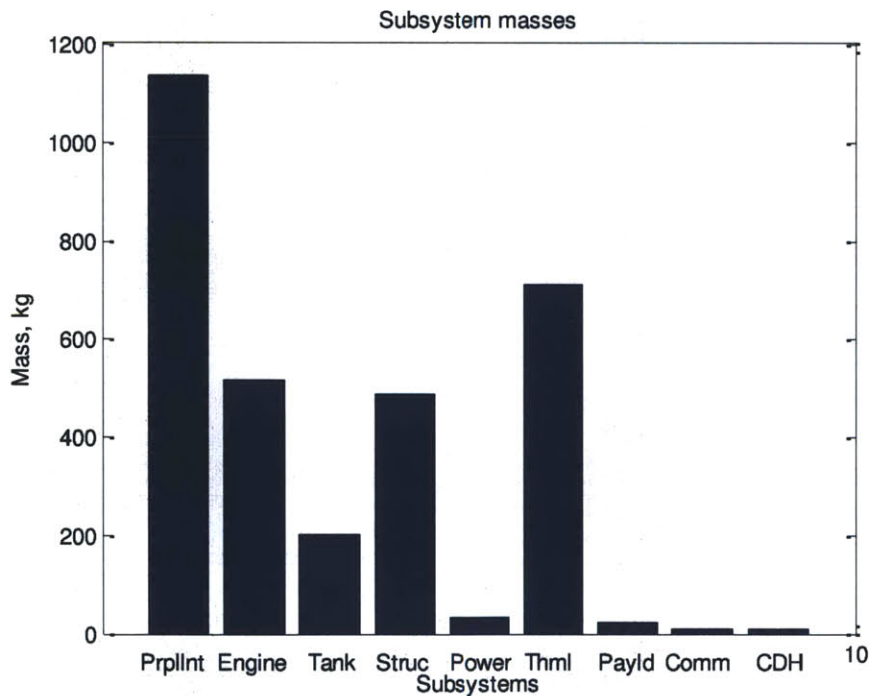


**Figure 64. Subsystem mass breakdown of a hopping vehicle for a Titan hopping mission.**

Note the relative prominence of the thermal subsystem, which has in no small part contributed in turn to the growth of the propellant, tank, engine, and structure subsystems. The thermal system includes multiple hundreds of kilograms of heaters, which are necessary to allow the hopping vehicle to survive for long periods on Titan. It should be noted that the model developed in this thesis accounts for heat lost due to convection in a surrounding fluid. This loss, in fact, constitutes the largest source of heat loss on the surface of Titan. The heat lost to this source is estimated based on thermal characteristics of the fluid and the hopping vehicle, including an estimated average traverse speed (which could also be taken as an average estimated speed of wind passage, which could be affected greatly by both traverse and local weather). On Titan, this constitutes a significant heat sink, and radiation to the cold surroundings of the planet constitute the second-largest heat sink. The net effect is that the cold, windy conditions on Titan act with the hopping vehicle's frequent motion to create a situation where a very large amount of heating power is required. This is a realistic concern: a hopping vehicle sent to visit Titan would need special attention paid to thermal issues, a point which is accurately flagged by the large project thermal subsystem mass generated by the model developed in this thesis. Even though a rover or flyer would also need a large thermal subsystem mass, this is a greater concern for a hopping vehicle, as its tendency to exhibit mass cascade effects renders it sensitive to increases in base subsystem mass in a way that a rover or flyer is not.

This is the case even though the result generated by the model is slightly skewed by the model design dynamics. For instance, the model always attempts to maintain a constant thermal equilibrium. On Titan, this requires a maximum of 82 kW of thermal power. Note that this is an extreme condition, requiring thermal equilibrium in conditions of the coldest ambient

temperature on Titan, with heat loss accelerated by wind passing by at maximum traverse speed. Realistically, this is not a situation which requires full thermal equilibrium, so the technical model of a hopping vehicle is very conservative here. However, some amount of heaters would be required on Titan, and these heaters would need to generate a large amount of energy. Practically this could be done either with a very heavy power system and simple electrical heaters, or it could be done with a heavy subsystem of RTG heating devices. The model assumes RTG heaters will be used to augment the thermal system, so the mass of that subsystem is very large. An electrical heater arrangement would result in a smaller thermal subsystem, but would simply offshore the mass requirement to the power subsystem instead. This would likely be even less effective, as RTG heaters deliver more heat energy per kilogram (if not more electrical energy per kilogram) than do standard electrical resistance heaters.

Finally, a look at the maneuvers which burned the most propellant can be seen in Figure 65.

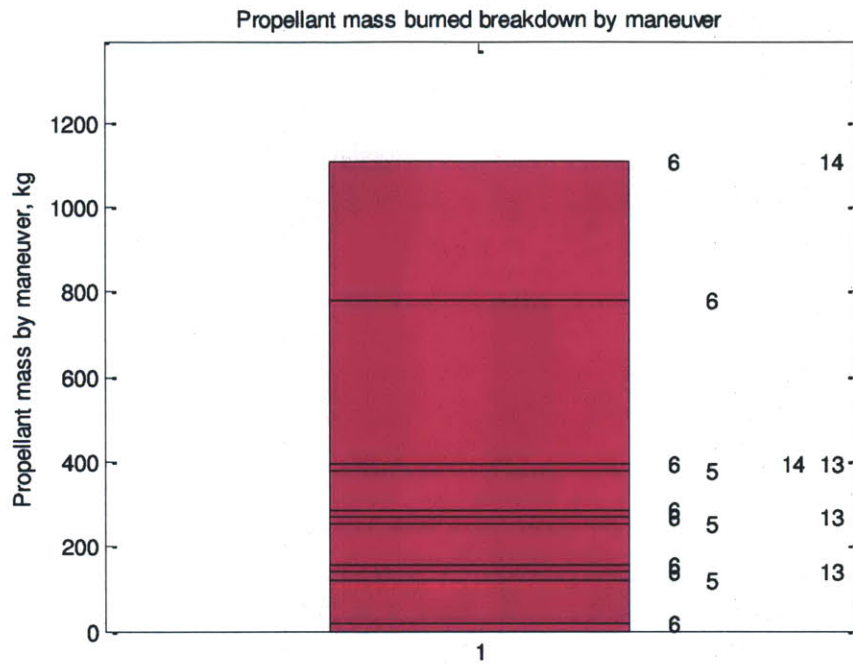
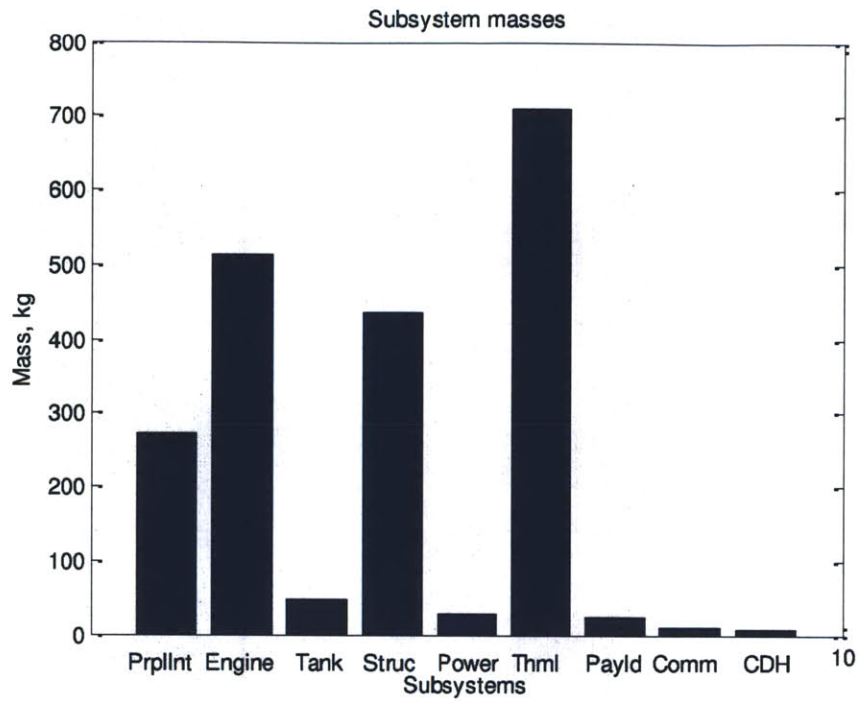


Figure 65. Propellant use breakdown for a Titan hopping mission.

The sounding hop's two vertical components dominate propellant expenditure. Clearly, if the sounding hop were not performed, a significant amount of mass could be saved. This is seen in Figure 66, which is based on performing the same mission without the sounding hop at the end.



**Figure 66. Subsystem mass breakdown for a variant Titan hopping mission.**

In addition to the mass breakdown seen in Figure 66, the propellant expenditure is seen in Figure 67, below.



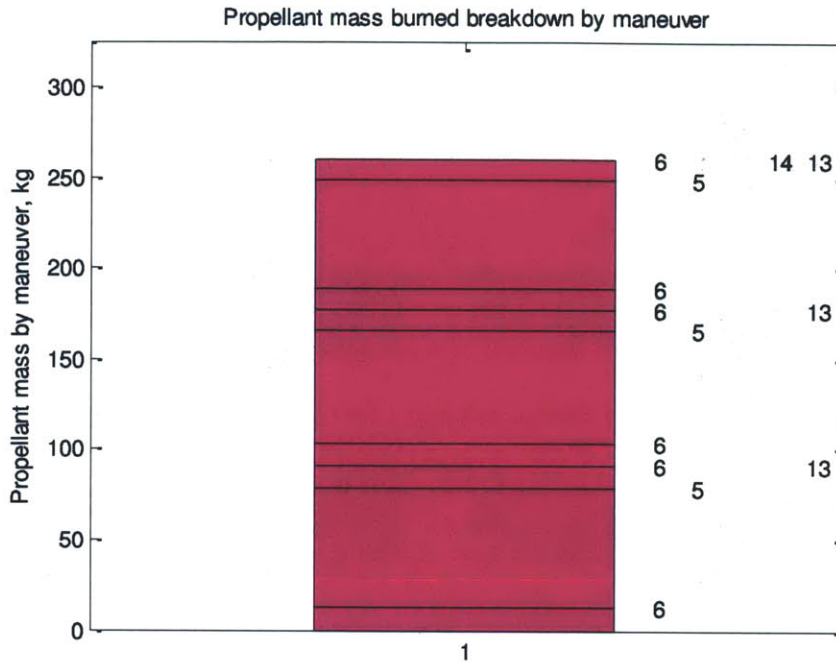


Figure 67. Propellant use breakdown for a variant Titan hopping mission.

Nearly a tonne of propellant could be saved by the decision to avert a sounding hop.

### 5.3 Analysis and Summary of Model Exercise Results

This chapter exercised the hopping vehicle model developed in Chapter 3 and validated and user-tested in Chapter 4. Model exercise focused first on investigating some of the major axes in the tradespace, and then focused on modeling and analysis of specific missions drawn from potentially interesting targets.

Major axes investigated in the tradespace include the planetary body axis, which was investigated by modeling the same hopping mission on every planetary body in the catalogue, the traverse type axis, which was investigated by changing traverses over various distances from

FA-FA to ballistic arc maneuvers, and the payload size axis, which was investigated by adding additional instances of a fixed-mass payload instrument.

### **5.3.1 Tradespace Investigation**

Major findings from the tradespace investigation exercises include the categorization of several planetary bodies as either impossible targets or special cases. The planetary bodies Venus, Io, and Mercury were all found to be infeasible as targets for hopping vehicles that can be investigated by the model developed in this thesis. This is in large part due to their extreme high temperatures on the surface, although in the case of Venus, the incredibly thick atmosphere (which would make hopping traverses prone to exceptionally high drag losses) also contributes. The planetary bodies Earth and Titan are found to be special cases, which require hopping vehicles that are typically much more massive than they would be on other planetary bodies. This is again due to the thick atmospheres found on Earth, and especially on Titan, although again the intense thermal conditions on Titan (albeit cold instead of hot) also contribute. Hopping is feasible on Earth and Titan, but the atmosphere brings additional considerations that do not apply to most other planetary bodies. Additionally, evidence was seen that an optimum traverse speed in atmosphere exists, although this optimum is probably a function of gravity as well as atmospheric density. The optimum occurs where drag losses (which are due to atmospheric density, and scale as the square of traverse velocity) and gravity losses (which are due to the need to hover against gravity, and scale as the time taken to make a traverse increases) are balanced such that the sum of all losses is minimal. The effect of traverse velocity on total hopping vehicle mass seems to scale with atmospheric density – Titan’s effect is larger than Earth’s, and the effect on Mars is almost unnoticeable.

However, without the main effects that planetary bodies can have on hopping vehicle mass, via thermal effects, atmospheric density, relatively high gravity, or some combination of the three, the size of a hopping vehicle for a given planetary body is likely to fall within a band close to hopping vehicles designed to perform similar missions on other planetary bodies. There is a cluster of planetary bodies, all with gravities near or lower than the gravity of Luna and Mars, for which a given hopping vehicle is likely to be of nearly constant mass across all bodies. This was seen when the baseline hopping missions for all bodies other than the impossible or special cases fell in a band from approximately 100-120 kg total mass. The mission profile and payload have an effect on the total vehicle mass, however, that is separate from this.

The effect of other axes, like the choice of maneuvers in the mission profile, was also investigated. Examining the effect of replacing FA-FA (or hover-hop) traverses with ballistic arc trajectories revealed a few limitations that affect ballistic arc trajectories. For instance, a small set of operational limitations, initially identified by Middleton (54), exists. These limitations are that any hopping vehicle performing a ballistic arc maneuver must first launch to an appropriate altitude (a ballistic arc cannot be performed from a position sitting on the ground), and must pitch over and pitch back at the ends of the ballistic arc as well. An additional limitation is that a ballistic arc requires more thrust (for a shorter period of time) than a hover-hop to cover the same distance over the surface. This typically requires a larger engine, which then requires more structure to hold it, which in turn leads to a need for additional propellant, and then even more tankage to carry the propellant. These limitations generally take away the theoretical efficiency advantages offered by the ballistic arc trajectory, meaning that in practical terms there is often

not much effective difference between a hover-hop and a ballistic hop, and sometimes a ballistic hop is actually disadvantaged.

Investigation of the effects of increasing payload mass showed a progression of mass, as payload masses have their own cascading effects in terms of more structure, more propellant, and more tank mass, which then lead to even more propellant mass, but this effect does not seem to be as pronounced as other effects.

### **5.3.2 Specific Hopping Mission Investigation**

Investigation of specific hopping missions found feasible hopping vehicle designs for missions to recover a sample from a permanently shadowed location in Shackleton Crater, make an initial descent into a hollow lava tube in the Mare Tranquilitatis, collect samples from several selenologically interesting sites located on the floor of Copernicus Crater, and conduct stratigraphy on a shallow slope in the Valles Marineris region of Mars. A feasible (if very large) hopping vehicle design was also found to perform island hopping near the shore of the Kraken Mare on Titan, followed by a high sounding hop vertically up and down.

A final specific mission investigation compared the performance of a hopper and a rover over a large fraction of the MER-A rover's traverse from near the Bonneville Crater in Mars to the nearby Columbia Hills. This comparison found a feasible hopping vehicle design, and the model indicated that the entire 500-sol traverse for the rover could potentially have been replicated in less than a day by a hopping vehicle. This does rely on the accuracy of the science mission segment durations, but stretching out these segments would not change the fact that the entire traverse can be completed by a hopping vehicle in a matter of minutes.

This highlights some of the fundamental distinctions between hopping and roving mobility. While hopping mobility is much faster over very long distances, it also has a lifetime limit when propellant runs out, while far-slower rovers can potentially travel longer overall distances over their lengthened lifetimes. Additionally, rovers can effectively touch any square meter of ground (barring terrain limitations) they can see, while a hopping vehicle actually has a certain effective minimum traverse range (e.g., hopping 2 meters laterally is not an efficient use of propellant in most situations). A hopping vehicle effectively emplaces a series of footprints over scattered spots throughout a region, while a rover can move its footprint slowly over most of what it touches.

This difference in aspect for hopping vehicles and rovers suggests a benefit to be found in working together. A hopping vehicle working in concert with a rover or a fleet of mini-rovers could in principle access nearly any spot in a region very rapidly, and then deploy rovers to search the immediate area around the hopping vehicle's immediate footprint. This concept (132) has the potential to apply the best characteristics of hopping and roving all at the same time, and is a very interesting subject for further future study.

An additional field of study with great interest for future work is the field of hopping vehicle operations and mission planning. As can be seen via comparison with some missions planned by Lanford (55), higher granularity in maneuvers and in subsystem fidelity results in larger hopping vehicle designs. This is sensible, as more precise maneuvering and more developed system designs always result in higher mass estimates than first-order initial estimates. The model

developed in this thesis is intended to serve as a bridge between first-order calculations and detailed design, and as such possesses an intermediate level of granularity. Nonetheless, the field of hopping vehicle operations is still in a nascent stage, and when additional study has been conducted, it would be fruitful to apply the results to the model developed in this thesis.

To summarize all the example missions modeled, Figure 68 shows the total landed masses of hopping vehicles modeled for example missions, with landed masses of flown spaceborne vehicles also shown for comparison. Figure 69 shows the total mission costs for the same set of all example missions and some key flown spaceborne missions. Both Figure 68 and Figure 69 show flown missions (Surveyor (133), Huygens (134), MER (135), MSL (136), Phoenix (119), and Viking (122)) from the same three bodies (Luna, Mars, and Titan) used for the example missions (to a well of eternal night, a lava tube, Copernicus Crater and a variant, a Mars crater, Valles Marineris, the MER-A site, and to the shore of Kraken Mare and a variant).

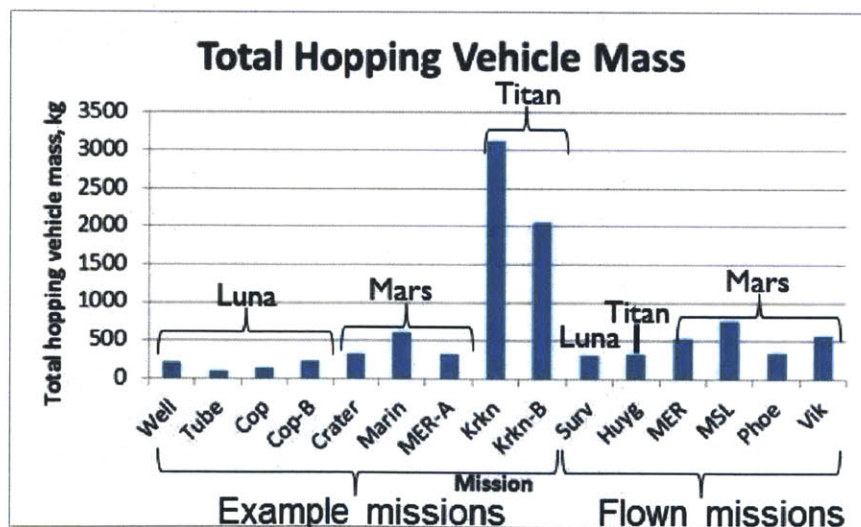


Figure 68. Total landed vehicle masses for example missions and flown missions to the same bodies.

Note that Apollo landed a vehicle with a mass of about 7500 kg at touchdown, for a program cost of about 130 billion dollars (in 2011 dollars). All the missions which appear in Figure 68 and Figure 69 fall well below this mass and cost. However, with the exception of the Titan example mission and its variant, all the example missions are such that their landed mass is similar to the masses previously landed on the target bodies. This is an additional indicator that the example missions as described previously in this thesis are feasible, and can provide a starting point for future exploration of the target planetary bodies.

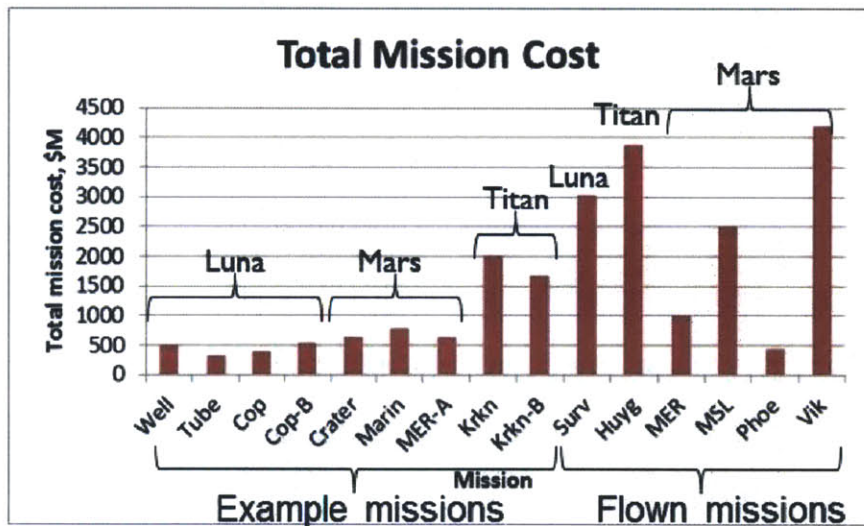


Figure 69. Total costs, in 2011 dollars, for example missions and flown missions to the same bodies.

Costs of example missions seem consistently lower than the costs for flown missions. However, costs for all example missions are shown for a single landed vehicle, while costs for flown missions are shown for entire programs, with multiple launched vehicles, in the case of Surveyor (seven vehicles), MER (two vehicles), and Viking (two vehicles). Additionally, all costs

produced by the model developed in this thesis are preliminary, Phase A or pre-Phase A estimates, and there is much uncertainty in these estimates. The high costs seen for Huygens, MSL, and Viking can be compared to the much lower costs shown for MER and Phoenix and interpreted as a sign that variability in final program costs can be high, and cost growth from initial estimates is also often high. The costs seen for the example missions, however, are not unreasonable compared to actual flown mission costs, and therefore the cost estimation provided by the model developed in this thesis can also serve as a starting point for deeper development of hopping vehicle designs.

#### **5.4 Tradespace Investigation Conclusions**

With model exercise completed, an initial picture of some of the tradespace dynamics is now available, and additionally a few specific missions have been evaluated as point designs in the model tradespace. Because these point designs are drawn from interesting concepts and the literature, they can serve as jumping-off points for more in-depth study of hopping vehicle missions based on these concepts. The model developed in this thesis permits in-depth analysis via the ability to manipulate payloads, flight profiles, and even a large suite of master parameters to investigate many variations in mission design.

Mission designers with an interest in evaluating hopping vehicles can use the material presented in this chapter to begin to understand the tradespace of hopping vehicle missions, or to select potentially viable missions from the specific missions already described. With this additional insight into the modeling capability delivered in Chapter 3, it should be feasible to begin



considering hopping vehicles as a viable alternative or supplement to rovers or landers in the exploration of planetary surfaces throughout the solar system.



## CHAPTER 6. Conclusions

In pursuit of the goal of bringing hopping vehicles into the option space for designers of planetary surface exploration missions in our solar system, this thesis has developed a framework for thinking about hopping mobility, used it to create a model that provides insight into hopping vehicle technical characteristics, and applied the model to several specific mission concepts.

In addition to the framework itself and the modeling tool, this has resulted in a few key insights into the design and operation of hopping vehicles. Among these is the assessment that some planetary bodies are not feasible hopping targets. While most of the small, solid planetary bodies in the solar system are feasible hopping targets, Venus, Io, and Mercury are not, due to the extreme thermal conditions that prevail on their surfaces (which would also create difficulties for rovers or flyers as well), and the thick, drag-inducing atmosphere on Venus. The thick atmospheres on Earth and Titan also mean additional mass requirements, due to the drag losses the atmospheres create. However, all of the other sixteen planetary bodies listed in Table 6 are feasible targets. A simple hopping maneuver, including a traverse of 500 m, can be conducted on each of these planetary bodies using a hopping vehicle which falls in a range of masses between 100 kg and 120 kg. Thus the approximate lower limit on mass for a hopping vehicle is about 100 kg.

Adding in additional maneuvers for a more complex flight profile or longer traverses or hovering times will increase the total mission delta-V, and the total mass will scale greater than linearly with delta-V, not allowing for in-situ propellant production or other means of refueling. Adding in additional payload will cause the hopping vehicle mass to scale linearly. Moving to a

planetary body with higher gravity will also cause approximately linear scaling of the total vehicle mass. Linear scaling of mass will occasionally be broken by the need to upgrade from one engine size to the next, resulting in a stairstep discontinuity in the overall linear trend.

An additional insight is that operational and technical limitations on engines may prevent the theoretically more-efficient ballistic arc hopping maneuvers from being more useful than the more steady-state fixed-altitude, fixed-attitude hops (also known as hover-hops). This is due to the stairstep effect of upgrading to a larger engine size. As a ballistic arc hopping maneuver is extended in length, the requirement for the delta-V to be delivered at the start and end of the arc grows, and this means that a larger engine, with higher thrust, must be used. A larger engine implies additional mass of propellant, which in turn implies additional mass cascade effects.

While a fixed-altitude, fixed-attitude hop is carried out in a near steady-state pose for the duration of the hop, and thus does not require an upgrade to a larger engine until the hop has grown long enough that the propellant mass necessitates an engine upgrade, the ballistic arc hop requires an engine upgrade by requiring larger thrust, which in turn feeds back into propellant mass. Because engine upgrades are needed sooner for ballistic hops of long distance than for hover-hops of long distance, the theoretically increased efficiency of a ballistic arc hop is reduced, and both modes of traverse should be modeled to discover the more efficient mode for a given mission flight profile.

Finally, although a hopping vehicle's native speed means it can traverse much greater distances much more quickly than can a rover, the converse aspect is that a rover does not greatly increase its energy requirements by stopping to look at an interesting science target that it may discover

during a traverse, while a hopping vehicle must cease its traverse, land, and then relaunch and resume its traverse if it wishes to examine a science target mid-flight. This generates a significant amount of additional delta-V requirement for the hopping vehicle. Thus, a rover is better at examining targets of opportunity, while a hopping vehicle is better at making rapid visits to small pre-defined target areas. This insight suggests that the two different types of planetary surface exploration vehicle have complementary strengths, and that future research on hybrid or teamed vehicles would be a valuable investment.

## **6.1 Intellectual Contributions**

Intellectual contributions generated by the work done for this thesis include the development of a motion and action grammar to describe hopping activities, the creation of a validated technical model of hopping vehicles, and early exploration of the tradespace of hopping vehicles which this model investigates. Underpinning this work is also a description of the key advantages of hopping vehicles.

### **6.1.1 Motion and Action Grammar**

The motion and action grammar for hopping vehicles, detailed in Chapter 3 of this thesis, provides a language for describing hopping maneuvers and related activities in depth. The grammar system consists of a small vocabulary of motions and other actions, and rules for combining these actions together. When combined, the actions can be used to describe almost any hopping mission to a high level of granularity, much as a language can be used to construct a theoretically infinite number of sentences using limited words.

This ability to describe hopping missions in great detail affords high flexibility to the mission designer interested in hopping missions. A quick pass can be used to describe a mission at a broad level, which can provide early insight into a mission. As a mission concept matures and more specific maneuvers are developed, or perhaps as a generic mission is shaped around specific terrain features, the model developed for this thesis permits successively more accurate formulations of the mission flight profile. In addition to the ability to define smaller or more intricate maneuvers, users can also adjust parameters of the model to fine-tune a mission design and investigate the effects of small design changes.

Thus, the motion grammar provides an important way to formalize discussion and analysis of hopping vehicle motions and actions, and to describe these motions and actions in a rigorous fashion.

### **6.1.2 Validated Technical Model of Hopping Vehicles**

The motion and action grammar was used, together with technical and physical analysis of the characteristics of a hopping vehicle and the relevant dynamics, to create a hopping vehicle model that analyzes a user's preferred formalized mission concept, including a description of the payload, target planetary body, and flight profile. The model then outputs a technical description of a hopping vehicle which can perform the mission, including information on total mass, subsystem masses and power levels, and subsystem technology choices, as well as cost information and data storage information. Users can then examine this technical model, which also includes details of operational interest, and either update the design or make a decision about whether to proceed further in the process to detailed design phases.

The model was validated against three existing vehicles, all planetary landers. These were the Apollo LM, the Viking Mars lander, and the Phoenix Mars lander. Additionally, the model was validated against a proposed design for a lunar hopping vehicle, the Next Giant Leap GLXP vehicle.

The model provides extensive insight into the technical and operational aspects of building and using a hopping vehicle, which can be used to aid mission designers in evaluating the feasibility of a hopping vehicle for a planetary surface exploration mission.

### **6.1.3 Early Tradespace Exploration for Hopping Vehicles**

Some key dynamics in the tradespace of hopping vehicles were also identified in this thesis, including the growth of hopping vehicle mass with increasing traverse distance, as driven by the need to provide engines which can both produce an appropriate maximum thrust and which can be throttled low enough to produce a low-enough minimum thrust. This often leads to a need to use larger (and thus heavier) engines on longer traverses, which in turn drives up vehicle mass by cascading into structure, propellant, and tank masses.

Additionally, a set of specific planetary surface exploration missions was investigated. These missions took place on Luna, Mars, and Titan, and were based on mission concepts previously described in the open literature or proposed as potentially scientifically beneficial. These mission concepts include missions to Shackleton Crater, Mare Tranquilitatis, and Copernicus Crater on the Moon, as well as the Valles Marineris on Mars and Kraken Mare on Titan.

Scientific knowledge related to the history of Luna's formation, the history of Mars, and the presence of volatiles on Luna and Titan could be gathered from these missions.

These missions, of attested scientific interest, are all formalized and evaluated in Chapter 5 of this thesis. With the information provided, mission designers will be able to assess an early design picture of hopping vehicles for these missions, and make decisions to either proceed with hopping concepts for these exploration missions, or to invest effort into evaluating other mission concepts instead.

#### **6.1.4 Description of Advantages of Hopping Vehicles**

An additional contribution of this thesis is an initial description of the capabilities of hopping vehicles and the advantages provided by these capabilities. This description, in Chapter 1 of this thesis, elucidates how the basic characteristics of hopping vehicles can be combined to offer additional advantages. For example, two characteristics of hopping vehicles are comparatively long range (on the order of kilometers) and high traverse speed (up to on the order of tens of meters per second), and these can either be used advantageously in individual ways, or can be combined to provide rapid regional access, which permits close contact between scientific instruments and widely separated terrain features in a comparatively short time window.

A discussion of hopping vehicle limitations is also produced. Limitations on hopping vehicles include the fact that they must carry all the propellant they need, and this limits their maximum size before cascading mass growth sets into the design. Other limitations are the fact that hopping mobility implies that system failures can result in damaging crashes rather than simply



shutdown in place, leading to an operational risk profile with heightened risk during the traverse phases, and the fact that a hopping vehicle must expend propellant to launch and descend to access any region, no matter how close, if it is outside the hopping vehicle's immediate reach. This creates a situation where exploring rock-to-rock is inefficient, although it is possible.

The description of characteristics and advantages is intended to provide an early roadmap to the ways in which hopping mobility and hopping vehicles should be considered for use in exploring planetary surfaces. For instance, while rovers may display advantages in lifetime mobility, as they can potentially operate on solar power for extended lifetimes, only hopping vehicles have the sort of terrain freedom afforded by their ability to maneuver around a landscape multiple times without needing to act against a fluid or the ground itself. This description can provide initial insight into the best ways in which to take advantage of hopping as a new form of mobility.

## **6.2 Future Work**

Work following this thesis could take any of several directions. Possibly chief among these directions are improving the technical hopping vehicle model, exploring the tradespace of hopping vehicles more thoroughly, and developing hopping mission concepts in more depth.

### **6.2.1 Model Improvements**

The technical hopping vehicle model developed in this thesis must retain a high degree of generality in order to remain applicable to the many potential hopping target planetary bodies in the solar system, but must also deliver results as specific as possible in order to provide

maximum insight into the design and operations of the hopping vehicles it generates. Although the model is effective at delivering initial insight, it could be expanded to provide more in-depth insight as well, especially for advanced users. One way to provide this insight might be to generate planet-specific subsystem models, or subsystem models with unique constraints (such as a thermal subsystem with a heat buffer, such that it could survive for a limited time in a very hot or very cold environment, rather than a system which is designed to provide a thermal steady state). A set of advanced subsystem or planetary body models, with time-varying characteristics, could be used to improve the applicability of the technical model to specific situations, but it would also be necessary to expand the ability of the model to cater to advanced or experienced users in order to make best use of improved capability. The incorporation of new code modules to handle in-situ propellant production or other means of in-mission refueling (such as fuel replenishment from a depot or by nearby human agents) would also be desirable, and would expand the variety of actions that could be performed on a mission. It might also be feasible to expand the model's list of user-controllable master parameters, but this would also require additional effort on the part of users to understand the parameters and learn how to apply them.

Another desirable improvement to the model would be an improved user interface, with additional functionality. One additional functionality that is very desirable is the ability to edit flight planning information after entering it into the model without needing to restart the process. A graphical user interface, with multi-level user interaction and the ability to actively update any aspect of the payload, target planetary body, or flight profile, would improve the ability of users to use the technical model, and would provide for constant editing of the flight planning information. Such an interface could also offer multi-level interaction with the information

produced by the model, including permitting detailed analysis of the characteristics of any subsystem or of any flight segment. A conceptual image of such a user interface appears in Figure 70, with specific sections labeled in orange.

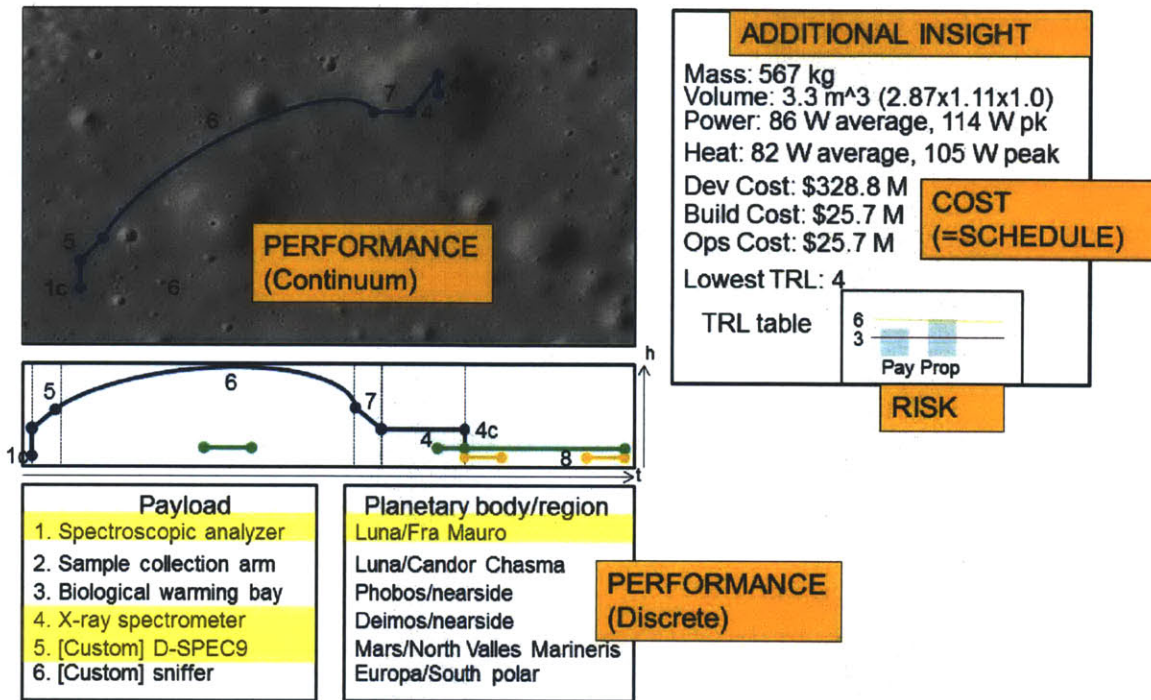


Figure 70. Concept for a continuously-editable graphical user interface.

Additional improvements to user interaction with the technical model are also possible, now that the engineering validity of the model's underlying algorithms has been established. For instance, as currently operated, the model works from mission requirements to a technical design. However, it would offer increased value to users if the model could also function in an inverse fashion, by taking in a baseline set of mission requirements and then optimizing them to meet specific constraints on technical and operational details. Furthermore, the model currently is able to deliver output data to an Excel file for further analysis, but it would also be desirable to

enable active loading of old work into the MATLAB environment of the model, and to enable users to export data to other file formats as well.

### **6.2.2 Tradespace Exploration**

The further exploration of the tradespace for hopping vehicles, including plotting of additional dynamics in the tradespace, would also be a beneficial step. For instance, it might be of value to plot out the longest possible hover-hop traverse and the longest possible ballistic arc traverse on every planetary body in the catalogue. Or it might be desirable to plot out the effects of changes in every single one of the dozens of master parameters over the evolution of a series of flight profiles on one planetary body. One area which would be very valuable to investigate would be more study on the contours of vehicle mass and subsystem mass as a function of maneuver speed on planetary bodies with dense atmospheres, including Titan, which is a target of high potential scientific value.

The tradespace produced by the model is multi-dimensional, and complexly interacting. Further exploration of the tradespace might elicit further insight into the best ways and places to use hopping vehicles, and as such would be a logical next step.

### **6.2.3 Mission Concept Development**

Finally, a significant amount of following work should focus on the location of interesting mission concepts in the tradespace, and the further development of these concepts. Of particular interest are concepts which make best use of the advantages of hopping vehicles.

An example of a hopping mission concept enabled by but not completely centered around hopping vehicles is the human-robot collaborative mission to the neighborhood of Mars described in (50). Because hopping vehicles are a new method of planetary surface mobility, it would be desirable to consider using them in new and unique ways. The list of hopping vehicle advantages can serve as a starting point for developing these concepts, but is not necessarily the ending point as well.

Additionally, the advantages of hopping vehicles (rapid regional mobility and terrain freedom, affording access to many small target areas very quickly) and of rovers (low cost for targets of opportunity, extended lifetime due to lack of propellant limitations) may be complementary, and further research on the ways in which hopping vehicle advantages and rover advantages could be turned to benefit planetary surface exploration would be advisable. This research may take the direction of investigating hybrid rover/hopper designs, or of investigating the abilities of teams of vehicles, perhaps with microrovers embarked aboard a fleet of hopping vehicles, as initially proposed in (132).

### **6.3 Future of Hopping Vehicles**

Given the great potential to explore planetary surfaces in new ways that hopping vehicles represent, the work done in this thesis likely comprises only the early stages of development for the concept of hopping vehicles as a means of exploring planetary surfaces. However, this thesis has provided a means to think about hopping mobility from an abstract perspective (with the description of hopping vehicle characteristics and advantages and the motion and action grammar system to formalize hopping mission concepts), as well as a model to evaluate hopping

vehicle designs from the more concrete perspectives of technical, operational, and programmatic details.

With these tools, and the recent upsurge in interest in hopping vehicles reflected in the work described in Chapter 2 of this thesis, it is possible to project a viable future for hopping mobility and hopping vehicles as a means of exploring the planetary surfaces of the solar system in new and interesting ways.

# BIBLIOGRAPHY

1. **Review of U. S. Human Spaceflight Plans Committee.** *Seeking a Human Spaceflight Program Worthy of a Great Nation.* Washington, D. C. : National Aeronautics and Space Administration, 2009.
2. *Dispelling the Myth of Robotic Efficiency.* **Crawford, Ian A.** 2, s.l. : Astronomy and Geophysics, Vol. 53.
3. **Lafleur, Claude.** Costs of US piloted programs. *The Space Review.* [Online] March 8, 2010. [Cited: April 21, 2012.] <http://www.thespacereview.com/article/1579/1>.
4. *Small Lunar Exploration and Delivery System Concept.* **Cohanim, B. E., N. A. Harrison, T. J. Mosher, J. Heron, K. Davis, J. A. Hoffman, P. M. Cunio, J. de Luis, and M. Joyce.** Pasadena, CA : AIAA, 2009. AIAA Space 2009 Conference and Exhibition.
5. **Bell, E. II.** Luna 1. *National Space Science Data Center.* [Online] National Aeronautics and Space Administration, April 20, 2012. [Cited: April 21, 2012.] <http://nssdc.gsfc.nasa.gov/nmc/spacecraftDisplay.do?id=1959-012A>.
6. **Bell, E., II.** Luna 21/Lunokhod 2. *National Space Science Data Center.* [Online] National Aeronautics and Space Administration, April 10, 2012. [Cited: April 16, 2012.] <http://nssdc.gsfc.nasa.gov/nmc/masterCatalog.do?sc=1973-001A>.
7. *New Platforms for Science on the Lunar Surface.* **Cohanim, B. E., J. A. Hoffman, B. P. Weiss, and J. N. Hewitt.** s.l. : Lunar Science Forum, 2011.
8. *Options in the Solar System for Planetary Surface Exploration via Hopping.* **Cunio, P. M., F. Alibay, P. Meira, T. Sheerin, E. Lanford, E. Krupczak, and J. A. Hoffman.** Big Sky, MT : IEEE, 2010.
9. **Dori, Dov.** *Object-process methodology: a holistic systems paradigm.* Berlin : Springer, 2002. 3540654712.

10. **Lamamy, Julien-Alexandre.** *Methods and Tools for the Formulation, Evaluation, and Optimization of Rover Mission Concepts (PhD Thesis)*. Cambridge, MA : Massachusetts Institute of Technology, 2007.
11. **Cohanim, Babak E.** *Planetary Hopper Navigation and Targeting (PhD Thesis)*. Cambridge, MA : Massachusetts Institute of Technology, 2012.
12. **X PRIZE Foundation.** *Google Lunar X PRIZE*. [Online] 2012. [Cited: April 3, 2012.] <http://www.googlelunarxprize.org/>.
13. **National Aeronautics and Space Administration.** *Surveyor Program Results*. 1969. NASA-SP-184.
14. *The Lunar Pogo Stick*. **Seifert, H. S.** 1967, *Journal of Spacecraft and Rockets*, pp. 941-943.
15. *Propulsion Dynamics of Lunar Hoppers*. **Meetin, Ronald J., and Seifert, Howard S.** 1974, *Journal of Spacecraft and Rockets*, pp. 852-856.
16. *Hopping Transporters for Lunar Exploration*. **Kaplan, Marshall H. and Seifert, Howard S.** 1969, *Journal of Spacecraft and Rockets*, pp. 917-922.
17. *Dynamical Equations for the Plane Change Maneuver of the Lunar Hopping Laboratory*. **Kaplan, Marshall H.** 1970, *Journal of Spacecraft and Rockets*, pp. 491-493.
18. *Design Study of a One-Man Lunar Transportation Device*. **Sandford, J. 1,** s.l. : AIAA *Journal of Spacecraft and Rockets*, 1965, Vol. 3.
19. *Lunar Flying Vehicle Propulsion System*. **Carey, L., and Stricklin, C. 4,** s.l. : AIAA *Journal of Spacecraft and Rockets*, 1971, Vol. 8.
20. *Robotic lunar exploration: Architectures, issues, and options*. **Mankins, John C., Vallerani, Ernesto, Della Torre, Alberto.** 2007, *Acta Astronautica*, pp. 475-483.
21. *Comparison of Alternative Concepts for Lunar Surface Transportation*. **Apel, Uwe.** 1988, *Acta Astronautica*, pp. 445-456.



22. *Lunar Lander Configuration Study and Parametric Performance Analysis*. **Donahue, Benjamin and Fowler, C. Robert**. Monterey, CA : AIAA, 1993. 29th Joint Propulsion Conference and Exhibit. AIAA-93-2354.
23. *A System Overview of the First Lunar Outpost*. **Ruff, T., et al., et al.** Huntsville, AL : AIAA, 1993. AIAA 93-4134.
24. *High Autonomy Lunar Surface Mobility Systems*. **Vallerani, Ernesto, Della Torre, Alberto, Guizzo, Gian Paolo, and Vukman, Igor**. 2006. International Astronautical Conference. IAC-06-A3.6.08.
25. *In Situ Propellant Production: The Key to Global Surface Exploration of Mars?* **Hoffman, S. J., Niehoff, J. C., and Stancati, M. L.** San Diego, CA : AIAA, 1982. AIAA/AAS Astrodynamics Conference. AIAA-82-1477.
26. *The Ballistic Mars Hopper: An Alternative Mars Mobility Concept*. **Sercel, J. C., Blandino, J. J., and Wood, K. L.** San Diego, CA : AIAA, 1987. AIAA/SAE/ASME/ASEE 23rd Joint Propulsion Conference. AIAA-87-1901.
27. *Diborane/CO2 Rockets for Use in Mars Ascent Vehicles*. **Zubrin, Robert**. San Diego, CA : AIAA, 1995. 31st AIAA/ASME/SAE/ASEE Joint Propulsion Conference and Exhibit. AIAA-95-2640.
28. *Methods for Achieving Long Range Mobility on Mars*. **Zubrin, R.** Nashville, TN : AIAA, 1992. AIAA/SAE/ASME/ASEE Joint Propulsion Conference and Exhibit. AIAA-92-3862.
29. *A Mars Rocket Vehicle Using In-situ Propellants*. **Landis, Geoffrey A., Linne, Diane L., and Taylor, David**. Huntsville, AL : AIAA, 2000. 36th AIAA/ASME/SAE/ASEE Joint Propulsion Conference and Exhibit. AIAA-2000-3120.
30. *Mars Rocket Vehicle Using In Situ Propellants*. **Landis, Geoffrey A., and Linne, Diane, L.** 2001, Journal of Spacecraft and Rockets, pp. 730-735.
31. *Mars Hopper versus Mars Rover*. **Shafirovich, E., Salomon, M., and Gokalp, I.** 2006, Acta Astronautica, pp. 710-716.

32. *The MITEE Hopper: A Compact NTP Spacecraft to Explore Multiple Surface Sites Using In-Situ Propellants.* **Powell, J., Maise, G., and Paniagua, J.** 2006. International Astronautical Conference 2006. IAC-06-D2.8/C3.5/C4.7/D3.5.06.
33. **Martinez-Cantin, R.** *Moonhoppers Colony.* Universidad de Zaragoza. Zaragoza, Spain : s.n.
34. *Mechanical Design of a Hopper Robot for Planetary Exploration Using SMA as a Unique Source of Power.* **Montminy, Steeve, Dupuis, Erick, and Champlaud, Henri.** 2006. International Astronautical Conference. IAC-06-C2.5.4.
35. *Diborane/CO2 Rockets for Use in Mars Ascent Vehicles.* **Zubrin, Robert.** San Diego, CA : AIAA, 1995. 31st AIAA/ASME/SAE/ASEE Joint Propulsion Conference and Exhibit. AIAA-95-2640.
36. **Smith, G. E., Gebhard, D. F., Schaffer, A. P.** *Application of LEM Technology to NASA Lunar Landing Research Program.* s.l. : NASA, 1963. LED-470-2.
37. **National Aeronautics and Space Administration.** *A Renewed Spirit of Discovery: The President's Vision for U. S. Space Exploration.* 2004.
38. *Project Alshain: A Lunar Flying Vehicle for Rapid Universal Surface Access.* **Beal, Sarah, et al., et al.** Pasadena, CA : AIAA, 2009. AIAA 2009-6710.
39. *LEAPFROG: Lunar Entry and Approach Platform For Research On Ground.* **Hendry IV, M. L., Rojdev, K., Cheng, J., Faghfoor, O., Garcia, A., Giuliano, P., Hoag, L., Raskin, C., Rudolph, M., and Rahman, O.** Rohnert Park, CA : s.n., 2007. AIAA Infotech@Aerospace 2007 Conference and Exhibit. AIAA-2007-2704.
40. *Initial Development of an Earth-Based Prototype for a Lunar Hopper Autonomous Exploration System.* **Cunio, P. M., Babuscia, A., Bailey, Z. J., Chaurasia, H., Goel, R., Golkar, A. A., Selva, D., Timmons, E., Cohanim, B. E., Hoffman, J. A., and Miller, D. W.** Pasadena, CA : AIAA, 2009.
41. *Further Development and Flight Testing of a Prototype Lunar and Planetary Surface Exploration Hopper: Update on the TALARIS Project.* **Cunio, P. M., Nothnagel, S. L., Lanford, E.,**

**McLinko, R., Han, C. J., Olthoff, C. T., Hoffman, J. A., and Cohanin, B. E.** Anaheim, CA : AIAA, 2010.

42. *TALARIS Project Update: Overview of Flight Testing and Development of a Prototype Planetary Surface Exploration Hopper.* **Rossi, C., Cunio, P. M., Alibay, F., Morrow, J., Nothnagel, S. L., Steiner, T., Han, C. J., Lanford, E., and Hoffman, J. A.** Cape Town, SA : International Astronautical Federation, 2011. IAC-11.A3.2A.7.

43. **Anderson, Allison P.** Personal Communication. April 25, 2012.

44. *Advancing Exploration Risk Reduction and Workforce Motivation through Dynamic Flight Testing.* **Barnhart, David, Sullivan, Joseph, and Will, Peter.** Long Beach, CA : s.n., 2007. AIAA Space 2007 Conference and Exhibition. AIAA-2007-0040.

45. *Development of a Local Transportation Infrastructure for Human Lunar Exploration.* **Akin, David L.** Pasadena, CA : AIAA, 2009. AIAA 2009-6782.

46. *Project Morpheus Main Engine Development and Preliminary Flight Testing.* **Morehead, Robert L.** San Diego, CA : 47th AIAA/ASME/SAE/ASEE Joint Propulsion Conference and Exhibit, 2011. AIAA-2011-5927.

47. *Planetary Lander Dynamic Model for GN&C.* **Frampton, R., K. Oittinen, J. M. Ball, A. Khodadoust, D. Kirshman, G. Grayson, P. Sundaram, J. Goff, D. Masten.** Pasadena, CA : AIAA, 2009. AIAA-2009-6571.

48. *Sea-Level Flight Demonstration & Altitude Characterization of a LO<sub>2</sub> / LCH<sub>4</sub> Based Ascent Propulsion Lander.* **Collins, J., Hurlbert, E., Romig, K., Melcher, J., and Eaton, P.** Denver, CO : AIAA, 2009. AIAA-2009-4948.

49. *Demonstration of a Safe and Precise Planetary Landing System On-board a Terrestrial Rocket.* **Paschall, S., and Brady, T.** Big Sky, MT : IEEE Aerospace 2012, 2012.

50. *Shared Human and Robotic Landing and Surface Exploration in the Neighborhood of Mars*. **Cunio, P. M., Cohanim, B. E., Corbin, B. A., Han, C. J., Lanford, E., Yue, H. K., and Hoffman, J. A.** Anaheim, CA : AIAA, 2010.
51. **Lanford, Ephraim**. *SM Thesis*. 2010.
52. **Michel, Wendelin X**. *Use and Sizing of Rocket Hoppers for Planetary Surface Exploration (SM Thesis)*. Cambridge, MA : MIT, 2010.
53. *Integrated Model for a Cost Tradeoff Study Between a Network of Landers and Planetary Hoppers*. **Yue, H. K., Corbin, B. A., Han, C. J., Michel, W. X.** Prague, Czech Republic : International Astronautical Federation, 2010. IAC-10.D1.3.8.
54. **Middleton, Akil J**. *Modeling and Vehicle Performance Analysis of Earth and Lunar Hoppers (SM Thesis)*. Aeronautics and Astronautics, Massachusetts Institute of Technology. Cambridge : Massachusetts Institute of Technology, 2010. Master's Thesis.
55. **Lanford, Ephraim Robert**. *Unique Abilities of Hopper Spacecraft to Enable National Objectives for Solar System Exploration (Master's thesis)*. Cambridge, MA : MIT, 2011.
56. *Jump Propulsion Systems for Soldier Mobility and Power*. **White, P.A., and Lewis, M. J.** Reno, NV : American Institute of Aeronautics and Astronautics, 2002. AIAA-2002-1032.
57. **Lamamy, Julien-Alexandre**. *Enhancing the Science Return of Mars Missions via Sample Preparation, Robotic Surface Exploration, and In-Orbit Fuel Production (SM Thesis)*. Cambridge, MA : Massachusetts Institute of Technology, 2004.
58. **Larson, W. J. and Wertz, J. R.** *Space Mission Analysis and Design, 3rd edition*. El Segundo, CA : Microcosm Press and Kluwer Academic Publishers, 1999. 1-881883-10-8.
59. **Costes, N. C., Farmer, J. E., and George, E. B.** *Mobility Performance of the Lunar Roving Vehicle: Terrestrial Studies - Apollo 15 Results*. Washington, D. C. : National Aeronautics and Space Administration, 1972. NASA Technical Report R-401.

60. *Soviet Rover Systems*. **Carrier, Dave**. Huntsville, AL : AIAA Space Programs and Technologies Conference, 1992. AIAA-1992-1487.

61. *Return to the Red Planet: An Overview of the Mars Pathfinder Mission*. **Thurman, Sam W**. Clearwater Beach, FL : AIAA Aerodynamic Decelerator Systems Technology Conference, 1995. AIAA-1995-1534.

62. **Webster, Guy**. Mars Exploration Rover Mission: Press Releases. *Mars Exploration Rovers*. [Online] NASA Jet Propulsion Laboratory, January 24, 2012. [Cited: March 29, 2012.] <http://marsrover.nasa.gov/newsroom/pressreleases/20120124a.html>.

63. —. Mars Science Laboratory Mission Status Report. *Mars Science Laboratory*. [Online] NASA Jet Propulsion Laboratory, March 26, 2012. [Cited: March 29, 2012.] <http://mars.jpl.nasa.gov/msl/news/whatsnew/index.cfm?FuseAction=ShowNews&NewsID=1211>.

64. *Shape Grammars and the Generative Specification of Painting and Sculpture*. **Stiny, G., and Gips, J. s.l.** : IFIP Congress 71, 1971.

65. *Size-frequency distributions of rocks on the northern plains of Mars with special reference to Phoenix landing surfaces*. **Golombek, M. P., A. Huertas, J. Marlow, B. McGrane, C. Klein, M. Martinez, R. E. Arvidson, T. Heet, L. Barry, K. Seelos, D. Adams, W. Li, J. R. Matijevic, T. Parker, H. G. Sizemore, M. Mellon, A. S. McEwen, L. K. Tamppari, and Y. Cheng**. E00A09, s.l. : Journal of Geophysical Research, 2008, Vol. 113.

66. *Crater and Rock Hazard Modeling for Mars Landing*. **Bernard, D. E. and M. P. Golombek**. Albuquerque, NM : AIAA Space 2001 Conference and Exhibition, 2001. AIAA-2001-4697.

67. **Griffin, Michael D. and French, James R**. *Space Vehicle Design*. Reston, VA : American Institute of Aeronautics and Astronautics, 2004. 1-56347-539-1.

68. **(webmaster), Maryia Davis**. Alpha Particle X-ray Spectrometer (APXS). *MSL Science Corner*. [Online] NASA. [Cited: January 21, 2012.] <http://msl-scicorner.jpl.nasa.gov/Instruments/APXS/>.

69. *The Rosetta Alpha Particle X-Ray Spectrometer (APXS)*. Klingelhofer, G., Brueckner, J., D'Uston, C., Gellert, R., Rieder, R. 1-4, s.l. : Space Science Reviews, 2007, Vol. 128.
70. **Canadian Space Agency Media Relations**. The Maple Leaf Returns to Mars. [Online] Canadian Space Agency, November 26, 2011. [Cited: January 21, 2012.] [http://www.asc-csa.gc.ca/eng/media/news\\_releases/2011/1126.asp](http://www.asc-csa.gc.ca/eng/media/news_releases/2011/1126.asp).
71. **(webmaster), Maryia Davis**. Chemistry & Camera (ChemCam). *MSL Science Corner*. [Online] NASA. [Cited: January 21, 2012.] <http://msl-scicorner.jpl.nasa.gov/Instruments/ChemCam/>.
72. **Maurice, S., R. Wiens, G. Manhes, D. Cremers, B. Barraclough, J. Bernardin, M. Bouye, A. Cros, B. Dubois, E. Druand, S. Hahn, D. Kouach, J.-L. Lacour, D. Landis, T. Moore, L. Pares, J. Platzer, M. Saccoccio, B. Salle, R. Whitaker**. ChemCam Instrument for the Mars Science Laboratory (MSL) Rover. *36th Lunar and Planetary Sciences Conference*. [Online] March 2005. [Cited: January 21, 2012.] <http://www.lpi.usra.edu/meetings/lpsc2005/pdf/1735.pdf>.
73. *Rock Abrasion Tool: Mars Exploration Rover mission*. **Gorevan, S. P., T. Myrick, K. Davis, J. J. Chau, P. Bartlett, S. Mukherjee, R. Anderson, S. W. Squyres, R. E. Arvidson, M. B. Madsen, P. Bertelsen, W. Goetz, C. S. Binou, and L. Richter**. E12, s.l. : Journal of Geophysical Research, 2003, Vol. 108. 8068.
74. Honeybee Robotics - History. [Online] Honeybee Robotics. [Cited: January 21, 2012.] <http://www.honeybeerobotics.com/about/history>.
75. Mars Science Laboratory (MSL) Mast Camera (Mastcam). [Online] Malin Space Science Systems, Inc., 2008. [Cited: January 21, 2012.] [http://www.msss.com/msl/mastcam/MastCam\\_description.html](http://www.msss.com/msl/mastcam/MastCam_description.html).
76. **(webmaster), Maryia Davis**. Mast Camera (Mastcam). *MSL Science Corner*. [Online] NASA. [Cited: January 21, 2012.] <http://msl-scicorner.jpl.nasa.gov/Instruments/Mastcam/>.
77. **Malin, M. C., J. F. Bell, J. Cameron, W. E. Dietrich, K. S. Edgett, B. Hallet, K. E. Herkenhoff, M. T. Lemmon, T. J. Parker, R. J. Sullivan, D. Y. Sumner, P. C. Thomas, E. E. Wohl, M. A. Ravine, M. A. Caplinger, and J. N. Maki**. The Mast Cameras and Mars Descent Imager (MARDI) for the

2009 Mars Science Laboratory. *36th Lunar and Planetary Sciences Conference*. [Online] March 2005. [Cited: January 21, 2012.] <http://www.lpi.usra.edu/meetings/lpsc2005/pdf/1214.pdf>.

78. MSSS Delivers First Science Instrument to JPL for 2009 Mars Rover Mission Payload. [Online] Malin Space Science Systems, 2010. [Cited: January 21, 2012.] <http://www.msss.com/news/index.php?id=4>.

79. NASA Selects MSSS to Provide Three Science Cameras for 2009 Mars Rover Mission. [Online] Malin Space Science Systems, 2010. [Cited: January 21, 2012.] <http://www.msss.com/news/index.php?id=5>.

80. **(webmaster), Maryia Davis**. Mars Hand Lens Imager (MAHLI). *MSL Science Corner*. [Online] NASA. [Cited: January 21, 2012.] <http://msl-scicorner.jpl.nasa.gov/Instruments/MAHLI/>.

81. Mars Science Laboratory (MSL) Hand Lens Imager (MAHLI) Instrument Description. [Online] Malin Space Science Systems, 2010. [Cited: January 21, 2012.] <http://www.msss.com/science/msl-mahli-instrument-description.php>.

82. **Malin, M. C., M. A. Caplinger, K. S. Edgett, F. T. Ghaemi, M. A. Ravine, J. A. Schaffner, J. N. Maki, R. G. Willson, J. F. Bell III, J. F. Cameron, W. E. Dietrich, L. J. Edwards, B. Hallet, K. E. Herkenhoff, E. Heydari, L. C. Kah, M. T. Lemmon, et al.** The Mars Science Laboratory (MSL) Mars Descent Imager (MARDI) Flight Instrument. *36th Lunar and Planetary Sciences Conference*. [Online] March 2005. [Cited: January 21, 2012.] <http://www.lpi.usra.edu/meetings/lpsc2009/pdf/1199.pdf>.

83. **Bell, E., II**. Biology (GEX/LR/PR). *National Space Science Data Center*. [Online] NASA, November 4, 2011. [Cited: January 22, 2012.] <http://nssdc.gsfc.nasa.gov/nmc/masterCatalog.do?sc=1975-075C&ex=03>.

84. **(webmaster), Maryia Davis**. Sample Analysis at Mars (SAM). *MSL Science Corner*. [Online] NASA. [Cited: January 22, 2012.] <http://msl-scicorner.jpl.nasa.gov/Instruments/SAM/>.

85. *The Search for Organic Substances and Inorganic Volatile Compounds in the Surface of Mars*. **K. Biemann, J. Oro, P. Toulmin III, L. E. Orgel, A. O. Nier, D. M. Anderson, P. G. Simmonds, D.**

**Flory, A. V. Diaz, D. R. Rushneck, J. E. Biller, A. L. Lafleur.** 28, s.l. : Journal of Geophysical Research, 1977, Vol. 82. doi:10.1029/JS082i028p04641 .

86. *Size-frequency distributions of rocks on Mars and Earth analog sites: Implications for future landed missions.* **Golombek, M. and Rapp, D.** E2, s.l. : Journal of Geophysical Research, February 25, 1997, Vol. 102, pp. 4117-4129.

87. *Rock size-frequency distributions on Mars and implications for Mars Exploration Rover landing safety and operations.* **Golombek, M. P., A. F. C. Haldemann, N. K. Forsberg-Taylor, E. N. DiMaggio, R. D. Schroeder, B. M. Jakosky, M. T. Mellon, and J. R. Matijevic.** E12, s.l. : Journal of Geophysical Research, 2003, Vol. 108.

88. **Corbin, B. A.** *RASC-AL Link Budget - Distant.* [Excel spreadsheet] Cambridge, MA : s.n., May 26, 2010.

89. *A Look Back at Assembly and Test of the New Horizons Radioisotope Power System.* **Harmon, B. A., and Bohne, W. A.** s.l. : American Institute of Physics, 2007. AIP Conf. Proc. 880, 339 (2007); doi: 10.1063/1.2437472.

90. *Dynamic Performance of Surveyor Throttleable Rocket Engine Operating on Propellants Containing Dissolved Gas.* **McDermott, C. E., R. B. Breshears, and J. McCafferty.** Boston, MA : AIAA, 1966. AIAA-1966-949.

91. *CECE: A Deep Throttling Demonstrator Cryogenic Engine for NASA's Lunar Lander.* **Giuliano, V. J., T. G. Leonard, W. M. Adamski, and T. S. Kim.** Cincinnati, OH : 43rd AIAA/ASME/SAE/ASEE Joint Propulsion Conference and Exhibit, 2007. AIAA-2007-5480.

92. *Northrup Grumman TR202 LOX/LH2 Deep Throttling Engine Technology Project Status.* **Gromski, J. M., A. N. Majamaki, S. G. Chianese, V. D. Weinstock, and T. S. Kim.** Nashville, TN : 46th AIAA/ASME/SAE/ASEE Joint Propulsion Conference and Exhibit, 2010. AIAA-2010-6725.

93. *Dual-Mode, 100:1 Thrust Modulation Rocket Engine.* **Carey, L.** 2, s.l. : Journal of Spacecraft and Rockets, 1968, Vol. 5.



94. **Collier, Patrick.** Kaiser Marquardt Rocket Engines. *The Artemis Project: Private Enterprise on the Moon*. [Online] Artemis Society International, May 7, 1998. [Cited: February 7, 2012.] <http://www.asi.org/adb/04/03/09/01/kaiser-marquardt.html#05-05>.
95. **Dismukes, Kim.** Shuttle Orbiter RCS Overview. *National Aeronautics and Space Administration - Human Spaceflight*. [Online] NASA, April 7, 2002. [Cited: February 7, 2012.] <http://spaceflight.nasa.gov/shuttle/reference/shutref/orbiter/rcs/overview.html>.
96. *Monopropellant Hydrazine 700 lbf Throttling Terminal Descent Engine for Mars Science Laboratory.* **Dawson, M., G. Brewster, Conrad, C., Kilwine, M., Chenevert, B., and Morgan, O.** Cincinnati, OH : 43rd AIAA/ASME/SAE/ASEE Joint Propulsion Conference and Exhibit, 2007. AIAA-2007-5481.
97. *The Descent Engine for the Lunar Module.* **Elverum, Jr., G., P. Staudhammer, J. Miller, A. Hoffman, and R. Rockow.** Washington, D. C. : AIAA 3rd Propulsion Joint Specialist Conference, 1967. AIAA-1967-0521.
98. **Pratt & Whitney Rocketdyne.** RL10 Engine. *Space Launch Propulsion Solutions, Pratt & Whitney Rocketdyne*. [Online] [Cited: February 7, 2012.] [http://www.pratt-whitney.com/products/pwr/propulsion\\_solutions/rl10.asp](http://www.pratt-whitney.com/products/pwr/propulsion_solutions/rl10.asp).
99. —. RL-10B-2 Propulsion System. [Online] 2009. [Cited: February 7, 2012.] [http://www.pw.utc.com/products/pwr/assets/pwr\\_rl10b-2.pdf](http://www.pw.utc.com/products/pwr/assets/pwr_rl10b-2.pdf).
100. **Mankins, J. C.** *Technology Readiness Levels*. s.l. : NASA Office of Space Access and Technology, 1995.
101. **Charles Stark Draper Labs and MIT.** *Concept Exploration and Refinement Study*. Cambridge, MA : s.n., 2005.
102. **Jilla, Cyrus D.** *A Multiobjective, Multidisciplinary Design Optimization Methodology for the Conceptual Design of Distributed Satellite Systems (PhD Thesis)*. Cambridge, MA : Massachusetts Institute of Technology, 2002.

103. **Cyr, Kelley.** Spacecraft/Vehicle Level Cost Model. *NASA Cost Estimating Web Site*. [Online] NASA, May 25, 2007. [Cited: March 26, 2012.] <http://cost.jsc.nasa.gov/SVLCM.html>.
104. **NASA's Mission Operations and Communications Services.** Costing document for 2011 Announcement of Opportunity for Explorer 2011. *DSN Commitments Office*. [Online] December 21, 2010. [Cited: February 15, 2012.] [http://deepspace.jpl.nasa.gov/advmisss/docs/NASA\\_MOCSExp11.pdf](http://deepspace.jpl.nasa.gov/advmisss/docs/NASA_MOCSExp11.pdf).
105. **McCloskey, Scott H.** *Development of Legged, Wheeled, and Hybrid Rover Mobility Models to Facilitate Planetary Surface Exploration Mission Analysis (SM Thesis)*. Cambridge, MA : Massachusetts Institute of Technology, 2007.
106. **Orloff, Richard W.** Apollo by the Numbers: A Statistical Reference. [Online] September 27, 2005. [Cited: February 22, 2012.] <http://history.nasa.gov/SP-4029/SP-4029.htm>.
107. **Bell, E., II.** Apollo 15 Lunar Module / ALSEP. *National Space Science Data Center*. [Online] National Aeronautics and Space Administration, November 4, 2011. [Cited: February 14, 2012.] <http://nssdc.gsfc.nasa.gov/nmc/spacecraftDisplay.do?id=1971-063C>.
108. **Grumman Aerospace Corporation.** *Apollo Operations Handbook, LM 10 and Subsequent*. Bethpage, NY : s.n., 1971. LMA790-3-LM.
109. **Weiss, Stanley P.** *Apollo Experience Report - Lunar Module Structural Subsystem*. Washington, D. C. : National Aeronautics and Space Administration, 1973. NASA Technical Note D-7084.
110. **Rogers, William F.** *Apollo Experience Report - Lunar Module Landing Gear Subsystem*. Washington, D. C. : National Aeronautics and Space Administration, 1972. NASA Technical Note D-6850.
111. **White, Lyle D.** *Apollo Experience report - Electrical Wiring Subsystem*. Washington, D. C. : National Aeronautics and Space Administration, 1975. NASA Technical Note D-7885.

112. **Wertz, J. R., Everett, D. F., and Puschell, J. J. (editors).** *Space Mission Engineering: The New SMAD*. Hawthorne, CA : Microcosm Press, 2011. 978-1-881-883-15-9.
113. **Next Giant Leap, LLC.** *NGL Mission Element List, October 30, 2010*. [Microsoft Excel] 2010.
114. *Phoenix Landing Propulsion System Performance*. **McAllister, J. G., and C. Parish**. Denver, CO : 45th AIAA/ASME/SAE/ASEE Joint Propulsion Conference and Exhibit, 2009. AIAA-2009-5264.
115. **Whetsel, Charles W.** *Personal Communication*. [Email] January 24, 2012.
116. *Phoenix Electrical Power Subsystem - Power at the Martian Pole*. **Coyne, J. W., W. E. Jackson, and C. Lewicki**. Denver, CO : 7th International Energy CONversion Engineering Conference, 2009. AIAA-2009-4518.
117. Phoenix Mars Mission - Frequently Asked Questions. *Phoenix Mars Mission*. [Online] University of Arizona - Lunar and Planetary Laboratory. [Cited: March 29, 2012.] <http://phoenix.lpl.arizona.edu/faq.php>.
118. **National Aeronautics and Space Administration.** *Phoenix Launch: Mission to the Martian Polar North - Press Kit*. 2007.
119. **Bell, E., II.** Phoenix Mars Lander. *National Space Science Data Center*. [Online] National Aeronautics and Space Center, November 4, 2011. [Cited: February 22, 2012.] <http://nssdc.gsfc.nasa.gov/nmc/spacecraftDisplay.do?id=2007-034A>.
120. **U. S. Bureau of Labor Statistics.** CPI Inflation Calculator. *Bureau of Labor Statistics - Databases, Tables & Calculators by Subject*. [Online] United States Department of Labor, July 8, 2011. [Cited: March 29, 2012.] [http://www.bls.gov/data/inflation\\_calculator.htm](http://www.bls.gov/data/inflation_calculator.htm).
121. **Martin Marietta Corporation.** *Viking Lander System: Primary Mission Performance Report*. s.l. : National Aeronautics and Space Administration, 1977. NASA-CR-145148.

122. **Bell, E., II.** Viking 1 Lander. *National Space Science Data Center*. [Online] National Aeronautics and Space Administration, November 4, 2011. [Cited: February 22, 2012.] <http://nssdc.gsfc.nasa.gov/nmc/spacecraftDisplay.do?id=1975-075C>.
123. *Mars Scout Phoenix Parachute System Performance*. **Witkowski, A., Kandis, M., and Adams, D. S.** Seattle, WA : 20th AIAA Aerodynamic Decelerator Systems Technology Conference and Seminar, 2009. AIAA-2009-2907.
124. *Mars Exploration Rover Parachute Mortar Deployer Development*. **Vasas, R. E. and Styner, J.** Monterey, CA : 17th AIAA Aerodynamics Decelerator Systems Technology Conference and Seminar, 2003. AIAA-2003-2137.
125. *Historical Perspective: Viking Mars Lander Propulsion*. **Morrisey, D. C.** 2, s.l. : Journal of Propulsion and Power, 1992, Vol. 8.
126. **Proctor, Robert W., and Van Zandt, Trisha.** *Human Factors in Simple and Complex Systems, 2nd edition*. Boca Raton, FL : CRC Press, 2008. 978-0-8058-4119-0.
127. **Head, J. W., and Scott, D. R.** *Scientific Basis for the Exploration of Copernicus Crater, The Moon*. 2012.
128. —. *Copernicus Crater central peak (LOLA-LROC) - personal communication with J. Head*. [Presentation] Providence, RI : s.n., March 12, 2012.
129. **Viotti, Michelle.** Mars Exploration Rover Missions: All Spirit Updates. *Mars Exploration Rovers*. [Online] NASA Jet Propulsion Laboratory, May 24, 2011. [Cited: March 29, 2012.] [http://marsrover.nasa.gov/mission/status\\_spiritAll\\_2004.html](http://marsrover.nasa.gov/mission/status_spiritAll_2004.html).
130. **NASA Jet Propulsion Laboratory.** Spirit: Detailed Traverse Map. *Mars Exploration Rovers*. [Online] June 6, 2005. [Cited: March 29, 2012.] [http://marsrover.nasa.gov/mission/tm-spirit/images/MERA\\_A503\\_1.jpg](http://marsrover.nasa.gov/mission/tm-spirit/images/MERA_A503_1.jpg).

131. **Viotti, Michelle.** *Spacecraft: Surface Operations: Instruments. Mars Exploration Rovers.* [Online] NASA Jet Propulsion Laboratory. [Cited: March 29, 2012.] [http://marsrover.nasa.gov/mission/spacecraft\\_surface\\_instru.html](http://marsrover.nasa.gov/mission/spacecraft_surface_instru.html).
132. *A New Form of Planetary Surface Mobility: Hoppers.* **Alibay, Farah.** Providence, RI : Brown University MicroRover Space Horizons Workshop, 2012.
133. **Bell, E., II.** *Surveyor 1. National Space Science Data Center.* [Online] NASA, May 14, 2012. [Cited: May 24, 2012.] <http://nssdc.gsfc.nasa.gov/nmc/masterCatalog.do?sc=1966-045A>.
134. —. *Huygens. National Space Science Data Center.* [Online] NASA, May 14, 2012. [Cited: May 24, 2012.] <http://nssdc.gsfc.nasa.gov/nmc/spacecraftDisplay.do?id=1997-061C>.
135. —. *Spirit. National Space Science Data Center.* [Online] NASA, May 14, 2012. [Cited: May 24, 2012.] <http://nssdc.gsfc.nasa.gov/nmc/spacecraftDisplay.do?id=2003-027A>.
136. —. *Mars Science Laboratory (MSL). National Space Science Data Center.* [Online] NASA, May 14, 2012. [Cited: May 24, 2012.] <http://nssdc.gsfc.nasa.gov/nmc/spacecraftDisplay.do?id=2011-070A>.
137. **Saenz-Otero, Alvar.** *Design Principles for the Development of Space Technology Maturation Laboratories Aboard the International Space Station (PhD Thesis).* Cambridge, MA, United States : Massachusetts Institute of Technology, June 2005.
138. **Olthoff, Claas T.** *Application of Flexibility Principles and Strategies to the TALARIS Avionics System (Diplomarbeit).* Munich, Germany : Technische Universitaet Muenchen, 2010.



## **Appendix A. MATLAB Code**

The MATLAB code for the tradespace model, broken up into sections for each individual code module, is available from a CD attached to this thesis document. Code is also available from the author upon appropriate request, and may be made available online at a later date.

## Appendix B. Excel Databases for Tradespace Model

This appendix contains information from the databases used by the tradespace model. Each database is kept as an Excel spreadsheet, allowing it to be used by other programs, or to be modified by advanced users. Each spreadsheet database will be presented in two tables: one showing the data used, and the other showing the sources used to collect the data. Following the table of sources will be a listing of the references for the sources.

### B.1. Planetary Body Database

The planetary body database contains a catalogue of the planetary bodies in the solar system that might be interesting targets for hopping vehicles. This is a list of all the bodies with terrestrial surfaces and a surface gravity above  $0.25 \text{ m/s}^2$ . The cutoff gravity level is approximately the point where the process of landing and hopping over the surface becomes more akin to a docking and approaching process, and thus is the point where hopping algorithms and propulsion technologies can be replaced by docking algorithms and technologies. See Appendix D for more information on the cutoff level.

Table B-1. Catalogue of planetary body data.

Number	Name	Type	Gravity (m/s <sup>2</sup> )	Atmosphere (Pa)	Golombek-k	Day length (s)	Solar dist (AU)	Surf temp (Max. K)	Surf temp (Min. K)
1	Earth	Planet	9.81	101300	0.06	86400	1	330	184
2	Venus	Planet	8.87	9420900	0.06	20995200	0.72	740	740
3	Mars	Planet	3.71	709.1	0.3	88775	1.52	290	150
4	Ganymede	Moon - Jupiter 3	1.428325648	0.000001013	0.12	617760	5.2	41	35
5	Titan	Moon - Saturn 6	1.35862758	145872	0.3	1378080	9.6	96	92
6	Mercury	Planet	3.702909079	1.013E-07	0.3	5067014.4	0.3871	725	90
7	Callisto	Moon - Jupiter 4	1.245713763	1.4182	0.12	1442016	5.2	41	35
8	Io	Moon - Jupiter 1	1.8	0.001013	0.3	152841.6	5.2	1550	100
9	Luna	Moon - Terra 1	1.623711699	1.06365E-08	0.12	2360591.424	1	390	104
10	Europa	Moon - Jupiter 2	1.303783621	0.000001013	0.05	306720	5.2	41	35
11	Triton	Moon - Neptune 1	0.78	1.4182	0.12	507772.8	30.1	41	35
12	Eris	Dwarf planet	0.773882639	3.039	0.4	93240	67.67	55	35
13	Pluto	Dwarf planet	0.655047845	3.039	0.4	551836.8	39.44	55	35
14	Titania	Moon - Uranus 3	0.374917454	1.4182	0.12	752544	19.2	41	35
15	Rhea	Moon - Saturn 5	0.277617248	1.4182	0.12	390528	9.6	41	35
16	Oberon	Moon - Uranus 4	0.340341081	1.4182	0.12	1162944	19.2	41	35
17	Iapetus	Moon - Saturn 8	0.240832683	1.4182	0.12	6854112	9.6	41	35
18	Makemake	Dwarf planet	0.474524444	3.039	0.4	80928	45.79	55	35
19	Charon	Moon - Pluto 1	0.218024017	0.001013	0.4	551836.8	39.44	55	35
20	Umbriel	Moon - Uranus 2	0.245277019	1.4182	0.12	357696	19.2	41	35
21	Ariel	Moon - Uranus 1	0.258945448	1.4182	0.12	217728	19.2	41	35
22	Ceres	Dwarf planet	0.26674451	3.039	0.12	32666.4	2.77	55	35



Table B-2. Catalogue of planetary body data sources.

Name	Type	Grav ref	Atm ref	Gmbk ref	Day ref	Sdist ref	Stemp ref
Earth	Planet	-	-	11, analogy with Mars modal	-	-	7
Venus	Planet	1	1	12	1	1	1
Mars	Planet	1	1	10, near-far avg	1	1	1
Ganymede	Moon - Jupiter 3	1	1	14, medium-density	1	1	5
Titan	Moon - Saturn 6	1	1	13	1	1	1
Mercury	Planet	1	1	13	1	1	1
Callisto	Moon - Jupiter 4	1	5	14, medium-density	1	1	5
Io	Moon - Jupiter 1	1	1	1, 13	1	1	1
Luna	Moon - Terra 1	1	1	14, medium-density	1	-	1
Europa	Moon - Jupiter 2	1	1	14, low-density	1	1	5
Triton	Moon - Neptune 1	1, p. 399	1, p. 399	14, medium-density	1	1	1, p. 399
Eris	Dwarf planet	2	8	14, high-density	4	2	8
Pluto	Dwarf planet	1, p. 399, 2	1, p. 399	14, high-density	1	1, p. 399	1, p. 399
Titania	Moon - Uranus 3	1	5	14, medium-density	1	1	5
Rhea	Moon - Saturn 5	1	5	14, medium-density	1	1	5
Oberon	Moon - Uranus 4	1	5	14, medium-density	1	1	5
Iapetus	Moon - Saturn 8	1	5	14, medium-density	1	1	5, 6
Makemake	Dwarf planet	2	8	14, high-density	4	2	8
Charon	Moon - Pluto 1	1, p.515	9	14, high-density	1	1	8
Umbriel	Moon - Uranus 2	1	5	14, medium-density	1	1	5
Ariel	Moon - Uranus 1	1	5	14, medium-density	1	1	5
Ceres	Dwarf planet	2	8	2, 14-medium density	4	2	8
Pallas	Asteroid	3, 4	9	14, high-density	4	2	8
Vesta	Asteroid	2, 4	9	14, high-density	4	2	8
Enceladus	Moon - Saturn 2	1	5	13	1	1	5
Eros	Asteroid	2, 4	9	14, high-density	4	2	8

1	Encyclopedia of the Solar System, edited by P. R. Weissman, L. McFadden, T. V. Johnson, Academic Press, San Diego, 1999.
2	On the Origin of Planets by Means of Natural Simple Processes, Michael M. Woolfson, Imperial College Press, Singapore, 2011.
	Hubble Takes a Look at Pallas: Shape, Size and Surface. B. E. Schmidt, P. C. Thomas, J. M. Bauer, J.-Y. Li, L. A. McFadden, J. M. Parker, A. S. Rivkin, C. T. Russell, and S. A. Stern. Lunar and Planetary Science XXXIX (2008).
3	[ <a href="http://www.lpi.usra.edu/meetings/lpsc2008/pdf/2502.pdf">http://www.lpi.usra.edu/meetings/lpsc2008/pdf/2502.pdf</a> ]
4	JPL Small-Body Database Browser, <a href="http://ssd.jpl.nasa.gov/sbdb.cgi">ssd.jpl.nasa.gov/sbdb.cgi</a> , last accessed November 23, 2011.
5	Analogy with large outer-planet moon Triton "Iapetus Thermal Radiation Image." Cassini Solstice Mission page, dated January 10, 2005. Accessed November 23, 2011.
6	[ <a href="http://saturn.jpl.nasa.gov/photos/imagetails/index.cfm?imageId=1281">http://saturn.jpl.nasa.gov/photos/imagetails/index.cfm?imageId=1281</a> ] "Global Measured Extremes of Temperature and Precipitation." National Climatic Data Center page, updated August 20, 2008.
7	Accessed November 23, 2011. [ <a href="http://www.ncdc.noaa.gov/oa/climate/globalextremes.html">http://www.ncdc.noaa.gov/oa/climate/globalextremes.html</a> ]
8	Analogy with dwarf planet Pluto
9	Analogy with Luna
10	Bernard and Golombek 2001, AIAA-2001-4697
11	Golombek and Rapp, 1997
12	Analogy with Earth
13	Analogy with Mars
14	Golombek, Huertas et al. 2008, JGR 113

## B.2. Scientific Instrument Database

The instrument database contains a listing of a selection of scientific instruments, all of which have flown or are currently flying on a planetary surface exploration vehicle. Data for each instrument is taken from publications related to the relevant mission, save for the magnetometer, which is an extremely small and simple instrument.

**Table B-3. Catalogue of scientific instruments.**

Number	Name	Modes	Mass [kg]	Volume [m <sup>3</sup> ]	Active Power [W]	Passive Power [W]	Dev Cost [M\$]	Build Cost [M\$]	Data rate [kb/s]	Analysis per kb [p-hr]	Mission
1	Alpha X-Ray Spectrometer (APXS)	1	0.64	0.000178392	1.5	1.5	17.1	0.9	0.28444444	0.01171875	MSL
2	ChemCam	2	7	0.009	15	0	12.777632	0.55	86.6666667	1.20192E-05	MSL
3	Driller/corer	2	0.687	0.000726336	11	0	5.7	0.3	1.28	0.000651042	MER
4	Pancam	2	2	0.00763407	13	4	8.4552632	0.2	294912	4.361E-06	MER/MSL
5	Precise Cam	2	0.15	0.000972	15	5	6.4657895	0.1	1000	0.001286111	MSL
6	Magnetometer	1	0.35	0.0000025	1.5	1.5	1.5	0.1	0.28444444	1.95313E-06	--
7	Sample Analysis Bay	2	15	0.045	15	5	20	2	1.57407407	0.355764706	Viking/MSL

**Table B-4. Catalogue of instrument data sources.**

Number	Name	Modes	Mass [kg]	Volume [m <sup>3</sup> ]	Active Power [W]	Passive Power [W]	Dev Cost [M\$]	Build Cost [M\$]	Data rate [kb/s]	Analysis per kb [p-hr]	Mission
1	Alpha X-Ray Spectrometer (APXS)	Z	B	B	B	B	V	V	A	A	MSL
2	ChemCam	Z	C	C	C	Z	W	W	C	D	MSL
3	Driller/corer	Z	E	E	E	Z	U	U	E	Z	MER
4	Pancam	Z	H	G	H	H	O	N	F	F	MER/MSL
5	Precise Cam	Z	X	I	X	X	O	M	I, J, P	X	MSL
6	Magnetometer	Z	Z	Z	Z	Z	Z	Z	W	Z	--
7	Sample Analysis Bay	Z	L	K	L	Z	Z	Z	R	T	Viking/MSL

Z	Assumed
A	<a href="http://msl-scicorner.jpl.nasa.gov/instruments/APXS/">http://msl-scicorner.jpl.nasa.gov/instruments/APXS/</a>
B	The Rosetta Alpha Particle X-Ray Spectrometer (APXS), Klingelhofer et al., Space Science Reviews (2007) 128: 383-396
C	<a href="http://www.lpi.usra.edu/meetings/lpsc2005/pdf/1735.pdf">http://www.lpi.usra.edu/meetings/lpsc2005/pdf/1735.pdf</a>
D	<a href="http://msl-scicorner.jpl.nasa.gov/instruments/ChemCam/">http://msl-scicorner.jpl.nasa.gov/instruments/ChemCam/</a> - implies rapid turnaround with a team, so used 5 people for 15 minutes
E	JGR 108, No. E12, 8068
F	<a href="http://www.msss.com/msl/mastcam/MastCam_description.html">http://www.msss.com/msl/mastcam/MastCam_description.html</a> - note that time assumes 10 sec thumbnail, 2 min image, 15 min x 5 people image
G	<a href="http://msl-scicorner.jpl.nasa.gov/instruments/Mastcam/">http://msl-scicorner.jpl.nasa.gov/instruments/Mastcam/</a>
H	<a href="http://www.lpi.usra.edu/meetings/lpsc2005/pdf/1214.pdf">http://www.lpi.usra.edu/meetings/lpsc2005/pdf/1214.pdf</a>
W	Analogy with APXS
X	Analogy with other cameras
I	<a href="http://msl-scicorner.jpl.nasa.gov/instruments/MAHLI/">http://msl-scicorner.jpl.nasa.gov/instruments/MAHLI/</a>
J	<a href="http://www.msss.com/science/msl-mahli-instrument-description.php">http://www.msss.com/science/msl-mahli-instrument-description.php</a>
K	<a href="http://msl-scicorner.jpl.nasa.gov/instruments/SAM/">http://msl-scicorner.jpl.nasa.gov/instruments/SAM/</a>
L	<a href="http://nssdc.gsfc.nasa.gov/nmc/masterCatalog.do?sc=1975-075C&amp;ex=03">http://nssdc.gsfc.nasa.gov/nmc/masterCatalog.do?sc=1975-075C&amp;ex=03</a>
M	<a href="http://www.lpi.usra.edu/meetings/lpsc2009/pdf/1199.pdf">http://www.lpi.usra.edu/meetings/lpsc2009/pdf/1199.pdf</a>
N	Analogy with M
	<a href="http://www.msss.com/news/index.php?id=4">http://www.msss.com/news/index.php?id=4</a> , divided by three and scaled by
O	<a href="http://www.msss.com/news/index.php?id=5">http://www.msss.com/news/index.php?id=5</a>
P	Analogy with MARDI, see also H
Q	<a href="http://www.lpi.usra.edu/meetings/lpsc2005/pdf/1337.pdf">http://www.lpi.usra.edu/meetings/lpsc2005/pdf/1337.pdf</a>
R	JGR Vol. 82, no. 28, Biemann et al.
S	JGR 108 No. E12, 8063, Bell et al.
T	Datarate, then use 21 people (full science team) for three days x 8 hours per day
	From <a href="http://www.honeybeerbots.com/about/history">http://www.honeybeerbots.com/about/history</a> , then assume half of annual revenue is from NASA, and NASA uses a 2-year contract; plus 95% = dev, 5% = bld
U	<a href="http://www.asc-csa.gc.ca/eng/media/news_releases/2011/1126.asp">http://www.asc-csa.gc.ca/eng/media/news_releases/2011/1126.asp</a> , and use 95% = dev rule
V	
W	Half of each for APXS and Precise Cam

### B.3. Engine Database

The engine database is populated with engines across a range of thrust levels and throttling ratios. Data is drawn from the technical literature.

Table B-5. Catalogue of engines.

Name	Max thrust (N)	Max throttle ratio	Fuel	Oxidizer	Isp (s)	Engine mass (kg)	TRL (est)
DM-LAE	500	20	N4H4	N2O4	315	4.54	8
Bell 8414	500	90	N2H4-UDMH	N2O4	254	3.86	6
R-40A/STS-RCS	5000	20	MMH	N2O4	281	10.25	9
MR-80B	5000	90	Hydrazine	None	204	7.68	7
LMDE	50000	75	N2H4-UDMH	N2O4	300	224.1	9
TR202	50000	90	CH4	LOX	309	127.3	4
CECE/RL-10B	250000	90	CH4	LOX	275	301.8	5

Table B-6. Catalogue of engine data sources.

Name	Max thrust (N)	Max throttle ratio	Fuel	Oxidizer	Isp (s)	Engine mass (kg)	TRL (est)
DM-LAE	9	9	9	9	9	9	Z
Bell 8414	3	3	3	3	3	3	Z
R-40A/STS-RCS	7, 8	9	7, 8	7, 8	7	7	Z
MR-80B	10	10	10	10	10	11	Z
LMDE	1	1	1	1	1	1	Z
TR202	2	2	2	2	2	2	Z
CECE/RL-10B	5	4	4	4	6	6	Z

1	Elverum et al. 1967, AIAA-1967-0521
2	AIAA-2010-6725
3	"Dual-Mode, 100:1 Thrust Modulation Rocket Engine," L. Carey, 1968, JSR vol. 5 No. 2
4	"CECE: A Deep Throttling Demonstrator Cryogenic Engine for NASA's Lunar Lander," Giuliano, Leonard, Adamski, and Kim, AIAA-2007-5480
5	<a href="http://www.pratt-whitney.com/products/pwr/propulsion_solutions/r110.asp">http://www.pratt-whitney.com/products/pwr/propulsion_solutions/r110.asp</a>
6	<a href="http://www.pw.utc.com/products/pwr/assets/pwr_r10b-2.pdf">http://www.pw.utc.com/products/pwr/assets/pwr_r10b-2.pdf</a>
7	<a href="http://www.asi.org/adb/04/03/09/01/kaiser-marquardt.html#05-05">http://www.asi.org/adb/04/03/09/01/kaiser-marquardt.html#05-05</a>
8	<a href="http://spaceflight.nasa.gov/shuttle/reference/shutref/orbiter/rcs/overview.html">http://spaceflight.nasa.gov/shuttle/reference/shutref/orbiter/rcs/overview.html</a>
9	SMAD
10	Dawson et al. 2007, AIAA-2007-5481
11	"Historical Perspective: Viking Mars Lander Propulsion," D. C. Morrissey, 1992, JPP vol. 8 no. 2
Z	Estimated from approximate maturity

## **Appendix C. User Guide**

The tradespace model of a hopping vehicle is intended to provide users with additional insight into hopping vehicles by producing designs for hopping vehicles based on user-specified target planetary bodies, scientific payloads, and flight profiles. This user guide briefly introduces the screens used to enter this information.

The tradespace model user interface relies on command line input in MATLAB, and produces a combination of textual and visual outputs as the user proceeds. Inputs are the payload, the target planetary body, and the flight profile. Outputs include feedback and guidance as the user proceeds, a visual display of the hopping vehicle's trajectory which is auto-updated as the user inputs more maneuvers, textual information on the hopping vehicle, and plots showing the subsystem mass breakdown and operational timeline.

### **C.1. User Inputs**

The user first enters a payload and a planetary body, selecting from options presented by the model in the MATLAB environment. While the user enters information via the command line, the model provides feedback and guidance, as shown in Figure C-1.

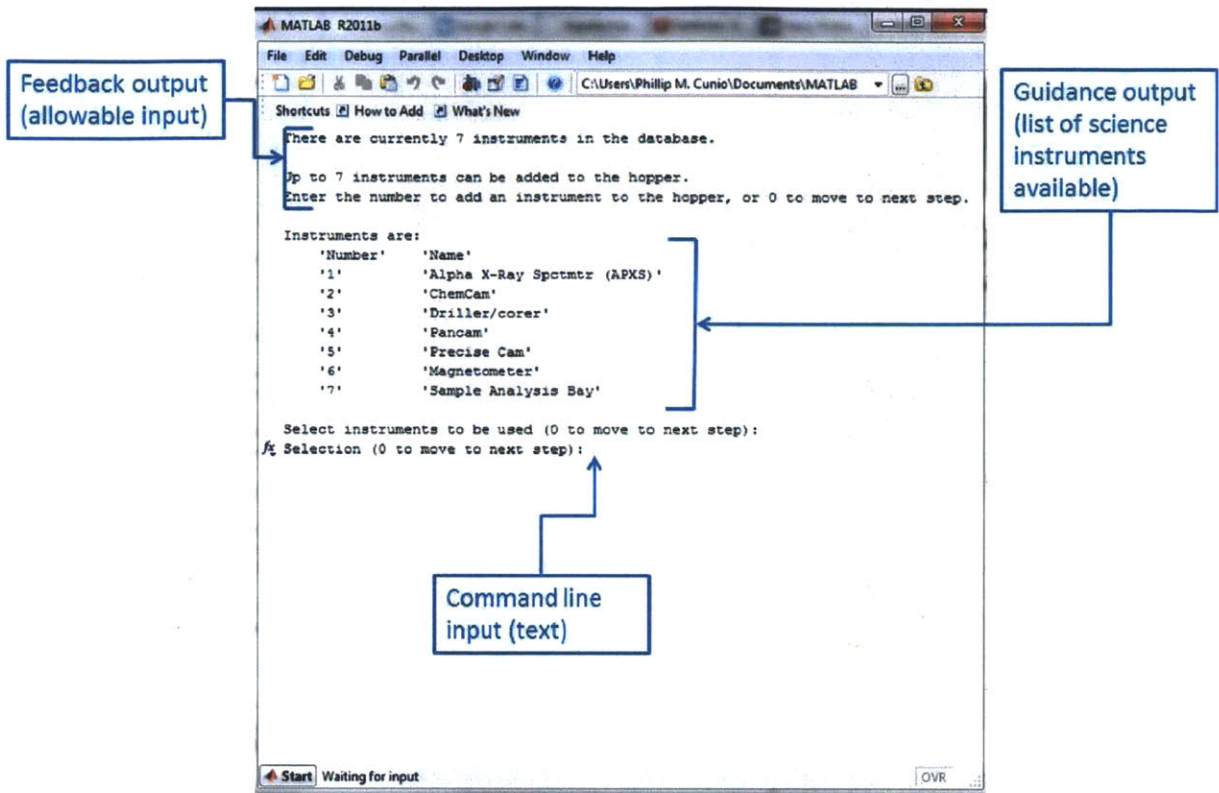


Figure C-1. Payload entry screen.

The user then similarly selects a planetary body as a target for the hopping vehicle mission, using the screen shown in Figure C-2.

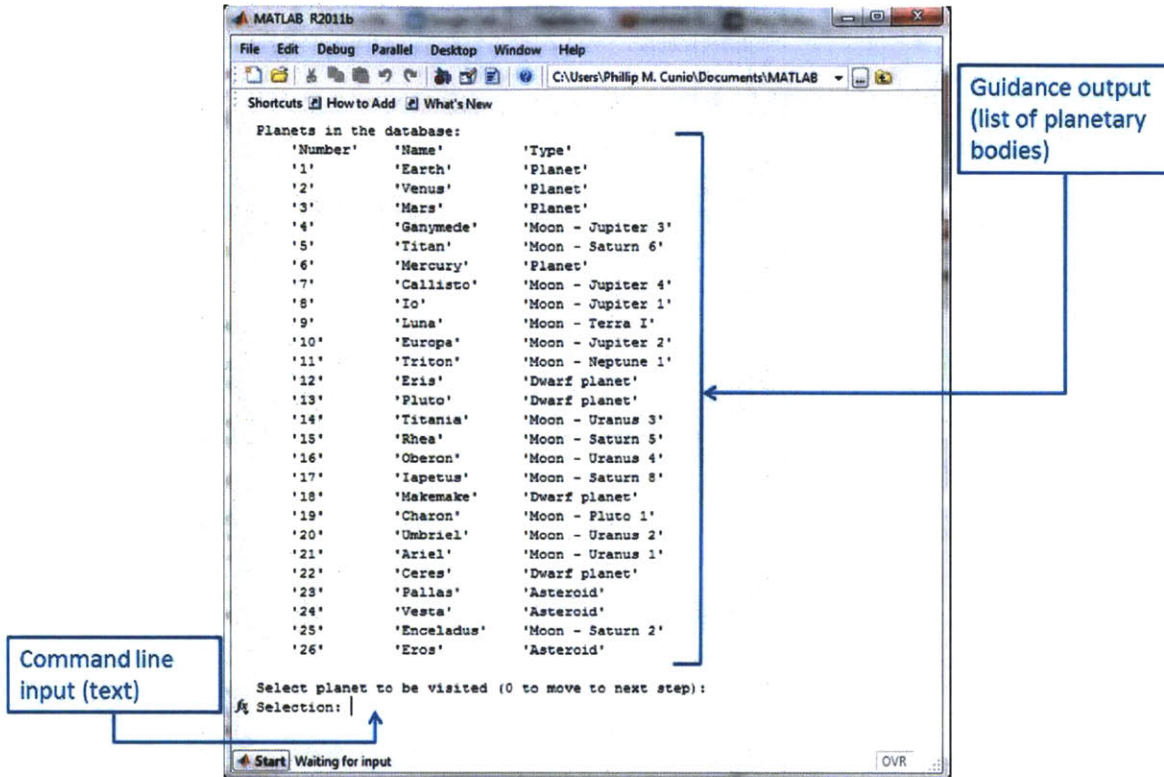


Figure C-2. Planetary body selection screen.

After this is complete, the user defines a flight profile one maneuver at a time, using feedback and guidance from the model to do so. The user is able to visualize the flight path on a three-dimensional plot generated and actively updated by the model as the flight profile is created. Figure C-3 shows the flight profile entry screen and the three-dimensional plot.

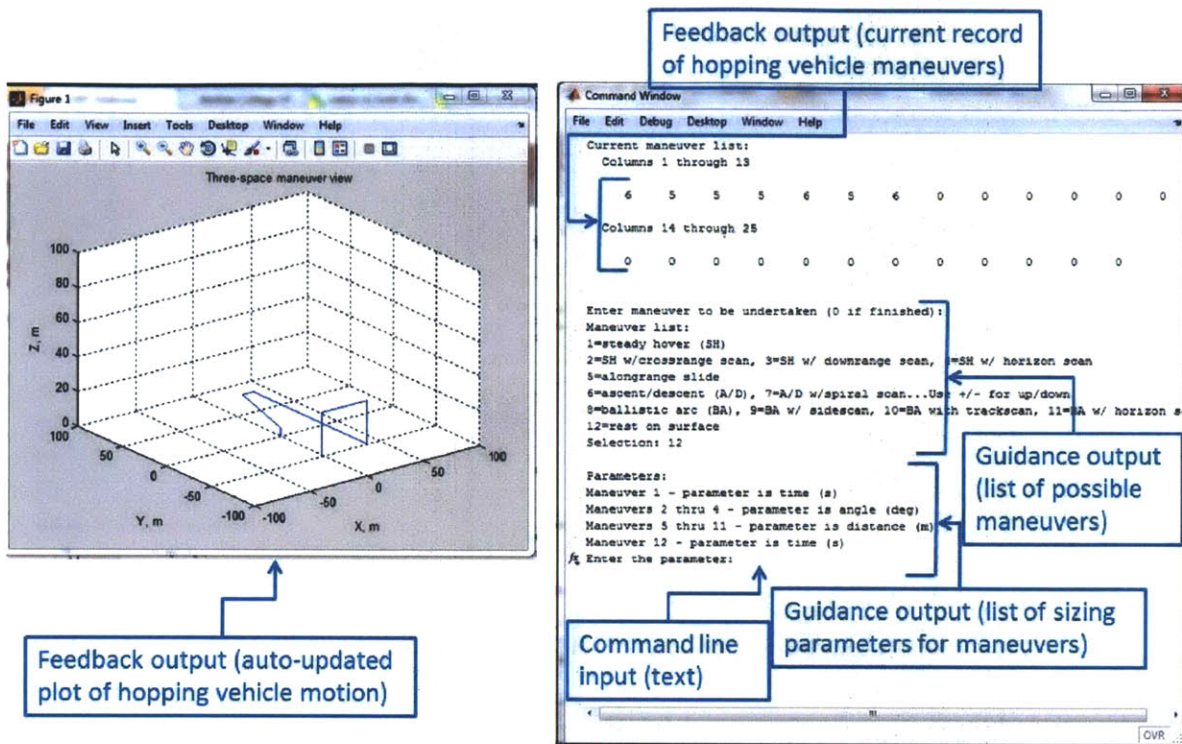


Figure C-3. Flight profile entry screen.

Finally, the user tags each segment of the mission to mark whether or not science and communications activities are being performed. With this operational information prepared, as shown in Figure C-4, the model is ready to perform its analysis.



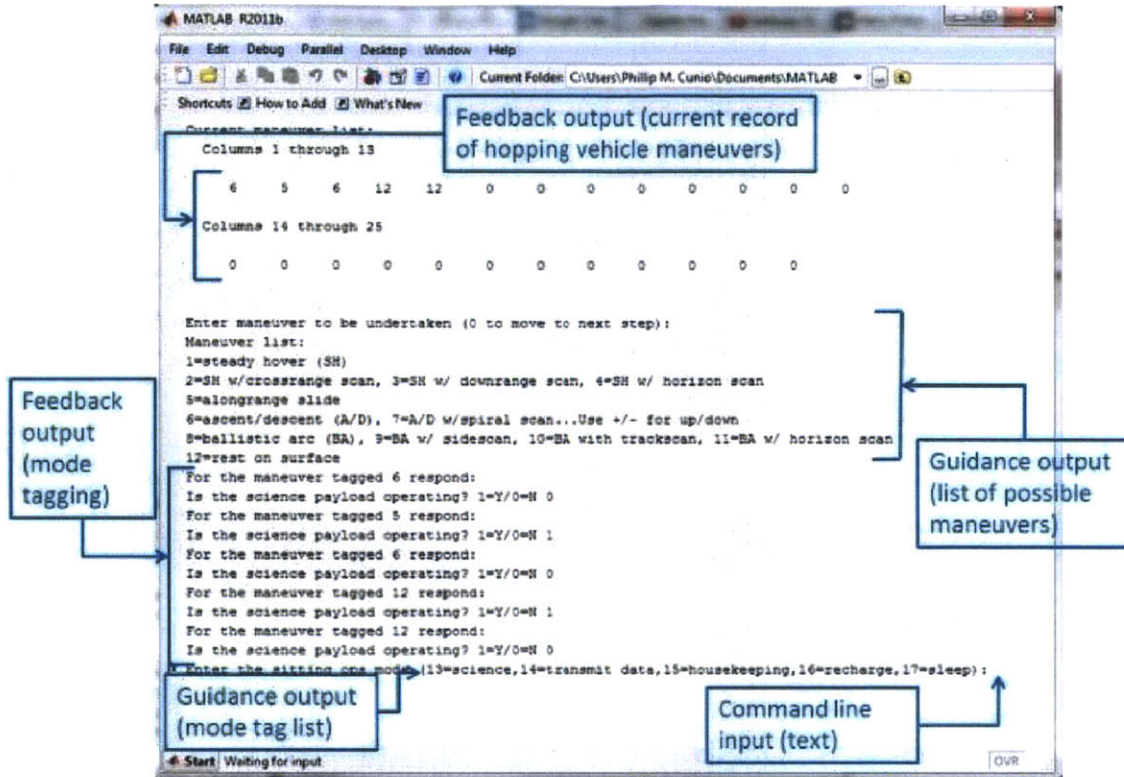


Figure C-4. Operations entry screen.

The output produced by the model is shown in Figure C-5. Textual information and plots showing the operational timeline and the subsystem mass breakdown, are given.



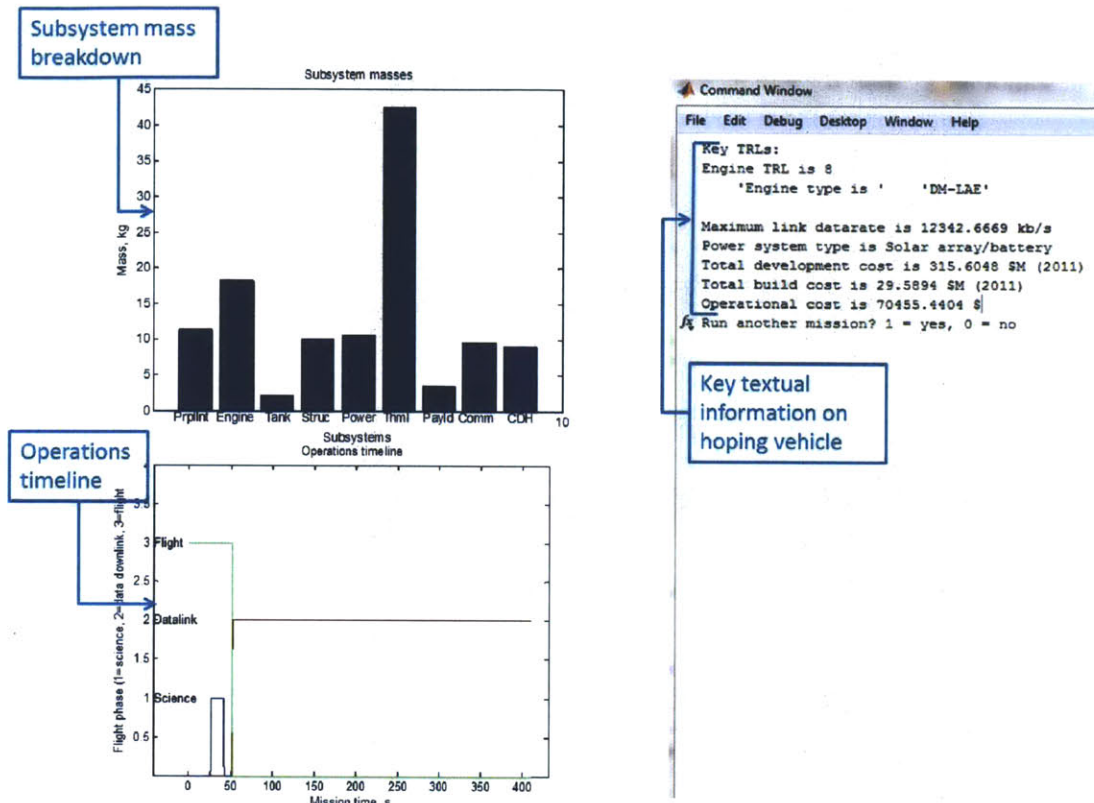


Figure C-5. Model outputs.

## C.2. Logical Information Flow

Data begins to flow through the model by being entered by a user. The user starts with a mission concept, which is a simple description of a planetary surface exploration mission to be performed. The user then formalizes this mission concept, using the action grammar presented in Chapter 3 of this thesis. The mission concept is formalized into a flight profile, a target planetary body, and a scientific payload. Figure C-6 shows these three sets of user choices outlined in blue.

The model then internally calculates the hopping vehicle size and other technical characteristics, using the algorithms described in Chapter 3 of this thesis. These calculations result in sizing and

technical information for each subsystem of the hopping vehicle, and a master parameter list provides another avenue for advanced user input. After the hopping vehicle is sized, cost models are used to calculate cost estimates. Figure C-6 shows the technical portions of the model outlined in orange.

Finally, the model produces output for user review. This output, which provides insight into the hopping vehicle design and its place in the tradespace of hopping vehicle designs, consists of the information detailed in Section 4.3.3 of this thesis. Figure C-6 shows outputs outlined in green.

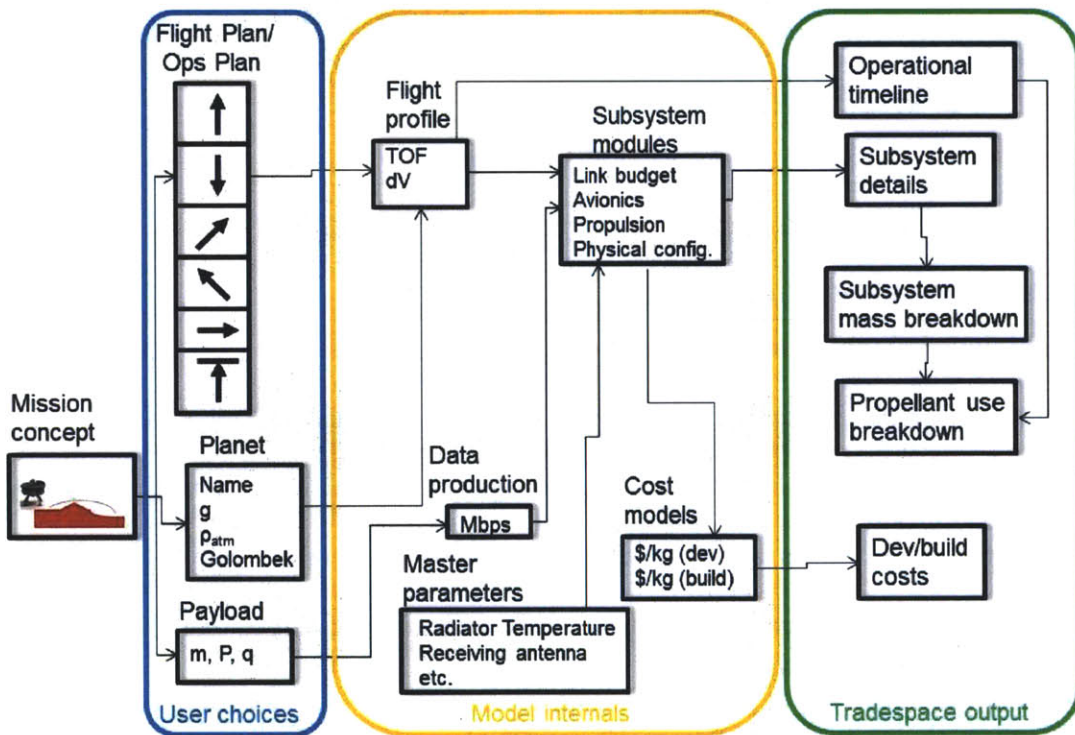


Figure C-6. Model logical flow.

## Appendix D. Lower Limit of Gravity for Hopping

Description: The motion performed by a hopping vehicle is known to be very similar to the motion performed by a lander, but the distinction breaks down somewhat when the target planetary body is very small. A very small planetary body, like an asteroid, presents a problem more akin to rendezvous and docking than to landing. Therefore, it may be advantageous in classifying future engineering problems to distinguish between missions which require docking-like approaches and missions which require landing-like approaches. Because hopping is still a technology in the embryonic stage, and because most landing has occurred on bodies which are either sufficiently small as to clearly be docking problems (Dawn/Vesta) or sufficiently large as to clearly be landing problems (Mars, Venus, Titan), the dividing line has not been specified to date, even though any solid-surfaced body in the solar system is a potential target for landing/hopping at some point.

Minimum gravity condition: The dividing line between rendezvous and docking and hopping/landing can perhaps best be specified by reference to the gravity of the target body. If the gravity is on the lower side of the line, the mission is akin to docking with the target, much as if it were just a very large ISS. If the gravity is on the high side of the line, then the mission is a landing/hopping mission, much like a touchdown on a very small Mars.

State that defines minimum gravity condition: We may assume that a practical limitation of maneuvering in the vicinity of a small planetary body obtains. This limitation takes the form of the minimum effective force that a maneuvering thruster can deliver. If the lowest possible force from a maneuvering engine is such that the vehicle attempting to encounter the target body experiences more force from such a thruster than from the target body's gravity whenever the thruster is active, then the vehicle must either be attracted to the body at the rate dictated by gravity or must fire its engines in careful pulses, essentially bouncing away from the target body briefly before continuing its gravity-driven approach. This situation is very similar to docking maneuvers, where careful pulsed firing and coasting of thrusters is used to rendezvous two vehicles of similar (or approximately similar, on a planetological scale) size. However, if the lowest possible engine force is such that it equals or falls below the gravity force, then the vehicle will continue to fall toward the surface at a lowered rate. This situation is much more akin to hopping or decelerated landing. Put simply, if the vehicle encountering the target body can throttle down far enough to descend smoothly without shutting its engines down entirely, then the situation is more akin to a landing or hopping scenario.

Calculation of limiting gravity condition: The minimum-gravity condition implies that the vehicle can attain a hovering state when it has throttled all the way down and is at minimum mass (i.e., has burned all its propellant). In this state, the gravity of the local body will be just enough to continue to drag the vehicle down to the surface. Under ideal operational conditions, this would equate to the hopper's touching down after completing its final hopping maneuver, with dry propellant tanks.

If we assume that a hopping vehicle's mass is made up of fuel plus some constant mass containing the payload, power systems, and other bus elements, then we can indicate that the

final, minimum mass of the hopping vehicle is equal to the constant mass. Therefore, in this state, the hopper's weight is equal to or greater than the thrust, as:

$$m_{min}g_{body} \geq R_{low}T_{max}$$

Note that the minimum thrust is described by  $R_{low}T_{max}$ , where  $T_{max}$  is the maximum thrust, and  $R_{low}$  is the lowest throttling ratio, i.e. the lowest fraction of the maximum thrust that can be produced. Because the minimum mass  $m_{min}$  is equivalent to the constant mass  $m_c$  (the hopper with all propellant expended), we can simplify to:

both when the engines are at maximum thrust (and the fuel tanks are consequently at maximum mass), and when the engines are at minimum thrust (when the fuel tanks are nearly empty). This condition can be expressed as:

$$g_{body} \geq R_{low} \frac{T_{max}}{m_c}$$

Additionally, since the hopper must also be able to hover when it begins its hopping maneuvers, i.e. when it is at its heaviest, the maximum thrust must be equivalent to that required to hold up the empty hopper and its full weight of propellant. This condition can be expressed by  $T_{max} = m_{max}g_{body}$ , which again simply equates weight and thrust.

Substituting this into the expression for  $g_{body}$ , we obtain:

$$g_{body} \geq R_{low} \frac{m_{max}}{m_c} g_{body}$$

Noting that  $m_{max}$  is effectively the initial mass, and  $m_c$  is the burnout mass (as described in the rocket equation,  $\frac{m_{bo}}{m_0} = e^{\frac{-\Delta V}{I_{sp}g_{earth}}}$ ), we can substitute in to obtain:

$$g_{body} \geq R_{low} e^{\frac{\Delta V}{I_{sp}g_{earth}}} g_{body}$$

Simplifying, we see:

$$1 \geq R_{low} e^{\frac{\Delta V}{I_{sp}g_{earth}}}$$

Taking the natural logarithm of both sides, we have:

$$0 \geq \ln(R_{low}) + \ln\left(e^{\frac{\Delta V}{I_{sp}g_{earth}}}\right)$$

Simplifying again, we arrive at:

$$-\ln(R_{low}) \geq \frac{\Delta V}{I_{sp}g_{earth}}$$

We may here also make the relationship that describes the  $\Delta V$  delivered. The connection between hovering time and delta-V runs directly through the local gravity:  $\Delta V = g_{body}t_{hover}$ , where the term  $t_{hover}$  refers to the total time spent hovering or approximately hovering.

Simplifying to a final form, we see that:

$$\frac{I_{sp}g_{earth}\ln\left(\frac{1}{R_{low}}\right)}{t_{hover}} \geq g_{body}$$

So long as this statement holds, then the hopper can smoothly descend to the surface of the local planetary body.

However, the term  $R_{low}$ , the lowest throttling ratio, is not exceptionally useful. We can replace it with a term relating the masses of fuel and the body of the hopper.

Noting that  $R_{low} = \frac{T_{min}}{T_{max}}$ , and that this is effectively equivalent to  $R_{low} = \frac{m_c}{m_c+m_p}$ , as detailed above, we can then simplify to see that:

$$\frac{1}{R_{low}} = (1 + m'_p),$$

where  $m_p$  is the mass of the propellant.

Thus the final equation is:

$$\frac{I_{sp}g_{earth}\ln(1 + m'_p)}{t_{hover}} \geq g_{body}$$

This equation relates technical parameters of the vehicle, such as the engine's specific impulse, and operational parameters of the hopping mission, such as the time spent hovering, to the gravitational attraction of the local planetary body. The parameter  $m'_p$ , the propellant mass fraction, is intrinsically related to both the technical vehicle characteristics and the mission plan.

Estimating parameter values: The various parameters may have a range of values, which vary widely according to the detailed design of the mission and vehicle. However, for the purposes of estimating the lowest value of  $g_{body}$  for which hopping is likely to be feasible in general, we can make some assumptions.

Assumptions: 1) the hover time may range from 60 to 600 seconds. One minute to ten minutes covers a wide range of hopping mission scenarios. 2) the fuel specific impulse is somewhere between 150 and 250 seconds. This covers a range of potential propellants. 3) The fuel mass fraction cannot be driven lower than 5-10%. This in turn implies a lowest required throttling ratio,  $R_{low}$ , that is close to unity, as the mass of the hopper payload and bus dominate the system.

Given these assumptions, the lowest values seen for  $g_{body}$  that still permit hopping conditions (with a smooth landing) to apply are in the vicinity of  $0.25 \text{ m/s}^2$ . This result ties well with physical conditions in the solar system, as the largest asteroid (Ceres) and all minor planets fall above this cutoff, as do many of the larger moons. However, smaller asteroids and moons fall below it.

## **Appendix E. TALARIS History**

This section describes the history of the TALARIS project, which provides the detailed context for the incorporation of flexibility principles into the development of small advanced prototype vehicles.

### **E.1 Definition of the TALARIS Project**

The TALARIS project seeks to develop an advanced prototype testbed vehicle for lunar and planetary surface hopping. Because the project's staff consists of no more than a few thesis-seeking graduate students and one Principal Investigator, as well as a small number of associated graduate students, research assistants, and undergraduate researchers, it is characterized as small. In the scheme of a university research project, it is of a fairly respectable size, but the number of people working on TALARIS is less than the number who might be working on a new technology development project at NASA or corporate institutions. Furthermore, the funding level for TALARIS is much more commensurate with a small project than with a medium or large project – to date, all the hardware that has been developed and tested has been developed and tested on a budget in the low six figures. This is a relatively small budget for a complex, hardware-centric project in the aerospace field.

TALARIS is an advanced prototype vehicle development project. Advanced prototypes are here defined as systems which have limited or no heritage; although the high-level design heritage of hoppers stretches back to the 1960s, few similar systems have ever been built, and no hopper design has ever been put into mass production. The hopper with the most extensive record to date is the LLTV (36), which flew most of its flights in the 1960s as part of the Apollo training

program. Therefore, little direct heritage for TALARIS exists, and accordingly, the collection of modeling data for TALARIS and similar projects will be difficult. TALARIS is also a vehicle development project; this means that there is an element of binary performance in the project's success. A vehicle must move to be considered successful; TALARIS is a flight vehicle, and therefore must fly to be considered successful at the most basic level. Because TALARIS is a development, rather than a simple test or pure design project, it also encompasses the entire system lifecycle, even including operation and eventual retirement of the system.

The TALARIS hopper is a testbed, meaning it is intended to enable a field of study, per the design principles advanced in (137). Enabling a field of study means that the testbed must be able to adapt to a series of different contexts and a series of different components. That is, in order to function properly as a testbed, the TALARIS hopper must enable a number of different testable items to undergo trials in a number of different ways. The primary type of testable item envisioned for TALARIS is software GNC algorithms, although some tests of various hardware components, especially GNC-related sensors, may also take place. The primary type of different ways to test these items will be the mission profile. TALARIS will fly different mission profiles, with different levels of gravity offset, different loft times, and different acceleration and velocity profiles, in order to simulate the effects of flight on different planetary bodies around the solar system. The Google Lunar X-Prize contest is simply the first instantiation of TALARIS' mission.

Accordingly, the mission statement for TALARIS can be encapsulated as:



*To test, without leaving Earth, guidance, navigation, and control capabilities for hopping missions on planetary bodies around the solar system.*

Several characteristics of this mission statement lend themselves to multipoint interpretations. GNC capabilities may refer to a number of different implementations of algorithms in different ways, and there are a number of bodies around the solar system where hopping is feasible.

## **E.2 Early Conceptual Designs**

After the announcement of the Google Lunar X-Prize contest in late 2007, early indications of private and corporate interest began to appear around the world. Indications of interest were also present among student groups at MIT, including some of those who attended an AIAA student conference held in late 2007. During MIT's Independent Activity Period in January 2008, a group of students, faculty, and interested parties from corporate and research partners met several times to brainstorm the design space and begin to develop an initial concept for entry into the contest.

An MIT graduate design class developed a high-level mission concept for the GLXP contest in Spring 2008, and this was followed up by a summer working group that further refined the design and developed the necessary partnerships to advance it. The class and working group concurred on a recommendation that a testbed demonstrator be built.

- Mechanical ballistic launching
  - Springs – boot jackets
  - Springs – torsion legs
  - Piezoelectrics
    - Issues: travel distance, energy storage
  - General issues: Resetting springs? Regenerable springs? Stability?
- Chemical ballistic launching
  - Cold gas [probable choice, max  $dV = O(5 \text{ m/s})$ ]
  - Chemical combustion
- Overall issues
  - N hops: better control, smaller  $dV$  (coupled with propellant)
  - 1 hop: safer and more reliable
  - Redundancy
    - MIRVs
    - Multiple landings
  - Existing hardware?

Figure E-1. Early design work.

## E.2 Initial Prototype Hopper Demonstrator Design

In the Fall 2008 semester, a special-topics graduate design class addressed the conceptual and detailed design of a hopper demonstrator as a first step to competing in the GLXP contest. The class developed an initial design, seen in Figure E-2.

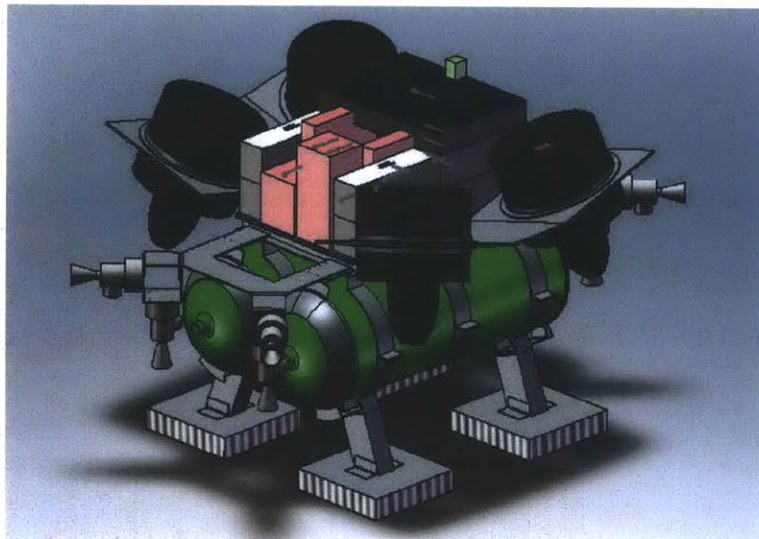
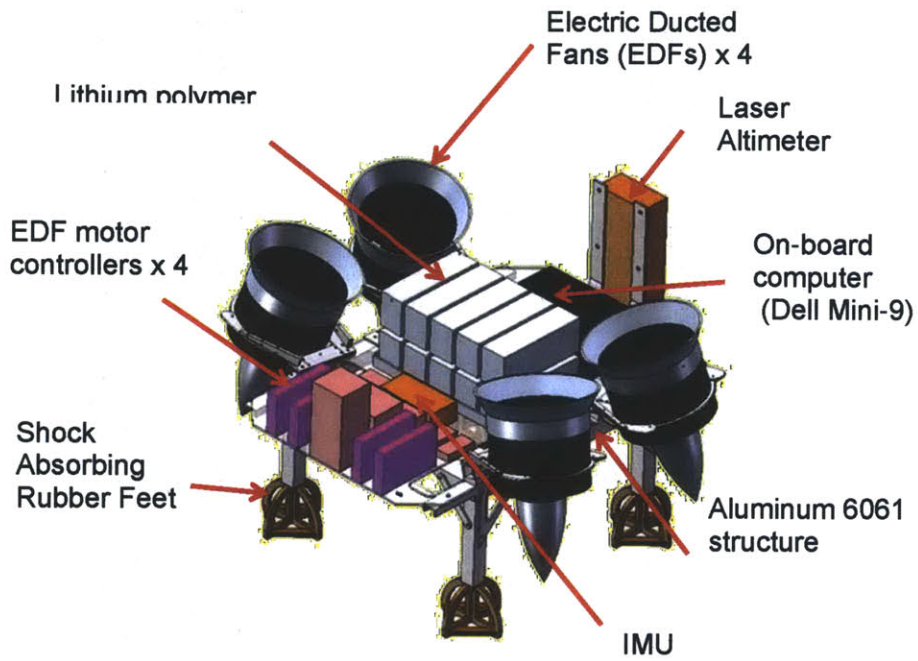


Figure E-2. Initial Design for a Hopper Demonstrator.

This initial design relied on Electric Ducted Fans (EDFs) for weight relief of 5/6 of a g, and used a Cold Gas Spacecraft Emulator (CGSE) system of compressed nitrogen to deliver the remaining 1/6-g lift force. It was determined that, for an Earth-based prototype hopper, the ability to simulate variable gravity is important, as is a relatively high frequency of testing, easy human access for repair, replacement, refueling, and part swap-out, plus the ability to demonstrate publicly or to corporate sponsors. The TALARIS prototype hopper design was developed as a means of meeting all these goals. A Critical Design Review was held and passed at the end of the semester.

### **E.3 Initial Hopper Demonstrator Construction and Testing**

In the Spring of 2009, a team of undergraduate and graduate students comprised of members from two capstone design classes was assembled to build and test the hopper demonstrator. This team, which first developed the name TALARIS, built and integrated many of the sub-systems necessary for the hopper: the air-breathing EDF (Electric Ducted Fan) propulsion system that removes the main part of the vehicle's weight, plus the first-generation structure and the avionics and other flight hardware. The vehicle was assembled and placed on a 1-degree-of-freedom test stand. Figure E-3 shows the components of the first-generation vehicle.



**Figure E-3. First-generation TALARIS vehicle.**

The first-generation hopper, after its initial construction, was taken through an extensive campaign of tests. After initial engine checkout and component integration, as seen in Figure E-4, the hopper was certified for flight.



**Figure E-4. Initial Engine Checkout.**

#### **E.4 Hopper Demonstrator Maturation and Flight Testing**

The Spring 2009 semester ended with the prototype hopper assembled and ready to fly. After the first full flight, in which the hopper demonstrated a thrust-to-weight ratio of greater than unity, further tests were conducted in the lab using a 1-degree of freedom test stand. Several obstacles were overcome in the ensuing months, including a crash after which the student team spent three weeks disassembling, carefully checking out, and reassembling every component on the vehicle. Other major obstacles included the development of a robust control algorithm that would be stable at high power levels during maneuvers and wear and tear on several of the EDF engines, which necessitated their replacement. Every major obstacle was turned into a redesign opportunity, with the vehicle's hardware and fasteners being upgraded after the crash, the vehicle's avionics being replaced and upgraded while controls algorithm development was underway, and the EDF replacement being used as an opportunity to infuse EDFs of a similar size but greater power into the system.

The vehicle in its configuration as of March 2010 is seen in Figure E-5. The overall architecture is similar to the first-generation layout, but improved components, including more powerful EDFs and improved avionics (modularized into an easily-replaceable box) have been added to the vehicle.

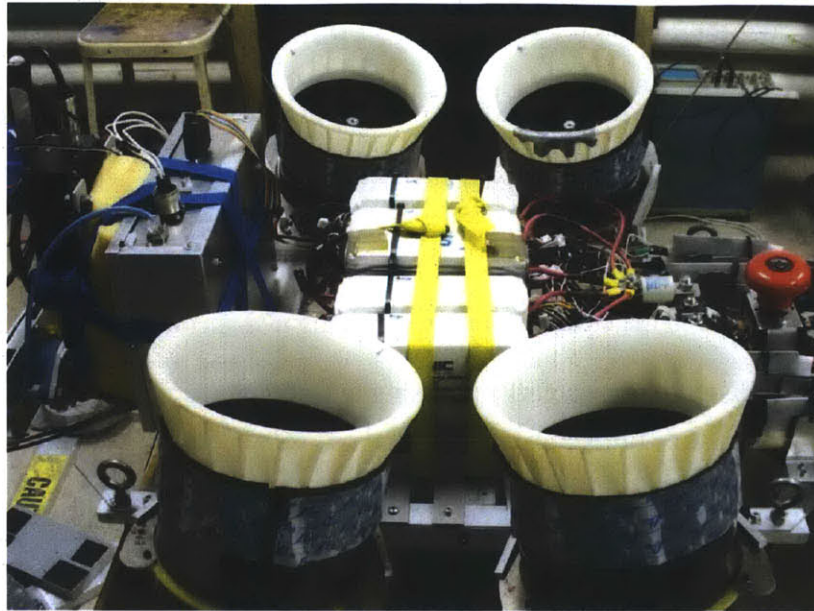


**Figure E-5. First-generation EDF and avionics layout.**

In concert with this design activity, the TALARIS project was converted into a full-scale research project, with permanently-assigned graduate students, a Principal Investigator, and defined lab space.

### **E.5 Further Development and Testing**

During the spring semester of the 2009-2010 academic year, the remaining systems, including the fractional-gravity cold gas spacecraft emulator (CGSE) propulsion system and a second-generation structure, were built and underwent final testing. A full second-generation vehicle was integrated during March 2010, and tests began in early April.

The second-generation TALARIS hopper, as seen in Figure E-6, started an initial flight campaign in the summer of 2010.



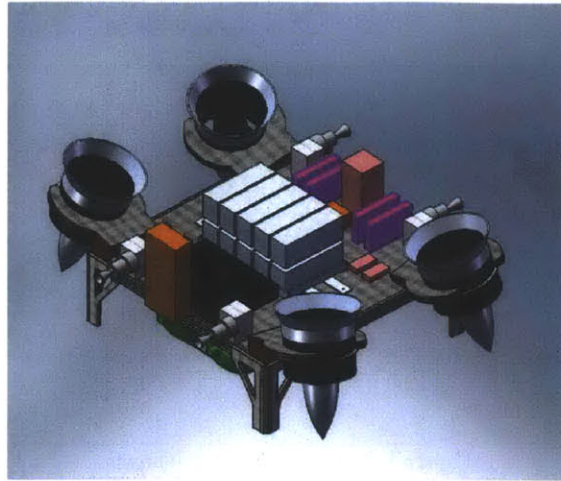


**Figure E-6. Second-generation TALARIS vehicle.**

After several incidents in which electrical components failed, a second complete overhaul of the avionics and power systems was carried out in late 2010 and early 2011. All control avionics were integrated into printed circuit boards (PCBs), and were given a system of fuses to protect against further failures. Older and aging batteries in the main power system were replaced with new batteries.

Once this redesign was complete, final development focused on launch systems and software algorithm development. Some algorithm development required adaptation of the second-generation vehicle, such as the 2-D navigation and guidance testing shown in Figure E-7, where the vehicle was mounted on an air bearing (to reduce vibration) and simulated a hovering traverse.

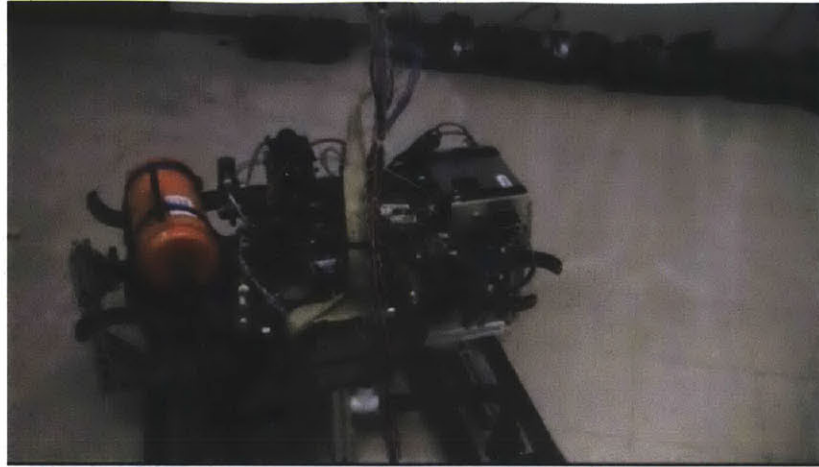


**Figure E-7. Air bearing GNC tests.**

Once advanced algorithm development had been carried out, more advanced testing proceeded.

Figure E-8 shows a descent test, with the vehicle hanging from a high overhead mount.



**Figure E-8. Descent tests and public demonstration.**



The test setup shown in Figure E-8 was also used to perform a public demonstration of the vehicle's capabilities at the MIT150 event in April 2011.

After this, development proceeded with the production of a quick-release launch stand, which minimized stand dynamics and ground effect during launch. This enabled launch and hover testing, as shown in Figure E-9.



**Figure E-9. Launch and hover test with new launch stand.**

The final development of the project was transition of knowledge gained to other projects. After a period of frequent flight testing, the algorithm and operational knowledge gained was transferred to other flight efforts, including the GENIE navigation system developed by Draper Laboratory, and contributed to the successful flight of GENIE onboard the Masten Space System Xombie vehicle in early 2012.